

# Investigating Dysbiosis as a Cause and Predictor of Intestinal Pathology

PhD Biomedical and Life Sciences

This thesis is submitted in partial fulfilment of the requirements for  
the Degree of Doctor of Philosophy

To

**Lancaster University**

August 2017

By

**Emma Leigh Beamish**

MSci (Hons)

## **Abstract**

Intestinal dysbiosis involves a shift in microbial composition and abundance within the gut and compelling evidence has highlighted the pivotal role dysbiosis plays in the onset and pathogenesis of numerous diseases, including inflammatory bowel disease (IBD), allergies and even mental health disorders. The intestinal microbiota is largely defined by host diet; a recent mouse model of total parenteral nutrition (TPN) showed that a dysbiotic shift in microbial dominance occurs following enteral nutrient deprivation. Furthermore, metabolomics studies have identified that IBD patients can be discriminated from healthy based on their urinary metabolite profiles, but whether such profiles are accountable to intestinal dysbiosis remains uncertain. The research presented herein employed two human models; a novel TPN model in loop ileostomy patients, and patients with IBD, to assess microbial shifts and associated physiological consequences as well as determine whether urinary metabolite profiles are reflective of the intestinal microbiota.

Using 16S rDNA-qPCR and -DGGE methods we revealed extensive variations in the microbiota of functional and defunctioned ileum following enteral nutrient deprivation, with a significant relative decrease in the Firmicutes phylum and concomitant increases in  $\gamma$ -Proteobacteria. Immunohistochemical techniques exposed a distinct physiological environment associated with a dysbiotic microbiota. Such environment was defined by reduced epithelial cell proliferation and mucosal atrophy that is likely due to altered host-microbiota interactions at the epithelial surface. We also observed post-operative complications that were potentially dysbiosis-mediated in almost 50% of the study cohort.

Urinary NMR and Illumina 16S next-generation sequencing multi-omics statistical analyses identified correlations between dietary-associated urinary metabolites, particularly epicatechin, and distinct enterotype-like microbiota profiles. Application of this principle to prediction of IBD, as an example of a dysbiosis-associated disease, proved to be difficult due to limited sample numbers confounding interpatient variability.

This research furthers the utilisation of intestinal microbiota as a therapeutic target, possibly via novel prebiotic administration to the defunctioned ileum with the potential to restore microbiota function prior to reanastomosis and reduce post-operative complications. Furthermore, it also provides promise for inexpensive, non-invasive detection of dysbiosis as a risk-factor of associated diseases. Further research, employing greater numbers of participants, is required to fully evaluate the potential predictive value of dysbiosis.

## **Acknowledgements**

I would like to take this opportunity to thank my primary supervisor, Dr. Rachael Rigby for her invaluable guidance and support throughout my time at Lancaster. In addition, to Prof. Peter Fielden for his continued enthusiasm and prompting collaborations that proved crucial to the success of this project. I am privileged to have worked with such encouraging, patient and hardworking academics and have learnt a lot along the way. My gratitude also extends to Professor James Morris, University Hospitals of Morecambe Bay NHS Trust and Bowel Cancer and Research for funding this research. The highly collaborative and clinical nature of this project has been most enjoyable and has taught me that we should recognise the boundaries of our own knowledge then embrace opportunity to learn from and teach others.

Additional thanks extend to our collaborating surgical team, Mr Arnab Bhowmick, Mr Nigel Scott and Judith Johnson, at Royal Preston Hospital for their combined efforts with provision of patient samples and contribution to our research paper. Judith in particular stretched herself to the limit to maximise patient recruitment and ensure the consistency of sample collection. Likewise, I am grateful to our collaborators in Gastroenterology at Furness General Hospital and Royal Preston Hospital; consultant gastroenterologists, Dr Albert Davies and Dr Abhishek Sharma and our research nurses, Emma Durant and Ailsa Watt, as well as the R&D departments at each respective site. Their combined efforts made provision of patient samples possible, despite facing almost every setback imaginable.

A huge thank you is owed to Dr. Geoffrey Akien, Dr. Marie Phelan and Dr. Frank Dondelinger for their generous provision of training, guidance and feedback with our metabolomics research. This area of the project has been a steep learning curve for me and I would not have reached this point without their expertise and advice. Furthermore, I gratefully acknowledge our collaborators, Dr. Sheena Cruikshank and Maria Glymenaki, at The University of Manchester. Their initial training in DGGE and bacterial enumeration techniques, as well as providing the TopoTA plasmid with permission from Professor Lora Hooper at UT South Western Medical Centre, enabled swift advancement of the project.

Thanks go to Dr. Karen Wright and all past and present members of the gut research group for their constructive criticism during our lab meetings and my departmental seminars. Particularly to Dr. Emily Smith for welcoming me to the Rigby lab and her initial, very patient, training during my masters year. Also to Charlotte and Meghan for their assistance with sample processing in the first year of this project.

On a more personal level, a special thank you is owed to Dr. Elisabeth Shaw for all the little yet significant ways in which she helped out, from answering my daft technical questions and offering encouragement at conferences, to our cake and hot chocolate breaks. We have formed a great friendship over the past four years and I would have been lost without her.

To my amazing friends, Kim, John and Caroline, for all of our European adventures, escape rooms, dinner parties, theme park trips, Tuesday quiz nights and general uncontrollable laughter that has kept me sane throughout this process. Kim's ingenious 'two week countdown survival kit' deserves a special mention too; such admirable creativity and kindness that has brightened these last few weeks, thank you so much! Also, to my fellow PhD student and good friend, Michelle for all of our long catch ups and trips to see each other, which offered us both a change of scenery and a fresh perspective.

I am infinitely grateful to my wonderful partner, Gary, for the limitless advice, reassurance and wit and for knowing me better than I know myself. There are not enough words to describe how thankful I am for everything you do and I cannot wait to see what the next chapter has in store for us.

Last but by no means least, I am forever indebted to my incredible family who are always filled with encouragement, support and challenge. I know for a fact that without such a strong foundation, I never would have embarked on this amazing journey, let alone made it to the end!



**Declaration**

I, Emma Beamish, declare that this thesis is my own work and has not been submitted elsewhere either in part, or as a whole, for the award of a higher degree or qualification. Published sections of this thesis are indicated in relevant figure legends.

Emma Beamish, MSci

## Contents

<b>Abstract</b> .....	<b>i</b>
<b>Acknowledgements</b> .....	<b>ii</b>
<b>Declaration</b> .....	<b>iv</b>
<b>List of Figures</b> .....	<b>xii</b>
<b>List of Tables</b> .....	<b>xv</b>
<b>Abbreviations</b> .....	<b>xvi</b>
<b>Chapter 1: Literature Review</b> .....	<b>1</b>
1.1 – Introduction.....	2
1.2 – Structure and Diversity of the Human Intestinal Microbiota.....	2
1.3 – Acquisition and Stability of the Intestinal Microbiota.....	5
1.4 – Functionality of Human Intestinal Microbiota.....	6
1.5 – Metabolism of the Intestinal Microbiota.....	8
1.6 – Intestinal Homeostasis Modulated by the Intestinal Microbiota.....	12
1.7 – Maintenance of Tolerance to Resident Microbiota.....	14
1.8 – Intestinal Dysbiosis.....	18
1.9 – Aetiology of Dysbiosis and Influence of Diet.....	22
1.10 – Intestinal Microbiota in Dysbiosis-associated Diseases.....	27
1.11 – Defining a Characteristic Dysbiotic Intestinal Microbiota.....	29
1.12 – Intestinal Microbiota Modulation: Aiming for Rebiosis and Implications for Therapies.....	30
1.13 – Research Aims.....	34
<b>Chapter 2: Materials and Methods</b> .....	<b>35</b>
<b>2.1 – Materials</b> .....	<b>36</b>
2.1.1 - Reagents.....	36
2.1.2 - Antibodies.....	37

2.1.3 - PCR Primers.....	37
2.1.4 - Buffers and Solutions.....	38
<b>2.2 Methods.....</b>	<b>39</b>
<b>2.2.1 - Research Ethics.....</b>	<b>39</b>
<b>2.2.2 - Surgical Patient Recruitment .....</b>	<b>39</b>
<b>2.2.3 - Provision of Surgical Specimen.....</b>	<b>40</b>
<b>2.2.4 - Surgical Specimen DNA Extractions.....</b>	<b>40</b>
2.2.4.1 - Mucosal Tissue DNA Extraction.....	40
2.2.4.2 - Luminal Swab and MEM Media DNA Extraction.....	40
<b>2.2.5 - Denaturation gradient gel electrophoresis (DGGE).....</b>	<b>41</b>
2.2.5.1 – Generation of a Standard DNA Marker for DGGE Analyses.....	41
2.2.5.2 – Polymerase Chain Reaction (PCR) for DGGE.....	41
2.2.5.3 - DGGE Profiling.....	42
2.2.5.4 – Digital Processing of DGGE Profiles.....	42
2.2.5.5 – DGGE Band Excision and Purification.....	43
2.2.5.6 - Sanger Sequencing and Analysis.....	43
<b>2.2.6 – Phylum-specific 16S ribosomal-deoxyribonucleic acid quantitative real-time PCR (16S rDNA qRT-PCR).....</b>	<b>43</b>
<b>2.2.7 – Quantification of Total Bacterial Load.....</b>	<b>44</b>
2.2.7.1 – Preparation of Luria Broth (LB) + Kanamycin Agar Plates.....	44
2.2.7.2 – pCR®2.1-TOPO® Plasmid Transformation.....	44
2.2.7.3 – Clone Selection using LB Kanamycin Plates.....	44
2.2.7.4 – Clone Amplification.....	44
2.2.7.5 – Isolation of Plasmid DNA.....	45
2.2.7.6 – Generation of pCR®2.1-TOPO® Plasmid Standard Curve.....	45
2.2.7.7 - pCR®2.1-TOPO® Plasmid 16S rDNA qRT-PCR.....	45
<b>2.2.8 - Histological Analyses.....</b>	<b>46</b>

2.2.8.1 - Tissue Fixation and Sectioning.....	46
2.2.8.2 - Haematoxylin and Eosin (H&E) Staining.....	46
2.2.8.3 - Morphological Analyses.....	46
2.2.8.4 – Inflammation Scoring.....	47
<b>2.2.9 - Immunofluorescence Proliferating Cell Nuclear Antigen (PCNA) Analysis.....</b>	<b>47</b>
<b>2.2.10 – Click-iT® Terminal Deoxynucleotidyl Transferase-dUTP Nick End Labelling (TUNEL) Assay.....</b>	<b>48</b>
<b>2.2.11 – Statistical Analyses.....</b>	<b>48</b>
<b>2.2.12 – Endoscopy Outpatient Recruitment.....</b>	<b>48</b>
<b>2.2.13 – Urine and Colonic Biopsy Sample Acquisition and Processing.....</b>	<b>49</b>
2.2.13.1 – Sample Acquisition.....	49
2.2.13.2 – Urine Sample Processing.....	50
2.2.13.3 – Colonic Biopsy DNA Extraction and Purification.....	50
<b>2.2.14 – 1D <sup>1</sup>H NMR Spectroscopy.....</b>	<b>50</b>
2.2.14.1 – 1D <sup>1</sup> H NMR Sample Preparation.....	50
2.2.14.2 – 1D <sup>1</sup> H NMR Spectroscopy.....	51
2.2.14.3 – NMR Spectroscopy Data Preprocessing.....	51
<b>2.2.15 – Illumina® MiSeq Sequencing.....</b>	<b>53</b>
2.2.15.1 – Library Preparation.....	53
2.2.15.2 – Cluster Generation.....	54
2.2.15.3 – Sequencing-by-Synthesis.....	54
2.2.15.4 – Illumina® Sequencing Data Processing.....	54
2.2.15.5 – Plotting Sequence Data.....	55
<b>2.2.16 – Multivariate Statistical Analyses of Illumina MiSeq Sequencing and Urinary NMR Metabolomics Datasets.....</b>	<b>57</b>
2.2.16.1 – Hierarchical Cluster Analyses.....	57
2.2.16.2 – Principal Components Analyses.....	57
2.2.16.3 – Orthogonal Partial Least Squares Discriminant Analyses (OPLS-DA).....	57

2.2.16.4 – Linear Regression Analysis.....	58
<b>Chapter 3: Investigating the effect of enteral nutrient deprivation on intestinal microbiota composition utilising a novel human model in patients undergoing ileostomy reversal surgery.....</b>	<b>59</b>
3.1 - Rationale.....	60
3.2 - Research Aims.....	63
3.3 - Methods Summary.....	63
3.4 - Results.....	64
3.4.1 – Sanger sequencing of extracted DGGE bands enables accurate identification of microbes to genus level.....	64
3.4.2 – Total bacterial load is significantly reduced in defunctioned intestine.....	67
3.4.3 – Luminal-associated microbiota profiles differ in functional and defunctioned intestine.....	67
3.4.4 – Luminal-associated microbial dysbiosis is apparent at phylum and genus level in defunctioned ileum.....	71
3.4.5 – Mucosal-associated microbial profiles differ in functional and defunctioned intestine following ileostomy-mediated enteral nutrient deprivation.....	73
3.4.6 – Mucosal-associated microbial dysbiosis is apparent at phylum, order and genus level in defunctioned ileum.....	76
3.5 - Discussion.....	83
<b>Chapter 4: Investigating the morphology of functional and defunctioned ileum following ileostomy-mediated faecal stream diversion.....</b>	<b>88</b>
4.1 - Rationale.....	89
4.2 - Research Aims.....	91
4.3 - Methods Summary.....	91
4.4 - Results.....	92
4.4.1 - Defunctioned ileum is atrophied but not inflamed at the time of loop ileostomy reversal.....	92

4.4.2 – Villous atrophy accountable to reduced IEC proliferation in defunctioned crypts rather than increased anoikis.....	94
4.4.3 – Blood CRP levels are raised but albumin and WBC levels remain normal post ileostomy reversal surgery.....	98
4.4.4 – Ileostomy reversal surgery is associated with substantial morbidity.....	98
4.4.5 – Exploratory analysis of participant demographics revealed associations with clinical outcomes.....	99
4.4 - Discussion.....	102
<b>Chapter 5: Utilising NMR Spectroscopy-Based Urinary Metabolite Profiling for Prediction of Intestinal Microbiota Composition.....</b>	<b>106</b>
5.1 - Rationale.....	107
5.2 - Research Aims.....	109
5.3 - Methods Summary.....	109
5.4 - Results.....	110
5.4.1 - Hierarchical clustering analysis of microbiota sequencing data revealed five enterotype-like groups.....	110
5.4.2 - Substantial interpatient variation observed in human urinary metabolite profiles.....	114
5.4.3 - Various urinary metabolites are correlated with intestinal microbiota profiles in humans.....	117
5.4.4 - Urinary metabolites are also associated with specific microbial populations.....	118
5.5 - Discussion.....	121
<b>Chapter 6: Investigating the Potential Application of Diagnosing Dysbiosis via Urinary NMR Metabolomics for Detection of Disease Susceptibility. ....</b>	<b>127</b>
6.1 - Rationale.....	128
6.2 - Research Aims.....	130
6.3 - Methods Summary.....	130
6.4 - Results.....	131

6.4.1 – Partial separation observed between IBD and control intestinal microbiota profiles.....	131
6.4.2 – No distinct differences observed in urinary metabolite profiles of IBD and control cohorts.....	138
6.4.3 – Participant demographics demonstrated well matched study cohorts but a variety of confounding variables exist between IBD patients.....	143
6.5 – Discussion.....	145
<b>Chapter 7: Discussion and Future Directions.....</b>	<b>148</b>
7.1 - Discussion and Future Directions.....	149
7.2 - Dysbiosis as a Cause of Intestinal Pathology.....	149
7.3 - Dysbiosis as a Predictor of Disease. ....	152
<b>Bibliography.....</b>	<b>155</b>
<b>Publication.....</b>	<b>172</b>
<b>Appendices.....</b>	<b>185</b>
Appendix 1 - Surgical Study Clinical Documentation.....	186
Appendix 2 - Binary DGGE Banding Profiles of Luminal and Mucosal-associated Microbiota.....	191
Appendix 3 - Mucosal and Luminal DGGE band extraction and purification.....	193
Appendix 4 - DGGE Band Class Consensus Sequences and Taxonomic Assignments for Optimisation Experiment, Mucosal and Luminal Microbiota Profiles.....	195
Appendix 5 - pCR2.1-TOPO® Standard Curve Calculations.....	199
Appendix 6 - Measurement of Villous Height and Crypt Depth using ImageJ Software .....	201
Appendix 7 - Endoscopy Study Clinical Documentation.....	202
Appendix 8 - Pattern File for Computational Bucket Processing of <sup>1</sup> H NMR Spectral Peaks.....	211
Appendix 9 - PQN Normalised and Pareto Scaled Relative Concentrations of Annotated Urine Metabolites.....	216
Appendix 10 - Scatterplot Matrix.....	229

Appendix 11 - Complete and Annotated Proportionate Microbiota Data at Order Level.....230

Appendix 12 - Complete and Annotated Proportionate Microbiota Data at Genus Level.....232



## List of Figures

Figure 1.1 - Microbiota of the GI tract in humans.....	3
Figure 1.2 - Intestinal microbiota-mediated metabolism of host dietary fibre.....	9
Figure 1.3 - Mechanisms of SCFA influence on intestinal physiology and immunology.....	11
Figure 1.4 - Homeostatic tolerance mechanisms sustaining host health.....	16
Figure 1.5 - Loss of intestinal homeostasis associated with dysbiosis.....	20
Figure 1.6 - Aetiology of dysbiosis and associated diseases.....	23
Figure 2.1 - Illumina® sequencing workflow.....	56
Figure 3.1 - Defunctioning loop ileostomy formation in surgical resection patients.....	60
Figure 3.2 - Structure of the intestine during loop ileostomy and following reanastomosis....	62
Figure 3.3 - Microbial DGGE profiles for band extraction and sequencing.....	65
Figure 3.4 - Species assignment for extracted and sequenced microbial DGGE bands.....	66
Figure 3.5 - Enumeration of total bacterial load.....	67
Figure 3.6 - Inpatient comparisons of luminal-associated intestinal microbiota profiles between functional and defunctioned intestine.....	68
Figure 3.7 - Luminal DGGE band analysis.....	69
Figure 3.8 - Hierarchical cluster analysis of luminal-associated DGGE profiles.....	70
Figure 3.9 - Luminal band class quantification and sequencing.....	71
Figure 3.10 - Relative quantification of predominant luminal-associated phyla.....	72
Figure 3.11 - Inpatient comparisons of mucosal-associated intestinal microbiota profiles between functional and defunctioned intestine.....	74
Figure 3.12 - Mucosal DGGE band analysis.....	73
Figure 3.13 - Hierarchical cluster analysis of mucosal-associated DGGE profiles.....	75
Figure 3.14 - Mucosal band class quantification and sequencing.....	76
Figure 3.15 - Relative taxonomic composition of 16S rRNA amplicon sequences in mucosal-associated microbiota samples, at phylum level.....	77
Figure 3.16 - Relative taxonomic composition of 16S rRNA amplicon sequences in mucosal-associated microbiota samples, at order level.....	79

Figure 3.17 - Relative taxonomic composition of 16S rRNA amplicon sequences in mucosal-associated microbiota samples, at genus level.....	80
Figure 3.18 - PCA of functional and defunctioned mucosal-associated microbiota.....	82
Figure 4.1 - Histological analysis of villous height in functional and defunctioned intestine....	92
Figure 4.2 - Histological analysis of crypt depth in functional and defunctioned intestine.....	93
Figure 4.3 - Histological analysis of inflammation in functional and defunctioned intestine.....	94
Figure 4.4 - Assessment of IEC proliferation in functional versus defunctioned intestine.....	95
Figure 4.5 - Relative quantification of IEC proliferation in functional versus defunctioned intestine.....	96
Figure 4.6 - Assessment of apoptosis in functional versus defunctioned intestine.....	97
Figure 4.7 - Noteworthy scatterplots correlating participant demographics with post-operative clinical data.....	100
Figure 5.1 - Relative taxonomic composition of 16S rRNA amplicon sequences in human intestinal biopsy samples, at phylum level.....	111
Figure 5.2 - Hierarchical cluster analyses of Illumina 16S intestinal microbiota profiles.....	112
Figure 5.3 - Relative taxonomic composition of 16S rRNA amplicon sequences from human intestinal biopsy samples, at order level, depicting 5 hierarchical clusters.....	113
Figure 5.4 - Representative <sup>1</sup> H NMR spectra of patient urine samples.....	115
Figure 5.5 - Hierarchical cluster analysis of <sup>1</sup> H NMR urinary metabolite NMR profiles.....	116
Figure 5.6 - Penalised multinomial regression analysis of urinary metabolites against enterotype-like microbiota profiles.....	117
Figure 5.7 - Penalised linear regression analysis of urinary metabolites against intestinal microbiota taxa at order level .....	119
Figure 5.8 - Penalised linear regression analysis of urinary metabolites against intestinal microbiota taxa at phyla level .....	120
Figure 6.1 - Relative taxonomic composition of 16S rRNA amplicon sequences from human intestinal biopsy samples, at phylum level.....	132
Figure 6.2 - Relative taxonomic composition of 16S rRNA amplicon sequences from human intestinal biopsy samples, at order level.....	133
Figure 6.3 - Hierarchical cluster analyses of intestinal microbiota profiles in IBD and control patients.....	134

Figure 6.4 - PCA of intestinal microbiota profiles from IBD and control patients.....	136
Figure 6.5 - OPLS-DA of intestinal microbiota profiles from IBD and control patients.....	137
Figure 6.6 - Hierarchical cluster analysis of <sup>1</sup> H NMR urinary metabolite NMR profiles from IBD and control cohorts.....	138
Figure 6.7 - Representative <sup>1</sup> H NMR spectra of IBD and control urine samples.....	139
Figure 6.8 - PCA of urine metabolite profiles from IBD and control patients.....	141
Figure 6.9 - OPLS-DA of urine metabolite profiles from IBD and control patients.....	142

## List of Tables

Table 1.1 - Differentiated cell types of the intestinal epithelium.....	13
Table 1.2 - Macronutrient influence on intestinal microbiota composition.....	25
Table 1.3 - Composition and dose of reputable poly-biotics and probiotics.....	31
Table 2.1 - Reagents and products with supplier details.....	36
Table 2.2 - Antibodies.....	37
Table 2.3 - PCR Primers.....	37
Table 2.4 - Buffers and Solutions.....	38
Table 2.5 - Inclusion and exclusion criteria for patient recruitment to surgical study.....	39
Table 2.6 - Inclusion and exclusion criteria for patient recruitment to endoscopy study.....	49
Table 2.7 - Amplicon PCR reaction components for Illumina® MiSeq library preparation.....	53
Table 2.8 - Amplicon and index PCR cycle parameters for Illumina® MiSeq library preparation.....	53
Table 4.1 - Mean participant demographics and Post-operative clinical data.....	98
Table 4.2 - Incidence of post-operative complications following ileostomy reversal surgery.....	99
Table 5.1 - Human metabolites and associated intestinal microbiota.....	108
Table 6.1 - Participant demographics and clinical characteristics of IBD cohort.....	143

## Abbreviations

16S rDNA qRT-PCR	16S Ribosomal-DNA Quantitative Real-Time PCR
AMP	Antimicrobial peptide
APES	3-Aminopropyltriethoxysilane
ASP	Ammonium Persulfate
BAFF	B-cell Activating Factor
BLASTn	Nucleotide Basic Local Alignment Search Tool
Bp	Base Pair
CCK	Cholecystokinin
CD	Crohn's disease
Cq	Quantification Cycle
DC	Dendritic cell
DGGE	Denaturation Gradient Gel Electrophoresis
dH <sub>2</sub> O	Distilled H <sub>2</sub> O
DSS	Dextran Sodium Sulphate
EBF	Epithelial Barrier Function
EGFR	Epidermal Growth Factor Receptor
FID	Free Induction Decay
FLASH	Fast Length Adjustment of Short Reads
FMT	Faecal Microbiota Transplantation
GF	Germ-free
GI	Gastrointestinal
GLP	Glucagon-like Peptide

GPCR	G Protein-Coupled Receptor
GPI	Glycosylphosphatidylinositol
H&E	Haematoxylin and Eosin
HAA	Heterocyclic Aromatic Amines
HDAC	Histone Deacetylases
HIER	Heat-Induced Epitope Retrieval
HSP	Heat Shock Protein
IBD	Inflammatory Bowel Disease
IBS	Irritable Bowel Syndrome
IEC	Intestinal Epithelial Cell
IESC	Intestinal Epithelial Stem Cell
IFN	Interferon
Ig	Immunoglobulin
IL	Interleukin
IRAS	Integrated Research Application System
KEGG	Kyoto Encyclopaedia of Genes and Genomes
LPS	Lipopolysaccharide
Lypd8	Ly6/PLAUR Domain-containing 8
M Cell	Microfold Cell
NF- $\kappa$ B	Nuclear Factor- $\kappa$ B
NHS	National Health Service
NLR	Nod-like Receptor
NMR	Nuclear Magnetic Resonance

NOESY	Nuclear Overhauser Enhancement Spectroscopy
OPLS-DA	Orthogonal Partial Least Squares-Discriminant Analysis
OTU	Orthogonal Taxonomic Unit
PAMP	Pathogen-Associated Molecular Pattern Motif
PCA	Principal Components Analysis
PCNA	Proliferating Cell Nuclear Antigen
PCR	Polymerase Chain Reaction
PNG	Portable Network Graphic
PRR	Pattern Recognition Receptor
PSA	Polysaccharide A
QIIME™	Quantitative Insights into Microbial Ecology
RD	Relaxation Delay
RDP	Ribosomal Database Project
rDNA	Ribosomal Deoxyribonucleic Acid
RPM	Revolutions per Minute
rRNA	Ribosomal Ribonucleic Acid
SCFA	Short Chain Fatty Acids
SEM	Standard Error of the Mean
TameNMR	Tools for Analysis of Metabolic NMR
TEMED	N,N,N',N'-Tetramethylethylenediamine
TFF3	Trefoil factor 3
TGF-β	Transforming Growth Factor-β
TLR	Toll-like Receptor

TNF	Tumour Necrosis Factor
TPN	Total Parenteral Nutrition
TSP-d4	Deuterated (Trimethylsilyl)-propionic-2,2,3,3-d4 acid sodium salt
TUNEL	Terminal Deoxynucleotidyl Transferase-dUTP Nick End Labelling
UC	Ulcerative Colitis
UMP	Uridine Monophosphate
UPGMA	Unweighted Pair Group Method with Arithmetic Mean
UTI	Urinary Tract Infection
VLDL	Very-low-density Lipoprotein
WBC	White Blood Cell
WHO	World Health Organisation



# **Chapter 1:**

## **Literature Review**

## **1.1 - Introduction**

This project aims to investigate intestinal dysbiosis both as a cause and a potential predictor of various associated diseases. First, molecular and biochemical techniques will be employed to explore dysbiosis and consequences for intestinal physiology utilising a novel human model which controls for confounding interpatient genetic and environmental variability. In addition, urinary NMR metabolomics and Illumina® 16S deep sequencing will be utilised to determine whether host urine metabolites are reflective of intestinal microbiota composition.

To provide a contextual background for this research and the data collected, the literature review will be presented with particular focus on the following topics:

- Diversity, structure and function of the human intestinal microbiota
- Acquisition and stability of the intestinal microbiota
- Maintenance of homeostasis and tolerance to commensal microbes
- Intestinal dysbiosis and associated diseases
- Dysbiosis aetiology and influence of diet
- Intestinal microbiota as a therapeutic target

## **1.2 – Structure and Diversity of the Human Intestinal Microbiota**

The gastrointestinal (GI) tract harbours a vast and diverse microbial community, referred to as the gut microbiota. This complex ecosystem comprises over  $10^{14}$  microorganisms of approximately 1000 different species, differing in composition and increasing in abundance and diversity with progression through the GI tract (figure 1.1) (Eckburg et al., 2005). The large intestine is resident to the vast majority of the human microbiota and is predominated by obligate anaerobes, which collectively outnumber all cells of human origin by an order of magnitude (Zhu et al., 2010). The composition of the intestinal microbiota is also thought to differ cross-sectionally with distinct microbes residing the intestinal lumen and mucosa (Eckburg et al., 2005). Bacteroidetes and Firmicutes phyla account for >90% of the intestinal microbiota, whilst the remaining populations consist of less predominant phyla including Proteobacteria, Actinobacteria, Fusobacteria and a small proportion of fungi and viruses (Eckburg et al., 2005, Reyes et al., 2010, Hoffmann et al., 2013).

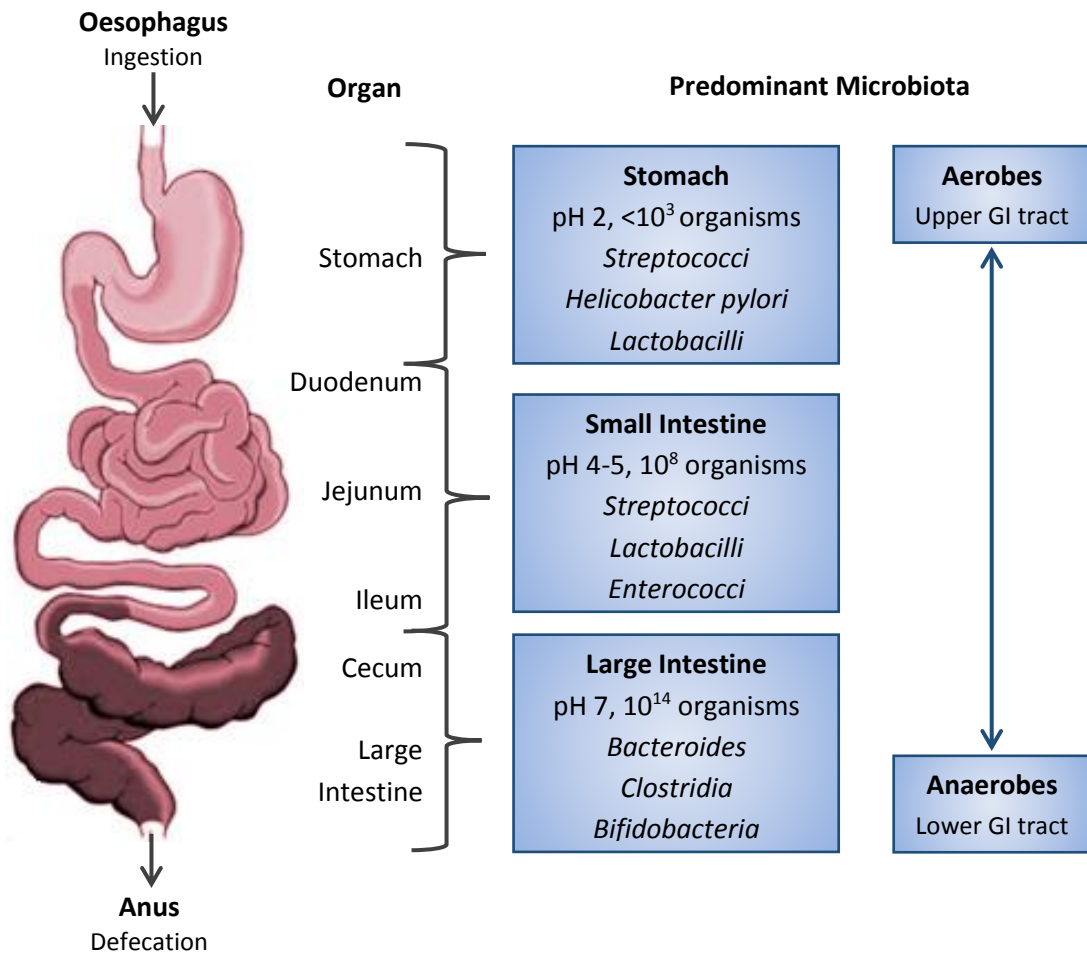


**Figure 1.1 – Microbiota of the GI tract in humans.**

The most diverse and abundant human microbiota is that of the GI tract which has coevolved with the host to reach a state of mutualism. A gradient exists in microbiota load with up to  $10^{14}$  prokaryotes of around 100 different species residing within the large intestine. Microbiota that are specially equipped to thrive under various host physiological conditions, such as pH and oxygen levels, predominant each organ of the GI tract, with anaerobes and facultative anaerobes significantly outnumbering aerobes.

*Figure adapted from (Tsabouri et al., 2014).*

Firmicutes is at present the largest phylum, containing no less than 200 genera, with most of the intestinal microbiota belonging to *Clostridium* and *Lactobacillus*. Firmicutes are Gram-positive bacteria with a low G+C DNA content that are particularly efficient at harvesting energy from host diet (Vos et al., 2009). The second most predominant phylum, Bacteroidetes comprises three broad classes of Gram-negative, non sporeforming, rod shaped bacteria; Flavobacteria, Sphingobacteria and the most well studied Bacteroida. The

genus *Bacteroides* provide important metabolic capabilities which promote a diverse metabolism in the human host (Wexler, 2007). The Proteobacteria phylum consist of five classes of Gram-negative bacteria, categorised primarily according to trophic status. Gammaproteobacteria is the most diverse class with many human pathogens including *Vibrio cholerae* and enteric bacteria including the most widely studied *Escherichia coli* (*E.coli*; (Garrity et al., 2005)). Actinobacteria are Gram-positive, high G+C DNA content microorganisms which harbour the clinically relevant bacterial genera *Bifidobacterium* and *Actinomyces* (Whitman et al., 2012).

The broad diversity of the intestinal microbiota has become increasingly well characterised with the development of high throughput sequencing technologies, enabling progression from limited culture-based methodologies. It was originally believed that all healthy adults harboured the same intestinal microbiota as the limited proportion of culturable intestinal bacteria were repeatedly isolated from different individuals. Since then, culture-independent studies such as the human microbiome project, have demonstrated substantial inter- and intra-individual variation in microbial diversity, despite the consistency of the “core” phyla (Consortium, 2012, Eckburg et al., 2005). Subsequent attempts to define a characteristic microbiota at species level in the adult intestine have identified various functionally important species, most notably *Faecalibacterium prausnitzii* (*F. prausnitzii*), which are shared across most individuals, albeit at varying abundances (Tap et al., 2009).

In 2011 it was suggested that despite the substantial inter-individual species variability, a common functionality, being the metabolism of nutrients within the lumen, is shared across each unique microbiota and would therefore result in different types of intestinal microbiota (Arumugam et al., 2011). The study identified three groups, termed enterotypes, across 4 combined datasets totalling more than 200 individuals from different cultures. Each enterotype is predominated by a different bacterial genera; *Bacteroides*, *Prevotella* and *Ruminococcus*, respectively. The first is also positively correlated with *Clostridia* and *Lactobacillus*, whilst the second and third are correlated negatively with *E. coli* (Arumugam et al., 2011). Since then a fourth enterotype has been suggested to be related to intestinal disease with an altered intestinal microbiota and is defined with an abundance of Proteobacteria, particularly *E. coli* (Harmsen and C., 2016). The ongoing effort to define

specific enterotypes enabling stratification of individuals into microbiota groups, analogous to the distinct A, B and O blood groups, is desirable as it would simplify the diverse microbiota to relatable and manageable subgroups. However, enterotype determination is subject to selection and application of sequencing and analytical methodologies (Koren et al., 2013). Furthermore, evidence has begun to demonstrate the vast temporal variability of the intestinal microbiota in healthy adults which is increasingly suggestive of a continuous dynamic ecosystem (Knights et al., 2014).

### **1.3 – Acquisition and Stability of the Intestinal Microbiota**

The intestine of an unborn child was until recently, considered sterile with initial microbial colonisation occurring during and immediately after birth (Escherich, 1988). However, recent studies have identified that foetuses are exposed to maternal microbiota that have infiltrated the amniotic fluid, likely via the placenta, suggesting microbiome acquisition may begin in utero (Collado et al., 2016). In addition, identification of bacteria in neonate meconium samples further supports this notion, although given that the bacterial profiles resemble maternal and later infant faecal profiles, rather than that of amniotic fluid or placenta, such findings may be a consequence of colonisation during child birth rather than in the womb (Collado et al., 2016).

Postpartum microbial colonisation of the intestine is determined by a variety of factors including method of delivery and feeding, duration of hospital stay and use of antibiotics (Penders et al., 2006). During vaginal delivery, the neonate is colonised with maternal vaginal and faecal microbiota via direct contact. However, neonates delivered by caesarean section are deprived of this direct contact resulting in a lack of maternally derived microbes, such as *Bifidobacteria* and are instead colonised by environmental microbes (Biasucci et al., 2008). Likewise, breastfed infants are colonised predominantly by *Bifidobacteria* and lactobacilli, whilst those fed on formula milk share microbial predominance between *Bacteroides* and *Bifidobacteria* and also harbour microbes such as *Escherichia coli* and *Staphylococci* (Harmsen et al., 2000). The precise influence of each of these factors on microbial diversity in children however is not yet well established but associations exist between disruptions in intestinal microbiota development and establishment of disease in later life, particularly allergies and obesity (Wang et al., 2008, Kalliomaki et al., 2008).

The intestinal microbiota is diverse and fluctuates considerably throughout infancy prior to development of a more stable microbiota in adulthood. During the first year of life, the intestinal microbiota has been shown to vary substantially both temporally within and between babies, largely as a consequence of environmental exposures, such as the microbiota of family members as well as diet (Palmer et al., 2007). By the age of 1, the microbial profiles converge toward a characteristic adult intestinal microbiota, predominated by Firmicutes and Bacteroidetes (Palmer et al., 2007). During adolescence, adulthood and through to old age, the intestinal microbiota remains relatively stable at the phylum level but is shaped by a variety of genetic and environmental factors to form a unique and continuously diverse microbiota. Host genetics are considered to influence intestinal microbiota composition, with twin studies reporting a high degree of similarity in microbiota profiles (Dicksved et al., 2008, Lee et al., 2011). However, subsequent studies have also reported a comparable level of similarity in the intestinal microbiota of monozygotic and dizygotic twins, suggesting that it is in fact environmental factors which interact with host genetics to shape intestinal microbiota composition, rather than genetic determinants exclusively (Turnbaugh et al., 2009). Likewise, studies investigating cultural differences in the intestinal microbiota composition have reported distinct profiles in healthy adults around the world. One study, which compared the intestinal microbiota profiles of healthy adults living in South Korea and the United States, found biogeographical signatures defined by significant increases in *Lactobacillales* and reductions in *Clostridiales* in the South Korean cohort (Lee et al., 2011). Although these cohorts undoubtedly have genetic differences, dissimilarity of the intestinal microbiota is considered to be a consequence of vastly contrasting lifestyles causing distinct environmental exposures (Lee et al., 2011).

#### **1.4 – Functionality of Human Intestinal Microbiota**

The intestinal microbiota has co-evolved with human hosts to reach a state of mutualistic symbiosis; humans provide nutritional sustenance and a superlative physiological environment, whilst the microbiota implement a broad range of essential functions which promote host health. The combined genomic capacity of the intestinal microbiota, referred to as the intestinal microbiome, has been calculated to exceed 3 million genes, which outnumbers that of the human host by several orders of magnitude (Qin et al., 2010). This

vast microbial ecosystem and its combined genomic repertoire provides a range of physiological and enzymatic functions which promote host health.

The broad mass of the intestinal microbiota provides barrier effects that protect the intestinal epithelium from potential invasion by toxins and pathogens also present in the lumen. Both germ-free (GF) and antibiotic treated mice have been shown to have an increased susceptibility to infection by enteric pathogens such as *Clostridium difficile* (Osawa and Mitsuhashi, 1964, Lawley et al., 2009). The dense population of resident microbes generates competition for shared nutrients and niches within the intestine, acting as a physical barrier to pathogenic invasion as well as attenuate overgrowth of opportunistic resident microbes. Resident microbes promote this defence via production of bacterial toxins that inhibit similar and thus competing species. Furthermore, the production of short chain fatty acids (SCFA) by bacteria such as *Bacteroides* can locally adjust the pH and consequently inhibit growth of intestinal pathogens, particularly enterohaemorrhagic *E. coli* (Shin et al., 2002).

It is also understood that the extent to which the intestinal microbiota contribute to host health far exceeds such protective functions. In particular, a range of gnotobiological studies have demonstrated that resident microorganisms are crucial for normal development of intestinal architecture in early life. For example, GF mice exhibit significant morphological defects in the development of various secondary lymphoid tissues, including Peyer's patches and lymphoid follicles, which usually provide innate immune functions against invasive microorganisms (Bouskra et al., 2008). In addition, a substantial reduction in the overall surface area of the intestine and thickness of the lamina propria was observed in GF mice compared to control groups (Abrams et al., 1963, Gordon and Bruckner-Kardoss, 1961). However, although the developmental consequences of intestinal microbiota depletion are well documented, the mechanisms by which microbes influence such development are not yet comprehensively defined.

In addition, commensal microbes are fundamental in establishment of proper host immune function that supports host-microbiota symbiosis, via immune cell training upon first

encounter. It has been suggested that exposure to commensal microbes within the first three months of life is essential for complete immune training (Arrieta et al., 2015). Research has shown that regulatory T cells present in the intestine express distinct cell surface receptors to those in the periphery, inferring a superior role for immune cell interactions with localised microbiota-derived antigens (Lathrop et al., 2011). Commensal interaction with such immune cells results in peripheral expansion of regulatory T cells rather than inflammatory effectors, as is observed with exposure to pathogenic microorganisms (Lathrop et al., 2011). Furthermore, research into this area has concluded that infants harbour a distinct premature immune system prior to microbiota-mediated immune cell training and an increased susceptibility for infection and disease has been correlated with perturbed microbiota-mediated immune training in early years (Arrieta et al., 2015).

### **1.5 – Metabolism of the Intestinal Microbiota**

The intestinal microbiota contribute to host metabolism via production of essential dietary SCFA, amino acids, lipids and vitamins which, due to a lack of host digestive enzymes, are otherwise absent (Zhu et al., 2010). Disaccharides and simple sugars, such as lactose and glucose, are hydrolysed and absorbed in the small intestine by host metabolism. However, complex carbohydrates, also referred to as dietary fibre, are polysaccharide chains such as starch and cellulose that are indigestible by host metabolic enzymes due to the configuration of glycosidic linkages between oligomers (figure 1.2B). These carbohydrates reach the large intestine undigested where various intestinal microbiota, including *F. prausnitzii*, are equipped with a specialised range of enzymes capable of metabolising such compounds. Complex carbohydrates are metabolised into simple oligosaccharide and monosaccharides and then fermented, for energy harvest, into SCFA end-products such as propionate and formate, by the intestinal microbiota (figure 1.2A) (Tremaroli and Backhed, 2012).

Propionate, acetate and butyrate are the principle SCFA produced within the large intestine and provide some nutritional value to the host as well as influencing intestinal health. SCFAs traverse the intestinal epithelium via transporters such as monocarboxylate transporter 1



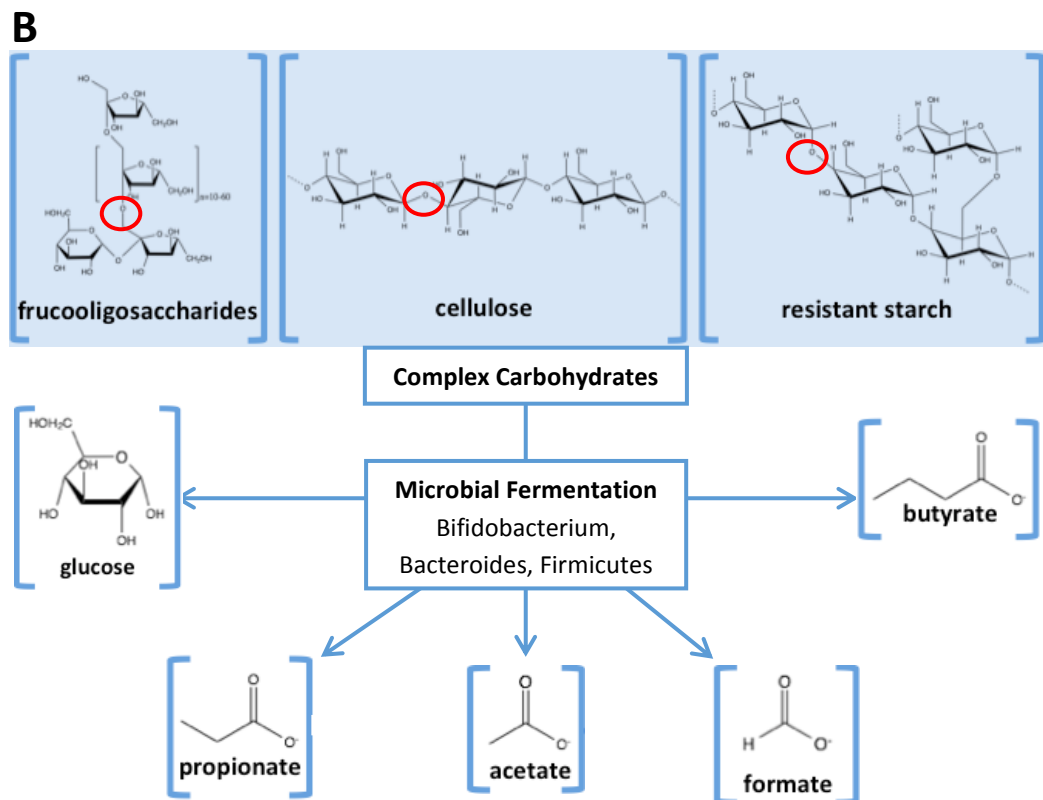
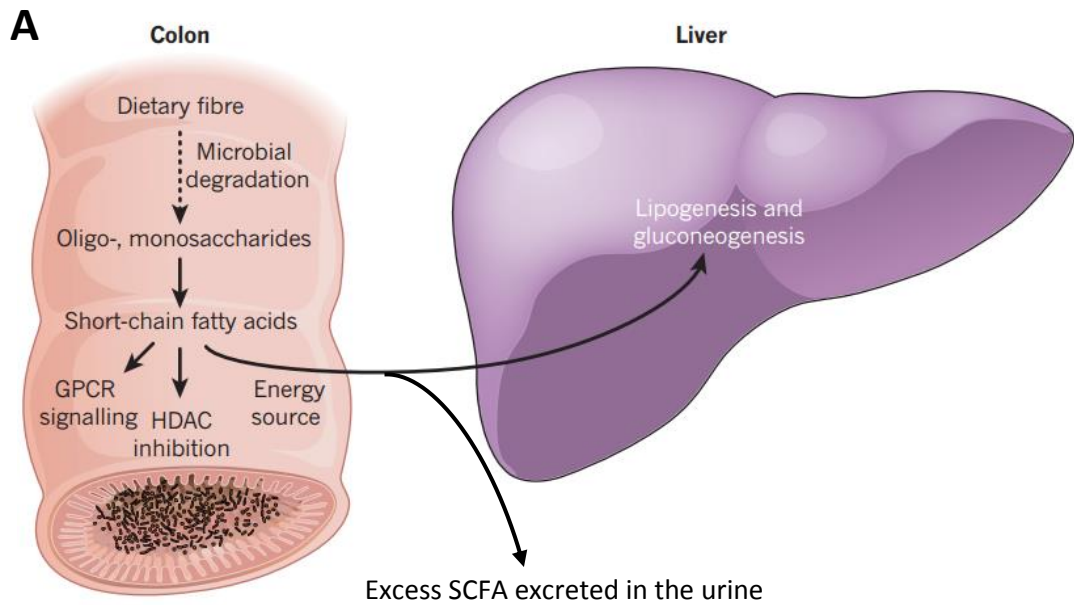


**Figure 1.2 – Intestinal microbiota-mediated metabolism of host dietary fibre.**

(A) Complex carbohydrates are first metabolised into oligo and monosaccharides then fermented into SCFAs by the intestinal microbiota where they serve a variety of functions both locally and on a systemic scale. Metabolites in excess are excreted in host urine. (B) Microbiota fermentation to produce SCFA end-products. Red circles depict glycosidic linkages indigestible by host metabolic capabilities.

*Figure adapted from Tremaroli and Backhed (2012).*

(MCT-1) where butyrate serves as an energy substrate for IECs whilst acetate and propionate function as substrates for gluconeogenesis and lipogenesis (figure 1.3) (den Besten et al., 2013). Additional mechanistic effects of SCFA have been suggested to influence host intestinal immunology and physiology. Such mechanisms are highlighted in figure 1.3 and discussed in relevant sections throughout.

In comparison to complex carbohydrates, there is limited research into microbiota-associated protein metabolism, likely due to the generally accepted opinion that all nine essential amino acids are provided by host diet. However, as research began to acknowledge the broad metabolic capability of the intestinal microbiome, investigative studies emerged demonstrating a role for microbiota-mediated *de novo* synthesis of amino acids. Studies employing a combination of radiolabelled carbon and nitrogen tracers with antibiotic treatments calculated the rate of microbiota contribution to leucine input to be up to 22% in healthy adults (Raj et al., 2008). Furthermore, a similar study identified lysine, proline and histidine contribution to be up to 21%, 41% and 52%, respectively (Metges, 2000). Furthermore, intestinal microbiota harbour proteolytic metabolic capabilities which promote catabolism of dietary protein into amino acids (Wallace, 1996). Dietary and microbiota derived amino acids are utilised for host and microbiota protein synthesis as well as modulating host nitrogen and energy balance in peripheral tissues (reviewed in Dai et al. (2011)).

As with most intestinal microbiota functions, early indications as to a role of the microbiota in host lipid metabolism was provided by comparison of GF mice with that of conventionally raised mice which found increased cholesterol and triglyceride levels in the serum of GF mice, indicative of decreased lipid clearance (Velagapudi et al., 2010). The intestinal microbiota have been identified to indirectly influence lipid metabolism via a variety of different mechanisms. Firstly, the intestinal microbiota are able to metabolise bile acids in the intestine that are responsible for emulsification, absorption and transport of dietary fats from the intestine to the liver. Deconjugation of bile acids by intestinal microbes delays absorption and enables further metabolism into secondary bile acids. A small portion of secondary bile acids that are absorbed into the periphery, act as ligands for the G protein-coupled receptor (GPCR), TGR5 which modulates systemic glucose and lipid metabolism via induction of glucagon-like peptide (GLP)-1 secretion (Thomas et al., 2009). Likewise, bacterial derived SCFAs are able to modulate host metabolism via localised signalling through GPCRs,

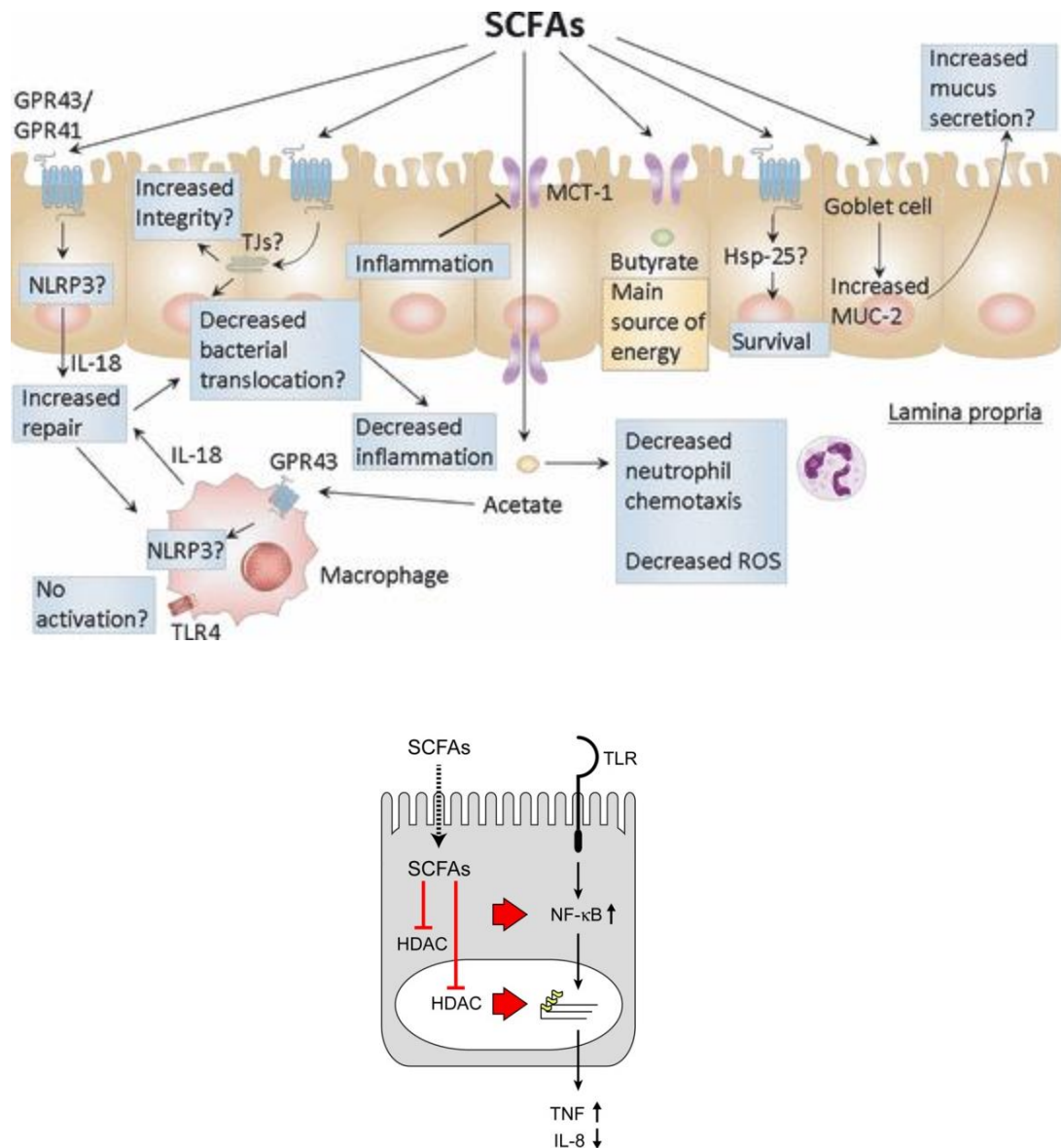


**Figure 1.3 – Mechanisms of SCFA influence on intestinal physiology and immunology.**

Microbiota derived SCFA metabolites are suggested to mediate host-microbiota and intestinal homeostasis via variety of mechanisms. SCFA IEC GPCR binding stimulates NLRP3-associated inflammasome formation, increased IL-18 secretion and fortification of immune responses. IEC MCT-1 regulate transport SCFA across the epithelial barrier where they influence chemotaxis of immune cells. Butyrate provides primary energy source for IECs. GPCR binding by SCFA upregulates heat shock protein-25 (Hsp-25) to promote cell survival and repair. SCFA stimulate mucin secretion, fortifying the mucosal barrier. SCFAs also inhibit HDAC activity resulting in histone hyperacetylation and modulation of gene transcription.

*Figures adapted from Macia et al. (2012) and Lin et al. (2015).*

GPCR41 and GPCR43 which also induce GLP-1 secretion (figure 1.3) (Tolhurst et al., 2012). On the other hand, choline, an important nutrient required for lipid metabolism and hepatic production of very-low-density lipoproteins (VLDLs), is metabolised by the intestinal microbiota into toxic trimethylamines. Trimethylamine is then further metabolised by the host in the liver to form trimethylamine-N-oxide which has been implicated in perturbation of cholesterol metabolism (Bennett et al., 2013).

Numerous essential vitamins including vitamin K, biotin, vitamin B12 and thiamine, are also produced by the intestinal microbiota, most notably by members of the genera *Clostridium*, *Bacteroides* and *Bifidobacterium* (Hill, 1997). In addition, various studies have demonstrated that indigenous microbiota are able to detoxify potentially damaging dietary compounds. For example, heterocyclic aromatic amines (HAA), produced during high-temperature cooking of meats, are implicated in the onset of colorectal cancer (CRC) (Helmus et al., 2013). Various species of *Lactobacillus* and *Bifidobacterium* directly bind to and alter the structure of HAAs, consequently reducing their mutagenicity (Stidl et al., 2008).

## **1.6 – Intestinal Homeostasis Modulated by the Intestinal Microbiota**

In addition to serving beneficial developmental, metabolic and protective functions within the host, the intestinal microbiota have been implicated in maintaining intestinal homeostasis. The intestinal epithelium is composed of a monocellular layer of intestine epithelial cells (IECs) arranged into specialised villi and crypts, referred to as the crypts of Lieberkuhn. To maintain intestinal health the IEC layer is continuously replenished by the division and differentiation of pluripotent intestinal epithelial stem cells (IESCs), residing at the base of crypts, into a range of functionally distinct IEC subsets (table 1.1; figure 1.4A). A state of intestinal homeostasis is achieved when the rate of IESC proliferation is equal to the rate of programmed cell death, via anoikis or apoptosis, thus maintaining cell numbers (Frisch and Francis, 1994). Early gnotobiotic experiments demonstrated the significant influence resident microorganisms have on intestinal homeostasis. For example, the rate of IEC turnover in GF mice was found to be significantly reduced as a result of decreased IEC proliferative activity, reduced rate of differentiation and upward migration within intestinal crypts and an overall decreased rate of IEC apoptosis (Abrams et al., 1963, Alam et al., 1994, Savage et al., 1981). Subsequent studies investigating the mechanisms underpinning such

observations have identified that microbial-mediated intracellular IEC signalling pathways serve a vital role in maintaining intestinal homeostasis (figure 1.4B) (Rakoff-Nahoum et al., 2004).

Differentiated Cell Type	Location and Abundance	Primary Function
Absorptive enterocytes	Distributed throughout the epithelium. Most abundant cell type in small intestine	Absorption of nutrients from the intestinal lumen
Goblet cells	Distributed throughout the epithelium. Increase in abundance in the colon and rectum.	Secretion of mucus into the intestinal lumen
Enteroendocrine cells	Represent <1% of cell numbers. Distributed throughout the epithelium	Secretion of a variety of hormones that impact gut motility and physiology
Paneth cells	Reside at the base of crypts below stem cell populations	Secretion of antimicrobial peptides for microbial regulation
Microfold cells (M cell)	Located above lymphoid Peyer's patches. Particularly rare cell type.	Selectively present microbial antigens to the underlying immune cells

**Table 1.1 - Differentiated cell types of the intestinal epithelium.**

*Table composed based on information presented in Barker et al. (2008) and Kucharzik et al. (2000).*

Conserved microbial molecular products such as lipopolysaccharide (LPS) and muramyl dipeptide (MDP) function as ligands for various pattern recognition receptors (PRRs) expressed on IECs. Microbial activation of different families of PRRs including, NOD-like receptor (NLR) and Toll-like receptor (TLR) families, provide distinct intracellular signals that promote and regulate homeostasis (figure 1.4B) (Hirota et al., 2011, Rakoff-Nahoum et al., 2004). The specificity of IEC PRRs for such highly conserved microbial ligands, provided the first indications that downstream functions of IEC signalling extend far beyond that of pathogen elimination. Since then, a variety of studies employing PRR signalling-deficient and antibiotic treated mice, have demonstrated the essential role of microbe-mediated IEC signalling in maintaining intestinal homeostasis. For example, broad-spectrum antibiotic treated mice as well as TLR-deficient mice were unable to recover from chemically induced colitis, using dextran sodium sulphate (DSS), whilst TLR2-deficient mice given oral doses of

LPS (a TLR4 ligand) were protected from mortality due to IEC repair and restored IEC homeostasis (Rakoff-Nahoum et al., 2004). Similarly, mice deficient in NLRP3, a member of the NLR family of receptors that oligomerise to form inflammasome complexes and initiate IL-18 release and immune activation, demonstrated an increased susceptibility to DSS-induced colitis as well as marked changes in the intestinal microflora, and reduced intestinal bactericidal capabilities (figure 1.3) (Hirota et al., 2011). Further studies have begun to elucidate the beneficial downstream effector mechanisms which influence intestinal homeostasis and have identified that such signalling pathways promote IEC survival and proliferation through expression of epidermal growth factor receptor (EGFR) ligands and trefoil factor 3 (TFF3; figure 1.4B) (Brandl et al., 2010, Taupin et al., 2000).

### **1.7 - Maintenance of Tolerance to Resident Microbiota**

Although the intestinal microbiota usually obtain a symbiotic relationship with the host, individual species are not necessarily benign, non-pathogenic microorganisms. Certain species, often referred to as pathobionts, reside within the intestinal microbiota but have the potential to establish infection or disease in particular environments. For example, *Clostridium difficile*, belonging to the Firmicutes phylum, comprises a small portion of the resident microbiota but can opportunistically induce pseudomembranous colitis following long term antibiotic therapy (Limaye et al., 2000). In addition, the vast antigenic nature of the intestinal microbiota paired with its residing proximity to the intestinal epithelium presents an enormous challenge to the host immune system. Given that the host immune system is specifically adapted to eliminate non-self cells, the intestinal microbiota pose a substantial threat of extensive immune activation. The host obtains several physiologic and immunologic defence mechanisms which serve to prevent adverse immunological responses to resident microorganisms.

Primary physiological defence mechanisms involve creating a physical barrier to attenuate direct contact between the intestinal microbiota and the underlying IECs. This is achieved through production of a mucus layer to the intestinal mucosa and formation of cell junctions which create tight, mostly impenetrable connections between IECs. The dense, gelatinous

mucus layer is formed via assembly of mucin glycoproteins into mesh-like polymers upon exocytosis from goblet cells (Johansson et al., 2008). The mucus layer in the large intestine is stratified and denser than that of the small intestine to account for the increased bacterial load. It consists of two layers and the innermost IEC-associated layer is firmly packed so largely devoid of bacteria (Johansson et al., 2008). The outer layer is less dense due to proteolytic degradation of mucin polymers by intestinal bacteria and is as a result inhabited by a vast number of microbes, known collectively as the mucosal-associated intestinal microbiota (Desai et al., 2016).

The small intestine has fewer goblet cells present in the epithelium and therefore does not harbour a stratified mucus layer. To prevent substantial bacterial penetration, as is observed in the colonic epithelium of mucin deficient mice, immunological and chemical barriers exist to maintain microbiota tolerance (Johansson et al., 2008). Immunoglobulin A (IgA) and antimicrobial peptides (AMPs) such as defensins are secreted by Paneth cells and IECs in the small intestine (figure 1.4A). AMPs are small cationic proteins which serve to modulate bacterial loads by non-specifically inducing cell lysis through a variety of killing mechanisms, including membrane disruption via pore formation (Brogden, 2005). Secretory IgA have a diverse repertoire for microbial specificity and which coat the cell surface of bacteria, upon transcytosis into the lumen by IECs, targeting them for destruction via phagocytic mechanisms (Kawamoto et al., 2014). IgA promotes diversification of the microbiota by limiting species predominance, particularly in the abundant Firmicutes phylum (Kawamoto et al., 2014).

A recent study has proposed a novel immune mechanism thought to support microbiota tolerance in the large intestine. A glycosylphosphatidylinositol (GPI)-anchored protein on the surface of IECs, referred to as Ly6/PLAUR domain-containing 8 (Lypd8), is released into the lumen during IEC turnover and favourably binds to flagellated microbes such as *Proteus mirabilis*, preventing bacterial invasion and translocation across the intestinal epithelium (Okumura et al., 2016). Mice absent of Lypd8 were found to harbour microbiota in the inner mucus layer as well as the presence of flagellated bacteria in the lamina propria, supporting a crucial role of Lypd8 in maintaining host-microbiota homeostasis (Okumura et al., 2016).

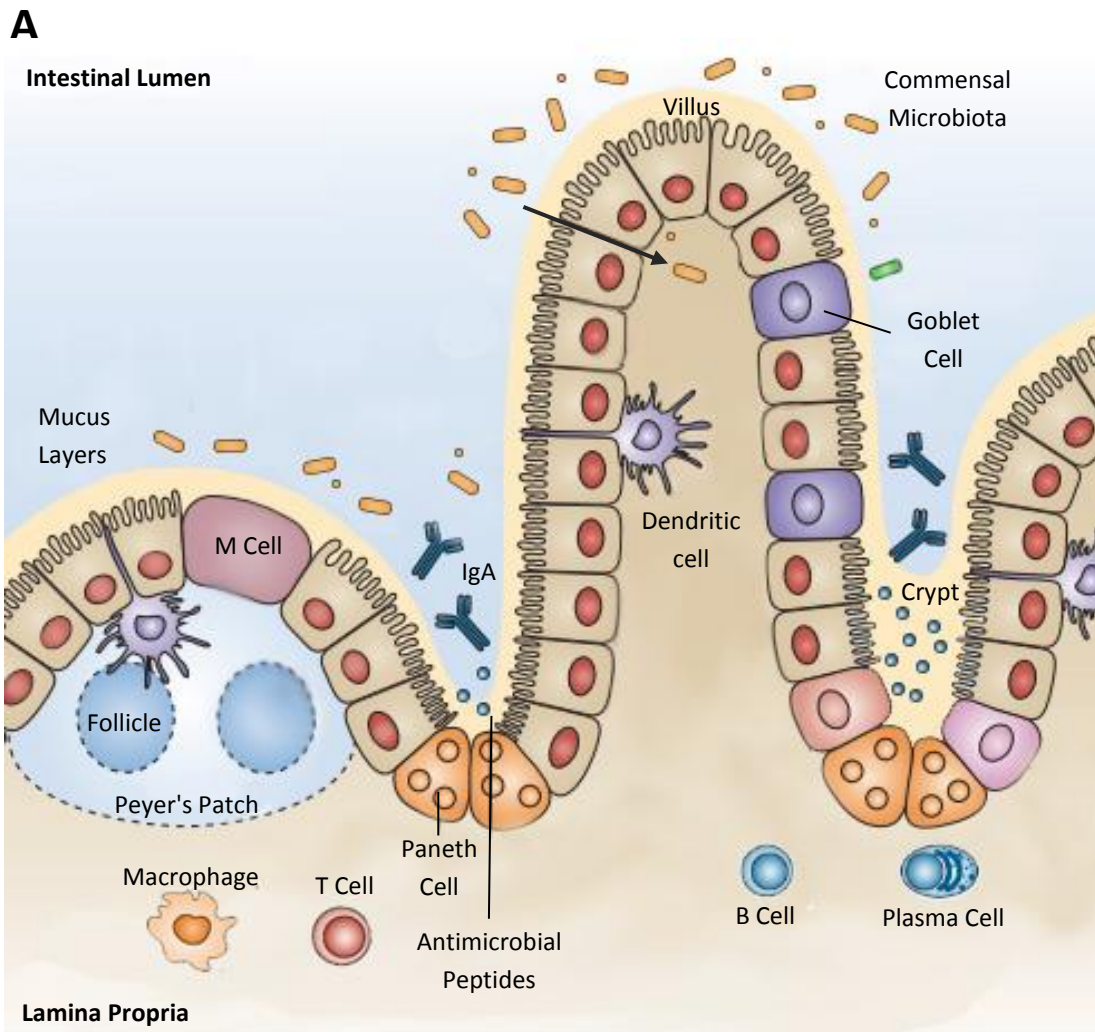


**Figure 1.4 A - Homeostatic tolerance mechanisms sustaining host health.** The single IEC layer presents a physical barrier separating the intestinal microbiota from the underlying lamina propria, rich in immune cells. A variety of host defence mechanisms function to prevent failure of this barrier and maintain host health. AMPs and IgA are secreted into the lumen by paneth and plasma cells, respectively, directly targeting commensal microflora to regulate abundance and prevent translocation. Goblet cells secrete mucin which coats the IEC layer and attenuates direct bacterial contact. A specialised subset of dendritic cells actively sample the lumen and promote immune cell differentiation and activation accordingly. Peyer's patches are organised lymphoid tissues which commit differentiation of B cells into IgA secreting plasma cells following antigen presentation and stimulation by the overlying M cells. These defence mechanisms and are mediated by a range of host-microbial interactions, particularly those which occur in the intestinal lumen following successful bacterial translocation (represented by bold black arrow).

*(Continued)*



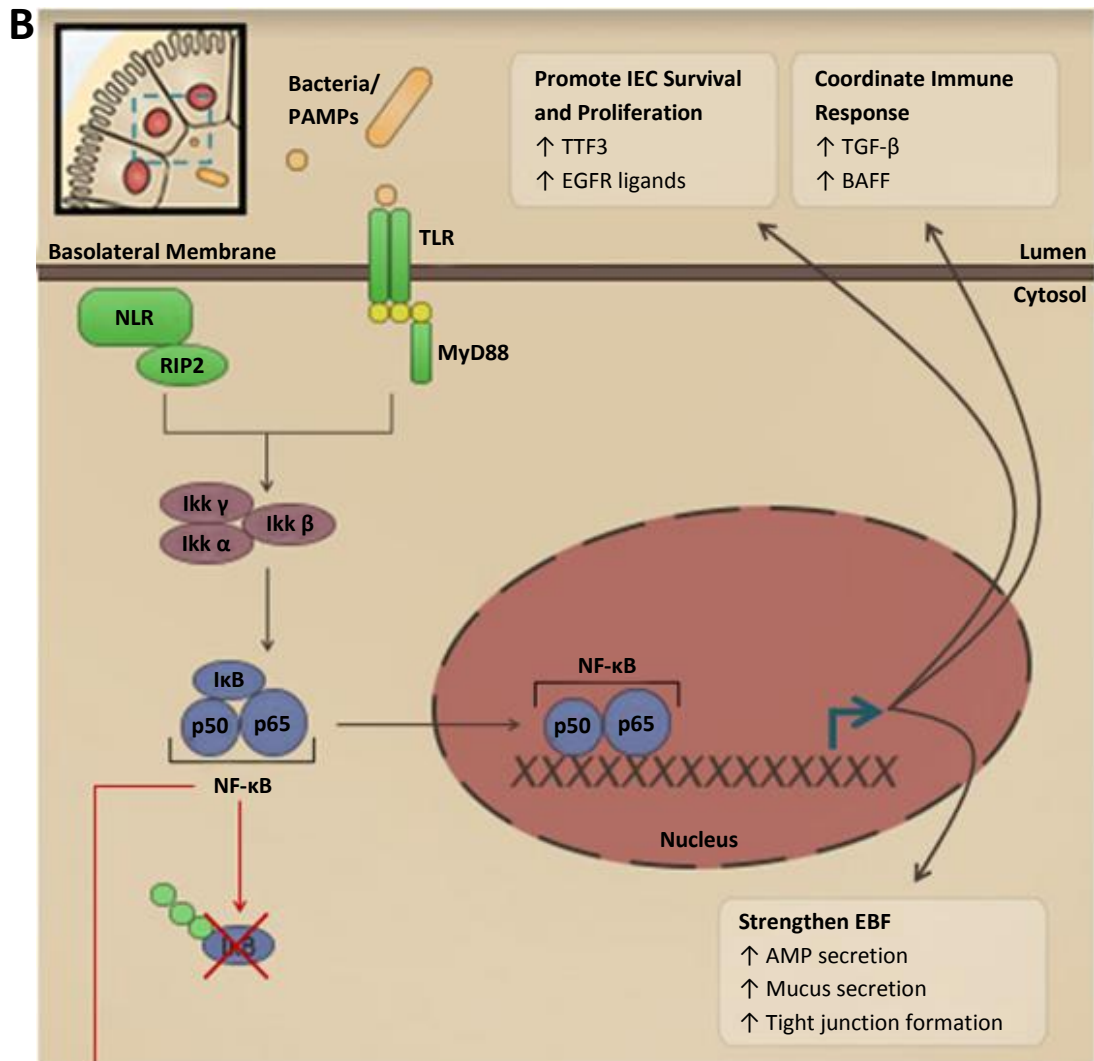


**Figure 1.4 (continued) B - Pattern recognition receptor signalling pathways in IECs promote intestinal health, in response to intestinal microbiota detection.** Recognition of bacterial products at the basolateral surface of the intestinal epithelium by TLRs, or in the cytosol by NLRs, triggers intracellular signalling cascades and activation of NF- $\kappa$ B. Expression of PRRs in IECs is polarised and aids differentiation between pathogens and commensals. Microbial activation at the apical IEC surface inhibits NF- $\kappa$ B translocation by targeting I $\kappa$ B for proteosomal degradation depicted in schematic using red arrow and cross. Blue arrow represents activation of NF- $\kappa$ B-associated gene transcription. Proliferation and survival of IECs is promoted via the production of EGFR ligands and TFF3, whereas the production of IgA is promoted by TGF- $\beta$  and BAFF synthesis. EBF is fortified by the increased secretion of mucus and AMP from goblet and paneth cells as well as an increase in tight junction formation. The blue dashed box highlights the location of such signalling events.

Figure composed based on information presented in Rakoff-Nahoum et al. (2004), Abreu (2010) and Peterson and Artis (2014).

A specialised subset of dendritic cells (DCs) are able to sample intestinal microbiota at different locations across the intestinal epithelium; the lamina propria and within organised lymphoid nodules referred to as Peyer's patches (figure 1.4A) (Rescigno et al., 2001, Lelouard et al., 2012). This sampling enables DCs to examine microflora located at the luminal side of the IEC surface and those which have penetrated the IEC surface, respectively. Bacterial activated DCs induce B lymphocyte differentiation into IgA secreting plasma cells which subsequently secrete bacterial specific IgA and promote swift clearance of penetrative microorganisms via phagocytic mechanisms (Lelouard et al., 2012).

The aforementioned physical, chemical and immunological barriers function concurrently in biological feedback processes to maintain intestinal microbiota-host homeostasis (figure 1.4B). Mucus secretion is stimulated by recognition of microbiota-derived metabolites such as butyrate and propionate by NLRs in the cytosol (figure 1.3) (Shimotoyodome et al., 2000). Whilst production of AMPs, tight junction expression and transcytosis of IgA is regulated by TLR and NLR signalling pathways on the basolateral membrane of the intestinal epithelium in addition to SCFA-mediated activation of GPCRs on IEC surface (figure 1.4B; figure 1.3) (Abreu, 2010, Rakoff-Nahoum et al., 2004). Furthermore, regulatory immune responses are co-ordinated by indirect expression of B cell activating factor expression (BAFF) and transforming growth factor- $\beta$  (TGF- $\beta$ ) to promote IgA synthesis and regulatory T cell activity (figure 1.4B) (Xu et al., 2007, Zeuthen et al., 2008). Therefore, increased bacterial infiltration and detection by PRRs subsequently escalates signalling cascades thus activating nuclear factor- $\kappa$ B (NF- $\kappa$ B) transcription factor and results in fortification of epithelial barrier function, increased IEC survival and immune response regulation (Abreu, 2010) (figure 1.4B).

## **1.8 – Intestinal Dysbiosis**

Under normal conditions the mechanisms discussed thus far maintain a state of homeostasis within the intestine and promote health of the human host. However, disruption of such mechanisms can pose severe pathological consequences. Intestinal dysbiosis is defined as a perturbation of the microbiota composition or abundance which usually promotes host health. Instead, dysbiosis often leads to a loss of host tolerance mechanisms and results in non-specific chronic inflammation. Dysbiosis is categorised by pathobiont expansion, commensal depletion and a reduction in overall diversity but often exists as a consequence

of all three deviations simultaneously. However, for the sake of clarity, each will be discussed as a separate entity and considered with associated immunological and clinical consequences.

Various intestinal microbiota have been branded as beneficial bacteria, or symbionts, as they promote host-microbiota homeostasis through a variety of different mechanisms which mitigate the host inflammatory response. For example, *Bacteroides fragilis* (*B. fragilis*) derived polysaccharide A (PSA) stimulates CD4+ T cells via TLRs which increases IL-10 levels and consequently suppresses inflammatory response mechanisms (Mazmanian et al., 2008). Furthermore, *Clostridia* strains from groups IV and XIVa stimulate Transforming Growth Factor- $\beta$  (TGF- $\beta$ ) release from IECs which promotes differentiation of regulatory T cells again suppressing inflammatory responses (figure 1.5) (Atarashi et al., 2013). Additionally, commensal *Lactobacillus paracasei* and *Lactobacillus casei* both produce lactocepin, a protease that degrades the inflammatory cytokine interferon gamma-induced protein 10 (IP-10) responsible for chemoattraction of lymphocytes (von Schillde et al., 2012). A loss of these symbionts defines dysbiosis and has been observed in clinical investigations of several dysbiosis-associated diseases. Notably, a reduction in *Clostridia* strains from groups IV and XIVa has been reported in the intestinal microbiota of inflammatory bowel disease (IBD) patients compared to healthy controls (Gophna et al., 2006). Furthermore, reductions in *Bacteroidetes* has been reported in the mucosal-associated microbiota of IBD patients (Frank et al., 2007). Symbiont decline wanes their protective mechanisms and generates a proinflammatory environment, creating an environmental niche which suits pathobionts (figure 1.5).

The abundance of pathobionts residing in the intestinal microbiota is usually controlled via host defence mechanisms and microbiota niche competition, as discussed. However, in various circumstances, expansion of such bacteria can occur contributing to disease pathology. Arguably the most frequently reported case of pathobiont expansion is that of the Enterobacteriaceae family and in particular *E. coli* and *Shigella* species. These flagellated bacteria have the ability to penetrate the inner mucus layer and intestinal epithelium and have been identified as increased in abundance in patients with IBD (Frank et al., 2007). An overgrowth of pathobionts leads to increased bacterial translocation and chronic stimulation

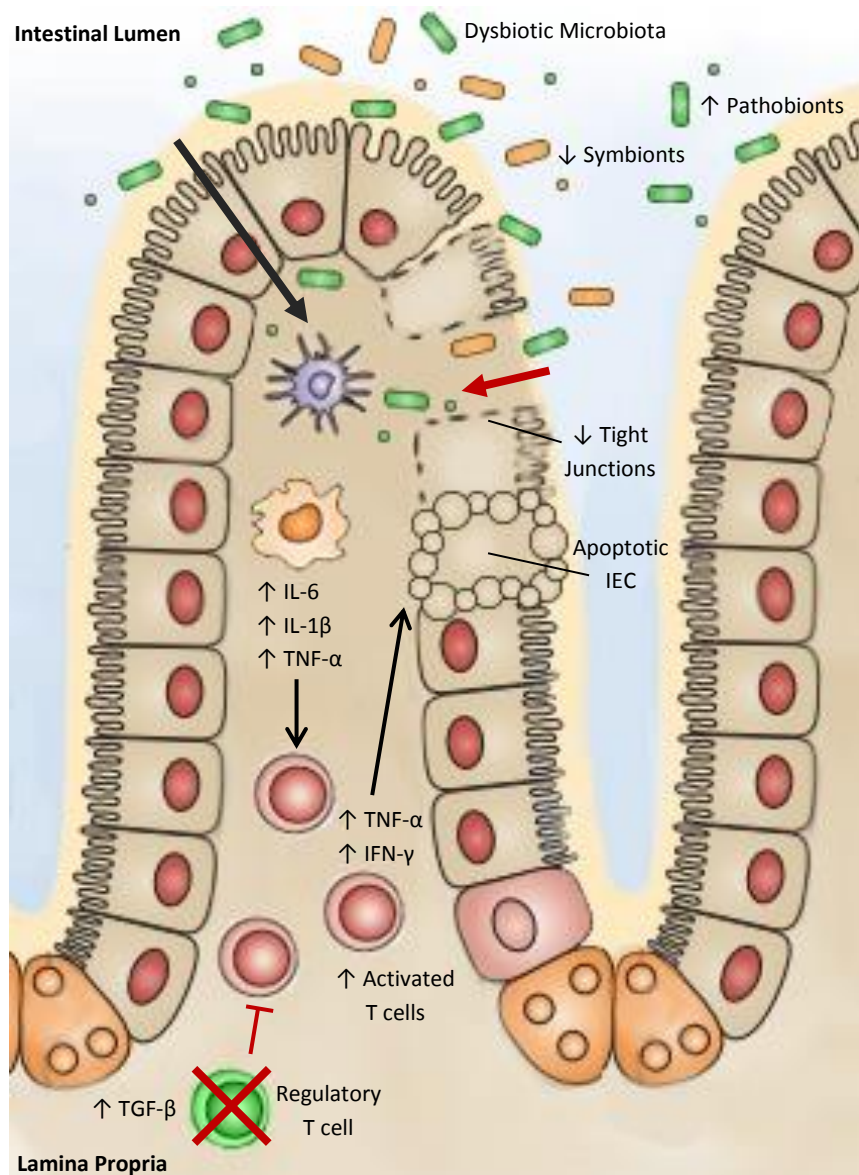


**Figure 1.5 - Loss of intestinal homeostasis associated with dysbiosis.** A depletion of symbionts, represented by bold red cross, prevents TGF- $\beta$  and PSA activation of regulatory T cells and IL-10 mediated suppression of inflammatory response mechanisms. Concurrent increased pathobiont expansion and translocation, as denoted with bold black arrow, leads to increased host-microbial basolateral interactions with chronic activation of IEC signalling and activation of innate immune cells. Subsequent proinflammatory cytokine expression recruits and activates T cells initiating a vast immune response. IFN- $\gamma$  and TNF- $\alpha$  expression lead to extensive immune cell recruitment, apoptosis of IECs and a loss of tight junctional complexes, respectively. Breakdown of intestinal homeostasis falls into a positive feedback loop due to the destruction of EBF and influx of microbiota, represented by bold red arrow.

Figure composed based on information in Su et al. (2013), Mazmanian et al. (2008) and Atarashi et al. (2013).

of TLR receptors on the basolateral IEC membrane and DCs in the lamina propria (figure 1.5). In response to activation, these immune cells secrete significant quantities of proinflammatory cytokines such as Tumour Necrosis Factor (TNF)- $\alpha$ , Interleukin (IL)-6 and IL-1 $\beta$  which stimulate effector T cell populations and induce substantial immune responses against the intestinal microbiota. It has been suggested that such immune responses fall into a positive feedback loops due to a consequential TNF- $\alpha$  and Interferon (IFN)- $\gamma$ -associated breakdown of epithelial barrier and increased translocation of resident microflora and associated products exacerbating the immune response (figure 1.5) (Su et al., 2013).

A depletion in microbiota diversity is the third defining feature of intestinal dysbiosis. As discussed, regulatory T cells are crucial in maintaining host-microbiota homeostasis. Gnotobiological studies identified that multiple species of *Clostridia* contribute to activation of regulatory T cells (Atarashi et al., 2013). However, this stimulation was abolished when colonised with single *Clostridia* species demonstrating the functional importance of less abundant commensal microbes. As with symbiont depletion and pathobiont expansion, reduction in intestinal microbiota diversity has been observed in IBD patients when compared to healthy controls demonstrating the functional decline of a diversity restricted microbiota (Willing et al., 2010).

A debate exists as to the cause or consequential role of dysbiosis in various associated diseases (reviewed in Butto and Haller (2016)). Understandably, the answer to such question will pose significant clinical implications, particularly if a causative relationship is established. However, considering the different features of dysbiosis, it is probable that disease connection is multifactorial. Logically, a loss of beneficial intestinal bacteria is likely to play a causative role with initiation in the attenuation of host tolerance mechanisms. This is likely later exacerbated by an outgrowth of pathobionts colonising a newly established, disease-associated niche within the intestine. Evidence to support this notion is provided by the observation that a loss of beneficial microbiota was observed in IBD patients regardless of active or remissive disease state, suggesting that it is not simply a reflection of inflammation but an underlying persistent issue (Gophna et al., 2006). Furthermore, familial IBD studies have demonstrated that pathobiont presence alone is not sufficient to induce disease, therefore a loss of beneficial microorganisms and microbiota diversity is also necessary

indicating a causative role for symbiont depletion and a consequential but detrimental role for pathobiont expansion (Joossens et al., 2011).

### **1.9 – Aetiology of Dysbiosis and Influence of Diet**

As is observed with intestinal microbiota development in early years, the aetiology of dysbiosis is highly multifactorial with factors such as genetics, lifestyle choices, medical practices and environmental exposures influencing microbiota composition (figure 1.6). These compound factors underpin dysbiosis by either depleting symbiont microorganisms or hindering host-microbiota tolerance mechanisms.

Genetic mutations in the NLR, nucleotide-binding oligomerisation domain protein 2 (NOD2), responsible for initiating AMP synthesis following commensal microbial stimulation, are implicated in 25-35% of all cases of Crohn's disease and have been shown to induce a state of immunodeficiency in the host (Economou et al., 2004). A range of genetic mutations, such as those which occur in the leucine rich regions (LLR) of the protein, alter the ability of NOD2 to recognise intracellular LPS and peptidoglycan fragments (Bonen et al., 2003). Such mutations therefore disrupt the ability of the immune system to monitor the intestinal microflora, rendering the host incapable of modulating microflora abundance and may consequently induce dysbiosis.

Although genetic factors undoubtedly play a vital role in the pathogenesis and aetiology of dysbiosis-associated diseases, it is becoming more apparent that genetic factors simply predispose certain individuals to disease by increasing sensitivity to fluctuations in the microflora. Instead, it is actually an array of environmental factors that directly alter microflora composition to induce dysbiosis and initiate disease. Evidence to support this notion is provided by various epidemiological and clinical studies which have reported a notable increase in the incidence of various dysbiosis-associated diseases, such as IBD and CRC, in developing populations, including India, Israel and China (Center et al., 2009). The rapid nature of the observed increase in disease incidence cannot be due to genetic factors alone and highlights the importance of environmental influences in dysbiotic disorders.

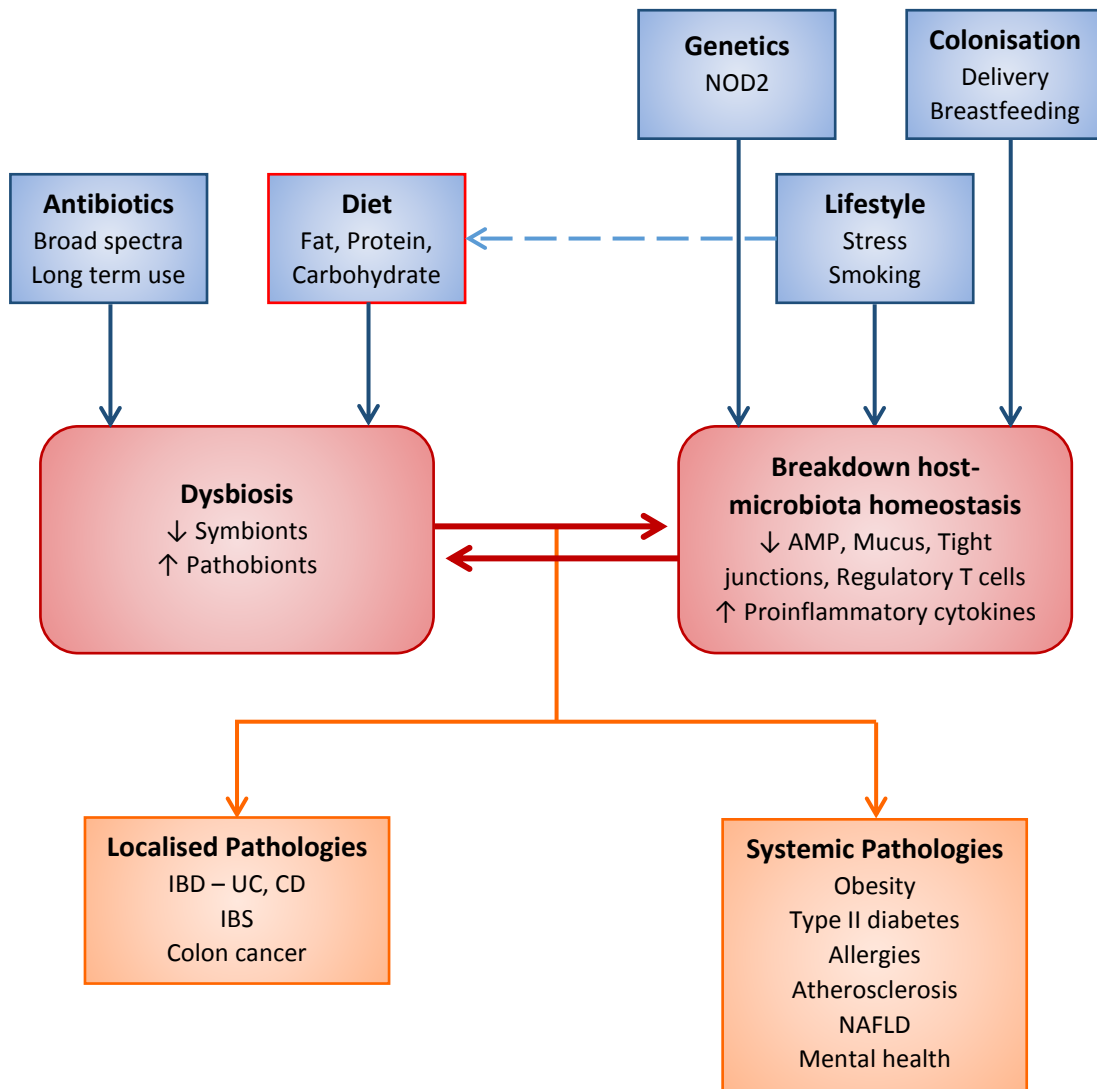


**Figure 1.6 – Aetiology of dysbiosis and associated diseases.**

The cause of intestinal dysbiosis is highly multifactorial with singular factors considered to predispose dysbiosis. Host genetics, lifestyle and colonisation in early years alter immunological and physiological host-microbiota homeostatic tolerance mechanisms whilst host diet and antibiotic use directly modulate microbiota composition. Lifestyle choices such as smoking and stress also indirectly alter the intestinal microbiota via influencing host diet, illustrated by blue dashed arrow. Diet is considered to be the most influential factor in dysbiosis as it directly modulates microbiota predominance on a frequent basis via composition of host dietary nutrients. A wide spectrum of dysbiosis-associated diseases have been identified and range from localised intestinal pathologies to more systemic disorders including obesity, allergies and schizophrenia.

Furthermore, migrant studies have shown that families emigrating from low incidence countries to Westernised regions with a high incidence of dysbiotic disorders can acquire diseases such as IBD, at a rate comparable to that of the native population, particularly in the case of migrant children (Pinsk et al., 2007).

Numerous environmental aetiological factors of dysbiosis have been identified and can be categorised into three primary groups; medical practices, lifestyle and diet (figure 1.6). Medical practices refer to an individual's historic and present use of therapeutics that have been linked to influencing intestinal dysbiosis. The most common and significant medicinal factor is undoubtedly antibiotic use. It is well understood that antibiotic therapies rapidly and non-specifically disrupt the diversity and abundance of intestinal microbiota and consequently impact on host health. For example, studies employing the use of broad spectrum antibiotics demonstrated that a significant disruption in the relative proportion of dominant phyla, Bacteroidetes and Firmicutes, with expansion of Proteobacteria occurs rapidly following first administration (De La Cochetiere et al., 2005). Furthermore, an association between antibiotic induced dysbiosis and disruption of intestinal homeostasis was identified in antibiotic treated mice. Significantly fewer IFN- $\gamma$  expressing regulatory T cells were identified in the lamina propria following antibiotic treatment, likely due to antibiotic-mediated destruction of symbionts and resultant pathobiont expansion dampening such anti-inflammatory mechanisms (Hill et al., 2010). Therefore, although the effects of short-term antibiotic use have been identified to stabilise naturally following use, long-term antibiotic exposure can both induce and sustain dysbiosis and has been associated with a significantly increased risk of developing dysbiotic-associated diseases such as Crohn's disease (De La Cochetiere et al., 2005, Card et al., 2004).

The intestinal microbiota is also defined by the major macronutrient components of host diet (table 1.2). Differences in intestinal microbiota profiles are reported in different types of diet, such as those associated with geographical locations or vegetarianism. Such observations are accountable to differences in predominating macronutrients: fats, proteins and carbohydrates. Transient alterations are observed in the intestinal microbiota with each predominant macronutrient as a consequence of complementary or contrasting bacterial metabolic capabilities. Increased complex carbohydrates, such as dietary fibre, results in an



increase in butyrate-producing microbiota capable of dietary fibre fermentation, whilst microbes with alternative metabolic preferences decline (De Filippo et al., 2010). This microbiota profile is often observed in vegetarians due to a high carbohydrate and low protein and fat diet (Liszt et al., 2009). Alternatively, a diet rich in protein increases microbiota with proteolytic capabilities which often results in a concomitant decline of butyrate-producing populations due to associated reduction in carbohydrate intake (Russell et al., 2011). A fat rich diet causes an increase in bile acid production which favours the expansion of bile acid metabolising microbiota whilst also reducing *Lactobacillus* populations through bactericidal activity (Islam et al., 2011). Furthermore, dysbiotic shifts in microbial abundance, including decreases in several *Bacteroides* species and significant overgrowth of members of the Firmicutes phyla, were reported in mice following transfer to a high sugar, high fat, 'Westernised' diet (Turnbaugh et al., 2006).

<b>Macronutrient Composition</b>	<b>Intestinal Microbiota Composition</b>	<b>Reference</b>
<b>Fat rich</b>	Increased <i>Bacteroides</i> Decreased <i>Bifidobacterium</i> and <i>Lactobacillus</i>	Islam et al. (2011)
<b>Carbohydrate rich</b>	Increased fermenting species – <i>Clostridium</i> cluster XVIII, <i>F. prausnitzii</i> and <i>Prevotella</i> Decreased <i>Bifidobacterium</i> , <i>Lactobacillus</i> and <i>Enterobacteriaceae</i>	De Filippo et al. (2010)
<b>Protein rich</b>	Decreased butyrate producing species – <i>Clostridium</i> cluster XIV, <i>F. prausnitzii</i> , <i>Bifidobacterium</i> and <i>Lactobacillus</i>	Russell et al. (2011)
<b>High-fat, high-sugar – 'Westernised diet'</b>	Increased <i>Enterococcus</i> and <i>Clostridium</i> Decreased <i>Bacteroides</i>	Turnbaugh et al. (2006)

**Table 1.2** – Macronutrient influence on Intestinal Microbiota Composition.

Several lifestyle choices have also been implicated in underpinning dysbiosis (figure 1.6). For instance, the mechanistic links between cigarette chemicals and intestinal disorders are well documented (reviewed in Birrenbach and Bocker (2004) and Liang et al. (2009) for IBD and CRC respectively), but only relatively recently has the effects of smoking on the intestinal microflora been suggested. Cessation of smoking in 15 healthy individuals was found to induce profound shifts in microbial populations, notably an increase in the number of Firmicutes and a decrease in Proteobacteria was observed (Biedermann et al., 2014). Studies have previously concluded that this observation suggests smoking directly influences dysbiotic microbial shifts in the intestine that may consequently induces disease pathogenesis. However, it should also be noted that cessation of smoking is linked to

increased hunger and eating, particularly high-fat, high-sugar foods (Hughes and Hatsukami, 1986). It is therefore more probable that smoking cessation indirectly modifies the intestinal microbiota via altered host diet.

Neuro-emotional stress has also been linked to intestinal dysbiosis with early studies demonstrating altered microbiota composition in Soviet cosmonauts with temporal reductions observed in faecal *Lactobacillus* and *Bifidobacterium* species (Lizko, 1987). Stress has been shown to increase hormone levels such as cortisol, which stimulate intestinal motility and thus clearance of predominant intestinal microbiota populations (Nakade et al., 2007). Furthermore, stress has been linked to decreased secretory IgA levels and dampened mucus secretion that subsequently supports growth of pathobionts (Drummond and Hewson-Bower, 1997, Lizko, 1987). However, similarly to smoking cessation, individuals enduring long periods of stress are more likely to make poor dietary choices, opting for convenience or comfort foods that are high in fat and refined sugars and will often overeat due to a hormonal dysregulation of appetite (Sinha and Jastreboff, 2013). Furthermore, the Soviet cosmonaut study failed to consider space-associated dietary restrictions (Lizko, 1987). Therefore, whilst stress directly hinders host-microbiota homeostatic tolerance mechanisms via the mechanisms described, it is also likely to indirectly modify the intestinal microbiota composition through altered macronutrient intake.

Despite many years of investigation, none of the factors discussed thus far can be held entirely accountable for development of dysbiosis. In fact, that majority of cases of dysbiosis are thought to occur as a result of exposure to a combination of causative factors which collectively induce major shifts in microbial profiles and attenuate host-microbiota homeostasis. However, host diet is becoming increasingly recognised to be the most significant environmental causative factor for dysbiosis. This is because it is the major variable factor that directly encounters the intestinal microflora on a frequent basis. Experimental support for this notion was provided by a comparative study which evaluated the relative influences of host genetics and diet on microbial composition in mice and subsequent metabolic syndrome complications. It was concluded that changes in dietary factors accounted for 57% of the total variation in gut microbiota, whilst less than 12% was due to underlying genetic mutations (Zhang et al., 2010).

### 1.10 – Intestinal Microbiota in Dysbiosis-associated Diseases

Intestinal dysbiosis has been associated with underpinning the pathogenesis of numerous chronic and degenerative diseases, ranging from various localised disorders such as IBD and CRC to more systemic pathologies including atherosclerosis, various mental health disorders and obesity (figure 1.6).

Dysbiosis-associated pathologies localised within the intestine have understandably received the most attention in attempts to elucidate causative mechanistic interactions. IBD is a class inflammatory conditions of the intestine that have been associated with a loss of symbiotic intestinal microbiota and their SCFA metabolites. Research has also investigated the potential of a singular causative pathogen for IBD onset with studies suggesting *Mycobacterium avium paratuberculosis* and *Clostridium difficile* as environmental infectious agents for IBD subgroups Crohn's disease (CD) and Ulcerative colitis (UC) (Pierce, 2010, Clayton et al., 2009). However, a lack of direct evidence to support these studies has led to scepticism regarding a one-disease-one-microbe theory. Instead, depletion of butyrate-producing microbiota and a concomitant increase in pathobionts have been implicated in breakdown of epithelial barrier function and induction of inflammation in the intestine (as detailed in section 1.8) (Frank et al., 2007). The same pattern of dysbiosis is also reported in CRC patients, with reduced SCFA producing microbiota and increased in *Enterobacteriaceae* pathobionts (Sobhani et al., 2011). A mouse model demonstrated a protective role for butyrate in CRC as administration to genetically susceptible mice fed on a high fat diets, typically associated with decreased SCFA production, led to a significant decrease in the occurrence of tumours (Schulz et al., 2014).

Similar to IBD and CRC, obesity has also been linked to dysbiosis but with a high fat and high sugar, 'Westernised' diet-associated microbiota. Most notably, a disrupted Bacteroidetes to Firmicutes ratio, in favour of Firmicutes, is frequently reported with an overall decrease in microbiota diversity (Turnbaugh et al., 2009). This characteristic microbiota has an increased metabolic capacity for energy harvest with a significantly enriched genomic repertoire to that of lean individuals. In addition, a high fat diet is linked to increased chylomicron lipid transporters in the intestine that indirectly facilitate absorption of bacterial derived LPS across the epithelium resulting in activation of innate immune responses. This process,

referred to as metabolic endotoxemia, is considered to cause low-grade chronic inflammation, often reported in obese patients and perpetuate disease pathology (Cani et al., 2007).

The metabolic functionality of the intestinal microbiota is associated with additional systemic pathologies, including atherosclerosis. The influence of the microbiota on host lipid metabolism, as discussed in section 1.5, is mediated through catabolism of bile acids into secondary bile acids. In peripheral organs and tissues, primary bile acids bind to farnesoid X receptors (FXRs) to negatively regulate bile-acid synthesis, whilst secondary bile acids bind to TGR5 and promote energy expenditure and maintain glucose homeostasis (Sinal et al., 2000, Thomas et al., 2009). A loss of bile acid metabolising populations, such as species of *Clostridia*, during dysbiosis can reduce the production of secondary bile-acids, concomitantly increasing the absorption of primary bile acids into the bloodstream and consequently creates excess levels of cholesterol due to a reduction in bile acid synthesis. In addition, FXR signalling exerts anti-homeostatic effects on endothelial cells, macrophages and vascular smooth muscle cells which collectively renders the host susceptible to atherosclerotic lesions and plaque formation (reviewed in Mencarelli and Fiorucci (2010)). Furthermore, an altered intestinal microbiota composition and its potentially increased capacity to metabolise choline into trimethylamines has been shown to have important implications in the onset of non-alcoholic fatty liver disease (NAFLD) as demonstrated in mice on a high fat diet (Dumas et al., 2006). Microbiota-mediated decreased choline bioavailability is suggested to cause a NAFLD characteristic accumulation of triglycerides in the liver due to impaired production of phosphatidylcholine production, responsible for triglyceride assembly to form VLDL and subsequent clearance from the liver (Dumas et al., 2006).

The intestinal microbiota have also been implicated in numerous mental health disorders primarily through metabolite-mediated influence of the central nervous system (CNS), via the gut-brain axis (GBA). Microbial derived products such as SCFA have neurotoxic effects which influence behaviour and brain development. Propionate produced by the intestinal microbiota is able to cross the blood brain barrier and influence behaviour in adolescent rats consistent with that observed in autism spectrum disorders (MacFabe et al., 2011). Furthermore, SCFAs are natural inhibitors of histone deacetylases (HDACs) which regulate

gene expression via modulation of DNA coiled histone proteins (figure 1.3). A dysbiosis-associated decrease in SFCA production causes an excess of HDAC expression which consequently alters gene expression and has been implicated in schizophrenia (Kurita et al., 2012). Administration of HDAC inhibitors have been shown to resolve schizophrenia-associated behavioural phenotypes, such as 'head-twitch', in mice (Kurita et al., 2012). However it should be noted that such research remains in its infancy and the full functional and mechanistic influences of intestinal microbiota on host mental health remain yet to be comprehensively elucidated.

Returning to localised-associated pathologies, irritable bowel syndrome (IBS) is a heterogeneous functional disorder of the intestine that does not have an observable pathology and has been associated with a dysbiotic microbiota. A typical microbiota has not been reliably identified in IBS patients, but increased temporal instability of predominant populations with overgrowth of aerobic organisms has been reported (Maukonen et al., 2006). Likewise to mental health disorders the microbiota is considered to influence IBS through the GBA in mechanisms largely related to stress-associated cortisol release and altered intestinal motility (Nakade et al., 2007). Furthermore, studies have identified that the intestinal microbiota of IBS patients have an altered fermentation capacity resulting in increased hydrogen gas production and this has been suggested to underpin the significant bloating observed in IBS patients (Tana et al., 2010).

### **1.11 – Defining a Characteristic Dysbiotic Intestinal Microbiota**

Despite extensive attempts to clarify dysbiosis and how such profiles modulate associated diseases, the findings from such research, although essential to improving our understanding of dysbiosis, remain yet to be translated into suitable therapeutic or diagnostic procedures. One major factor limiting such development is the variation in microbial profiles between species commonly utilised in models of dysbiosis and that of the human host. A comparative meta-analysis of the core gut microbiome between mice and humans demonstrated that although a considerable number of genera were shared, there were distinct quantitative differences in their relative abundance between the two species (Krych et al., 2013). Attempts to overcome this issue included the development of a mouse model referred to as human flora-associated (HFA) mice. This model involves inoculating GF mice with human

faeces and is considered to support a stable ecosystem representative of the human microbiota (reviewed in Hirayama and Itoh (2005)). However, it has also been reported that various genera which comprise a large portion of the human microbiota, such as *Lactobacilli* and *Bifidobacteria*, are lost upon transfer into the mouse intestine (Corpet, 2000). Therefore, although studies employing animal models have proved useful in identifying key physiological mechanisms that are influenced by the microbiota, the inability to extrapolate these findings directly to humans has significantly hindered clinical progression. Similar issues are also encountered in studies employing human participants. The considerable number of genetic and environmental factors, which contribute to intestinal dysbiosis, vary significantly between individuals and thus impedes the ability to perform interpatient comparisons during attempts to accurately profile the intestinal microflora. One study, extensively profiling just three individuals, noted substantial variations in presence of Bacteroidetes phylotypes (Eckburg et al., 2005), highlighting the difficulty in characterising a 'typical' microflora. Future research to design and evaluate robust scientific methods that can control for interpatient variability will aid in defining dysbiosis.

### **1.12 - Intestinal Microbiota Modulation: Aiming for Rebiosis and Implications for Therapies**

Given the pivotal role of the intestinal microbiota in the onset and pathogenesis of numerous disease, modulation of the microbiota utilising pre and probiotics are logical practices to restore and maintain host health. Prebiotics are rather generically defined as 'non-digestible food ingredients that, when consumed in sufficient amounts, selectively stimulate the growth and/or activity(ies) of one or a limited number of microbial genus(era)/species in the gut microbiota that confer(s) health benefits to the host' (Roberfroid et al., 2010). Probiotics on the other hand are defined as 'live organisms which, when administered in adequate amounts, confer a health benefit to the host' (FAO/WHO, 2002). Simply, the overall aim of pre and probiotic use is to inflate the beneficial effects of symbiotic intestinal microbiota, thus promoting host health.

*Lactobacilli* and *Bifidobacteria* are two bacterial genera that have received a lot of research focus and are therefore recognised to benefit health via mechanisms discussed throughout. Such beneficial microbiota are often used in combination, termed poly-biotics, to exploit complementary differences in bacterial functionality. For example, VSL#3 contains over 450 billion bacteria from 8 different strains, 7 of which are members of *Lactobacilli* and *Bifidobacteria* genera and is the most heavily dosed probiotic on the market (table 1.3; WWW, VLS#3 Polybiotic Food Supplement). It has been clinically proven to be therapeutically valuable in alleviating intestinal disease symptoms, including IBD and IBS by altering the composition and thus functionality of the intestinal microbiota (Tursi et al., 2004, de Boer et al., 2012).

<b>Poly- or Probiotic</b>	<b>Contributing bacterial species</b>	<b>Dose</b>
<b>VSL#3</b>	<i>Bifidobacterium breve</i> , <i>B. longum</i> , <i>B. infantis</i> , <i>Lactobacillus paracasei</i> , <i>L. acidophilus</i> , <i>L. delbrueckii subsp. Bulgaricus</i> , <i>L. plantarum</i> and <i>Streptococcus thermophiles</i> .	$4.5 \times 10^{11}$
<b>Symprove</b>	<i>Lactobacillus rhamnosus</i> , <i>L. acidophilus</i> , <i>L. plantarum</i> and <i>Enterococcus faecalis</i> .	$1.0 \times 10^{10}$
<b>Actimel</b>	<i>Lactobacillus casei</i>	$1.0 \times 10^{10}$
<b>Yakult</b>	<i>Lactobacillus casei</i>	$6.5 \times 10^9$

**Table 1.3** – Composition and dose of reputable poly-biotics and probiotics.

*Table composed based on information presented on WWW, VLS#3 Polybiotic Food Supplement.*

Conversely, common prebiotics include lactulose, inulin and oligofructose which function to promote the beneficial activities of symbiotic microbes. Oligofructose and inulin are naturally occurring polysaccharides present in plant foodstuffs that when artificially substituted into the host diet can influence both the intestinal microbiota composition and metabolic activity. Selective increases in *Bifidobacteria* and concomitant reductions in *Staphylococci* and *Streptococci* were observed in faecal microbial profiles following oligofructose and inulin administration. In addition, breath analysis revealed greater quantities of hydrogen and methane were excreted with prebiotic use, indicating an increase in carbohydrate fermentation and production of beneficial SCFAs (Gibson et al., 1995). Furthermore, lactulose has been clinically demonstrated to avert clinical complications of liver disease by upregulating metabolic activity of *Bifidobacteria* populations. *Bifidobacteria*-mediated lactulose metabolism lowers the pH within the intestine and converts gaseous ammonia into salt form which is excreted. This process consequently draws ammonia from

the liver and prevents hepatic encephalopathy onset which occurs as a result of accumulated ammonia crossing the blood brain barrier (Prasad et al., 2007).

One major limitation of pre and probiotic use is the temperamental nature of such beneficial effects, thus requiring long term administration. A relatively novel method for achieving intestinal rebiosis as a potential therapeutic for various diseases is faecal microbial transplantation (FMT). FMT involves broad antibiotic depletion of the intestinal microbiota of a diseased individual and subsequent oral or enema administration of intestinal microbes, obtained from healthy donor faeces, in large doses to the intestine. FMT has proven highly efficacious at treating recurrent *Clostridium difficile* infection, repeatedly restoring microbiota and host health in over 90% of patients over long periods (van Nood et al., 2013). A revolution in therapeutics for dysbiosis-associated diseases was anticipated with FMT following such impressive initial clinical outcomes. However, subsequent studies investigating the efficacy of FMT at inducing remission in UC and CD patients have been highly varied (Moayyedi et al., 2015, Paramsothy et al., 2017). Investigations to improve and standardise several confounding variables such as donor-recipient match criteria and sample collection and processing, in addition to number of donors and donor species are ongoing meaning FMT continues to hold promising future implications for treatment of dysbiosis-associated diseases (Moayyedi et al., 2015, Paramsothy et al., 2017).

In addition to being targeted for therapeutic potential, the intestinal microbiota have been implicated in determining the efficacy of numerous treatments. For example, the use of VSL#3 poly-biotic dually administered with reduced-doses of balsalazide was identified to be more efficacious in treating ulcerative colitis than balsalazide or mesalazine drugs alone suggesting the presence of anti-inflammatory host microbes can strengthen drug anti-inflammatory mechanisms (Tursi et al., 2004). However this study did not test sole administration of VSL#3 and so improved efficacy could be a direct result of enhanced microbiota composition rather than microbiota-drug associations. Moreover, intestinal microbiota impact the immunomodulatory effects of chemotherapeutics in the treatment of various cancers. A study by Lehouritis et al. (2015) investigated various bacteria and cancer cell lines both *in vitro* and *in vivo* for influences on the efficacy of 30 chemotherapeutic agents. In total, 30% of the drugs were identified to be significantly attenuated by *E. coli* and



*Listeria welshimeri* whilst 20% were improved by the same microbes and 50% were unaffected in cell toxicity assays. Furthermore, in vivo studies replicated such findings with tumours supporting *E. coli* growth and reduced toxicity of gemcitabine in the presence of *E. coli* (Lehouritis et al., 2015). This research indicates the potential future direction towards personalised medicines to accommodate individuality in the intestinal microbiota as well as potential modulation of microbiota composition to improve drug efficacy.

The principle of intestinal microbiota modulation is based upon the therapeutic potential of inducing rebiosis. Research thus far has presented substantial developments and breakthroughs in the treatment of dysbiosis associated diseases by targeting or utilising microbiota, however due to socioeconomic issues, prevention of disease is always better than cure. Given that dysbiosis is recognised as a major causative factor in numerous associated pathologies, perhaps research should be focusing on investigating novel techniques to enable detection or diagnosis of dysbiosis rather than merely acting upon clinical manifestation.

### **1.13 Research Aims:**

The intestinal microbiota is the most abundant, diverse and complex microbial ecosystem residing within the human host. A range of host- and microbiota-mediated immunological and physiological mechanisms have evolved to establish a mutualistic existence, but disruption of such mechanisms poses severe pathological consequences. Intestinal dysbiosis is associated with numerous chronic and degenerative diseases and therapeutics have therefore targeted the microbiota for rebiosis. However, clinical progression of such therapeutics is limited, mostly due to substantial individual variability in microbiota composition and lack of a characteristic profile of dysbiosis.

To advance understanding of the role of intestinal microbiota in health and disease this project aimed to employ two novel human models, in loop ileostomy patients and IBD patients, to achieve the following:

- Investigate dysbiosis as a causative factor of disease utilising a novel human model in loop ileostomy patients.
- Explore mechanisms by which different microbiota profiles impact upon physiology of the intestine utilising a novel human model of dysbiosis.
- Investigate the relationship between intestinal microbiota profiles and metabolites excreted in human urine, with regard to potential clinical application to complement diagnosis of dysbiosis-associated diseases.

## **Chapter 2:**

### **Materials and Methods**

## 2.1 - Materials

### 2.1.1 - Reagents

Reagent/Product	Supplier	Catalogue Number
QIAamp® <i>cador</i> ® Pathogen Mini Kit	Qiagen	54104
QIAamp® UCP Pathogen Mini Kit	Qiagen	50214
QIAamp® DNA Stool Mini Kit	Qiagen	51504
Pathogen Lysis Tube S	Qiagen	19091
MiniElute™ PCR Purification Kit	Qiagen	28004
Buffer ATL	Qiagen	19076
Proteinase K	Qiagen	19131
PowerClean® Pro DNA Clean-up Kit	MoBio Labs	12997
3-Aminopropyltriethoxysilane (APES)	Sigma Aldrich	440140
Bovine Serum Albumin (BSA)	Sigma Aldrich	A3294
Triton X-100	Sigma Aldrich	T8787
Tri-sodium citrate dihydrate	Sigma Aldrich	S1804
Goat Serum	Sigma Aldrich	G9023
PAP pen	Sigma Aldrich	Z377821
Click-iT® Plus TUNEL Assay for In Situ Apoptosis Detection, Alexa Flour® 594,	ThermoFisher Scientific	C10618
REDTaq® ReadyMix™ PCR Reaction Mix	Sigma Aldrich	R2523
Ammonium Persulfate (APS)	Sigma Aldrich	A3678
N,N,N',N'-Tetramethylethylenediamine (TEMED)	Sigma Aldrich	T7024
SYBR® Gold Nucleic Acid Gel Stain (10,000x)	ThermoFisher Scientific	S11494
SYBR® Green JumpStart™ Taq ReadyMix™	Sigma Aldrich	S4438
XL1-Blue Subcloning-Grade Competent Cells	Agilent Technologies	200130
SOC Outgrowth medium	New England BioLabs	B9020S
Low Salt Luria Broth	Duchefa Biochemie	L1705
GeneJET Plasmid Miniprep Kit	ThermoFisher Scientific	K0503
DUS 10 Reagent Strips for Urinalysis	Dream Future Innovation Co Ltd	3064
Sodium Azide	Sigma Aldrich	S2002
Deuterium oxide (D <sub>2</sub> O)	Sigma Aldrich	435767
Deuterated (Trimethylsilyl)-propionic-2,2,3,3-d <sub>4</sub> acid sodium salt (TSP-d <sub>4</sub> )	Sigma Aldrich	269913
Potassium Phosphate	Sigma Aldrich	P9791

**Table 2.1** – Reagents and products with supplier details.

### 2.1.2 - Antibodies

Antibody	Manufacturer	Catalogue Number	Source	Concentration	Working Dilution
anti-PCNA (PC10) primary antibody	Life Technologies	13-3900	Mouse	500 µg/ml	1:350
anti-mouse (H+L) Alexa-Fluor® 488 IgG	Life Technologies	A-11001	Goat	2 mg/ml	1:1000
Normal Mouse IgG	Santa Cruz	sc-2025		200 µg/0.5ml	1:20
Hoechst 33342 Nucleic Acid Stain	Life Technologies	H3570		10 mg/ml	1:1000

**Table 2.2** – Antibodies with working concentrations and supplier details.

### 2.1.3 - PCR Primers

Primer	Sequence	Product Size (bp)	Refs
<b>Universal</b> 926F + 1062R	<b>F:</b> 5'-AAACTCAAAGGAATTGACGG-3'	180	Bacchetti De Gregoris et al. (2011)
	<b>R:</b> 5'-CTCACRRCACGAGCTGAC-3'		
<b>γ-Proteobacteria</b> 1080γF + γ1202R	<b>F:</b> 5'-TCGTCAGCTCGTGTGTGA-3'	170	
	<b>R:</b> 5'-CGTAAGGGCCATGATG-3'		
<b>Bacteroidetes</b> 798cfbF + cfb967R	<b>F:</b> 5'-CRAACAGGATTAGATACCCT-3'	240	
	<b>R:</b> 5'-GGTAAGGTTCTCGCGTAT-3'		
<b>Firmicutes</b> 928F-Firm + Firm1040R	<b>F:</b> 5'-TGAAACTYAAAGGAATTGACG-3'	200	
	<b>R:</b> 5'-ACCATGCACCACCTGTC-3'		
<b>Eubacterial (Universal)</b> Uni344F + Uni514R	<b>F:</b> 5'-ACTCCTACGGGAGGCAGCAGT-3'	190	Hartman et al. (2009) Table S2
	<b>R:</b> 5'-ATTACCGCGGCTGCTGGC-3'		
<b>Universal 16S</b> 341f-GC Clamp + 518r	<b>F:</b> 5'- <u>CGCCCCCGCGCGCGCGGGCGGGCGG</u> <u>GGGCACGGGGGGCCTACGGGAGGCAGCA</u> G -3'	190	Muyzer et al. (1993)
	<b>R:</b> 5'-ATTACCGCGGCTGCTGG -3'		
<b>Universal V3/V4 16S + Illumina® Overhang</b> S-D-Bact-0341- b- S-17 + S-D-Bact- 0785-a-A-21	<b>F:</b> 5'- <u>TCGTCGGCAGCGTCAGATGTGTATAAGAGA</u> <u>CAGCCTACGGGNGGCWGCAG</u> -3'	550	Klindworth et al. (2013)
	<b>R:</b> 5'- <u>GTCTCGTGGGCTCGGAGATGTGTATAAGA</u> <u>GACAGGACTACHVGGGTATCTAATCC</u> -3'		

**Table 2.3** – PCR primer sequences.

Single underlined sequence denotes GC-rich clamp positioned at the 5' end of the forward primer. Double underlined sequences denote Illumina® overhang adapters.

### 2.1.4 - Buffers and Solutions

Solution	Composition
50 × Tris acetic acid (TAE) buffer (1 L)	242.0 g Tris base, 57.1 mL Acetic acid, 100.0 mL 0.5 M EDTA, <i>q.s</i> to 1 L with dH <sub>2</sub> O. Autoclaved prior to use. Stock diluted 1:50 to achieve 1 × solution as required.
Gradient dye (10 mL)	0.05 g Bromophenol Blue, 0.05 g Xylene Cyanol. <i>q.s</i> to 10 mL with 1 × TAE buffer.
2 × Gel Loading Dye (10 mL)	0.25 mL of 2% Bromophenol Blue, 0.25 mL of 2% Xylene Cyanol, 7.0 mL 100% Glycerol and <i>q.s</i> to 10 mL with dH <sub>2</sub> O. Solutions were degassed under a vacuum.
0% Denaturant (20 mL)	5.0 mL 40% Acrylamide, 0.4 mL 50 × TAE buffer <i>q.s</i> to 20 mL with dH <sub>2</sub> O.
100% Denaturant (20 mL)	5.0 mL 40% Acrylamide, 0.4 mL 50 × TAE buffer, 8.0 mL formamide and 8.4 g Urea. Solution was heated to 50 °C, whilst stirring continuously, to dissolve urea crystals. Solutions were degassed for 3 min under a vacuum.
10% APS (1 mL)	0.1 g APS then <i>q.s</i> to 1 mL with dH <sub>2</sub> O.
4% Paraformaldehyde (1 L)	800 mL 1xPBS was heated to 50°C. 40g paraformaldehyde was added to the heated solution. pH raised via addition of 1N NaOH dropwise until dissolved. Solution was filtered and pH adjusted to 6.9 with 1 N HCl. <i>q.s</i> to 1 L with PBS.
Sodium Citrate Buffer (10mM Sodium Citrate, 0.05% Tween 20, pH 6.0, 1 L)	Tri-sodium citrate dihydrate 2.94 g, 900 mL dH <sub>2</sub> O, mix to dissolve. pH to 6.0 with 1N HCl, add 0.5 mL of Tween 20 and mix well. <i>q.s</i> to 1L with dH <sub>2</sub> O.
2 × Phosphate Buffer (1M KH <sub>2</sub> PO <sub>4</sub> , 10% TSP-d4 in 100% D <sub>2</sub> O, pH. 7.4, 100 mL)	1M KH <sub>2</sub> PO <sub>4</sub> prepared by dissolving 13.6 g into 80 mL 100% D <sub>2</sub> O. 100 mg TSP-d4 was dissolved in 6 mL 100% D <sub>2</sub> O and both solutions were mixed via sonication. pH was adjusted to 7.4 with addition of KOH pellets then <i>q.s</i> to 100 mL with D <sub>2</sub> O.

**Table 2.4** – Buffers and Solutions.

## 2.2 - Methods

### 2.2.1 - Research Ethics

Favourable ethical opinion was obtained from North West Research Ethics Committee following submission of relevant study documentation through the Integrated Research Application System (IRAS) and formal assessment by an independent peer review panel (REC references 13/NW/0695 and 14/NW/1429 for surgical and endoscopy studies, respectively). Local Research and Development approval was achieved at each collaborating National Health Service (NHS) Trust; Lancashire Teaching Hospitals (Preston, UK) and University Hospitals of Morecambe Bay (Barrow-In-Furness, UK), in addition to authorisation from the study sponsor; Lancaster University Research Support Office.

### 2.2.2 – Surgical Patient Recruitment

Patients at Lancashire Teaching Hospitals, scheduled for loop ileostomy reversal surgery, were assessed against the inclusion and exclusion criteria of the study by the Surgical Care Practitioner (table 2.5). Suitable and willing patients provided full informed consent and were anonymised via study ID allocation (BCRGXXX). Non-identifiable patient information including age, gender, and BMI were recorded in addition to the following post-operative data: number of days with ileostomy, incidence of complications, C reactive protein (CRP), WBC and albumin blood levels. Relevant study documentation is presented in appendix 1.

Study Inclusion Criteria	Study Exclusion Criteria
<p>The participant may only enter the study if <b>ALL</b> of the following apply:</p> <ul style="list-style-type: none"><li>• Participant is willing and able to give informed consent for participation in the study.</li><li>• Male or Female, aged 18 years or above.</li><li>• Must be undergoing ileostomy reversal surgery.</li></ul>	<p>The participant may not enter the study if <b>ANY</b> of the following apply:</p> <ul style="list-style-type: none"><li>• Patients not undergoing ileostomy reversal surgery.</li><li>• Patients who are currently, or have taken <u>any</u> courses of antibiotics within the last 3 months.</li></ul>

**Table 2.5** – Inclusion and exclusion criteria for patient recruitment to surgical study.

### **2.2.3 – Provision of Surgical Specimen**

Ileostomy reversal surgery involves reanastomosis of functional and defunctioned intestine using a linear stapler. During this process, a short region of the intestine is removed from the end of each limb and are the specimens acquired for this study (figure 3.2). Immediately following acquisition, luminal associated microflora were sampled by inserting a sterile swab into the lumen of each specimen. Specimen were then transferred into sterile histopots and sustained with Minimum Essential Media (MEM). All specimen were transported from the operating theatre to the research laboratories at Lancaster University and were processed within two hours of collection.

To examine the mucosal associated microflora, an equal number of mucosal biopsies were dissected from each specimen. The number of biopsies obtained from each participant ranged between 2 and 5 per limb and was determined by availability of mucosa in the defunctioned specimen. For histological analysis, a full thickness portion was obtained from each limb at immediately transferred into paraformaldehyde fixative. MEM media was collected and processed to salvage loosely adhered bacteria which may have washed off during transport.

### **2.2.4 Surgical Specimen DNA Extractions**

**2.2.4.1 - Mucosal Tissue DNA Extraction** – Mucosal biopsies (~20 mg each), dissected from surgical specimen, were finely sliced to aid release of associated microflora. Biopsies were exposed to various DNA extraction pre-treatments associated with the QIAamp® Cador® Pathogen Lysis Minikit (Qiagen, Manchester, UK). First, samples were digested in proteinase K at 56 °C for 30 mins, centrifuged at 4000 × g for 30s to pellet tissue and the supernatant subjected to mechanical lysis, at maximum speed for 10 min, utilising Pathogen Lysis Tubes S (Qiagen) on a Vortex Genie 2 (Scientific Industries). Following mechanical lysis, total genomic DNA was extracted using QIAamp® Cador® Pathogen Lysis Mini Kit (Qiagen), according to the manufacturer's protocol. Eluted DNA was quantified using a NanoDrop™ 2000c Spectrophotometer (Thermo-Fisher) and stored at -20 °C until required.

**2.2.4.2 - Luminal Swab and MEM Media DNA Extraction** – Swab heads were separated from transport vials and placed in 650 µL buffer ATL (Qiagen). Samples were vortexed at full speed for 10 min, prior to incubation at 56 °C for 20 min, in a thermoshaker at 800 rpm. Media



samples were centrifuged at  $8000 \times g$  to pellet bacteria and resuspended in 500  $\mu\text{L}$  buffer ATL (Qiagen). Media and swab supernatants were subjected to mechanical lysis at maximum speed for 10 min utilising Pathogen Lysis Tubes S (Qiagen) on a Vortex Genie 2 (Scientific Industries), prior to DNA extraction using QIAamp® UCP Pathogen Mini Kit (Qiagen), according to the manufacturer's protocol. Eluted DNA from swab and media samples were pooled, quantified as described, then stored at  $-20\text{ }^{\circ}\text{C}$  until required.

## **2.2.5 - Denaturation gradient gel electrophoresis (DGGE)**

**2.2.5.1 – Generation of a Standard DNA Marker for DGGE Analyses** – A sample enriched in microbial diversity was generated from pooled human faecal DNA for use as a standard marker in DGGE analyses. Faecal samples were gifted from five healthy volunteers, differing in age (between 20 and 50 years old), gender, weight (between 9 and 18 stone) and geographical location to increase overall microbial diversity within the marker. All samples were transported on ice to research laboratories at Lancaster University and processed within two hours of collection in a class II microbiological safety cabinet (Baker), employing aseptic technique. Samples were processed in duplicate by weighing  $2 \times 200\text{ mg}$  sample into microcentrifuge tubes containing 1.4 mL buffer ASL (Qiagen). DNA extractions were performed using QIAamp® DNA Stool Mini Kit (Qiagen), according to the manufacturer's protocol, with the following modification; increased incubation temperature in lysis buffer from  $70\text{ }^{\circ}\text{C}$  to  $95\text{ }^{\circ}\text{C}$ , to improve lysis efficiency. DNA Eluted from 10 samples was pooled, quantified as described, then stored at  $-20\text{ }^{\circ}\text{C}$  until required.

**2.2.5.2 – Polymerase Chain Reaction (PCR) for DGGE** – A highly conserved 200 base pair (bp) sequence, neighbouring the V3 hypervariable region of the 16S ribosomal ribonucleic acid (rRNA) gene, was amplified using universal 16S rRNA primers, 341F\_GC and 518R (table 2.3; Muyzer *et al.*, 1993) on luminal and mucosal microbiol DNA samples. For PCR reactions performed for use in DGGE analysis, a 40 base pair nucleotide GC rich clamp was attached to the 5' end of the 341F forward primer (GC Clamp sequence listed in table 2.3). All PCR reactions were prepared in a designated PCR area, contained within Holten LaminAir™ HV Mini Airflow cabinet (Thermo-Fisher), using sterile filter pipette tips, sterile 0.2 mL PCR tubes and sterile-filtered PCR grade water (Sigma Aldrich). The PCR reaction mix ( $V_f = 25\text{ }\mu\text{L}$ ) contained 12.5  $\mu\text{L}$  REDTaq® ReadyMix™ PCR Reaction Mix (0.06 unit/ $\mu\text{L}$  Taq DNA polymerase, 0.4 mM dNTP mix, 20 mM Tris-HCl, 100 mM KCl, 0.002% gelatin and 3mM Magnesium

Chloride ( $\text{MgCl}_2$ ); Sigma Aldrich), 1  $\mu\text{L}$  BSA (0.5  $\mu\text{g}/\mu\text{L}$ ), 1  $\mu\text{L}$  341f primer (0.4 mM), 1  $\mu\text{L}$  518r primer (0.4 mM), X  $\mu\text{L}$  template DNA (100 ng/25  $\mu\text{L}$  reaction) and *q.s* to 25  $\mu\text{L}$  with PCR grade water. The PCR cycle was initiated with a denaturation step of 95 °C for 5 min; followed by 29 cycles of 95 °C for 30 sec, 57 °C for 30 sec, 72 °C for 30 sec and a concluding step of 72 °C for 5 min. PCR was performed using a PTC-100® Thermal Cycler (Bio-Rad) with a total run time of approximately 1.5 h.

**2.2.5.3 – DGGE Profiling** – Parallel DGGE was performed using a DCode™ Universal Mutation Detection System (Bio-Rad). DGGE analysis was conducted following the manufacturer's recommended protocol (BioRad). Briefly, PCR products were resolved with 40% polyacrylamide gels, composed with a 30 to 70% linear gradient of denaturants (table 2.4), which rise in concentration in the direction of electrophoretic migration. Polymerisation was initiated with the addition of 150  $\mu\text{L}$  10% APS and to each denaturant solution. Gels were cast using a BioLogic™ EP-1 Econo Pump (Bio-Rad) at a flow rate of 5 mL/min, whilst gradients were formed using a SG50 Gradient Maker (Hoefer, Massachusetts, USA) and visualised with the addition of 200  $\mu\text{L}$  gradient dye to the 70% denaturant solution (table 2.4). Samples composed of 5  $\mu\text{L}$  PCR sample (30 ng/ $\mu\text{L}$ ), 7.5  $\mu\text{L}$  loading dye (table 2.4) and 2.5  $\mu\text{L}$  sterile PCR grade water (Sigma), were loaded into individual lanes, whilst the standard faecal DNA marker was loaded into the two outermost lanes. Electrophoresis was conducted at 60 °C and ran at 60 V for 16 h. Gels were post-stained using 20 mL 1 × SYBR® Gold Nucleic Acid Gel Stain (Invitrogen) for 30 min, with constant, gentle agitation, rinsed in 1 × TAE buffer and imaged using a BioDoc-It™ 210 UV imaging system (Bio-Rad) with 4 sec exposure. Gels were stored in a refrigerated humidified chamber for up to 24 h prior to band excision.

**2.2.5.4 – Digital Processing of DGGE Profiles** – DGGE profiles were processed digitally using BioNumerics software (version 7.5; Applied Maths, TX, USA), following the manufacturer's guidelines; lanes and bands were automatically defined and manually corrected, followed by automatic normalisation against marker lanes. Next, band matching analysis was performed, dividing all bands into classes of common bands and generating a binary presence/absence banding profile (appendix 2). Percent presence was calculated for each band class and those differing in abundance between functional and defunctioned profiles were selected for extraction and sequencing.

Hierarchical cluster analysis was also performed on binary data, following manufacturer's guidelines for band based coefficients, with the following defined parameters: Similarity

coefficient, Jeffrey's X; Optimisation, 0.5%; Band matching tolerance, 0.5%; Uncertain bands, Include; Method, Unweighted Pair Group Method with Arithmetic Mean (UPGMA).

**2.2.5.5 – DGGE Band Excision and Purification** – Amplicons from DGGE bands of interest were reamplified directly from the gel, using the PCR parameters as described in 2.2.5.2. The purity of the PCR products was confirmed via DGGE and the process was repeated until a single band was obtained. Purification was confirmed by running extracted band neighbouring the original sample (appendix 3).

**2.2.5.6 - Sanger Sequencing and Analysis** – Following matched confirmation of target bands with original sample profiles, amplicons were subjected, in triplicate, to Sanger sequencing (Source Bioscience, Nottingham, UK), using primers 341F+GC Clamp and 518r. Consensus sequences were generated using the ClustalW Multiple Alignment tool accessory within BioEdit software (available online at, [www.mbio.ncsu.edu/BioEdit/bioedit.html](http://www.mbio.ncsu.edu/BioEdit/bioedit.html)). Alignment mismatches were manually corrected where possible or otherwise base-called as N. Using FASTA format, consensus sequences were individually submitted to Nucleotide Basic Local Alignment Search Tool (BLASTn; (Altschul et al., 1990) <https://blast.ncbi.nlm.nih.gov/Blast.cgi>). BLASTn parameters were defined as: Highly similar sequences (megablast), within the 16S ribosomal RNA sequences (Bacteria and Archaea) database. Each sequence and thus band class, was assigned a genus classification based on BLAST E values, Query cover and Max scores. Consensus sequences and taxonomic assignments for each experiment are presented in appendix 4.

## **2.2.6 – Phylum-specific 16S ribosomal-deoxyribonucleic acid quantitative real-time PCR (16S rDNA qRT-PCR)**

Predominant microbial phyla were compared using phylum-specific and universal 16S rDNA primers (table 2.3). PCR was performed in a 25  $\mu$ L reaction volume containing 12.5  $\mu$ L SYBR® Green JumpStart™ Taq ReadyMix™ (20 mM Tris-HCl, pH 8.3, 100 mM KCl, 7 mM MgCl<sub>2</sub>, 0.4 mM each dNTP, stabilizers, 0.05 unit/mL Taq DNA Polymerase, JumpStart Taq antibody, and SYBR Green I; Sigma-Aldrich), 30-50 ng of template DNA and 1  $\mu$ L each forward and reverse primer (10  $\mu$ M) and *q.s* to 25  $\mu$ L with PCR grade water. PCR parameters were as follows: 1 cycle of 95 °C for 5 min, 35 cycles of 95 °C for 20 sec, 61.5 °C for 10 sec, annealing, 72 °C for 30 sec and 1 cycle of 72 °C for 5 min. Data was normalised to total bacteria, using universal

primers, and the relative abundances of each phylum determined using the delta delta-Ct ( $2^{-\Delta\Delta Ct}$ ) algorithm method (Livak and Schmittgen, 2001).

### **2.2.7 – Quantification of Total Bacterial Load**

pCR<sup>®</sup>2.1-TOPO<sup>®</sup> plasmid DNA, containing a 179 bp cloned portion of the 16S rRNA gene was kindly provided by Dr Sheena Cruickshank at The University of Manchester, with permission from Professor Lora Hooper at University of Texas Southwestern Medical Centre. The recombinant pCR<sup>®</sup>2.1-TOPO<sup>®</sup> plasmid was generated at University of Texas Southwestern Medical Centre.

**2.2.7.1 – Preparation of Luria Broth (LB) + Kanamycin Agar Plates** – 15 g low salt LB (Duchefa Biochemie, Haarlem, NL) was dissolved in 500 mL dH<sub>2</sub>O. Agar was autoclaved for 20 min then left to cool. Prior to pouring, 500 µL kanamycin (30 mg/mL) was added and mixed thoroughly. Plates were poured in an Evanair Class II Bio2+ Microbiological Safety Cabinet with a lit Bunsen then stored at 2-5 °C until required.

**2.2.7.2 – pCR<sup>®</sup>2.1-TOPO<sup>®</sup> Plasmid Transformation** - The pCR<sup>®</sup>4-TOPO<sup>®</sup> plasmid was transformed into XL1-Blue competent cells (Agilent Technologies, California, USA). A single vial was thawed slowly on ice then 50 µL XL1-Blue competent cells and 1 µL pCR<sup>®</sup>2.1-TOPO<sup>®</sup> plasmid were gently mixed in a falcon tube. The suspension was incubated on ice for 30 min, heat-pulsed at 42 °C for precisely 45 sec and again placed on ice for a further 2 min. Next, 200 µL SOC Outgrowth medium (New England BioLabs, Hertfordshire, UK) was added prior to incubation at 37 °C for 1 h, shaking at 250 revolutions per minute (rpm).

**2.2.7.3 – Clone Selection using LB Kanamycin Plates** – The transformation suspension was streaked onto an LB kanamycin plate (30 µg/mL kanamycin; prepared as described in 2.2.7.1) and incubated overnight, upside-down, at 37 °C. Since the pCR<sup>®</sup>2.1-TOPO<sup>®</sup> plasmid contains a kanamycin resistance cassette, XL1-Blue competent cells which acquired the plasmid will selectively grow on the LB kanamycin plate, thus generating a single cell clone.

**2.2.7.4 – Clone Amplification** – Following overnight incubation, a single colony was transferred into 3 mL LB broth (Life Technologies) containing kanamycin at a final concentration of 30 µg/mL, using aseptic technique. Universal tube was incubated overnight at 37 °C, in a shaking incubator at 220 rpm.

**2.2.7.5 – Isolation of Plasmid DNA** – Following overnight incubation, 1ml aliquot of culture was transferred into an Eppendorf and centrifuged at 12000 × g for 3 min to pellet cells. Plasmid DNA was extracted and purified using GeneJET Plasmid Miniprep Kit (Thermo-Fisher), following manufacturer’s protocol A: ‘Plasmid DNA purification using centrifuges’. Eluted DNA was quantified using a NanoDrop™ 2000c Spectrophotometer (Thermo-Fisher) and stored at -20 °C until required.

**2.2.7.6 – Generation of pCR®2.1-TOPO® Plasmid Standard Curve** – Molecular weight of a single copy of recombinant plasmid was calculated using the equation:

$$m = (n) \left( \frac{1.096 \times 10^{-21} g}{bp} \right)$$

Where: m = calculated mass of single plasmid  
n = plasmid + insert size (bp)  
1.096 × 10<sup>-21</sup> = average base pair mass

Mass of plasmid copy number of interest was calculated. This was selected to be 3 × 10<sup>9</sup> to represent typical bacterial abundances within the small intestine:

$$\text{Copy \# of interest} \times \text{mass of single plasmid} = \text{mass of plasmid DNA required}$$

The following formula was applied for dilution calculation:

$$C_1V_1 = C_2V_2$$

Where C<sub>1</sub> = concentration in copy number of plasmid stock  
V<sub>1</sub> = volume of plasmid stock  
C<sub>2</sub> = desired concentration  
V<sub>2</sub> = volume of diluted plasmid

A full worked example of standard curve calculation is presented in appendix 5. Dilutions 1-5, corresponding to 3 × 10<sup>9</sup> – 3 × 10<sup>5</sup> copy numbers, were utilised for construction of standard curve with physiological representation of bacterial load in the small intestine.

**2.2.7.7 - pCR®2.1-TOPO® Plasmid 16S rDNA qRT-PCR** - Total bacterial load in the functional and defunctioned intestine was measured via qRT-PCR, employing universal eubacterial 16S rRNA primers, Uni334F and Uni514R (table 2.3). PCR was performed in triplicate 25 µL reactions containing 12.5 µL SYBR® Green JumpStart™ Taq ReadyMix™ (20 mM Tris-HCl, pH 8.3, 100 mM KCl, 7 mM MgCl<sub>2</sub>, 0.4 mM each dNTP, stabilizers, 0.05 unit/mL Taq DNA Polymerase, JumpStart Taq antibody, and SYBR Green I; Sigma-Aldrich), 0.75 µL each forward and reverse primer (10 µM), 1 µL template DNA and 10 µL PCR grade H<sub>2</sub>O. PCR was performed

using a CFX96 Real-Time PCR Detection System (Bio-Rad) and cycle parameters were: 1 cycle of 95 °C for 10 min followed by 39 cycles of 95 °C for 15 sec and 60 °C for 1 min.

The abundance of bacterial 16S rRNA gene was quantified via extrapolation from the pCR<sup>®</sup>2.1-TOPO<sup>®</sup> plasmid standard curve utilising quantification cycle (Cq) values for each sample. Bacterial quantification relates to total 16S rRNA gene copy number and not colony forming units or absolute cell counts.

## **2.2.8 - Histological Analyses**

**2.2.8.1 - Tissue Fixation and Sectioning** - Full thickness excised functional and defunctioned tissue sections were fixed in 4% paraformaldehyde solution for 24 h. Samples were transferred into cassettes and dehydrated through increasing concentrations of alcohol (70-100%; 1 h each) to 2 × 1 h incubations in xylene and paraffin wax. Samples were next embedded in liquid paraffin wax and cooled on ice overnight to form solid blocks. Histological sections 7 µM thick were prepared using a RM2125 RTS Microtome (Leica Microsystems, Milton Keynes, UK) on APES-coated, frosted microscope slides and incubated at 37 °C overnight to dry.

**2.2.8.2 - Haematoxylin and Eosin (H&E) Staining** - H&E sections were generated to assess tissue orientation and suitability for immunofluorescence experiments in addition to villous height and crypt depth analyses.

Tissue sections were deparaffinised in xylene for 2 × 5 min then rehydrated in graded alcohol (100-70%) for 2 × 1 min each. Slides were washed in running tap water and rinsed in distilled H<sub>2</sub>O (dH<sub>2</sub>O) prior to immersing slides in Haematoxylin (Sigma-Aldrich, Dorset, UK) for 5 min with gentle agitation. Next slides were washed in hot running tap water for 15 min then submerged into Eosin for 30 sec with gentle agitation. Slides were rinsed in running tap water for 1 min then dehydrated in graded alcohol (70-100%) for 2 × 5 min each followed by 2 × 5 min xylene. Sections were mounted using DPX (Sigma-Aldrich) and coverslips then stored at room temperature until analysed.

**2.2.8.3 - Morphological Analyses** - Morphological analysis was performed on suitable H&E tissue sections. Images were captured using Nikon Eclipse E600 microscope with 10 × magnification. Villous height and crypt depth were measured using ImageJ software as illustrated in appendix 6 (Schneider et al. (2012); <https://imagej.nih.gov/ij/>). Measurements

were converted from pixels to  $\mu\text{M}$  at  $3.63 \mu\text{M}/\text{pixel}$ . Percent change in villous height and crypt depth were calculated using functional measurements as control.

**2.2.8.4 – Inflammation Scoring** - Coded H&E sections were scored for inflammation by a blinded observer. Scoring applied a well-validated system which assigns a score of 0 – 4 for inflammation and mucosal damage based on degree and extent of transmural inflammation, goblet cell depletion, immune infiltrate and architecture distortion (Rath et al., 1996).

### **2.2.9 - Immunofluorescence Proliferating Cell Nuclear Antigen (PCNA) Analysis**

Immunofluorescence was performed on suitably orientated embedded functional and defunctioned human tissue sections. First, tissue sections were deparaffinised and rehydrated through xylene and decreasing concentrations of alcohol in  $\text{dH}_2\text{O}$  (100-70%) for  $2 \times 5 \text{ min}$  and  $2 \times 2 \text{ min}$  each prior to 0.5% NaCl in  $\text{dH}_2\text{O}$  for 5 min.

Heat-Induced Epitope Retrieval (HIER) was conducted to reveal antigen binding sites masked during the fixation process, by boiling in sodium citrate buffer pH 6.0 in a microwave oven for 15 min, followed by gradual cooling in  $\text{dH}_2\text{O}$  for 10 min. Samples were next permeabilised using TBS + 0.25% Triton X-100 for 10 min with gentle agitation to ensure free access of the primary antibody to its epitope, then washed in TBS + 0.025% Triton X-100 for  $2 \times 2 \text{ min}$ . A PAP pen (Sigma-Aldrich) was used to create a hydrophobic barrier around each tissue section. Non-specific antibody binding was attenuated via incubation in 10% goat serum in TBS + 3% BSA for 2 h at room temperature in a humidified container. Slides were next immunised with  $1.4 \mu\text{g}/\text{mL}$  mouse anti-PCNA (PC10) primary antibody in 3% BSA-TBS, overnight at  $4 \text{ }^\circ\text{C}$ , in a humidified container. A species matched isotype control was also included, incubated with  $1.4 \mu\text{g}/\text{mL}$  Normal Mouse IgG in 3% BSA-TBS only.

Following overnight incubation, slides were rinsed in TBS + 0.025% Triton X-100 for  $2 \times 2 \text{ min}$  then incubated with  $2 \mu\text{g}/\text{mL}$  Goat Anti-Mouse Alexa-Fluor® 488 antibody in TBS (Thermo-Fisher, Paisley, UK) for 1 h at room temperature, in a darkened humidified container. Slides were counterstained with Hoescht33342 Trihydrochloride nucleic acid stain (Life Technologies, Paisley, UK) and mounted using VectaShield® Mounting Medium (Vector Laboratories, Peterborough, UK), then sealed with a coverslip and stored in the dark at  $4 \text{ }^\circ\text{C}$  until visualised using a Zeiss LSM 880 confocal microscope.

The number of PCNA positive cells and all nucleated cells were counted by a blinded observer. Rate of IEC proliferation was calculated as the percent of PNCA-positive cells/crypt

to account for potential variation in total number of cells per crypt between functional and defunctioned samples.

#### **2.2.10 – Click-iT® Terminal Deoxynucleotidyl Transferase-dUTP Nick End Labelling (TUNEL) Assay**

Paraffin embedded functional and defunctioned tissue sections were assessed for apoptosis using Click-iT® Plus TUNEL Assay for In Situ Apoptosis Detection, Alexa Flour® 594, according to the manufacturer's protocol. A positive control slide, treated with DNase I, was prepared according to manufacturer's instructions. In addition, a negative control slide, treated only with Click-iT® Plus TUNEL Reaction Cocktail. Slides were counterstained with Hoescht33342 Trihydrochloride nucleic acid stain (Life Technologies) and mounted using VectaShield® Mounting Medium (Vector Laboratories, Peterborough, UK), then sealed with a coverslip and stored in the dark at 4 °C until visualised using a Zeiss LSM 880 confocal microscope. Due to the limited number of TUNEL positive cells, quantification of positive cells/crypt was not performed.

#### **2.2.11 – Statistical Analyses**

Univariate statistical analyses, employing a paired T-test, was performed using SPSS Statistics Desktop (IBM, New York, USA) to compare data from functional versus defunctioned samples.  $p \leq 0.05$  was deemed statistically significant (\*  $p \leq 0.05$ ; \*\*  $p \leq 0.01$ ; \*\*\*  $p \leq 0.001$ ; \*\*\*\* $p \leq 0.0001$ ).

#### **2.2.12 – Endoscopy Outpatient Recruitment**

Patients undergoing colonoscopy or flexible sigmoidoscopy at either Lancashire Teaching Hospitals (Lancashire, UK) or University Hospitals of Morecambe Bay NHS Foundation Trust (Cumbria, UK) were assessed against the study inclusion and exclusion criteria by the Research Nurse or Gastroenterologist (table 2.6). Upon receipt of informed consent, participants were anonymised via study ID allocation (LTHXXX/LANCXXX) and non-identifiable patient information including age, gender and relevant treatment history was recorded. Relevant study documentation is presented in appendix 7.



Study Inclusion Criteria	Study Exclusion Criteria
<p>The participant may only enter the study if <b>ALL</b> of the following apply:</p> <ul style="list-style-type: none"> <li>• Participant is willing and able to give informed consent for participation in the study.</li> <li>• Male or Female, aged 18 years or above.</li> <li>• Must be undergoing colonoscopy or flexible sigmoidoscopy examination.</li> <li>• Diagnosed with IBD (test group).</li> <li>• Must not be diagnosed with IBD, CRC or IBS to be included as a 'healthy' control.</li> </ul>	<p>The participant may not enter the study if <b>ANY</b> of the following apply:</p> <ul style="list-style-type: none"> <li>• Patients not undergoing colonoscopy or flexible sigmoidoscopy.</li> <li>• Participants who do not have IBD cannot be included in test group.</li> <li>• Participants who have ongoing bowel pathologies such as IBD, CRC and specifically IBS cannot be included in the 'healthy' control group.</li> <li>• Participants who are currently taking any antibiotic, or who have taken broad spectrum antibiotics within the last 3 months.</li> <li>• Participants who have or, within the last month, have had a urinary tract infection (UTI).</li> </ul>

**Table 2.6** – Inclusion and exclusion criteria for patient recruitment to endoscopy study.

### 2.2.13 – Urine and Colonic Biopsy Sample Acquisition and Processing

**2.2.13.1 – Sample Acquisition** - Immediately following collection, participant midstream urine samples were screened for indications of a UTI using DUS 10 Reagent Strips (Dream Future Innovation Co Ltd, Gyeongsangnam-do, Korea) following the manufacturer’s instructions. Patients with observed leukocyte and nitrite levels exceeding 125 WBC/ $\mu$ L and trace levels respectively were excluded from the study and referred to their GP for confirmatory diagnosis and treatment. For non-excluded participant samples, sodium azide was added to a final concentration of 0.02%, to prevent bacterial growth.

During the patients’ flexible sigmoidoscopy or colonoscopy procedure, two additional biopsies were obtained; one from the descending and one from the sigmoid colon. Biopsies were placed directly into a sterile 2 mL microcentrifuge tube containing 180  $\mu$ L Buffer ATL (Qiagen).

All samples were stored on ice, transported to the research labs at Lancaster University and processed within 4 h of collection. Human samples were processed within a class II microbiological safety cabinet (Baker), employing aseptic technique.

**2.2.13.2 – Urine Sample Processing** – Urine samples were prepared for analysis via centrifugation for 5 min at 3900 × g at 4 °C, to remove particulate matter. Aliquots of 1.5 mL urine were snap frozen in liquid nitrogen and stored at -80 °C prior to nuclear magnetic resonance (NMR) spectroscopy.

**2.2.13.3 – Colonic Biopsy DNA Extraction and Purification** – Biopsy samples were digested in 40 µL proteinase K at 56 °C for 1 h prior to bead beating, at maximum speed for 10 min, utilising Pathogen Lysis Tubes S (Qiagen) on a Vortex Genie 2 (Scientific Industries). Following mechanical lysis, total genomic DNA was extracted using QIAamp® Cador® Pathogen Lysis MiniKit (Qiagen), according to the manufacturer's protocol.

PCR inhibitors were removed from extracted DNA samples using PowerClean® Pro DNA Clean-up Kit (Mo Bio Laboratories, California, USA) following the manufacturer's instructions. Eluted DNA was quantified using a NanoDrop™ 2000c Spectrophotometer (Thermo-Fisher) and diluted to 50 ng/µL with a final volume of 50 µL. Samples were stored at -20 °C prior to Illumina® MiSeq sequencing.

## **2.2.14 – 1D <sup>1</sup>H NMR Spectroscopy**

NMR spectroscopy experiments were performed at The University of Liverpool NMR Centre for Structural Biology with technical guidance from Dr Marie Phelan and Dr Geoffrey Akien; NMR Facility Managers from University of Liverpool NMR Centre for Structural Biology and Lancaster University Chemistry Department, respectively.

**2.2.14.1 - 1D <sup>1</sup>H NMR Sample Preparation** – Urine samples were thawed at room temperature for approximately 1 h and processed as described with minor modifications (Beckonert et al., 2007). Briefly, after centrifugation at 6000 × g for 5 min, 500 µL aliquot each urine sample was mixed with 500 µL 2× phosphate buffer, containing 10% TSP-d4 (table 2.4). Samples were vortexed for 1 min and centrifuged at 13000 × g for 2 min room temperature. A 600 µL aliquot was transferred to a coded 96 deep well plate for automated acquisition and loading of 400 µL of each urine sample into racked 3mm NMR tubes by a Burkert-modified Gilson Nebular 215 liquid handler (Bruker BioSpin, Karlsruhe, Germany).

**2.2.14.2 - 1D <sup>1</sup>H NMR Spectroscopy** – Samples were processed consecutively at 298 K on a Bruker AVANCE III 600MHz spectrometer equipped with a 1H-optimised 5 mM helium TCI cryoprobe (Bruker BioSpin). Data were also acquired at 300 K, but due to the disappointing separation in the statistical analysis of the 298 K NMR data alone, and the limitations of time, no attempt was made at a detailed analysis. Furthermore, data was also acquired in 5 mm tubes on the 600 MHz instrument, as well as in both 3 mm and 5 mm tubes in a Bruker AVANCE III HD 700 instrument (Bruker BioSpin), but in all cases the lineshape and signal to noise were poorer compared to the 3 mm/600 MHz dataset.

Prior to running each batch of samples, the temperature was calibrated using MeOH-d<sub>4</sub>, and the 3D shims (Topshim 3d, TopSpin, version 3.5, Bruker Biospin) and water suppression frequency (O1) optimised manually using a 90% H<sub>2</sub>O/10% D<sub>2</sub>O sucrose test sample. Each sample was allowed a 5 min equilibration period in the magnet, before shimming, automated calibration of the 1H 90° pulse length (pulsecal). 1D <sup>1</sup>H spectrum were acquired using a standard vendor supplied, gradient enhanced, single pulse sequence with a 90° flip angle and water suppression, referred to as 1D nuclear Overhauser enhancement spectroscopy (NOSEY)-presat (or noesygprr1d), performed as previously described (Beckonert et al., 2007). A total of 32 scans were performed for each sample with an acquisition time of approximately 4 min per sample. The acquired free induction decay (FID) data were automatically processed to ensure consistency, with a line broadening of 0.3 Hz and zero-filled to 64k Fourier domain points prior to Fourier transformation. The automation routine included manual phasing, baseline correction and reference to TSP-d<sub>4</sub> at 0 ppm.

**2.2.14.3 – NMR Spectroscopy Data Preprocessing** - NMR spectra were overlaid in NMR processing and analysis software, TopSpin (Version 3.5, Bruker Biospin). Buckets were defined manually via visual analysis and annotated using Chenomx NMR Suite 6.0 (Chenomx Inc., Edmonton, Canada) to create a pattern file (appendix 8) that was imported into AMIX (Version 3.9.14, Bruker Biospin) for computational processing of the defined buckets. The Chenomx NMR Suite enables comparison spectral peaks against a reference library of defined common mammalian metabolites, facilitating spectral annotation. Ambiguous peaks were labelled as 'Unknown' for further investigation if found to be of significance. The AMIX-generated bucket table harboured a list of metabolite-annotated peaks and relative intensities, relating to total area under each peak, for each patient urine sample (appendix 9). Representative NMR spectra were labelled with assigned metabolite annotations using

Tools for Analysis of Metabolic NMR (TameNMR) within the Galaxy framework (available at [www.galaxy.liv.ac.uk](http://www.galaxy.liv.ac.uk) from autumn 2017).

Normalisation and scaling preprocessing methods for acquired spectroscopic metabolomics datasets are required to ensure amenability to downstream multivariate statistical analyses. Such techniques are continually scrutinised and debated within the literature and standardised methods do not currently exist. Various appropriate methods were considered in the context of the dataset generated, previous experimental literature and advice from NMR technicians.

Normalisation is applied to the data obtained from each sample to ensure comparability. This is important with urine due to drastic concentration variations between samples. Normalisation can be performed to a housekeeping metabolite considered to be constant across all samples, usually creatinine. However creatinine excretion rates have been shown to vary between individuals due to differences in age, gender and disease state (Slupsky et al., 2007). Another method is to normalise to the total intensity by expressing each data point in relative terms as a fraction of the total spectral integral, a method referred to as constant sum normalisation (Craig et al., 2006). This method assumes the total integral is constant throughout all samples but is considered ineffective if drug metabolites are expected to be present within the urine. This led us to consider probabilistic quotient normalisation (PQN) which scales spectra according to the most probable dilution factor in the dataset and has been shown to be more robust and accurate than other normalisation methods (Dieterle et al., 2006). PQN normalisation was therefore selected for processing of the dataset. Next, scaling functions to bring all variables to a comparable scale. Methods include mean centring, where all variables have the mean of respective samples subtracted to give a mean of 0, or unit variance, where each variable is divided by the standard deviation of all respective samples. Pareto scaling is a modification of the latter method which involves the division of each variable by the square root of the standard deviation of all respective samples and was selected for this study as it is considered to be more effective at minimising bias of abundant urinary metabolites, such as urea (van den Berg et al., 2006).

Normalisation and scaling were performed utilising the R programming language script 'NMRMetab\_Norm\_Scale.R' written and provided by collaborators at Liverpool University,

Computational Biology Facility, within the RStudio software interface (Version 1.0.143, RStudio Inc. Boston, MA; <https://www.rstudio.com/>).

### 2.2.15 – Illumina® MiSeq Sequencing

Purified DNA extracted from colonic tissue biopsies was outsourced to Source Bioscience for Illumina® MiSeq Sequencing and data processing. The full sequencing workflow is illustrated in figure 2.1 and described briefly as follows:

**2.2.15.1 – Library Preparation** – Samples were first subjected to Amplicon PCR (figure 2.1A) to amplify target DNA utilising S-D-Bact-0341- b-S-17 and S-D-Bact-0785-a-A-21 primers containing Illumina® overhang adapters (table 2.3). PCR reactions were composed as indicated in table 2.7 then subjected to PCR cycle parameters outlined in table 2.8.

PCR Reagent	Volume (µL)
2 × KAPA HiFi HotStart ReadyMix	12.5
Forward Primer (1 µM)	5.0
Reverse Primer (1 µM)	5.0
Template DNA (5 ng/µL)	2.5
Total	25.0

**Table 2.7** - Amplicon PCR reaction components for Illumina® MiSeq library preparation.

Cycle	Number of cycles	Temperature	Duration
<b>Initial Denaturation</b>	1	95°C	3 min
<b>Denaturation</b>	24 (Amplicon PCR) 8 (Index PCR)	95°C	30 sec
<b>Annealing</b>		55°C	30 sec
<b>Extension</b>		72°C	30 sec
<b>Final Extension</b>	1	72°C	5 min
<b>Hold</b>	1	4°C	∞

**Table 2.8** - Amplicon and index PCR cycle parameters for Illumina® MiSeq library preparation

Finally, PCR purification using AMPure XP beads was again performed prior to library validation checks utilising a Bioanalyzer DNA 1000 chip (Agilent, Santa Clara, CA) to verify amplicon size of 630 bp.

**2.2.15.2 – Cluster Generation** – Library quantification, normalisation and pooling were first conducted by diluting libraries to 4 nM and mixing 5  $\mu$ L aliquots from each library containing unique indices to generate a pooled amplicon library. Next, a 5  $\mu$ L aliquot was mixed with 5  $\mu$ L 0.2N NaOH, briefly vortexed, centrifuged at  $280 \times g$  for 1 min at 20 °C and diluted to 20 pM in pre-chilled HT1 hybridisation buffer to denature the pooled library in preparation for cluster generation. A PhiX quality control library was prepared as described for the amplicon library to a matched final concentration of 20 pM. Both libraries were then diluted to 4  $\mu$ M in HT1 buffer with a final volume of 600  $\mu$ L and combined at a PhiX control spike-in concentration of 25% (150  $\mu$ L PhiX and 450  $\mu$ L pooled). Finally, the combined library was heat denatured at 96 °C for 2 min and placed on ice immediately prior to MiSeq V3 reagent cartridge loading.

Cluster generation is an automated process by which single stranded DNA amplicons are hybridised and clonally amplified in a flow cell via bridge amplification (figure 2.1B). Reverse strands are cleaved and washed away leaving forward strands tethered to the flow cell for subsequent sequencing.

**2.2.15.3 – Sequencing-by-Synthesis** – Annealing of specific sequencing primers initiates sequencing-by-synthesis. Following the addition of a complementary nucleotide a light source excites the clusters resulting in emission of a distinguishing fluorescent signal. Automated detection and interpretation of emission wavelength and signal intensity defines the base call and thus the DNA sequence. This process is conducted twice, first for forward and second for reverse strand sequencing.

**2.2.15.4 – Illumina® Sequencing Data Processing** – First pooled sample libraries are separated based on the unique indices labelling system. Pre-processing raw Illumina® next-generation sequencing data involves trimming adapter sequences and merging paired-end reads. Sequencing reads were quality analysed and trimmed of adapter sequences using Skewer (Jiang et al., 2014). Next, paired-end reads are overlapped and merged to create longer read sequences using Fast Length Adjustment of Short Reads (FLASH; Magoc and Salzberg (2011)).

Quantitative Insights Into Microbial Ecology™ (QIIME™; Caporaso et al. (2010)) was utilised to pick orthogonal taxonomic units (OTU), compose OTU tables, perform taxonomic assignment and plot taxa sample data. OTU picking was set to a 97% minimum threshold for sequence similarity and subsequent clustering. Taxonomic assignments, connecting OTUs to an organism identification, were defined using the Ribosomal Database Project (RDP) Classifier reference database, with a confidence value of 0.8 (Wang et al., 2007). Taxonomic data is presented as a relative proportion of total OTUs for each patient and not precise OTU counts for each taxonomy.

**2.2.15.5 – Plotting Sequence Data** – The relative proportions of microbiota taxa present within each patient was visualised utilising bar charts. Such charts were generated using RStudio software (Version 1.0.143, RStudio Inc. Boston, MA) using the R package ggplot2 (Wickham, 2009). Microbiota variables with very low counts detected in few samples are considered to arise primarily due to sequencing errors and can cause difficulties in data interpretation. To control for this, a low count filter was applied to eliminate microbiota with a sample prevalence of <25%.

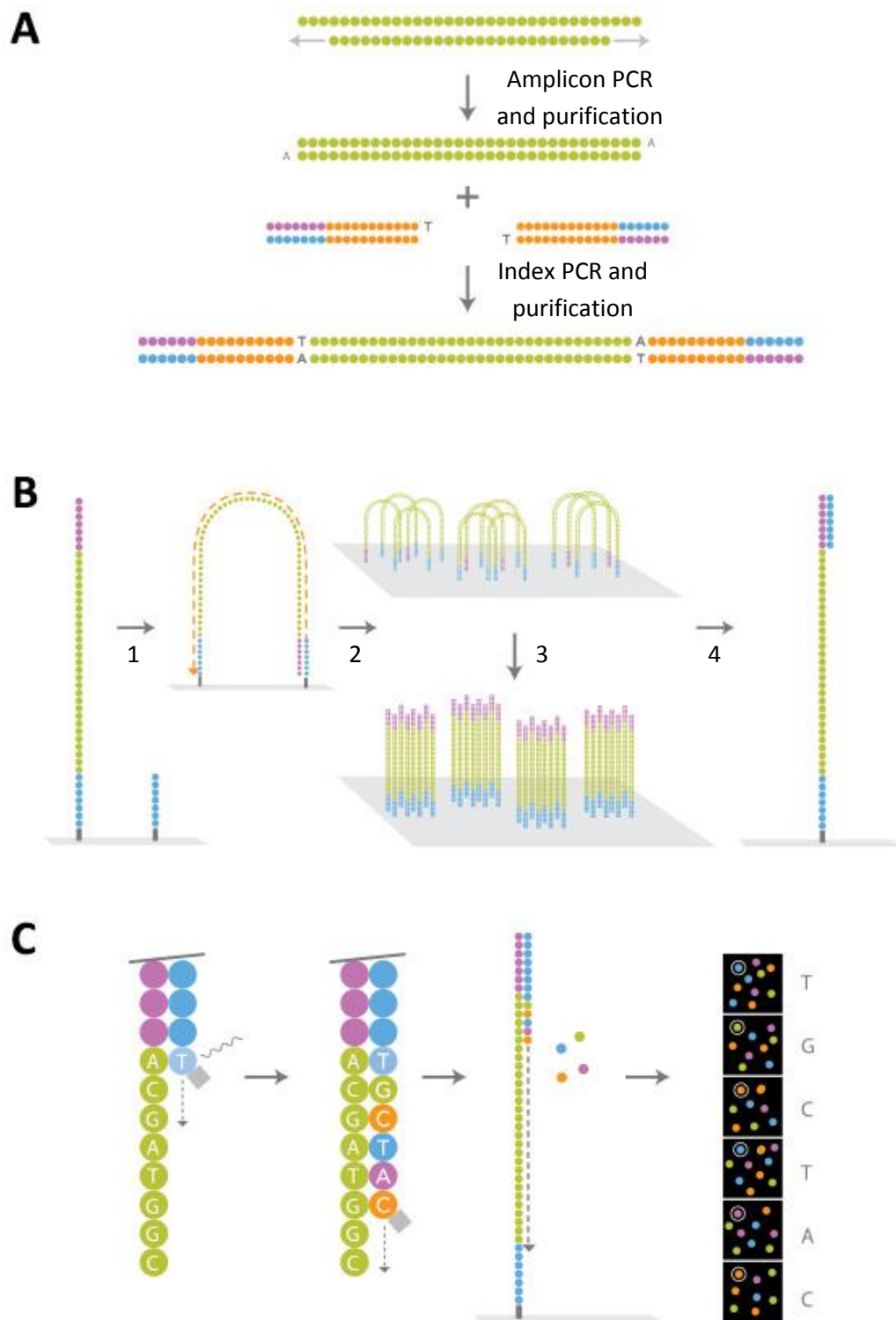


**Figure 2.1 – Illumina® sequencing workflow.** (A) Library preparation, to anneal sequencing binding site, indices and complementary sequence to flow-cell oligos to PCR amplicons (B) Cluster generation; 1. Hybridisation, strand synthesis and denaturation, 2. Bridge amplification and reverse strand synthesis, 3. Clonal amplification and 4. Reverse strand cleavage in preparation for (C) sequencing using sequencing-by-synthesis technology.

*Figure adapted from WWW, Illumina Inc®, 2012.*



### **2.2.16 – Multivariate Statistical Analyses of Illumina MiSeq Sequencing and Urinary NMR Metabolomics Datasets.**

Statistical analyses were performed with training and guidance provided by Dr Marie Phelan and Dr Frank Dondelinger at University of Liverpool NMR Centre for Structural Biology and Lancaster University Centre for Health Informatics, Computing and Statistics, respectively.

To account for the impact of metabolites on the measurement outcome (in this case control and IBD groups), multivariate statistical analyses were employed. Furthermore, multivariate models were utilised to identify metabolites contributing to, and predicting, such results.

Both unsupervised and supervised multivariate statistical methods were applied during data analysis. Unsupervised analyses such as hierarchical clustering and principal component analysis (PCA) are often the first step in data exploration as they involve application of statistical models without prior knowledge of sample classifications, such as disease group, whilst supervised models, including partial least squares-discriminant analysis, are built following exposure to a training subset of data with defined sample classifications that is then applied to the remaining dataset.

**2.2.16.1 – Hierarchical Cluster Analyses** – To investigate potential existence of subgroups within metabolomics and microbiota datasets, hierarchical clustering was performed. Cluster analysis was executed utilising RStudio software (Version 1.0.143, RStudio Inc. Boston, MA) and the accompanying hclust function. Within this script the Euclidean distance measure was utilised to inform the hierarchical clustering.

**2.2.16.2 – Principal Components Analyses** – PCA was performed to reduce the dimensionality of the metabolomics and microbiota datasets as well as visualising data structure. PCA scores and biplots were generated utilising the statistical analysis function of MetaboAnalyst (Version 3.0; Xia et al. (2015); <http://www.metaboanalyst.ca/faces/home.xhtml>). For metabolite data analysis the pre-processed NMR peak intensity data table was uploaded whilst the microbiota taxonomic order proportion data table was uploaded as a concentrations table. The datasets were then subjected to the inbuilt PCA multivariate statistical package and graphics were exported in portable network graphic (PNG) format as a resolution of 300 dpi.

**2.2.16.3 – Orthogonal Partial Least Squares Discriminant Analyses (OPLS-DA)** – OPLS-DA is required to enhance the variance between groups and minimise intrinsic variance within

groups (i.e. the systematic variation not related to test variables). Diagnostic parameters such as explained variance ( $R^2$ ) that are presented in the model overview are commonly utilised as a measure of model performance, with acceptable values considered to be  $R^2 > 0.6$  for biological cohorts (Worley and Powers, 2013).

OPLS-DA models were generated utilising the statistical analysis function of MetaboAnalyst (Version 3.0; Xia et al. (2015); <http://www.metaboanalyst.ca/faces/home.xhtml>). Datasets were uploaded as described above and subjected to inbuilt OPLS-DA statistical functions. Graphical score plots and model overviews were exported in PNG format at a resolution of 300dpi.

**2.2.16.4 – Linear Regression Analysis** – Penalised linear regression analysis was performed to investigate potential relationships between metabolite and microbiota profiles or predominant microbes via integration of multi-omics datasets utilising RStudio software (Version 1.0.143, RStudio Inc. Boston, MA) package glmnet (Friedman et al., 2010).

## **Chapter 3:**

**Investigating the effect of enteral nutrient deprivation on intestinal microbiota composition utilising a novel human model in patients undergoing ileostomy reversal surgery.**

### 3.1 – Rationale:

Surgical resection of the large intestine is commonly carried out in patients with intestinal pathologies, such as colon cancer. To facilitate healing, prevent septic complications and reduce requirement for repeat operations, a temporary defunctioning loop ileostomy is formed upstream of the surgical site (figure 3.1). It functions to protect the downstream anastomosis via redirection of faecal stream through the abdominal wall, into an ileostomy pouch. Diversion of the faecal stream in this way gives rise to two opposing nutritional environments; the proximal ileum remains functional with nutrient and water absorption occurring at the mucosal surface from peristaltic motioned chyme, whilst the distal ileum is wholly deprived of luminal contents and consequently rendered inactive (figure 3.2A).

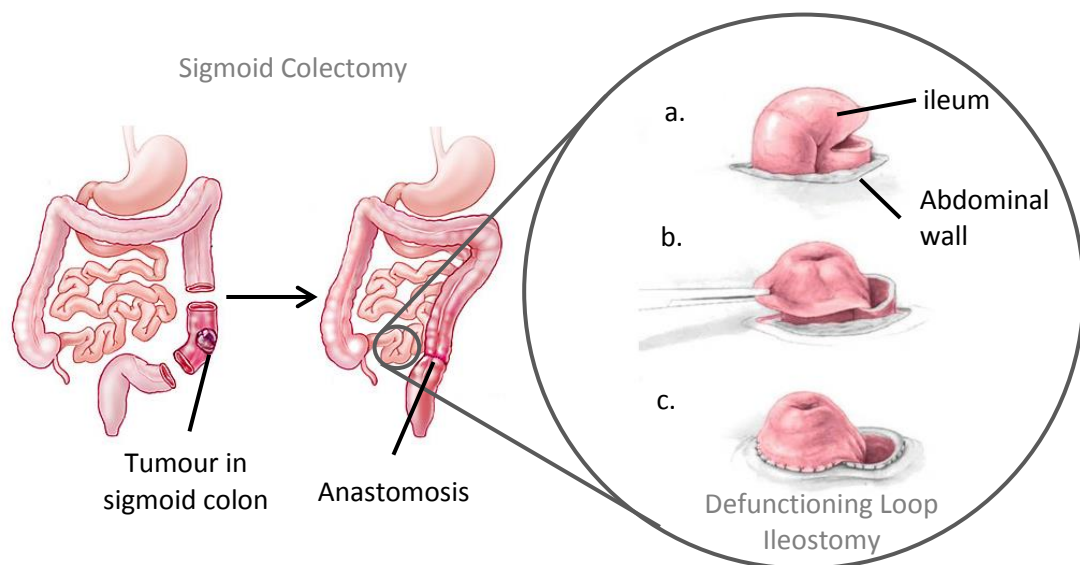


**Figure 3.1 - Defunctioning loop ileostomy formation in surgical resection patients.** A. ileum is lifted through the abdominal wall and divided longitudinally. B. Proximal ileum is everted, exposing the mucosa. C. Both limbs are sutured to surrounding skin.

The composition of the intestinal microbiota is modulated by various host genetic and environmental factors including medical practices such as antibiotic use, method of childbirth and most notably, host diet (De La Cochetiere et al., 2005, Gronlund et al., 1999, De Filippo et al., 2010). A plethora of literature now exists detailing the effects of diet modulation on the intestinal microbiota (Graf et al. (2015) and discussed in the literature review). An extreme example of diet modulation is demonstrated during medical interventions which

impose complete withdrawal of enteral nutrients. In such circumstances, total parenteral nutrition (TPN), a saline solution containing essential macronutrients, vitamins, electrolytes and water, is delivered intravenously to bypass the gastrointestinal tract (Gasser and Parekh, 2005). The use of TPN is debated due to numerous associated complications, including sepsis and hepatic dysfunction, motivating research to investigate the consequences of TPN on intestinal microbiota (Kudsk et al., 1992, Peyret et al., 2011). A mouse model of TPN demonstrated that deprivation of enteral nutrition leads to dysbiotic shifts in microbial dominance from Firmicutes to Proteobacteria and Bacteroidetes (Miyasaka et al., 2013). Similar observations were made in rats fed TPN for 14 days with changes in Bacteroidetes and Firmicutes ratio in favour of Bacteroidetes phylum (Hodin et al., 2012). This shift appears to be a consequence of loss of Firmicutes rather than an increase in Bacteroidetes.

Human studies investigating the impact of TPN on intestinal microbiota are few in number and limited, due to the feasibility of sample collection, to analysis of faecal microbiota. One recent study investigated the use of TPN in children with a functional disorder of the small intestine known as short bowel syndrome (Engstrand Lilja et al., 2015). Comparison of the faecal microbiome with both healthy siblings and short bowel syndrome children weaned from TPN demonstrated an overall loss of microbial diversity as well as a distinct increase in relative abundance of Proteobacteria. However, this study also reports long-term antibiotic use in short bowel syndrome patients and it can therefore not be determined whether the observed dysbiosis is a direct consequence of TPN (Engstrand Lilja et al., 2015). Furthermore, this study – and many others – utilise faecal samples to assess the intestinal microbiota with the assumption that they obtain similar microbial distribution and abundance, but faecal microbiota has been reported to have limited representativeness of the mucosal microbiota, largely under-representing bacterial diversity (Durban et al., 2011). In addition to interpatient genetic and environmental variability, issues such as antibiotic use and ideal versus feasible sample collection methods are common hindrances in clinical microbiome studies and efforts should be made to develop scientific models with minimise such issues.

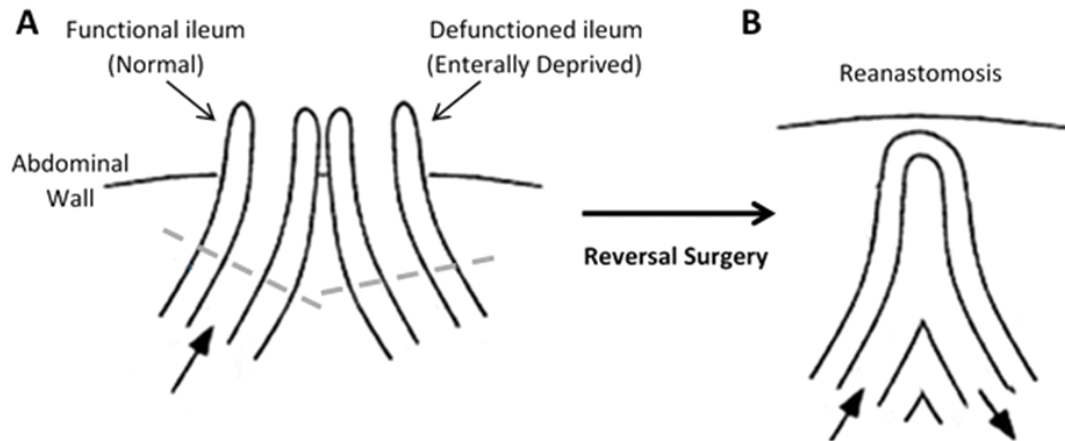


**Figure 3.2 - Structure of the intestine.** A. loop ileostomy and B. following reanastomosis. Block arrows denote presence and direction of luminal contents flow. Tissue located above dashed lines represent areas of intestine removed prior to reanastomosis and form the specimen acquired for our research.

*Figure published in Beamish et al. (2017).*

Patients undergoing loop-ileostomy reversal surgery present a novel human model of TPN (figure 3.2). The enterally deprived, defunctioned ileum receives only blood-borne nutrition and therefore simulates conditions observed with TPN use. Furthermore, the functional ileum serves as a paired control which enables inpatient comparisons, thus negating interpatient variations which often encumber human studies. Harnessing this human model provides unique opportunity to evaluate intestinal microbiota profiles in distinct *in vivo* nutritional environments, eliminating both interspecies and interpatient translational issues common in microbiota studies.

This thesis proposes that ileostomy-mediated faecal stream diversion and the resultant loss of enteral nutrition in the downstream intestine alters microbiota composition and abundance, causing dysbiosis. We aimed to investigate the mucosal- and luminal-associated microbiota in functional and defunctioned intestine, obtained from patients undergoing ileostomy reversal surgery, utilising a variety of biochemical and molecular techniques.

### **3.2 – Research Aims:**

- To investigate alterations in the composition and abundance of the microbiota following a period of enteral nutrient deprivation.
- Attempt to elucidate a characteristic dysbiotic microflora utilising a novel human model in loop ileostomy patients.

### **3.3 – Methods Summary:**

Tissue was obtained and processed from 35 study participants, recruited from Royal Preston Hospital, while 9 participants were excluded on medical grounds. All recruited patients had loop ileostomy to protect downstream anastomoses following resection of colorectal cancer tumours. Loop ileostomies were in place for an average of 12 months prior to reversal surgery.

Microbial DNA was extracted from functional and defunctioned luminal swab and mucosal tissue samples respectively, as described in section 2.2.4. DNA from luminal-associated microbiota was utilised to perform DGGE profiling and qRT-PCR analyses while mucosal-associated microbial DNA was expended in DGGE profiling, total bacterial load quantification and Illumina® 16S sequencing analyses.

### 3.4 – Results:

#### 3.4.1 – Sanger sequencing of extracted DGGE bands enables accurate identification of microbes to genus level.

Evaluation of DGGE band extraction and Sanger sequencing methods to identify unknown bacteria from patient loop ileostomy samples was conducted utilising bacterial DNA from four predominant phyla of the intestinal microbiota. DGGE analysis of DNA extracted from *B. longum*, *B. fragilis*, *E. faecalis*, and *E. coli*, pertaining to Actinobacteria, Bacteroidetes, Firmicutes, Proteobacteria, phyla respectively is presented in figure 3.3. In addition, luminal-associated DNA extracted from functional and defunctioned ileum from one patient are also presented. All sample lanes displayed more than one band despite containing purified DNA from a single species of bacteria, with *E. coli* presenting 4 distinct bands for example.

Figure 3.4 presents fourteen bands post extraction and purification with corresponding species assignment for ten samples sequenced. Visual analysis of the gel revealed that not all bands were successfully isolated; bands 1, 5, 6 and 7 presented multiple bands after one round of purification. In addition, bands 10 and 14 appeared to have amplified an incorrect band and as a result were not selected for sequencing. However successful isolation of bands 10-13, as determined via presence of single band, demonstrated that bands of interest can be extracted from complex mixed microbial samples.

Taxonomic species assignment, via BLAST analysis, was possible for nine of ten samples sequenced (figure 3.4). Confident taxonomic assignment was unsuccessful for the consensus sequence generated from band 1, likely due to contaminating DNA from another distinct band present in the sample (figure 3.4). In addition, band 4 was incorrectly assigned as uncultured *Bifidobacterium sp.* when it was in fact DNA extracted from *B. longum*. It was therefore decided that bacterial taxonomic assignment should be limited to genus level for unknown bands extracted from mixed samples. It was also concluded that multiple rounds of extraction and purification should be performed to obtain a single band prior to sequencing analysis.



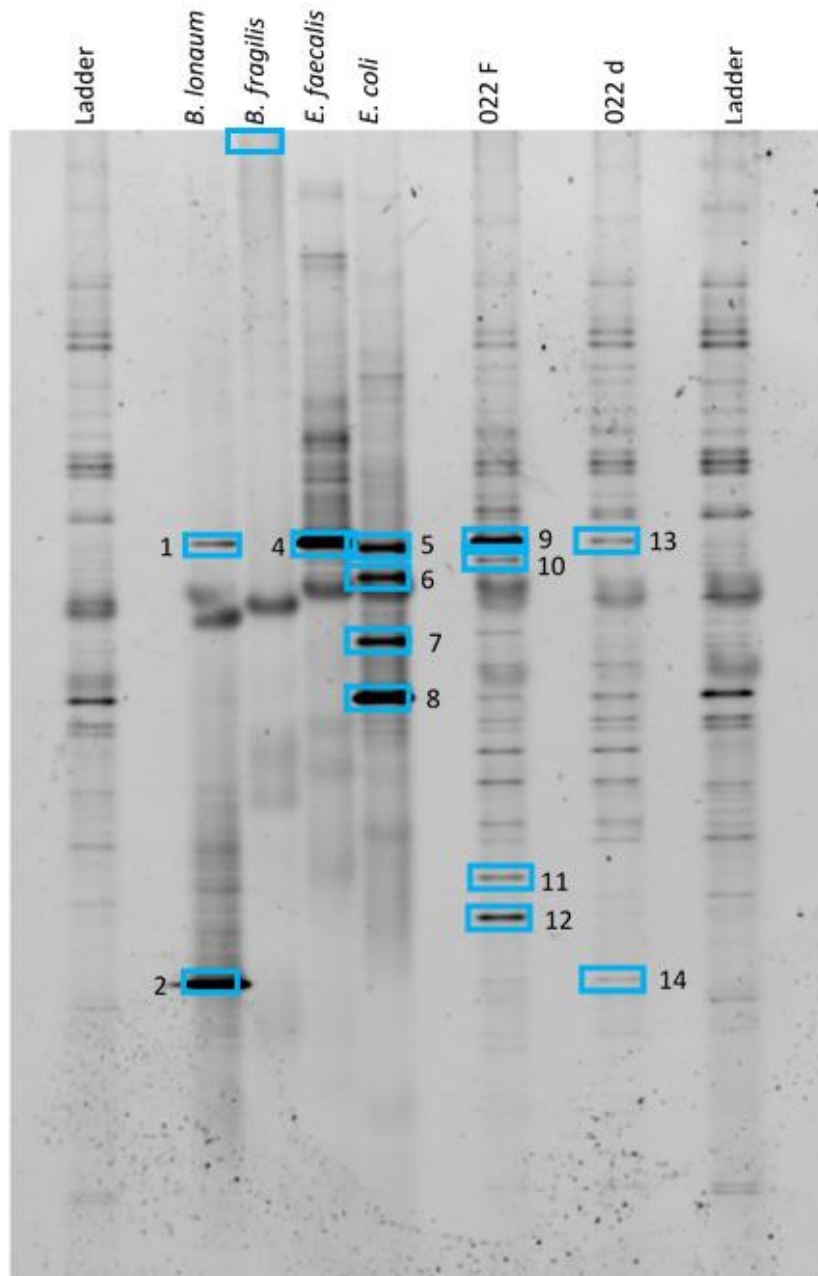


**Figure 3.3 – Microbial DGGE profiles for band extraction and sequencing.**

DGGE-PCR analysis of 16S rDNA PCR amplicons of bacterial species representing four predominant gut phyla: *B. longum*, Actinobacteria; *B. fragilis*, Bacteroidetes; *E. faecalis*, Firmicutes and *E. coli*, Proteobacteria, in addition to unknown functional and defunctioned paired profiles from patient 022. Blue boxes highlight bands selected for extraction.

Ladders composed from pooled faecal microbiota DNA to enable comparison between gels. Abbreviations: F, functional; D, defunctioned.

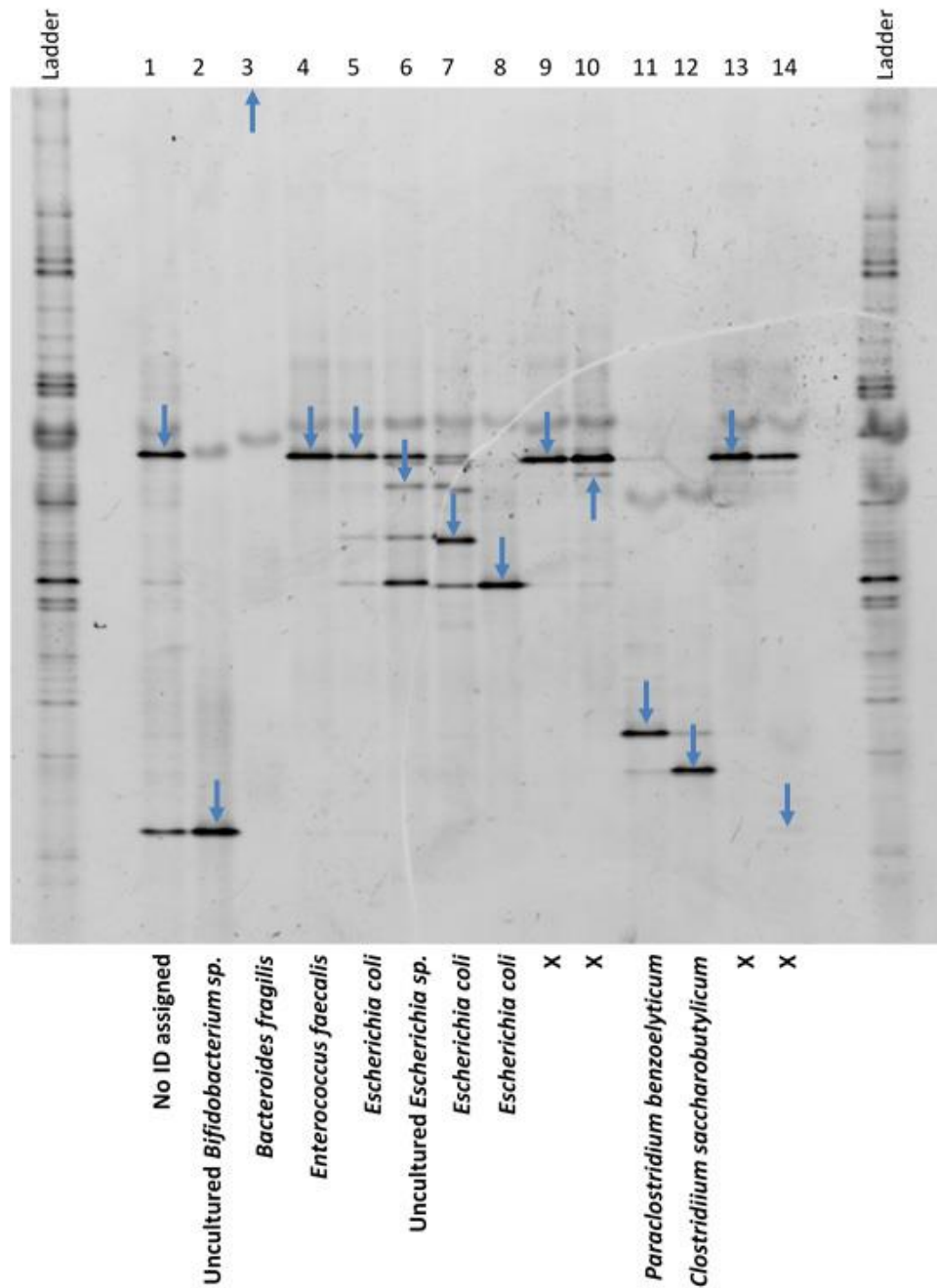


**Figure 3.4 – Species assignment for extracted and sequenced microbial DGGE bands.**

DGGE-PCR analysis of fourteen bands extracted and purified from microbial DGGE profiles presented in figure 3.3, as indicated by blue arrows. Ten of the fourteen bands were selected for sequencing. Inclined, the corresponding bacterial species ID for each band sequence is displayed. 'X' samples were not selected for sequencing. Consensus sequences and taxonomic assignments for each band class are presented in appendix 4.

Ladders composed from pooled faecal microbiota DNA to enable comparison between gels.

### 3.4.2 – Total bacterial load is significantly reduced in defunctioned intestine.

Quantification of total mucosal-associated bacterial load was conducted via determination of the 16S rRNA gene copy number. Small intestinal bacterial load is considered to be around  $10^8$  cells per mL of luminal content (Berg, 1996). In accordance with this, the average mucosal-associated bacterial load in the functional ileum was calculated to be  $2.63 \times 10^8$  gene copies per gram of tissue, compared with  $9.89 \times 10^7$  in the defunctioned (figure 3.5A). This constituted to a 62.4% average decrease in total bacterial load in the defunctioned ileum (figure 3.5A;  $n = 27$ ,  $p = 0.0003$ ). A reduction occurred consistently across all paired samples tested (figure 3.5B), suggesting that faecal stream diversion and consequential microbial enteral nutrient deprivation leads to a substantial reduction in total mucosal-associated bacterial load.

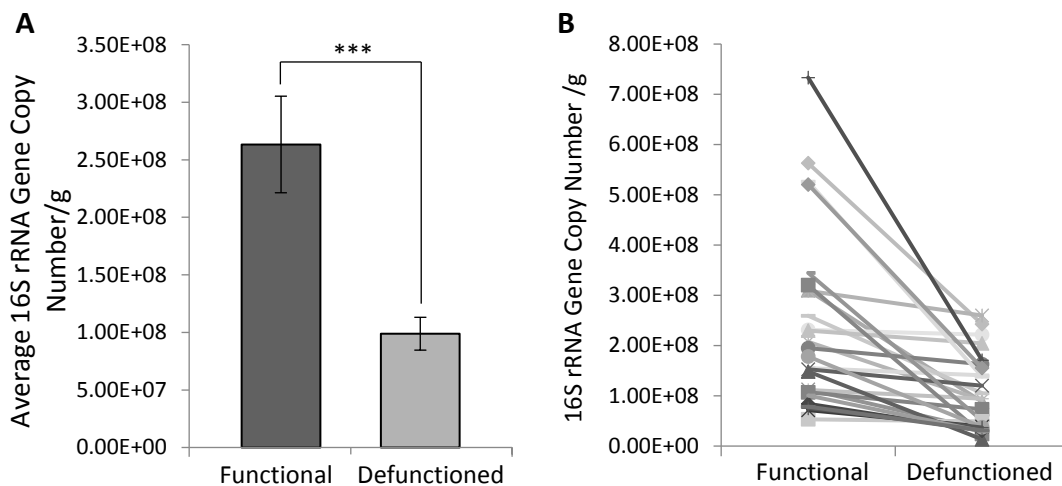


**Figure 3.5 - Enumeration of total bacterial load.** Bacterial enumeration of (A) average- and (B) absolute-16S rRNA gene copy numbers per gram of mucosal tissue in functional and defunctioned intestine ( $n = 27$ ;  $p = 0.0003$ ). *Data published in Beamish et al. (2017).*

### 3.4.3 – Luminal-associated microbiota profiles differ in functional and defunctioned intestine.

Inpatient comparisons of luminal-associated microbiota profiles from functional and defunctioned intestine were conducted to investigate potential variations in luminal microbial composition utilising universal 16S rDNA PCR and visualised via DGGE analysis (figure 3.6). Unsurprisingly, it is immediately evident from figure 3.6 that distinctive microbial profiles are apparent both between patient samples and within paired samples taken from our patient cohort, as evidenced by visibly diverse banding patterns.

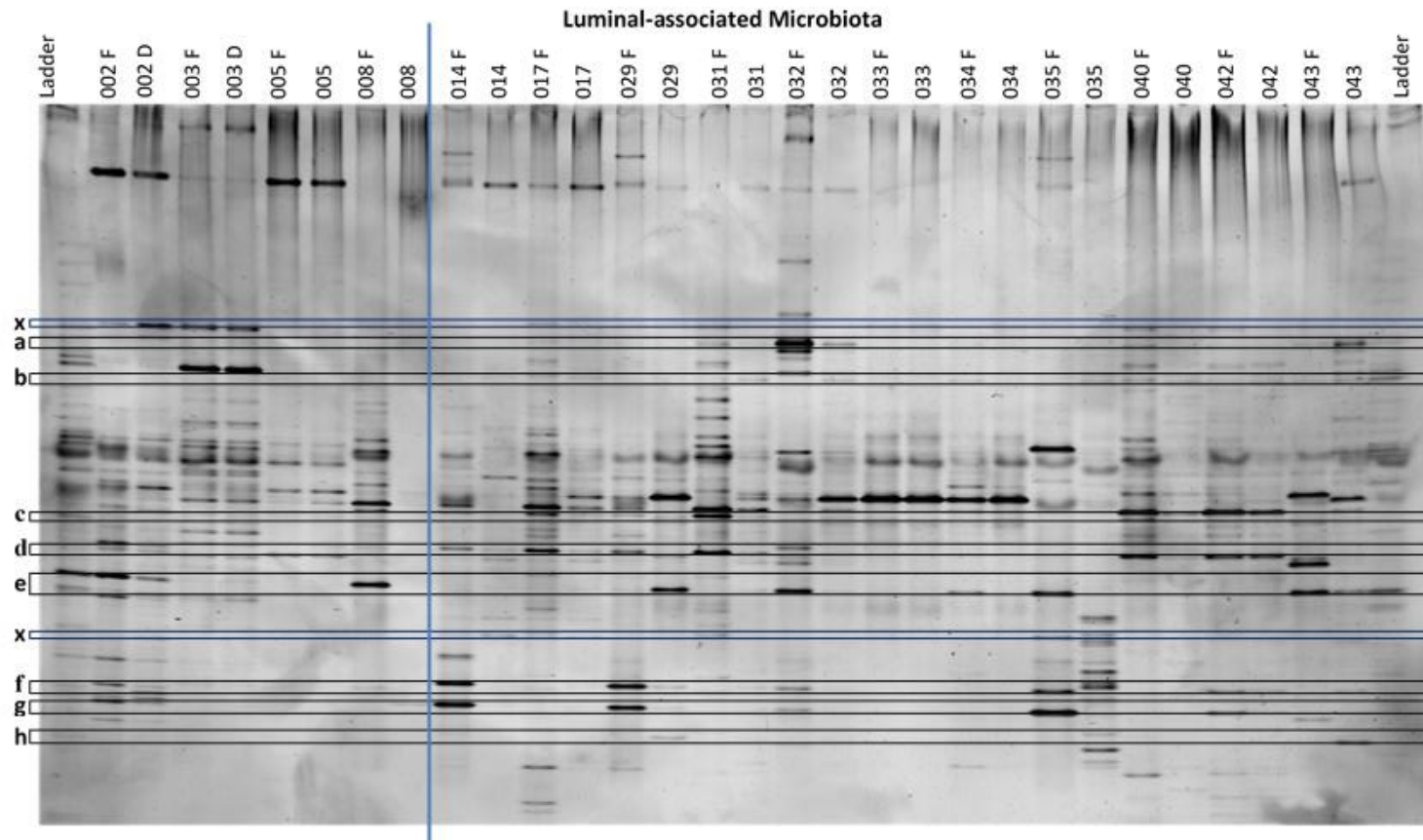


**Figure 3.6 - Inpatient comparisons of luminal-associated intestinal microbiota profiles between functional and defunctioned intestine.** DGGE-PCR analysis of 16S rDNA PCR amplicons. Band classes are depicted using characters a through h and corresponding bands are enclosed. X depicts band classes lost during extraction. Blue line segregates samples excluded from downstream analysis due to variant processing methods. Ladders composed from pooled faecal microbiota DNA. Abbreviations: F, functional; D, defunctioned.

*Data published in Beamish et al. (2017).*

Digital processing of the gel image enabled identification of common band classes shared between different samples, presented in the form of a binary presence or absence banding profile (appendix 2). Each band on a DGGE gel represents one or more closely related bacterial species therefore the number of bands in each profile can be considered to reflect the number of different bacterial species and thus overall microbial diversity. On average, the total number of bands in the defunctioned profiles was lower than the number observed in the functional profiles (average of 16 bands to 11 bands, respectively; figure 3.7A), indicating that faecal stream diversion reduces diversity of the intestinal microbiota. A reduction in diversity was not observed consistently across the cohort as three samples were found to have an equal or increased number of bands in the defunctioned profiles (figure 3.7B). Interestingly, such samples had the lowest diversity in the functional ileum (figure 3.7).

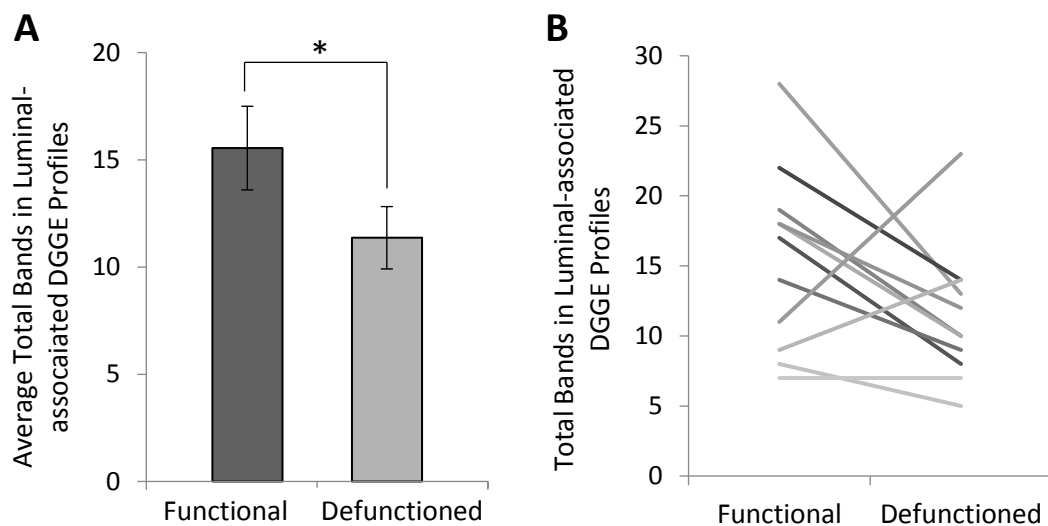


**Figure 3.7 - Luminal DGGE band analysis.** (A) average- and (B) absolute-number of bands in luminal-associated DGGE profiles, representing microbial diversity. n = 11, p ≤0.05.

*Data published in Beamish et al. (2017).*

Subsequent hierarchical cluster analysis of the binary data, presented in figure 3.8, revealed considerable similarity between the defunctioned profiles as they frequently clustered together rather than with their paired functional counterparts. Profiles from functional intestine were also observed to cluster together demonstrating that, irrespective of natural interpatient genetic and environmental variability, distinct luminal-associated microbial populations exist within the functional and defunctioned intestine.

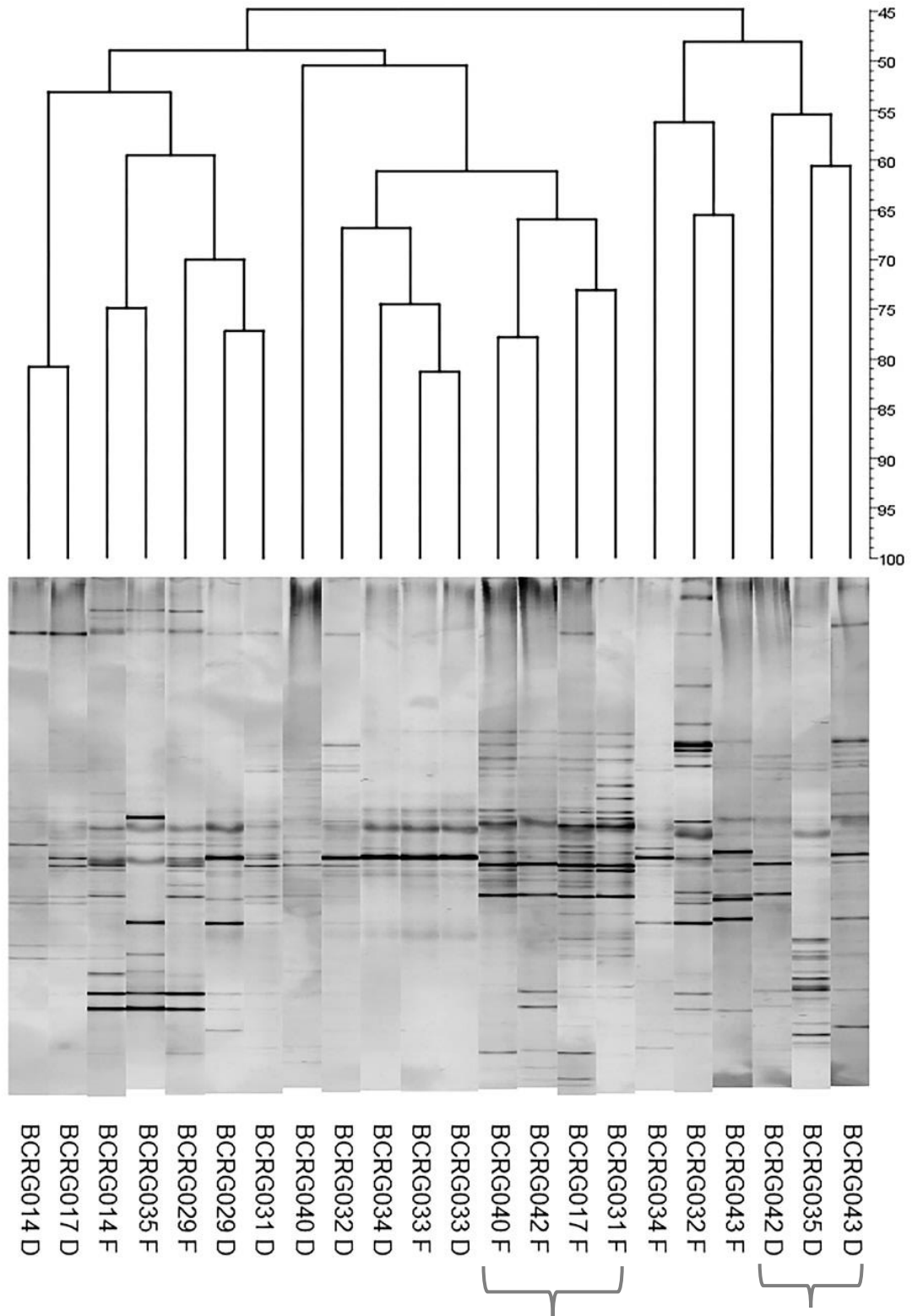


**Figure 3.8 – Hierarchical cluster analysis of luminal-associated DGGE profiles** represented in graphical form as an UPGMA dendrogram. Braces highlight examples for functional and defunctioned profile clusters F: functional ileum, D: defunctioned ileum. n = 11. *Data published in Beamish et al. (2017).*

### 3.4.4 – Luminal-associated microbial dysbiosis is apparent at phylum and genus level in defunctioned ileum.

To further characterise the apparent disparity in luminal-associated microbial profiles between the functional and defunctioned intestine, Sanger sequencing analysis was performed on extracted band classes of interest (figure 3.9). In total, 73 distinct band classes were identified across 22 DGGE profiles (11 functional and 11 defunctioned paired samples). A total of 10 band classes, differing in percent presence between functional and defunctioned profiles, were selected and of these 8 were successfully extracted, purified and sequenced (appendix 3; figure 3.9). Subsequent BLAST analysis revealed the highest matched identities from NCBI nucleotide databases for each band class and the highest sequence similarity (99-100%) match was assigned at genus level. Band classes a and b were assigned to the *Bacteroides* genus, band class c and d to *Streptococcus*, band class e to *Shigella*, band class f and g to *Clostridium* and band class h to *Spirosoma*. *Shigella* is a human pathogen that is not commonly associated with the intestinal microbiota. Therefore it is likely that Band e was misclassified and is actually the closely related common commensal, *Escherichia*.

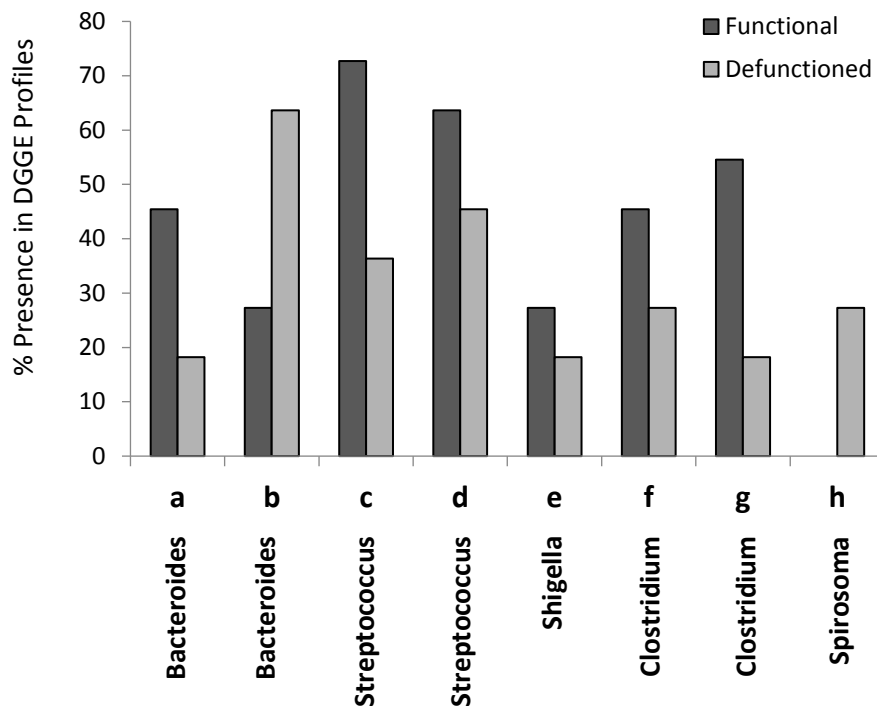


**Figure 3.9 – Luminal band class quantification.** Luminal-associated DGGE band classes differing in functional versus defunctioned profiles expressed as a percentage presence across all patients. Characters a-h correspond to the band classes highlighted in figure 3.6. Inclined, the corresponding bacterial genus ID for each band class is displayed. Consensus sequences and taxonomic assignments for each band class are presented in appendix 4.

*Data published in Beamish et al. (2017).*

Figure 3.9 also demonstrates percent reductions in *Clostridium* (18.2% and 36.3% band class f and g, respectively), *Shigella* (9%, band e) and *Streptococcus* (36.3% and 18.2%, band c and d) genera across defunctioned profiles, compared with functional. Conversely, an increase in the percentage presence of *Spirosoma* (27% increase, band h) was observed in the defunctioned ileum. Interestingly, members of the Bacteroides genus were observed to increase or decrease in percent presence across the functional and defunctioned profiles (27.3% reduction and 36% increase, band a and b, respectively; figure 3.9).

Furthermore, the relative percent abundance of three predominant intestinal microbial phyla, Firmicutes, Bacteroidetes and  $\gamma$ -Proteobacteria, were calculated in the defunctioned intestine compared to the paired functional control, utilising qRT-PCR (figure 3.10). A significant reduction in the relative abundance of the Firmicutes phylum was observed in the defunctioned intestine (21% reduction,  $n = 18$ ;  $p = 0.02$ ), in addition to a concomitant small but significant increase in the  $\gamma$ -Proteobacteria phylum (6.9% increase,  $n = 9$ ,  $p = 0.05$ ). Consistent with the DGGE sequencing data, no significant difference was observed in the relative abundance of the Bacteroidetes phylum, due to substantial variation in phylum abundance across the patient cohort ( $n = 17$ ,  $p = 0.22$ ).

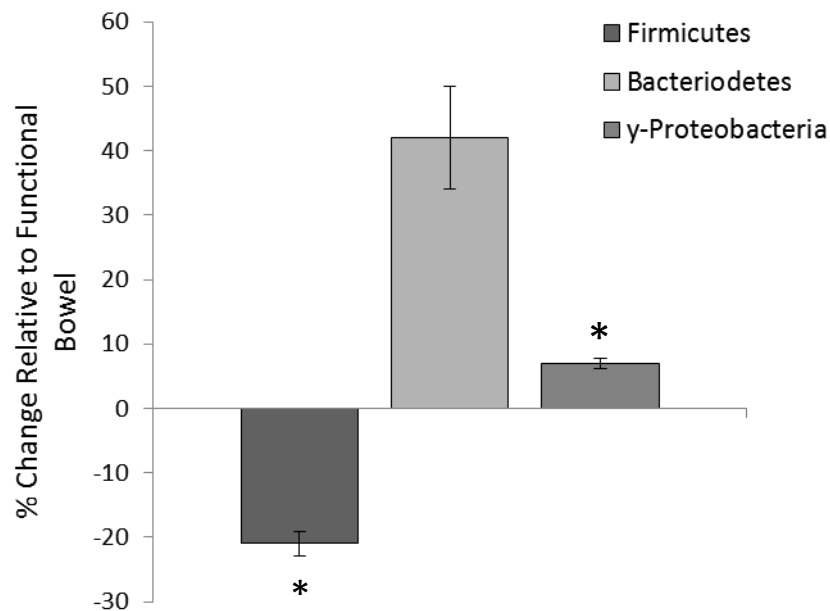


**Figure 3.10 – Relative quantification of predominant luminal-associated phyla.** Percent change of phylum abundance in defunctioned intestine relative to functional. Data normalised to universal 16S rDNA primers (Firmicutes ( $n = 18$ ,  $p = 0.02$ ), Bacteroidetes ( $n = 18$ , NS),  $\gamma$ -Proteobacteria ( $n = 9$ ,  $p \leq 0.05$ )). *Data published in Beamish et al. (2017).*



### 3.4.5 – Mucosal-associated microbial profiles differ in functional and defunctioned intestine following ileostomy-mediated enteral nutrient deprivation.

Inpatient comparisons of mucosal-associated microbial profiles were performed to assess the extent of dysbiosis within microbial populations at mucosal level utilising universal 16S rDNA PCR and visualised via DGGE analysis (figure 3.11). As with luminal-associated DGGE profiles, distinct mucosal-associated microbial populations were observed both between and within paired patient samples, as evidenced by clearly diverse banding patterns. No difference was observed in the number of DGGE bands between the mucosal-associated functional and defunctioned profiles suggesting that the diversity of mucosal-associated microbiota is maintained despite enteral nutrient deprivation (figure 3.12).

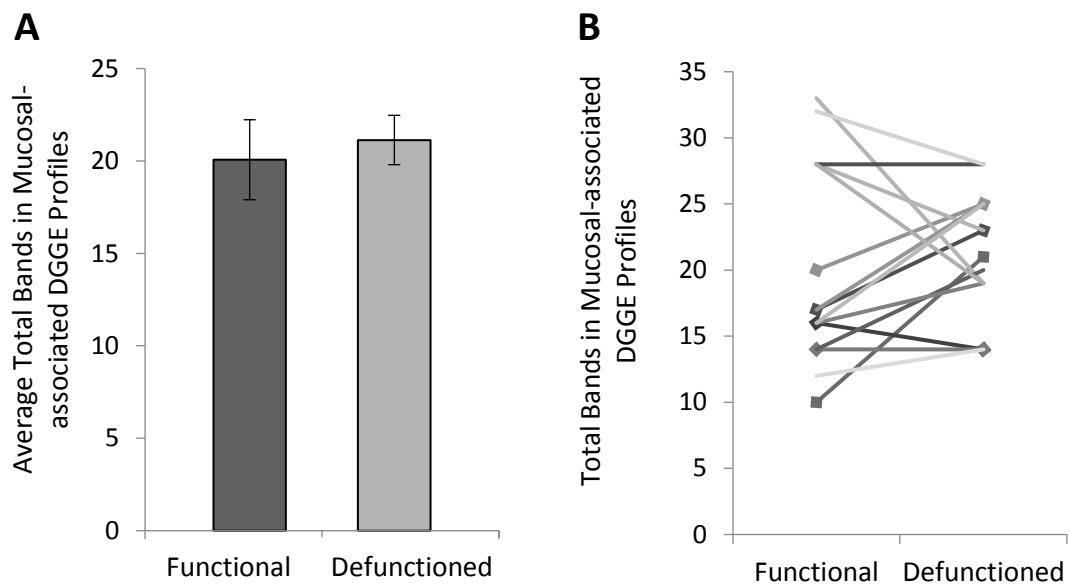


**Figure 3.12 - Mucosal DGGE band analysis.** (A) average- and (B) absolute-number of bands in mucosal-associated DGGE profiles, representing microbial diversity.  $n = 15$ ,  $p > 0.05$ .

Hierarchical cluster analysis of binary data, representing common band classes shared between sample profiles, revealed that distinct mucosal-associated microbial profiles exist in defunctioned and functional ileum as the profiles were observed to cluster together (figure 3.13). However mucosal-associated microbiota in defunctioned ileum appear less affected by ileostomy-mediated nutrient diversion compared to luminal-associated microbiota as four patient's defunctioned samples clustered with their functional counterparts thus maintaining paired nature (figure 3.13 arrows).

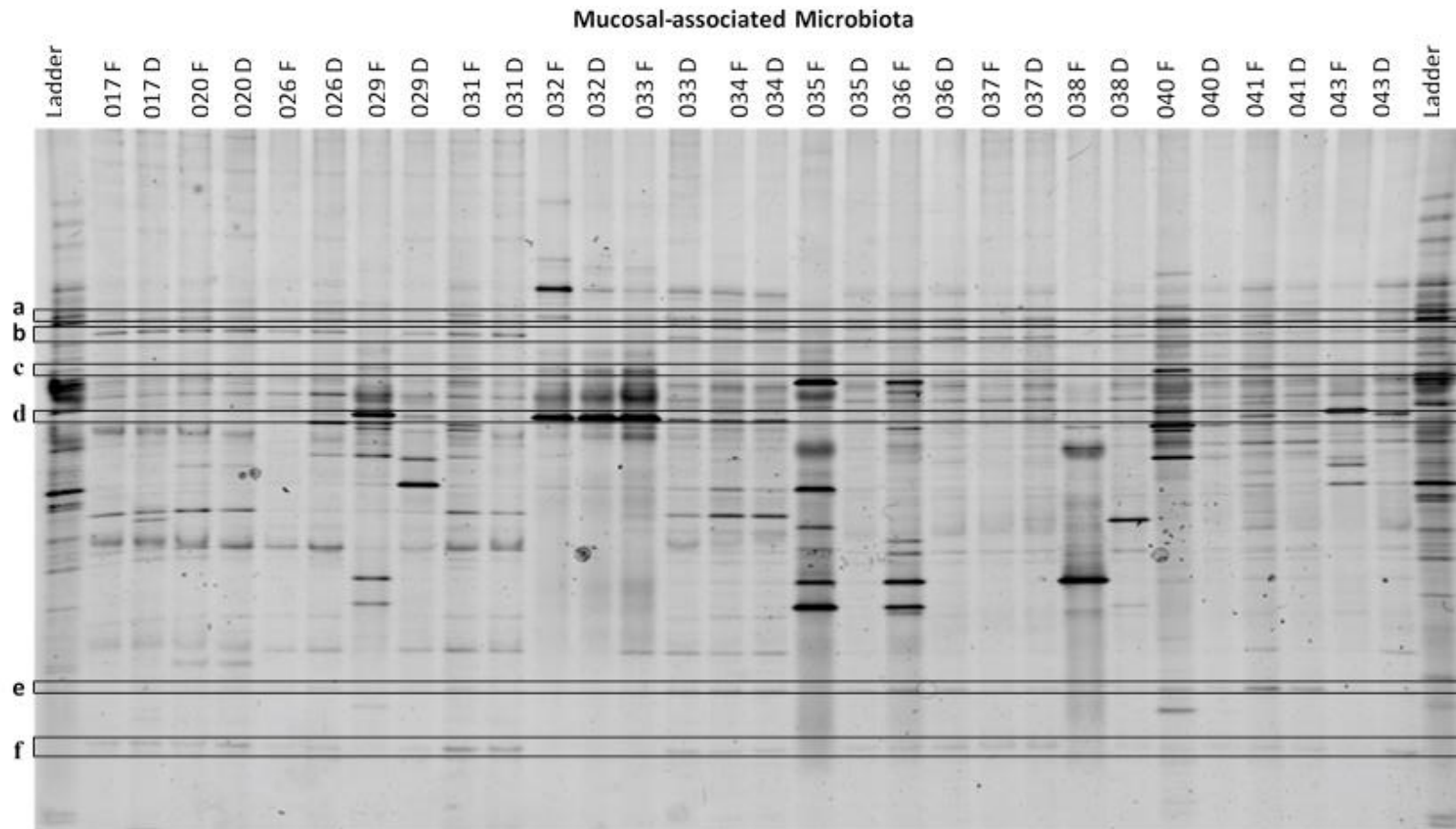


**Figure 3.11** - Inpatient comparisons of mucosal-associated intestinal microbiota profiles between functional and defunctioned intestine. DGGE-PCR analysis of 16S rDNA PCR amplicons. Band classes are depicted using characters a through f. Ladders composed from pooled faecal microbiota DNA. Abbreviations: F, functional; D, defunctioned.

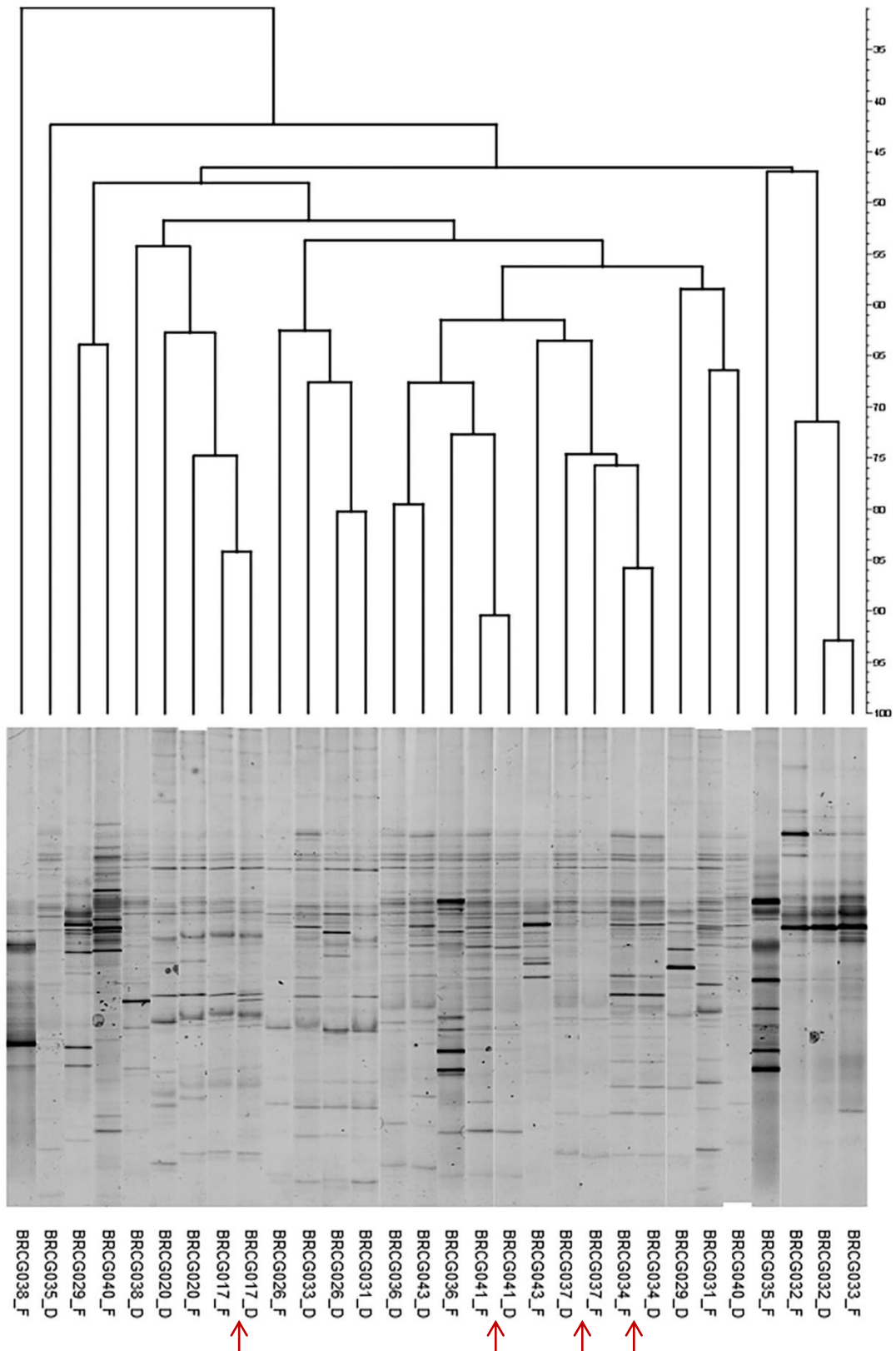


**Figure 3.13 - Hierarchical cluster analysis of mucosal-associated DGGE profiles** represented in graphical form as an UPGMA dendrogram. Red arrows highlight samples with retained paired sample nature. F: functional ileum, D: defunctioned ileum. n = 15.

### 3.4.6 – Mucosal-associated microbial dysbiosis is apparent at phylum, order and genus level in defunctioned ileum.

To further elucidate mucosal-associated microbial profiles in functional and defunctioned intestine, band classes of interest were extracted and purified for Sanger sequencing analysis. A total of 96 distinct band classes were identified across 30 DGGE profiles (15 functional and 15 defunctioned paired samples). Band classes were assessed for percent presence in functional and defunctioned profiles and from a selection of 10, 6 were successfully extracted and purified and sequenced (appendix 3; figure 3.14). Due to limited sequence read quality, confident genus assignment, with a sequence similarity of 99-100%, was successful with only 3 band classes during subsequent BLAST analysis using NCBI nucleotide databases (figure 3.14). The generated data demonstrates a reduction in the *Gemella* and *Enterococcus* genera and a concurrent increase in the *Bacteroides* genus in the defunctioned ileum compared to functional (figure 3.14).

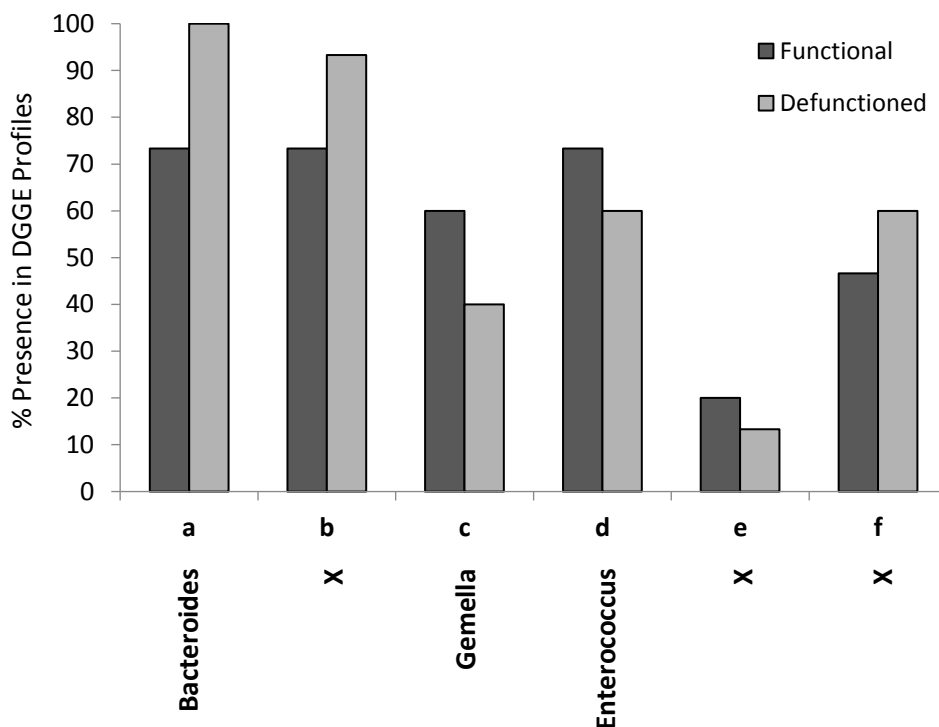


**Figure 3.14 - Mucosal band class quantification.** Mucosal-associated DGGE band classes, differing in functional versus defunctioned profiles, expressed as a percentage presence across all patients. Characters a-f represent band classes highlighted in figure 3.11. Inclined, corresponding bacterial genus ID for each band class. Consensus sequences and taxonomic assignments for each band class are presented in appendix 4.

Next-generation Illumina® sequencing analysis of the mucosal-associated microflora, classified to phylum level, revealed alterations in the proportions of three predominant phyla analogous to that observed in the luminal-associated profiles; relative increase in Proteobacteria, relative decrease in Firmicutes and a varied response in Bacteroidetes phylum in the defunctioned ileum compared to the functioned controls (figure 3.15). This trend was observed in all except one patient in which the defunctioned profile microbiota proportions remained relatively unchanged despite enteral nutrient deprivation (Patient 043). Contrastingly, a drastic shift in microbial profiles was observed in another patient, with microbial dominance shifting almost entirely from Firmicutes to Proteobacteria (Patient 029). Furthermore, less predominant bacterial phyla, including *Chloroflexi*, Fusobacteria, OD1, *Cyanobacteria* and Actinobacteria, were identified to increase in relative proportion in the defunctioned ileum.

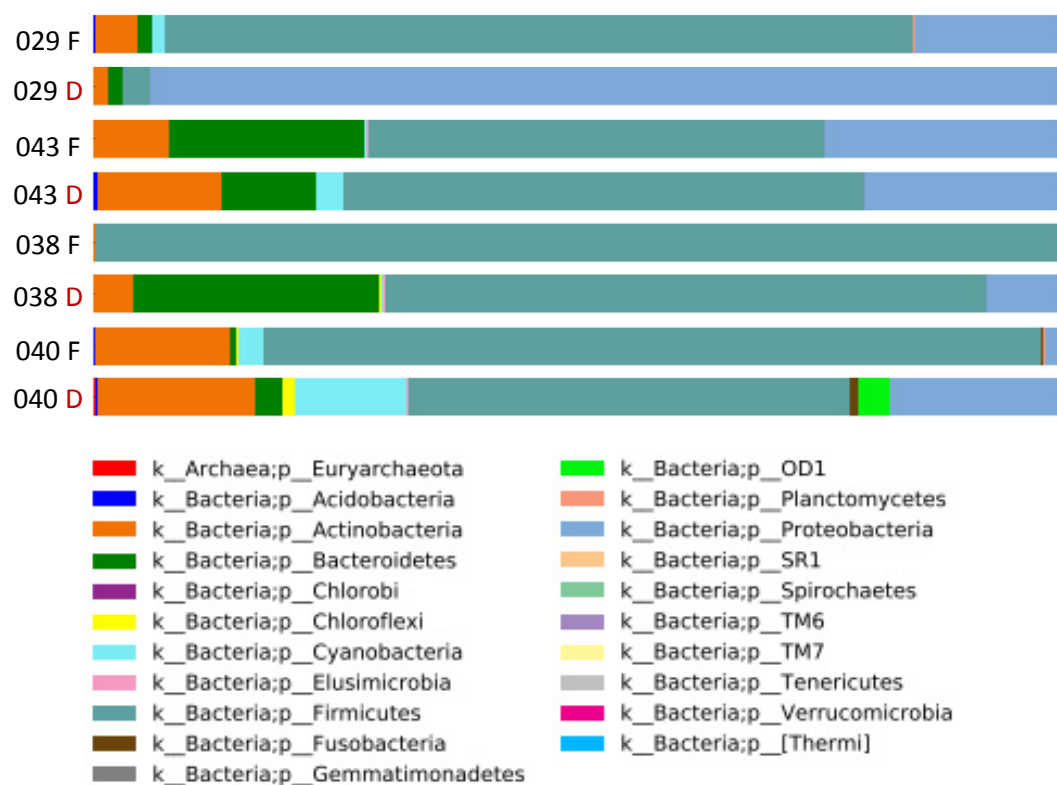


**Figure 3.15** - Relative taxonomic composition of 16S rRNA amplicon sequences in mucosal-associated microbiota, at phylum level. F, functional; D, defunctioned. n = 4.

Taxonomic classification of sequencing data to order and genus level was carried out in attempt to further characterise dysbiosis in the defunctioned ileum. This revealed the order Clostridiales and Lactobacillales, of the Firmicutes phylum, are predominantly associated with the functional intestine, often decreasing in relative terms in the defunctioned ileum (figure 3.16). Likewise, Enterobacteriales and Pseudomonadales are the predominant order of the Proteobacteria phylum, appearing to increase in relative abundance in the defunctioned ileum. Interestingly, several less abundant order, including Xanthomonadales, Rhizobiales and Burkholderiales are primarily acquired in the defunctioned ileum and contribute to predominance of Proteobacteria. The order, Actinomycetales and Bifidobacteriales compose the Actinobacteria phylum and appear to remain stable within the defunctioned ileum often presenting near equivalent relative abundance that observed in paired functional profiles.

Further analysis of sequencing data revealed a large variation in microbial diversity within both functional and defunctioned profiles is also apparent across the cohort, at genus level, highlighting the extent of interpatient variability in the intestinal microbiome (figure 3.17). In addition, increased bacterial diversity in the functional ileum appears to support greater preservation of microbial profiles in the defunctioned ileum, despite enteral nutrient deprivation. For example, patient 043 hosts numerous genera within the Firmicutes phylum which are largely maintained in the defunctioned ileum. In contrast, patients 029 and 040 host predominately *Enterococcus* and *Streptococcus* within the functional ileum, respectively and are observed to lose substantial portions of such microbes in the defunctioned ileum. However, this data requires quantification, using OTU counts for each paired sample, to confirm such suggestions.

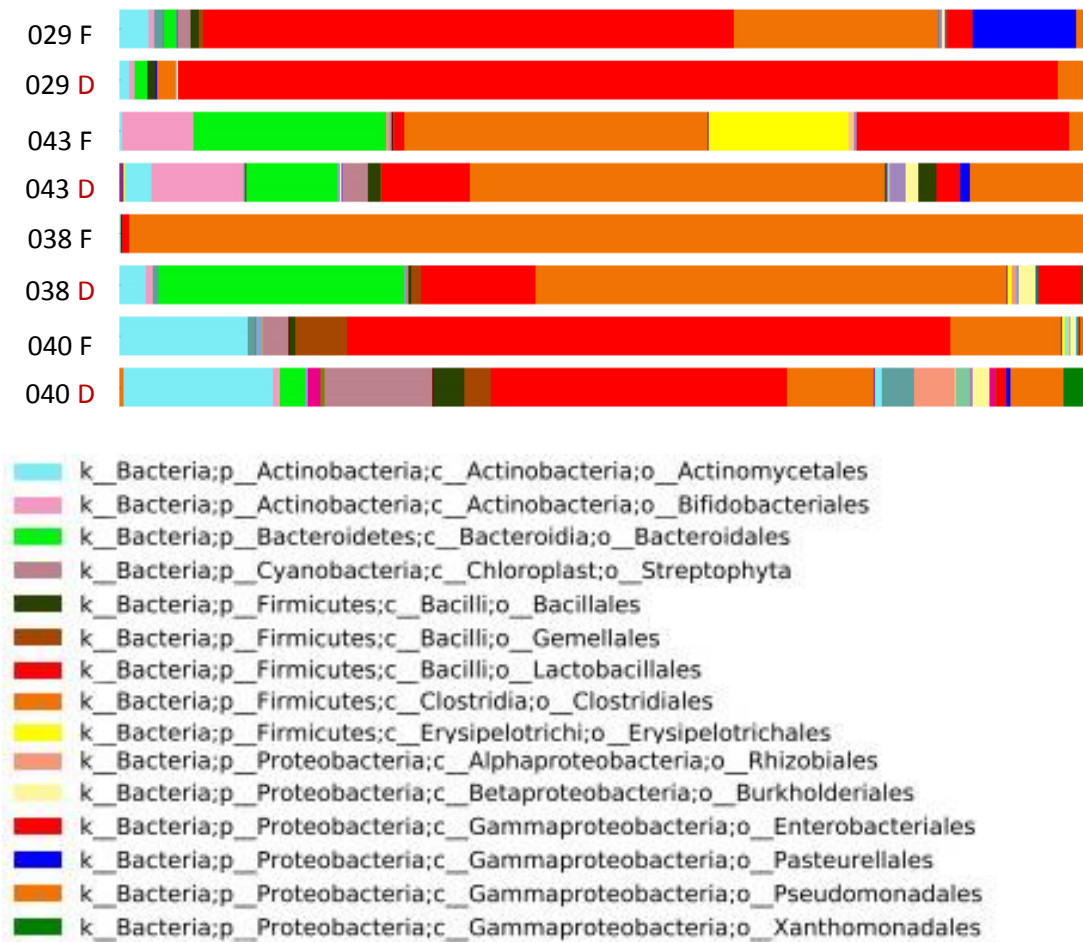


**Figure 3.16** - Relative taxonomic composition of 16S rRNA amplicon sequences in mucosal-associated microbiota, at order level. F, functional; D, defunctioned. n=4.

Key presents predominant order. Annotated figure and complete key detailing all assigned taxonomic classifications is presented in appendix 11. F, functional; D, defunctioned. n = 4.

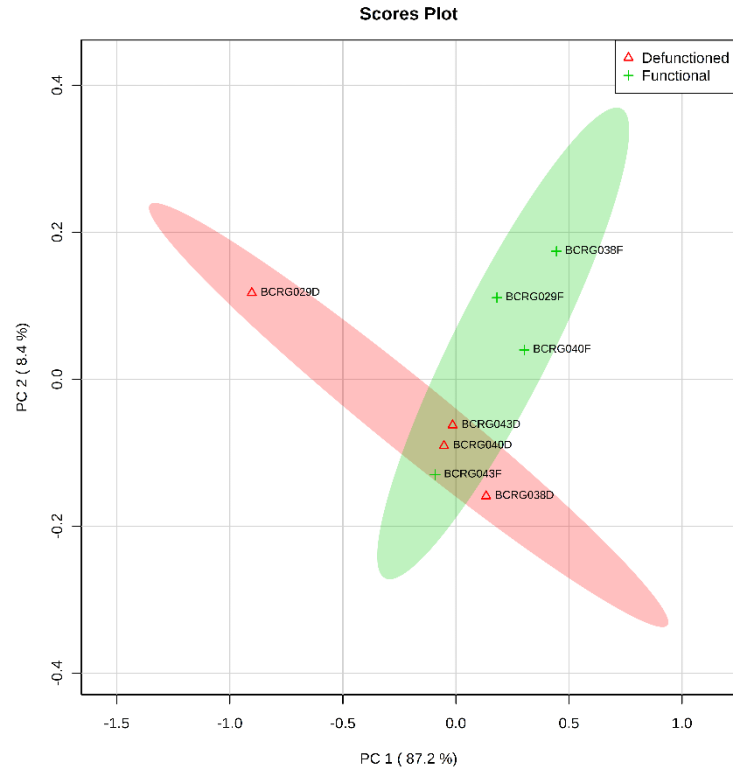
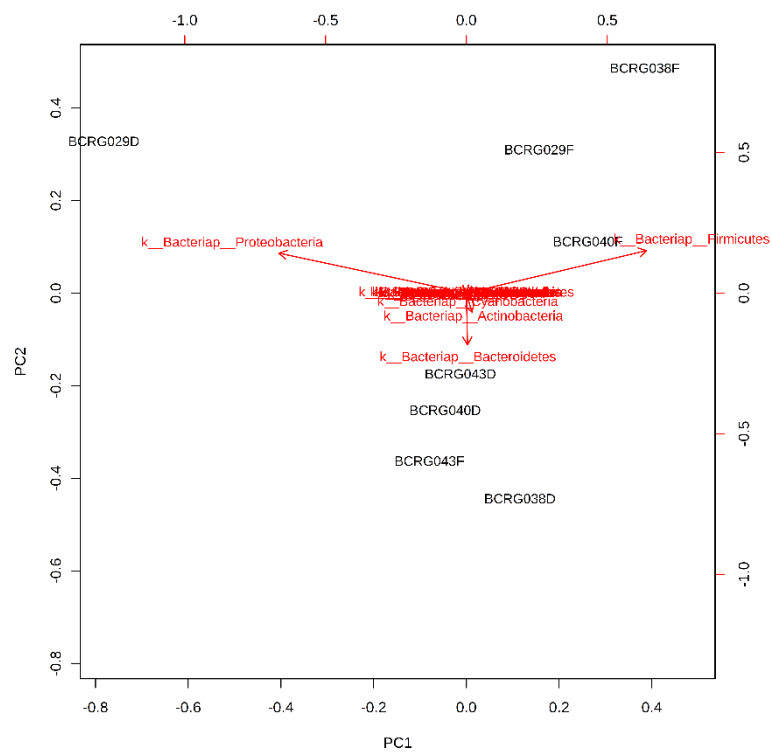


**Figure 3.17** - Relative taxonomic composition of 16S rRNA amplicon sequences in mucosal-associated microbiota, at genus level. F, functional; D, defunctioned. n=4.

Key presents predominant genera. Annotated figure and complete key detailing all assigned taxonomic classifications is presented in appendix 12. F, functional; D, defunctioned. n = 4.



Finally, PCA was executed to visualise structure within the microbiota sequencing data (figure 3.18). Separation was observed between the functional and defunctioned microbiota profiles with an overlap occurring due to the similarity of 043 functional sample with defunctioned profiles (figure 3.18A). The associated PCA biplot suggested that relative proportions of Firmicutes, Bacteroidetes and Proteobacteria defined the variability between clusters with Firmicutes correlating with the majority of functional samples whilst proportions of Bacteroidetes and Proteobacteria correlate with defunctioned profiles, as evidenced by the magnitude and direction of respective vectors (figure 3.18B). The similarity of sample 043F with defunctioned profiles is observed to be a result of reduced Firmicutes proportions (figure 3.18B). Sample 029D was identified to be a potential outlier with substantial proportions of Proteobacteria, but this cannot be confirmed due to limited sample numbers.

**A****B**

**Figure 3.18 – PCA of functional and defunctioned mucosal-associated microbiota. (A)** PCA scores plot and **(B)** corresponding biplot of proportionate mucosal-associated microbiota profiles, at phylum taxonomic level, from functional (green; F) and defunctioned (red; D) ileum.

### 3.5 – Discussion:

For the first time, this research demonstrated a strong relationship between loop ileostomy-mediated faecal stream diversion and profound alterations in the intestinal microbiota of the defunctioned ileum at the time of reversal. A significant reduction in total bacterial load in the defunctioned intestine was identified, as determined by a reduction in 16S rRNA gene copy number, as well as broad shifts in microbiota composition between functional and defunctioned intestine. Of particular note, a significant loss of the predominant phylum Firmicutes was observed with a concomitant increase in  $\gamma$ -Proteobacteria in the defunctioned ileum. Such dysbiotic characteristics are also reported in IBD, suggesting that the microflora in the defunctioned ileum may potentially disrupt homeostasis and/or promote disease (Baumgart et al., 2007, Sokol et al., 2008). Furthermore, these results are also consistent with that reported in the study investigating the effects of TPN on the microbiota of human small intestine (Ralls et al., 2014). Interestingly, the study reports a correlation between duration of TPN use and increased severity of dysbiosis; participants fed with TPN either partially, or for less than 6 weeks, somewhat maintained microbial diversity compared to one participant given TPN for >2 months. Given that the downstream intestine in participants of this study remained defunctioned for an average of one year, it is unsurprising that such profound dysbiosis was observed.

The copy number of the 16S rRNA gene is frequently utilised as a measure of bacterial load in microbial studies for both clinical and environmental samples as it is highly conserved between species of bacteria and contains 9 hypervariable regions which enable reliable taxonomic classification (Klappenbach et al., 2001). The 16S rRNA gene copy number varies considerably between bacterial species, with *E. faecalis* of the Firmicutes phylum obtaining 4 copies whilst *E. coli* of Proteobacteria harbours between 7 and 9 copies (Klappenbach et al., 2001). In this study, gene quantification revealed an average of 62.4% reduction in total bacterial load in the defunctioned ileum across the patient cohort. However, the reduction in bacterial cell numbers may be underestimated due to dysbiotic shift in favour of Proteobacteria which appear to obtain more copies of the 16S rRNA gene per bacteria. Despite this, the overarching conclusion that total bacterial load is significantly reduced in the defunctioned ileum remains the same.

Loss of total microbiota is also reported in patients with anorexia nervosa when compared to gender and age matched controls (Morita et al., 2015). Anorexia nervosa patients electively halt their intake of food, without receiving artificial nutrition such as TPN, meaning the intestine is consequently defunctioned and the microbiota starved. The observed reduction in total bacteria was attributed to significant losses of members of the Firmicutes phylum, including *Clostridium* and *Streptococcus*, as well as *Bacteroides* of the Bacteroidetes phylum (Atarashi et al., 2013). These observations are consistent to that reported in defunctioned limb of loop-ileostomy patients in this study with a loss of *Streptococcus* and *Clostridium* reported in both DGGE and Illumina® deep sequencing analyses. Moreover, expansion of the Firmicutes phylum is frequently found in obese humans and also correlated with adaption of a westernised diet, which is likely due to an increased capacity for energy harvest from high fat diet (Turnbaugh et al., 2006, De Filippo et al., 2010). Considering this, such drastic losses of predominant microbial phyla in the nutritionally deprived defunctioned intestine is to be expected. This research also reported parallel increases in the abundance of the Proteobacteria phylum following a period of enteral nutrient deprivation. Such shifts in microbial abundance are likely due to changes in nutrient availability within the intestine. Members of the Proteobacteria phylum have previously been shown to achieve increased survival rates in nutritionally restricted environments, including sterile PBS and sewage water when compared with other bacterial populations (Sinclair and Alexander, 1984). In addition, literature has recently begun to consider Proteobacteria as a microbial signature of dysbiosis in the intestine due to its recurrence in various dysbiosis-associated diseases, particularly IBD (Baumgart et al., 2007). It is also important to note that the microbiota sequencing data is presented as relative proportions in abundance meaning increases reported in certain microbiota populations, such as Actinobacteria and Proteobacteria, may be a reflection of the reduced total bacteria load, rather than increases in their numbers.

Illumina sequencing of mucosal-associated microflora provided detailed insights into the microbial profiles of the functional and defunctioned intestine and distinct differences were observed throughout the cohort. Despite analysing phylogenetic profiles to genus level, we were unable to define a specific microbial profile characteristic of either nutritional environment. Although disappointing, this is largely unsurprising considering culture-independent sequencing studies have demonstrated that an individual can host up to 200 of

a possible 1,000 species-level phylotypes and reports have noted significant variation in species composition within the intestinal microbiota between healthy individuals (Avershina and Rudi, 2015, Eckburg et al., 2005). Given the enormous and unique diversity of the intestinal microbiota, it is becoming seemingly unlikely that a determinative loss or gain of specific bacterial genera for dysbiosis will be identified, meaning a 'one microbiome fits all' principle will not extend past the phylum level. To transition into clinical application the individuality of intestinal microbiota must be accommodated and it may be that diagnostic and therapeutic techniques will become personalised. Furthermore decreasing costs of next generation sequencing technologies will promote such clinical advancements.

The data presented herein also suggests that increased taxonomic diversity in functional ileum may better preserve microbial profiles through a period of enteral nutrient deprivation. Previous studies have demonstrated that communities rich in diversity are more resistant and resilient to perturbing environmental factors and biological invasion. For instance, the invasive capacity of the weed, *Crepis tectorum*, was found to be limited in areas with high resident plant diversity due to limited nutrient and light availability, increasing biological competition (Naeem et al., 2000). Furthermore, soil microbial communities high in species richness were found to be more resilient to various environmental stressors, such as copper and excessive heat, than those with low diversity (Griffiths et al., 2005). This was suggested to be due to a larger functional capacity of the diverse microbiota. Such principle can also extend to the intestinal microbiota as low microbial diversity in the intestine has been correlated with IBD, but it has not been yet determined whether such observations are causative or consequential of disease (Willing et al., 2010, Butto and Haller, 2016). Considering this, techniques to promote the intestinal microbiota diversity prior to loop ileostomy formation may prove to increase microbial resilience to enteral nutrient deprivation and thus attenuate dysbiosis. Nonetheless, additional analyses employing OTU counts to quantify and compare microbiota populations and overall diversity within the functional and defunctioned intestine, with increased sample numbers, is required to confirm such suggestions.

Here we present a novel human model of dysbiosis that enables assessment of variations in the presence and profile of the intestinal microbiota, as a consequence of dietary modification. The primary advantage of this model is the paired functional sample obtained from the same individual at the same time as the defunctioned. The paired sample nature enables control of genetic and environmental bias as consequences of potential perturbing factors, such as contaminants from showering or changing ileostomy pouch for example, will be apparent in both functional and defunctioned samples and therefore eliminated during subsequent analyses. However, despite such unique advances, this model is not without its limitations. Firstly, the anaerobic environment of the intestine is likely compromised during ileostomy as the limbs are sutured to the abdominal wall. Due to this, we cannot determine whether possible key bacteria have been eliminated from both limbs due to inadequate growth conditions. Furthermore, this model is executed utilising the ileum of the small intestine and although the majority of enzymatic digestion and absorption occurs here, bacterial fermentation of indigestible complex carbohydrates, crucial mediators of host health and disease, occurs in the colon (Tremaroli and Backhed, 2012). The consequences of dietary modification in the small intestine are therefore arguably less relevant than those observed in the colon. Future studies applying this model to colostomy patients may prove beneficial, however only 35% of colostomies are temporary, potentially making recruitment of patients undergoing reversal surgery problematic (WWW, Colostomy Association).

In the context of patients recruited to this study, despite loop ileostomy generating such drastic nutritional environments, research had not yet been conducted to elucidate potential effect on the intestinal microbiota in the defunctioned ileum. This data demonstrates patients undergoing loop ileostomy reversal surgery harbour substantial dysbiosis in the defunctioned ileum with profound shifts observed in microbiota predominance. Previous research has demonstrated the crucial impact microbiota have on maintenance of intestinal homeostasis as well as rapid breakdown of EBF associated with dysbiosis (as discussed in literature review). Considering we have observed such profound dysbiosis in the defunctioned ileum, future studies should investigate the consequences of dysbiosis on defunctioned ileal morphology and homeostasis in view of potential implications for the success of ileostomy reversal surgery.

Collectively, findings presented within this chapter revealed that dysbiosis occurs in the defunctioned ileum of loop ileostomy patients following enteral nutrient deprivation.

Furthermore, we have presented a novel human model of dysbiosis which can be utilised in future studies to determine host microbiota profiles influence on intestinal physiology with consideration to dysbiosis associated diseases.

## **Chapter 4:**

# **Investigating the morphology of functional and defunctioned ileum following ileostomy-mediated faecal stream diversion**



#### 4.1 – Rationale:

The structure of the human intestine has evolved to support its primary function; the absorption of nutrients and water from luminal contents. This function is aided considerably by diverse metabolic actions of the intestinal microbiota and in return such resident microorganisms receive sustenance from host enteral nutrition, inducing a state of host-microbiota mutualism. Loop ileostomy deprives the downstream intestine of enteral nutrition, rendering it inactive until reversal surgery is carried out an average of 12 months post formation. Research presented in chapter 3 demonstrated that loop ileostomy-mediated enteral nutrient deprivation leads to profound disruptions to microbial structure and abundance, termed dysbiosis, in the defunctioned ileum. However, the physiological consequence of this dysbiosis remain yet to be investigated.

Previous mouse models have demonstrated that TPN use, which deprives the intestine of enteral nutrition equal to that of loop ileostomy, leads to microbial dysbiosis (Miyasaka et al., 2013). In addition, rats fed on exclusive TPN for 8 days were observed to develop circumferential atrophy with remodelling of the intestinal wall, such as increased thickness of the submucosal layers, throughout the intestine when compared to identically housed rats fed and watered *ad libitum* (Ekelund et al., 2007). It is also known that recognition of commensal microbes by IEC TLR mediates host-microbiota crosstalk and is crucial for maintaining intestinal homeostasis (Rakoff-Nahoum et al., 2004). Collectively, this research supports a probable role for the microbiota in influencing intestinal physiology in the defunctioned intestine, consequential to enteral nutrient deprivation.

Chapter 3 utilised loop ileostomy patients undergoing reversal surgery, to investigate nutritional influence on the presence and profile of the intestinal microbiota. The same patients also lend themselves as a novel human model for analysis of how distinct microbial populations may alter intestinal physiology, promoting either health or disease. Likewise to chapter 3, the paired nature of obtained samples will enable inpatient analysis of intestinal morphology following enteral nutrient deprivation-induced dysbiosis whilst controlling for interpatient genetic and environmental variability.

This research model will also enable consideration of post-operative clinical outcomes for patients undergoing loop-ileostomy reversal surgery. In addition to the inconvenience of a second operation for loop closure, the reversal procedure is associated with a substantial morbidity of 21-70% (Shabbir and Britton, 2010). Small bowel obstruction and anastomotic leakage are the most common post-operative complications with respective incidence rates up to 22% and 19% (Pemberton et al., 1987, Phang et al., 1999, El-Hussuna et al., 2012). Further complications include prolonged postoperative ileus and faecal incontinence, as well as incisional hernia and wound infections at the site of stoma formation (El-Hussuna et al., 2012). Due to such complications, around 5% of cases prove to be irreversible, leaving patients with a permanent stoma and a reduced quality of life (Bailey et al., 2003). Investigation of ileostomy-mediated enteral nutrient deprivation and resultant influence of dysbiosis on intestinal structure and function, with particular consideration to the rate of post-operative complications, may potentially identify a novel therapeutic target for improving the success of ileostomy reversal surgeries.

This thesis proposes that dysbiosis associated with loop ileostomy-mediated enteral nutrient deprivation in the downstream intestine results in distortion of intestinal morphology, potentially via a loss of host-microbial interaction at the mucosal surface. We also suggest that these mechanisms underpin the substantial morbidity associated with ileostomy reversal surgery.

#### **4.2 – Research Aims:**

- Investigate the consequence of enteral nutrient deprivation and resultant dysbiosis on intestinal function and morphology, utilising a novel human model.
- Explore possible mechanisms by which microbiota impact intestinal function and how these may influence clinical outcome of ileostomy reversal surgery.

#### **4.3 – Methods Summary:**

Full thickness excised functional and defunctioned tissue sections, obtained from 35 patients undergoing ileostomy reversal surgery, were fixed, embedded and sectioned, as described in section 2.2.8.1. Morphological analyses measuring villous height, crypt depth and inflammation were performed on tissue sections from paired samples. IEC proliferation and apoptosis rates were assessed using immunofluorescence PCNA and Click-iT TUNEL assays. Participant demographics and post-operative clinical data were recorded and compiled for exploratory data analysis using a scatterplot matrix.

#### 4.4 – Results:

##### 4.4.1 - Defunctioned ileum is atrophied but not inflamed at the time of loop ileostomy reversal.

Assessment of intestinal morphology was conducted via qualitative and quantitative analysis of histological sections. Atrophy of villi in the defunctioned ileum is immediately apparent from figure 4.1A, with visibly distorted and stunted villi, in comparison to that of the paired functional control. Following quantification, a 47%  $\pm$ 15% reduction in average villous height was observed in defunctioned ileum of all patients, compared with functional (figure 4.1B). This reduction in villous height was found consistently across all paired samples tested (figure 4.1C).

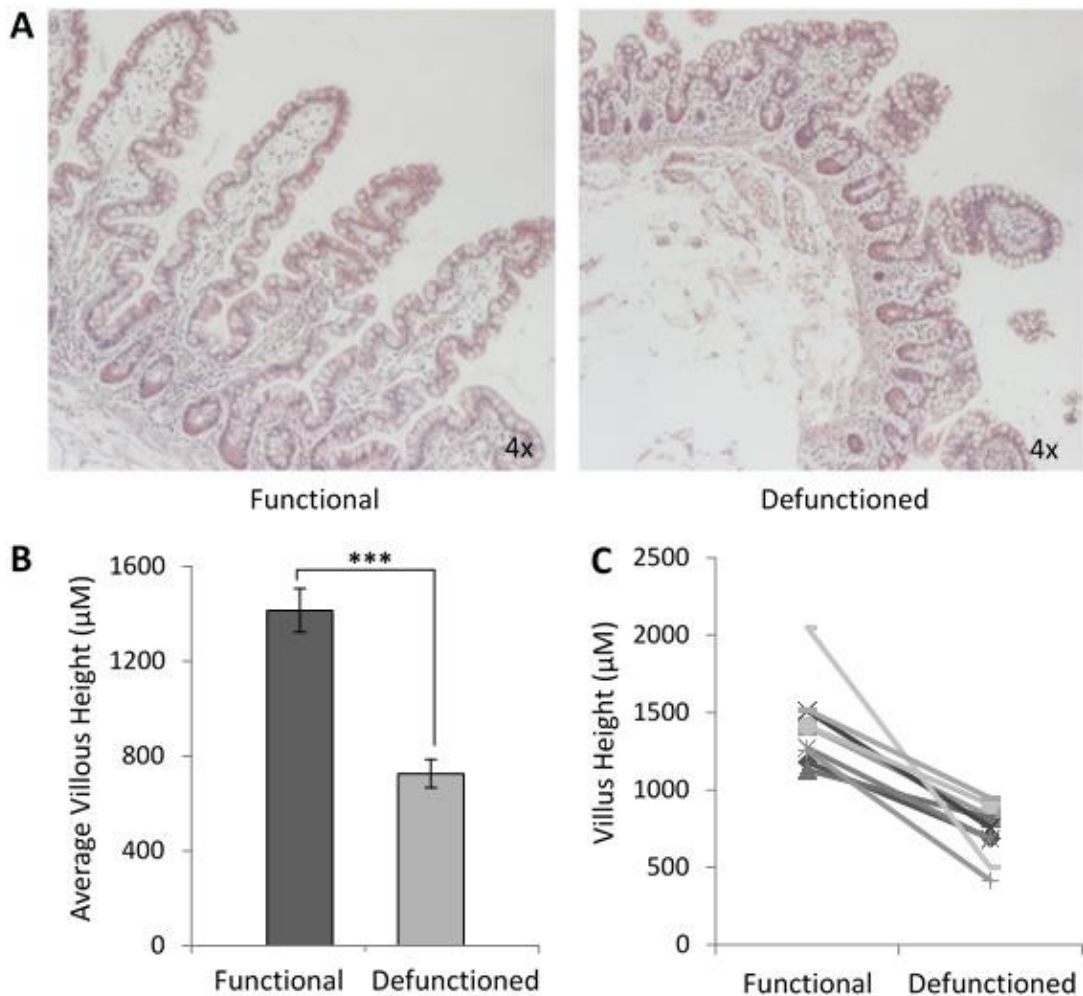


**Figure 4.1 – Histological analysis of villous height in functional and defunctioned intestine.** (A) Representative H&E stained sections, magnification 4 ×. (B) Average villous height  $\pm$  SEM (n = 9, p = 0.0004) (C) Paired villous height (n = 9).

*Data published in Beamish et al. (2017).*

Histological analysis of crypt depth was performed to assess total mucosal height and atrophy of the mucosa found to extend to the crypts with a significant reduction in average crypt depth in the defunctioned limb following enteral nutrient deprivation (figure 4.2A). The average crypt depth in the functional ileum was  $306 \mu\text{M} \pm 48 \mu\text{M}$ , decreasing to  $266 \mu\text{M} \pm 31 \mu\text{M}$  in the defunctioned ileum, which constitutes to an  $11.5\% \pm 12\%$  overall reduction observed in average crypt depth across all patients tested (figure 4.2A). Analysis of paired data revealed a varied response to enteral nutrient deprivation across the cohort with the shortest of functional crypts seeing a slight increase in crypt depth in the defunctioned ileum (figure 4.2B).

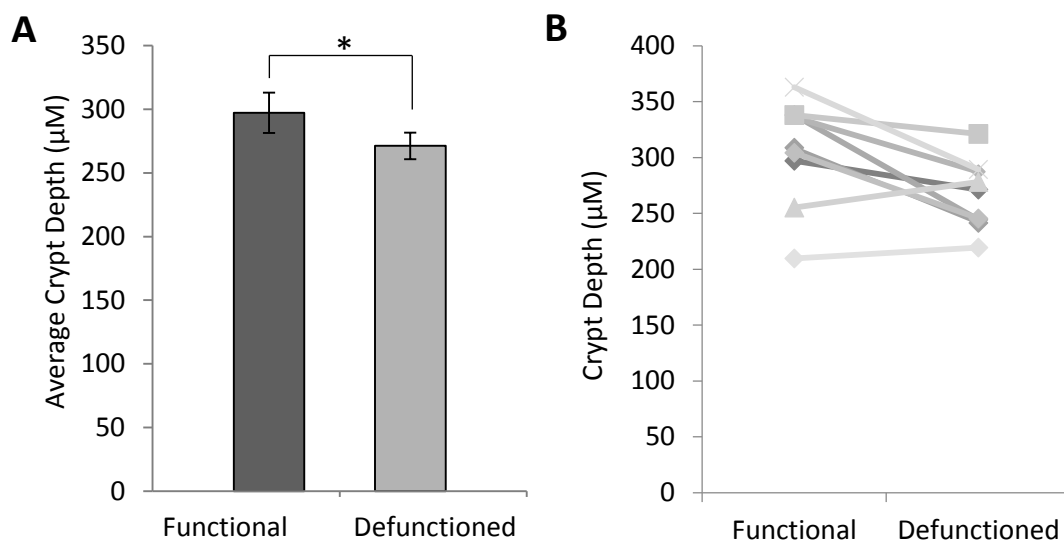


**Figure 4.2 – Histological analysis of crypt depth in functional and defunctioned intestine.** (A) Average crypt depth  $\pm$  SEM (n = 9, p = 0.02) (B) Paired crypt depth (n = 9).

Despite drastic mucosal atrophy identified in defunctioned ileum, scoring the extent of mucosal damage, immune infiltrate and goblet cell depletion, revealed no significant inflammation in the defunctioned ileum compared with functional (figure 4.3), suggestive of an absence of chronic inflammation at time of reversal surgery.

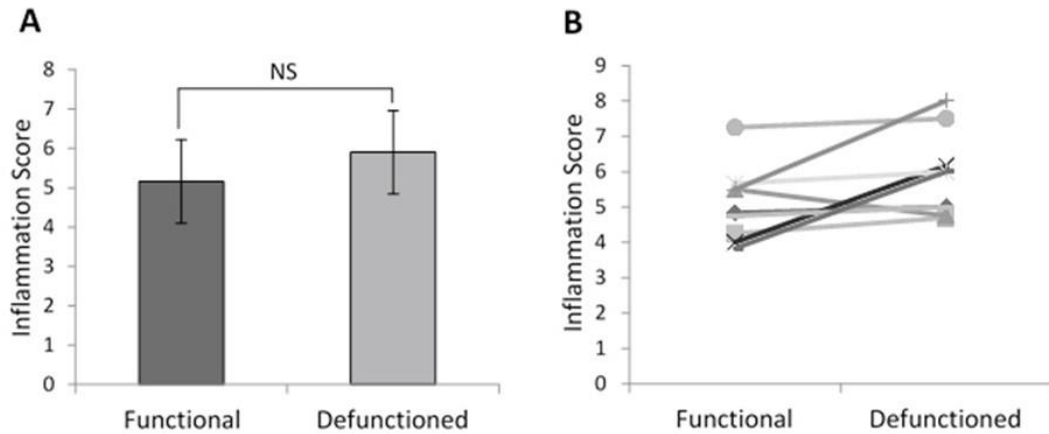


**Figure 4.3 – Histological analysis of inflammation in functional and defunctioned intestine.** (A) Average inflammation score  $\pm$ SEM (n = 9, p = >0.05) (B) Paired inflammation score (n = 9).

*Data published in supplementary material of Beamish et al. (2017).*

#### 4.4.2 – Villous atrophy accountable to reduced IEC proliferation in defunctioned crypts rather than increased anoikis.

Homeostasis of the intestine is maintained by a fine balance of epithelial cell proliferation in the intestinal crypts and anoikis at the tip of the villi (Frisch and Francis, 1994). To assess potential functional impact of enteral nutrient deprivation upon epithelial replenishment, the proportion of proliferative cells per crypt and rate of apoptosis was determined via immunofluorescent PCNA antibody and TUNEL staining (figure 4.4, figure 4.6).

Loop ileostomy-mediated defunctioning resulted in a decline in the percent of proliferating cells, visualised as PCNA-positive IECs per crypt (38.1%  $\pm$ 8.3%; figure 4.5) compared to that observed in the functional controls (61.8%  $\pm$ 11.9%; figure 4.5). This represents an overall average reduction of 23.7%  $\pm$ 4% (n = 5, p = 0.01; figure 4.5A), supporting evidence that microbial changes influence IEC proliferation.

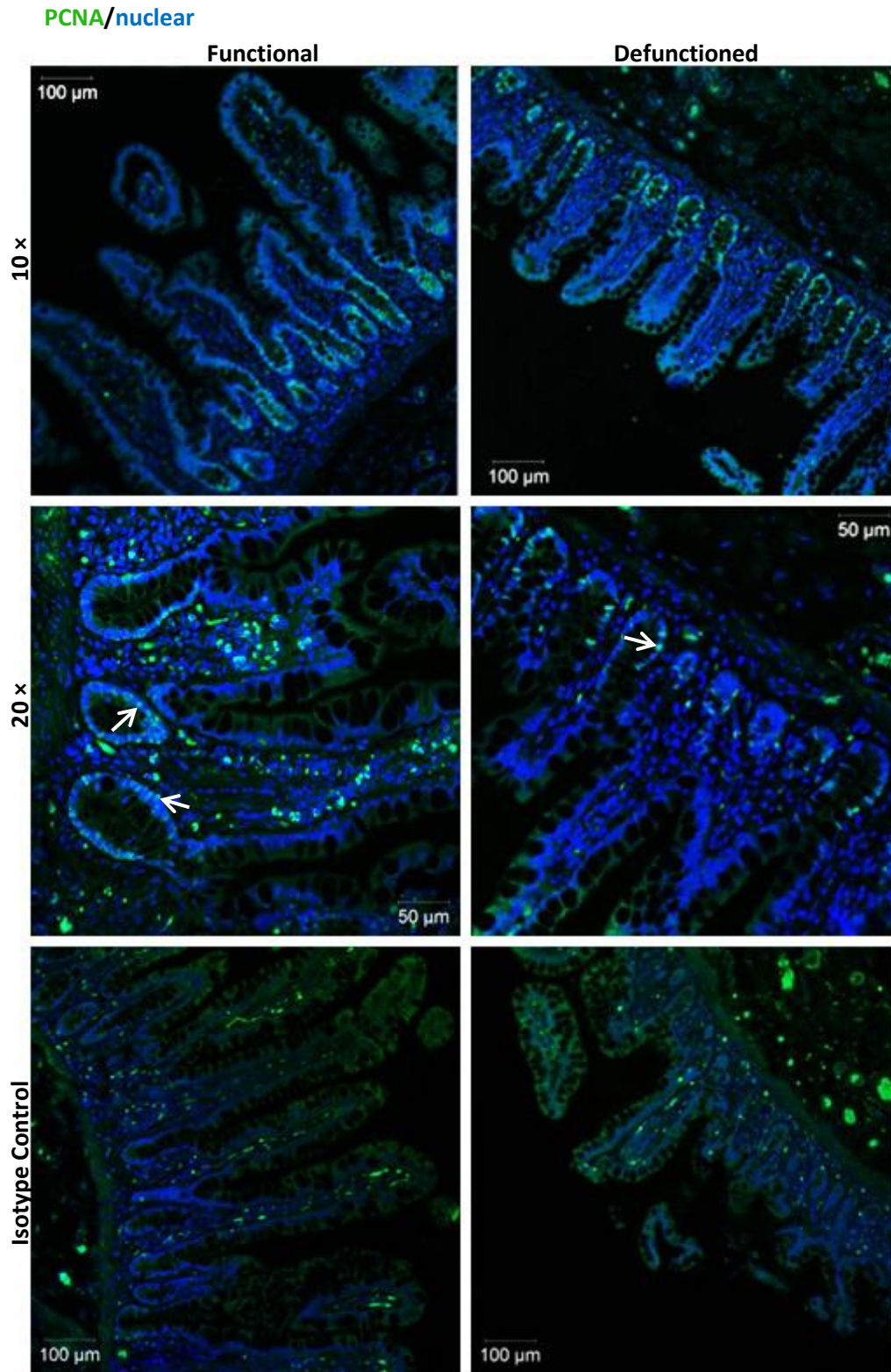


**Figure 4.4 – Assessment of IEC proliferation in functional versus defunctioned intestine.** Representative immunofluorescent PCNA labelling (green) to measure proliferation. White arrows illustrate individual proliferating cells identified for quantification. All nucleated cells, counterstained using Hoechst 33342, are coloured blue. Isotype control represents non-specific antibody binding. *Data published in Beamish et al. (2017).*

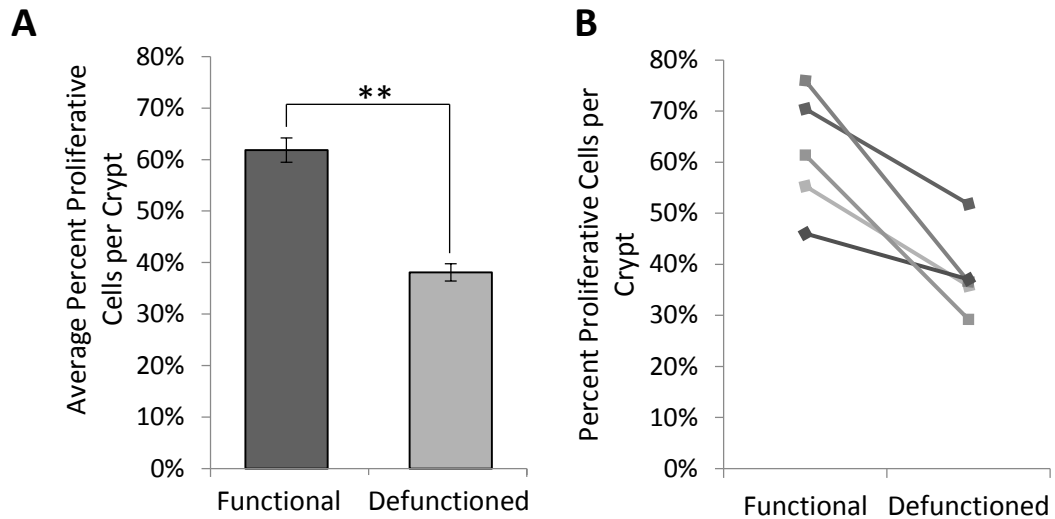


**Figure 4.5 – Relative quantification of IEC proliferation in functional versus defunctioned intestine.** (A) Average percent proliferating PCNA positive cells/crypt  $\pm$  SEM (n = 5; p = 0.01). (B) Paired percent PCNA-positive cells per crypt in the functional and defunctioned intestine (n = 5).

*Data published in Beamish et al. (2017).*

TUNEL staining, which measures the extent of double strand DNA breaks generated during apoptosis, revealed no difference in rates of apoptosis between the functional and defunctioned ileum (figure 4.6). This suggests that reduction in villous height is likely due to decreased proliferation of IEC rather than increased apoptosis, which may be due to a dysbiosis-associated lack of pro-proliferative microbial signals.



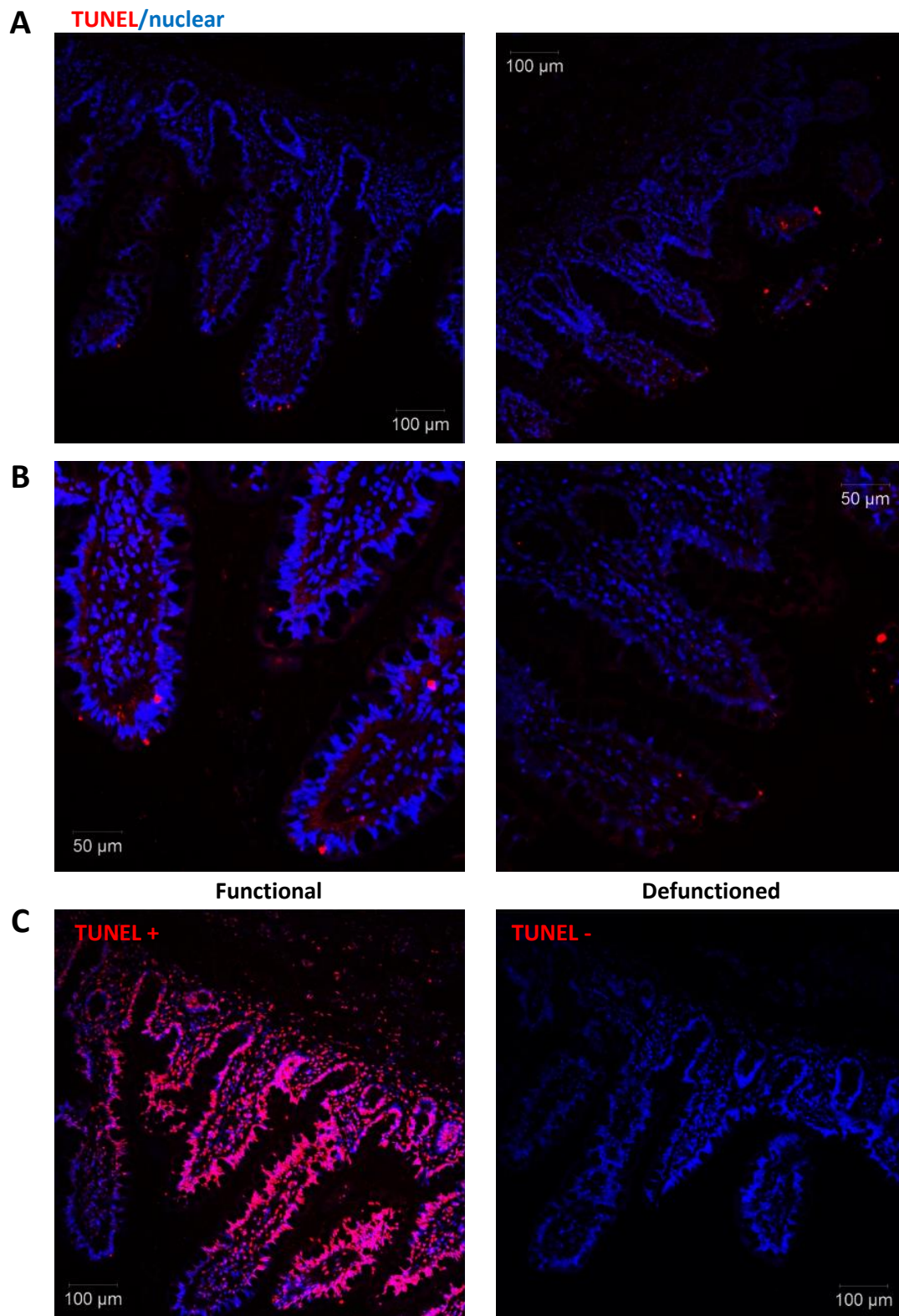


**Figure 4.6 – Assessment of apoptosis in functional versus defunctioned intestine.** Representative immunofluorescent TUNEL labelling (red) to measure apoptosis. All nucleated cells, counterstained using Hoechst 33342, are coloured blue. (A) Magnification 10 ×. (B) Magnification 20 ×. (C) TUNEL +ve control treated with DNase and TUNEL –ve control treated with TdT reaction cocktail only. Magnification 10×.

#### 4.4.3 – Blood CRP levels are raised but albumin and WBC levels remain normal post ileostomy reversal surgery.

To monitor post-operative clinical outcomes, routinely obtained serum CRP, Albumin and WBC levels were recorded (table 4.1). As per Lancashire Teaching Hospitals NHS Trust guidelines, the healthy reference ranges for serum albumin, CRP and WBC levels are as follows: 34-54 g/L, 0-5 mg/L and 4.0-11.0  $\times 10^9/L$ , respectively. We found a substantial elevation in post-operative CRP levels with an average of 87.9 mg/L, and normal levels of serum albumin (average 38.1 g/L) across the patient cohort. Furthermore, all WBC counts remained within reference range with an average of 9.4  $\times 10^9/L$ .

<b>Table 4.1 - Mean Participant Demographics and Post-operative Clinical data</b>	
<b>Age (years)*</b>	58 ( $\pm 16$ )
<b>BMI*</b>	26.0 ( $\pm 2.4$ )
<b>Days since ileostomy formation*</b>	392 ( $\pm 264$ )
<b>Gender (% females)</b>	51
<b>Length of Hospital Stay (Days)</b>	6 ( $\pm 4$ )
<b>Post-op CRP (mg/L)</b>	87.9 ( $\pm 54.8$ )
<b>Post-op Albumin (g/L)</b>	38.1 ( $\pm 3.4$ )
<b>Post-op WBC (<math>\times 10^9/L</math>)</b>	9.4 ( $\pm 1.7$ )

\* The mean is given with standard deviation in parentheses.

Abbreviations: BMI, body mass index; CRP, C-reactive protein; WBC, white blood cells.

*Data published in Beamish et al. (2017).*

#### 4.4.4 – Ileostomy reversal surgery is associated with substantial morbidity.

Patient post-operative clinical outcomes were documented to investigate potential influence of dysbiosis on clinical outcome of ileostomy reversal surgery (table 4.2). A total morbidity rate of 48.6% was observed post-operatively across the cohort, with wound associated complications being the most common with 14% incidence, followed by post-operative ileus and erratic bowel function both with 11% incidence. Less prevalent complications included abdominal distension and anastomotic leak with 8.6% and 2.9% incidence, respectively. Finally, 51.4% of patients recovered without complication, despite prolonged enteral nutrient deprivation.

Interestingly, two of the patients who developed post-operative ileus were also measured for total bacterial load and were found to have a higher than average reduction in total bacterial load than the patients who did not (average reduction of 62.4%; patient 001 had 71.6% decrease, 038 had 97.2% decrease in total bacterial load).

<b>Post-operative Complications</b>	<b>#</b>	<b>%</b>
Ileus	4	11.4
Wound	5	14.3
Bowel function	4	11.4
Anastomotic Leak	1	2.9
Abdominal Distension	3	8.6
<b>Total Complications</b>	<b>17</b>	<b>48.6</b>
<b>Without Complication</b>	<b>18</b>	<b>51.4</b>

**Table 4.2 – Incidence of post-operative complications following ileostomy reversal surgery.** #, number of patients affected; %, percent of patients affected across cohort.

#### **4.4.5 – Exploratory analysis of participant demographics revealed associations with clinical outcomes.**

Scatterplot matrix analysis was performed to investigate potential associations between sample variables, particularly regarding changes in intestinal microbiota and clinical outcomes. Full scatterplot matrix is located in appendix 10 whilst noteworthy correlations are presented in figure 4.7. First it was identified that percent decrease in total bacterial load positively correlated with mean post-operative CRP levels, mean post-operative WBC count and with increased duration of hospital stay post loop ileostomy reversal surgery. Furthermore, a strong positive correlation was identified between mean post-operative CRP levels and relative increases in Bacteroidetes and  $\gamma$ -Proteobacteria phyla and concomitant relative decreases in the Firmicutes phylum. Interestingly, duration of hospital stay was found to have no correlation with patient age or BMI, factors which may have existed as confounding variables.

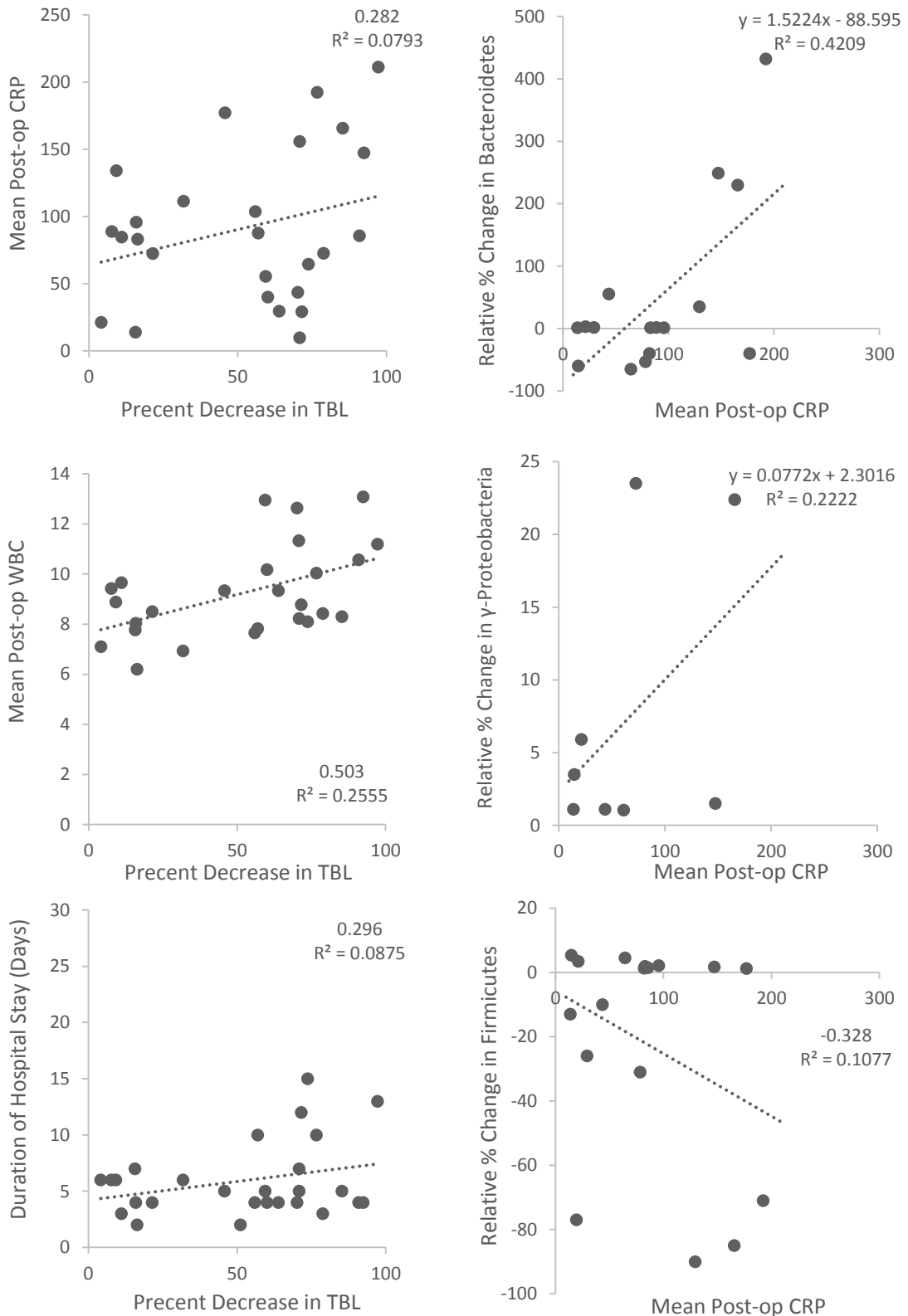


**Figure 4.7 – Noteworthy scatterplots correlating participant demographics with post-operative clinical data.**  $R^2$  estimates fit of model to data and is the square of the Pearson correlation coefficient.

(Continued)

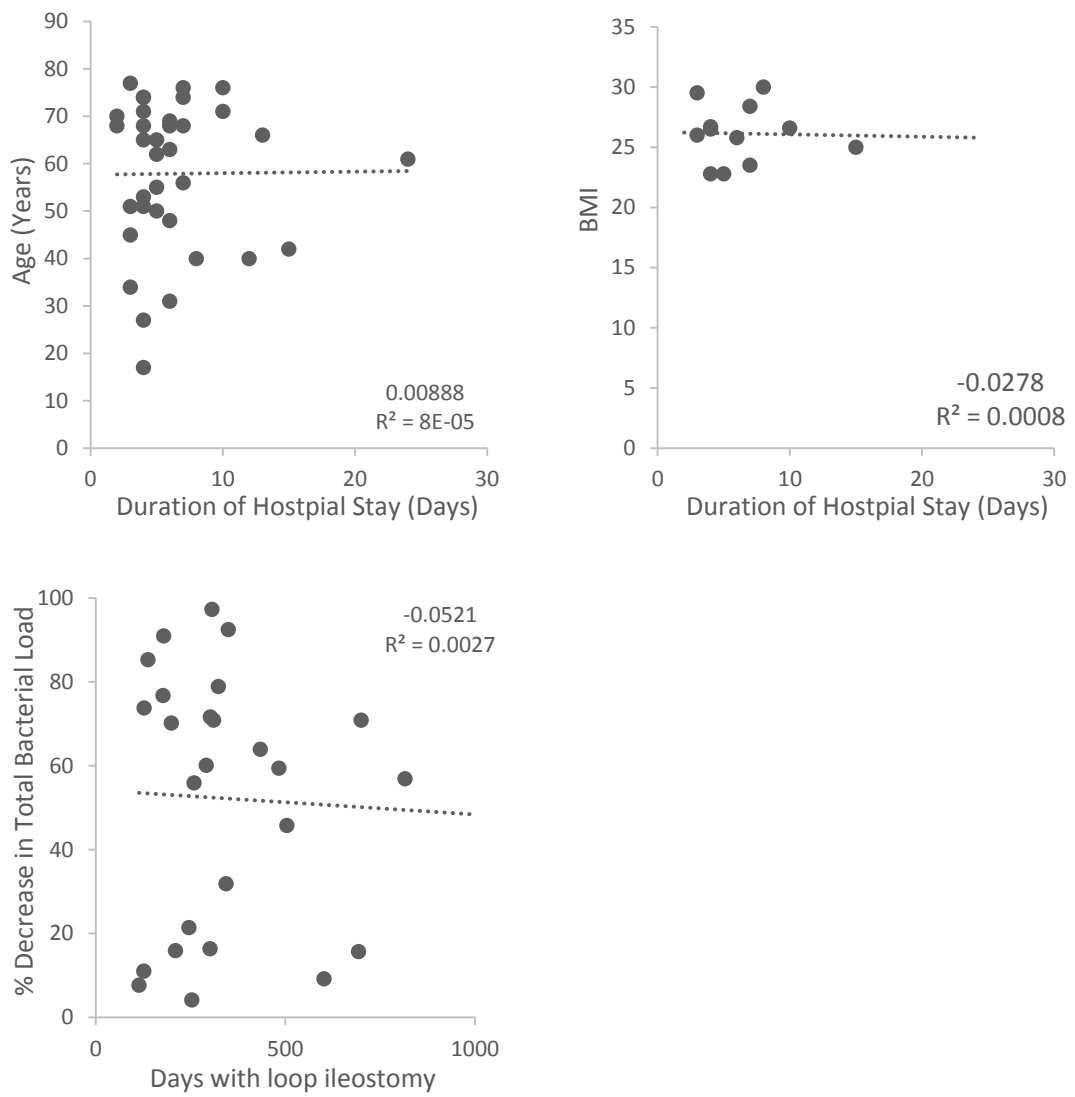


**Figure 4.7 – (continued)** – Full scatterplot matrix is presented in appendix 10.

#### 4.5 – Discussion:

The data presented reveals substantial distortion of intestinal mucosal architecture following enteral nutrient deprivation, with significant atrophy of villi in the defunctioned ileum. Similar results were also reported in the rat jejunum following defunctioning by a blind end Roux-en-y anastomosis (Kovalenko and Basson, 2012). Likewise to ileostomy patients, food is provided for the rat, offering nutritional sustenance, whilst the bypassed jejunum remains sedentary. This study reported mucosal and fibromuscular atrophy when compared with adjacent functional bowel and remarkably such changes were observed within only 3 days following initial anastomosis formation.

Previous studies have hypothesised that morphological dysfunction observed in defunctioned ileum is likely a direct consequence of nutrient depletion. It is understood that SCFA such as butyrate, act as nutritional substrates for epithelial cells and so such assumptions are plausible (Csordas, 1996). The research presented herein demonstrated that ileostomy-associated defunctioning results in a reduction in IEC proliferation. Miyasaka *et al.* reported that mice fed exclusively on TPN demonstrated a reduction in IEC proliferation in a MyD88 dependent manner (Miyasaka *et al.*, 2013). MyD88 knockout (-/-) mice, which lack TLR signalling pathway function that is crucial in host-microbiota homeostasis, presented normal levels of IEC proliferation irrespective of enteral nutrient deprivation, but wild-type TPN mice, with reduced IEC proliferation, demonstrated a characteristic significant shift in microbial dominance from Firmicutes to Proteobacteria, consistent with findings in loop ileostomy patients presented in chapter 3. Furthermore, physiological preservation of epithelial barrier function in MyD88 -/- TPN fed mice was also reported, indicating minimal disruption to intestinal morphology, suggesting that intestinal microbiota influence host immunological responses and thus mucosal architecture. Considering this research with the data presented in chapters 3 and 4, it is reasonable to conclude that the reduction we observed in IEC proliferation and resultant intestinal atrophy is highly likely to be a consequence of dysbiosis, via altered host-microbial interactions at the intestinal surface, rather than exclusively due to nutrient deprivation.

Further support for this principle is provided by clinical studies which have attempted to stimulate the defunctioned intestine prior to reanastomosis and loop closure, utilising a

sterile saline solution (Miedema et al., 1998, Abrisqueta et al., 2013, Abrisqueta et al., 2014). Such studies were conducted with the aim of gradually activating cellular mechanisms of absorption and motility to restore functionality to the intestine prior to reversal surgery. However, there have been varied and limited reports of success at reducing post-operative complications, particularly post-operative ileus. The rationale and practice within these studies vastly disregards the importance of a healthy gut microbiome for proficient intestinal function. In particular, the absence of nutritional value to the stimulating solution used within these studies is likely to conserve dysbiosis and continue to promote mucosal distortion in the weeks prior to ileostomy reversal surgery.

Another possible mechanism which may underpin the observed physiological changes in the defunctioned ileum involves direct nutrient sensing by enteroendocrine cells. Postprandial nutrients including sugars, amino acids, SCFAs and bile acids are known to act as substrates for GPCRs and transporters on the luminal surface of enteroendocrine cells (reviewed in Gribble and Reimann (2016)). Such interactions induce secretion of gut hormones, glucagon-like peptide 1 (GLP-1) and cholecystokinin (CCK), which function to regulate intestinal mobility (Camilleri et al., 2012, Lin et al., 2002). Therefore a loss of enteral nutrition, as a consequence of loop ileostomy mediated faecal stream diversion, deprives enteroendocrine cells of luminal nutrients and thus attenuates CCK and GLP-1-mediated functional activity within the intestine. This mechanism likely occurs simultaneously to dysbiosis-associated disruption of host-microbiota interactions at the intestinal mucosal surface, consequently perpetuating the deterioration observed in intestinal morphology and function in the study cohort. Novel therapeutics to provide nutritional sustenance to defunctioned ileum may potentially achieve rebiosis and activate host cellular mechanisms prior to loop ileostomy reversal surgery.

Intestinal dysbiosis has been linked to the pathogenesis of numerous chronic diseases due to the induction of a proinflammatory state within the intestine (as discussed in the literature review). Interestingly, we identified that there was no significant inflammation observed in the defunctioned ileum at the time of loop ileostomy reversal. We propose that this finding is linked to the reduction observed in total bacterial load following nutrient deprivation. The intestinal microbiome is sensitive to local nutritional fluctuations and data presented in

chapter 3 indicated that nutrient deprivation in the defunctioned ileum significantly depleted bacterial load. It is likely that an initial period of inflammation following ileostomy formation occurs but a subsequent state of 'dysbiotic equilibrium' is reached and mucosal homeostasis, be it at a compromised capacity, is reinstated preventing chronic inflammation. However, reanastomosis to reinstate luminal flow through the defunctioned intestine (figure 3.2) could restore bacterial load while maintaining dysbiosis, therefore putting patients at risk of complications. This notion is also supported by our finding that the number of days between loop ileostomy formation and reversal is not correlated with clinical outcome or decrease in bacterial load, meaning that the observed physiological changes are likely to occur rapidly following loop ileostomy formation rather than progressively over a long period.

Blood tests, measuring CRP, albumin and WBCs are routinely used as predictors of post-operative complications and clinical outcomes (Ortega-Deballon et al., 2010, Hubner et al., 2016). Compiled patient data reported elevation of post-operative CRP levels with normal serum albumin and WBC levels across the patient cohort. Significantly elevated CRP and WBC levels are often signals of infection and in loop ileostomy reversal patients can be early indicators of anastomotic leak (Ortega-Deballon et al., 2010). The observed elevated CRP is possibly due to incompetent barrier function in the defunctioned intestine following reanastomosis. However, this would likely cause increased bacterial translocation and inflammation, yet the WBC count in these patients is considered to be normal. It is therefore more likely that, for the majority of patients, such responses occur in consequence of a natural inflammatory response to surgery. On the other hand, it was also identified that increases in the relative abundance of Bacteroidetes and  $\gamma$ -Proteobacteria and decreased Firmicutes are positively correlated with increased post-operative CRP levels, suggesting a role for dysbiosis in influencing post-operative inflammatory responses. Further research to perform precise time course analysis of CRP, WBC and albumin levels post-operatively may prove useful in elucidating possible influences.

The combined morbidity rate of the cohort was identified to be 48.6%, fitting centrally within the range of 21-70% previously reported in literature (Shabbir and Britton, 2010). The most frequently reported post-operative complication in the study cohort was associated with the surgical wound and is likely occur as a result of environmental factors such as infection, rather



than dysbiosis. However, all other recorded complications, including severe complications such as ileus and anastomotic leak, may potentially be linked to microbial dysbiosis. Studies have shown that depletion of microbiota populations within the Firmicutes phyla (as was observed in our study) is associated with altered intestinal permeability and activation of local immune cells in mice (Cani et al., 2009). It is plausible that dysbiosis driven changes in the defunctioned limb following reversal surgery, promote intestinal inflammation and contribute to an increased risk of developing post-surgical complications, such as ileus. We also identified a small positive correlation between decreased bacterial load and increased duration of hospital stay which, when paired with our observation that two patients who developed ileus were also found to have a higher than average reduction in total bacterial load, suggests that loss of intestinal microbiota populations may increase risk of post-operative complications that ultimately result in lengthier hospital stays. Factors such as patient age and BMI are usually crucial factors in patient prognosis following surgery however, for this procedure, this did not appear to be the case as no correlations were observed between such factors within the study cohort.

To strengthen our hypotheses, future studies exploring the expression levels of TLR receptors in defunctioned ileum following enteral nutrient deprivation would be most interesting as it would elucidate our suggested mechanism of dysbiosis-mediated distortion of the defunctioned intestine. In addition, clinical studies to measure levels of bacteria and/or associated products in the blood of patients pre, during and post loop ileostomy would offer interesting insights into the influence of dysbiosis on epithelial barrier function and subsequent clinical outcome. Finally, this research presents the microbiota as a potential novel therapeutic target for improving the outcome of ileostomy reversal surgery. Subsequent clinical feasibility studies to provide the defunctioned ileum with nutritional sustenance prior to reanastomosis, with the aim of promoting microbiome restoration, may prove to reduce post-operative morbidity in loop-ileostomy patients.

## **Chapter 5:**

# **Utilising NMR Spectroscopy-Based Urinary Metabolite Profiling for Prediction of Intestinal Microbiota Composition**

## 5.1 – Rationale:

The broad diversity and functional capacity of the intestinal microbiota is becoming increasingly recognised with the advancement of high-throughput sequencing technologies. However despite such advances, understanding of the functional role of even the most abundant bacteria within the gut remains limited. It is well accepted that microbiota-generated metabolic products are important in maintaining health and homeostasis, most notably during an inflammatory response (as discussed in literature review), but emerging studies indicate that such metabolites are also pivotal in the onset and pathogenesis of numerous systemic and gastrointestinal diseases.

The indigenous human metabolism is tightly integrated with that of the intestinal microbiota, whose vast genomic capacity provides a repertoire of supplementary enzymatic and biochemical capabilities of benefit to the host (Qin et al., 2010). The significant influence resident microbes have on the host metabolome is highlighted in a study that demonstrated humanised mice (mice transplanted with human faecal microbiota) harbour distinct urinary and faecal metabolome profiles to that of conventionally raised mice (Marcobal et al., 2013). This observation indicates that differing profiles of intestinal microbes can induce systemic changes in host metabolites, outweighing that of the indigenous host metabolism.

Metabolomics is defined as the systematic analysis of metabolites produced during specific cellular processes and in recent years efforts have been made to map the intestinal microbiota and their relationship to specific metabolites. A comprehensive review from Nicholson *et al.*, defined several chemical classes involved in host-microbiota co-metabolism via compilation of data presented in the literature thus far (table 5.1) (Nicholson et al., 2012). SCFA are considered to be the most significant microbial-associated metabolites due to their localised functional influence on gut motility and IEC turnover and associations with colorectal cancer (Park et al., 2016). However, choline metabolites, although primarily metabolised in the liver, are also converted by microbial enzymes into trimethylamine, which has been implicated in development of NAFLD (Dumas et al., 2006). Such systemic consequences of microbial-associated metabolites highlight the vast functional influence of the intestinal microbiome.

<b>Chemical classes with example metabolites</b>	<b>Associated microbiota</b>
<b>SCFA:</b> Acetate, propionate, butyrate	<i>Clostridia; Eubacterium and Faecalibacterium</i>
<b>Bile Acids:</b> Cholate, hyocholate, glycodeoxycholate	<i>Lactobacillus, Bifidobacteria, Enterobacter, Bacteroides, Clostridium</i>
<b>Choline:</b> Methylamine, trimethylamine, trimethylamine-N-oxide, betaine	<i>Faecalibacterium prausnitzii, Bifidobacterium</i>
<b>Phenol:</b> Hippuric acid, 2-hydroxybenzoic acid, phenylacetate, phenylpropionate,	<i>Clostridium difficile, F. prausnitzii, Bifidobacterium, Subdoligranulum, Lactobacillus</i>
<b>Indole derivatives:</b> Indoleacetate, indole-3-propionate, melatonin, serotonin,	<i>Clostridium sporogenes, E. coli</i>
<b>Vitamins:</b> Vitamin K, vitamin B12, biotin	<i>Bifidobacterium</i>
<b>Lipids:</b> Conjugated fatty acids, LPS, peptidoglycan, cholesterol, phosphatidylcholines, triglycerides	<i>Bifidobacterium, Roseburia, Lactobacillus, Klebsiella, Enterobacter, Citrobacter, Clostridium</i>
<b>Others:</b> D-lactate, glucose, urea, creatinine, succinate.	<i>Bacteroides, Ruminococcus, Faecalibacterium, Bifidobacterium, Lactobacillus</i>

**Table 5.1 - Human metabolites and associated intestinal microbiota.**

*Table modified from information presented in Nicholson et al. (2012).*

The majority of gut microbial-metabolome studies have to date focused on targeted analysis of covariation, such as with microbial SCFAs, but have not yet comprehensively explored the wider indigenous- and microbiota-metabolic interactions. Considering the broader nature of the intestinal microbiome, Li *et al* attempted to characterise key microbial populations which influence host metabolism via functional metagenomics analyses in Chinese and American families (Li et al., 2008). They reported that variation in *Bacteroides uniformis* was identified to be positively associated with citrate and 3-aminoisobutyrate. Furthermore, variation in *Faecalibacterium prausnitzii* is associated with modulation of eight different urinary metabolites, including 2-hydroxyisobutyrate and dimethylamine. Interestingly dimethylamine, produced during microbial catabolism of choline, has been linked with fatty liver and type 2 diabetes in mice (Dumas et al., 2006) and an increased abundance of the Firmicutes phylum, to which *F. prausnitzii* belongs, has been associated with obesity in humans (Ley et al., 2006). However, this study is limited by the employment of DGGE faecal sample analysis as such methodology may disregard key mucosal-associated microbiota.

Furthermore, the kindred study cohort share genetics and environmental exposures and are therefore not representative of the general population.

The research presented herein has focused on localised physiological consequences of dysbiosis when in reality, the effects are broadly systemic, with correlations reported between microbiota-associated metabolites and disorders such as obesity and cardiovascular disease. This thesis postulates that the metabolic signatures of human urine reflect gut microbiota composition and thus health or disease, and may potentially be exploited as an early clinical indicator of numerous dysbiosis-associated diseases.

## **5.2 – Research Aims:**

- To determine whether intestinal microbiota composition is reflected in the profile of host urinary metabolites.
- To evaluate the capability of urinary metabolites as early predictors of various dysbiosis-associated diseases via detection of dysbiosis.

## **5.3 – Methods Summary:**

Study participants were recruited from Gastroenterology outpatient clinics at Royal Preston Hospital and Furness General Hospital. A mid-stream urine sample and two biopsies were obtained from each patient; one each from the descending and sigmoid colon. All participants within the cohort were pooled, disregarding IBD or Control status, to facilitate investigation of the research aims within this chapter.

DNA extracted from colonic biopsies was utilised for Illumina® 16S sequencing to profile intestinal microbiota and each classified microbial taxa was presented as a relative proportion of the total number of OTUs/sample for subsequent analysis. Urine samples were subjected to urinary NMR analysis to profile metabolites. Relative NMR peak intensities of annotated urine metabolites were normalised and scaled to minimise bias due to variation in urine sample concentration and the presence of very abundant metabolites (e.g. urea), respectively. Hierarchical cluster and penalised linear regression analysis were utilised to investigate potential influence of intestinal microbiota on urinary metabolite profiles.

## 5.4 – Results:

### 5.4.1 – Hierarchical clustering analysis of microbiota sequencing data revealed five enterotype-like groups.

Intestinal microbiota was profiled via Illumina 16S sequencing of microbial DNA extracted from colonic biopsies that were obtained from 42 patients during endoscopic examination. Taxonomic classification of Illumina sequencing data identified a total of 20 microbial phyla, 42 class, 83 order, 172 family, 412 genus and 566 different species across the entire patient cohort. The vast interpatient variability of intestinal microbiota composition is apparent in figure 5.1 with broad diversity observed across the cohort in relative proportions of the 4 predominant phyla; Actinobacteria, Bacteroidetes, Firmicutes and Proteobacteria.

To assess similarity between the microbiota profiles, hierarchical clustering analysis was performed on proportionate sequencing data, at phylum, order and genus taxonomic levels (Figure 5.2). Hierarchical clustering analysis measures the distance, or dissimilarity, between samples by pairing the closest related samples first, then methodically linking such samples with those that are more distinct. Hierarchical cluster analysis revealed a crescendo in interpatient variability from phylum through to genus level as the first level branches were observed in increase in height at genus level indicating the presence of more dissimilar microbiota profiles. In addition, hierarchical analysis revealed 5 clusters with closely related microbiota profiles, at order level, at a branch cut position of 0.5 (Figure 5.2B).

Relative proportions of Illumina 16S sequencing data at taxonomic level order according to the 5 hierarchical-defined groups are presented in figure 5.3. Each group is observed to be defined by predominant microbial order in an Enterotype-like manner. Group 1 is defined by almost complete predominance of Enterobacteriales belonging to the phylum, Proteobacteria. Due to the limited patient numbers within group 1 it was excluded from downstream analyses. Group 2 equates to over one third of the cohort and is defined by what is considered to be a 'typical' microbiota; an abundance of Clostridiales with slightly fewer Bacteroidales and a small proportion of less predominant microbes, including Enterobacteriales and Verrucomicrobiales. Group 3 harbour reduced proportions of Clostridiales corresponding increased relative proportions of Verrucomicrobiales,

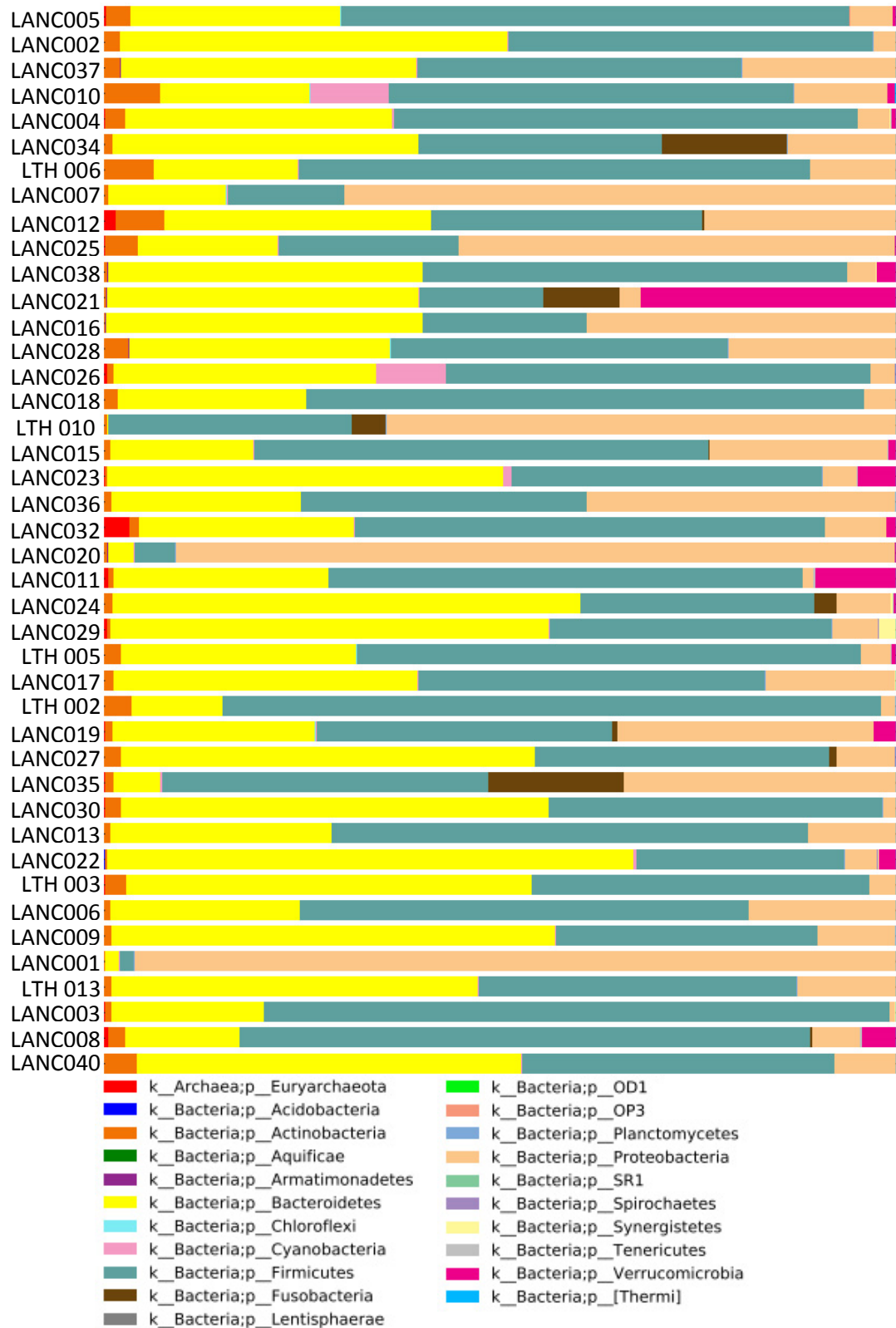


**Figure 5.1 - Relative taxonomic composition of 16S rRNA amplicon sequences from human intestinal biopsy samples, at phylum level.** K, kingdom; p, phylum. LTH and LANC prefix denote associated NHS site for recruited participants. LANC022 was retrospectively excluded from downstream analyses due to confirmatory IBS diagnosis.

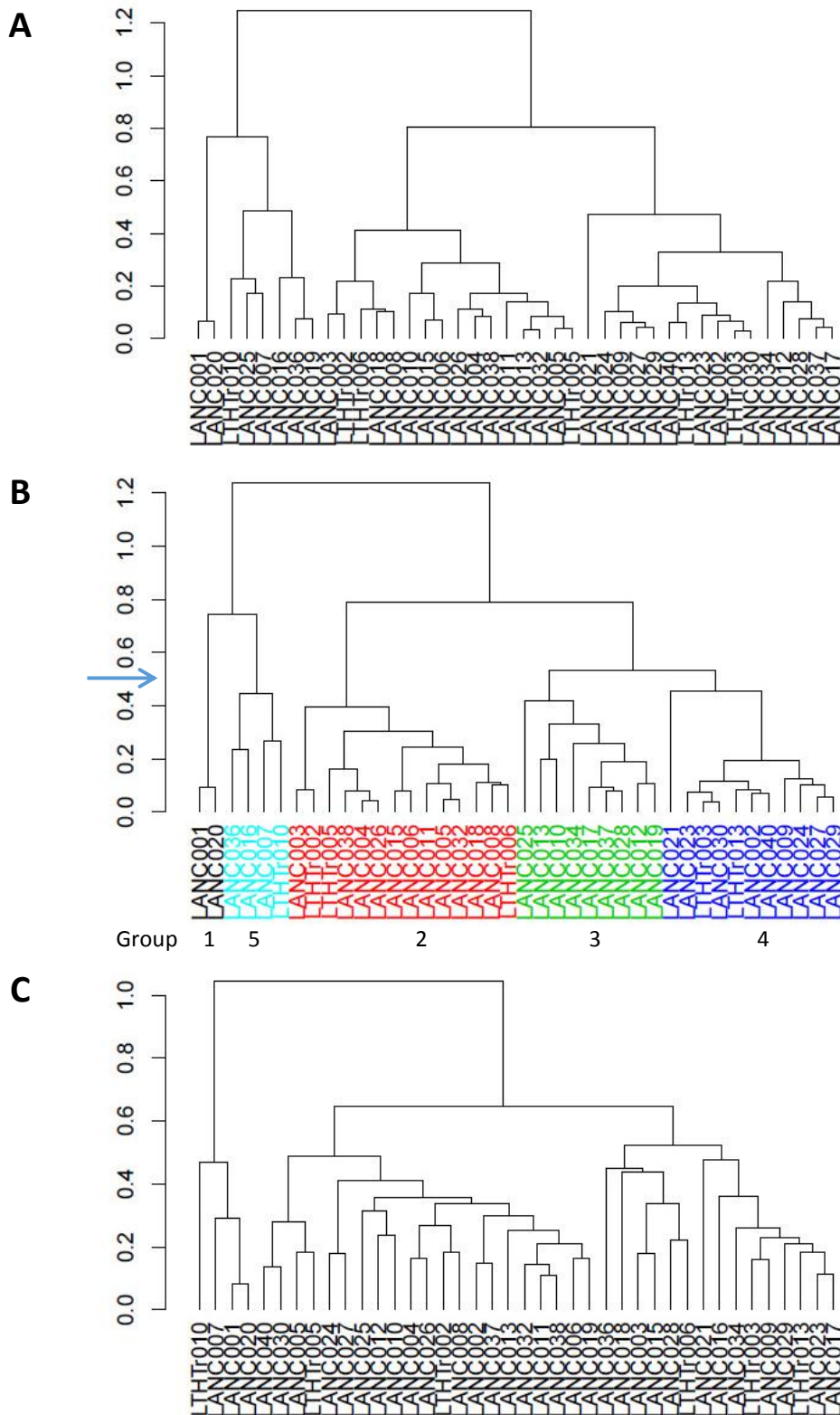


**Figure 5.2 - Hierarchical cluster analyses of Illumina 16S intestinal microbiota profiles at (A) phylum (B) order and (C) genus taxonomic level.**

Colours depict 5 groups with closely related microbiota profiles, as defined by blue arrow which represents branch cutting point.



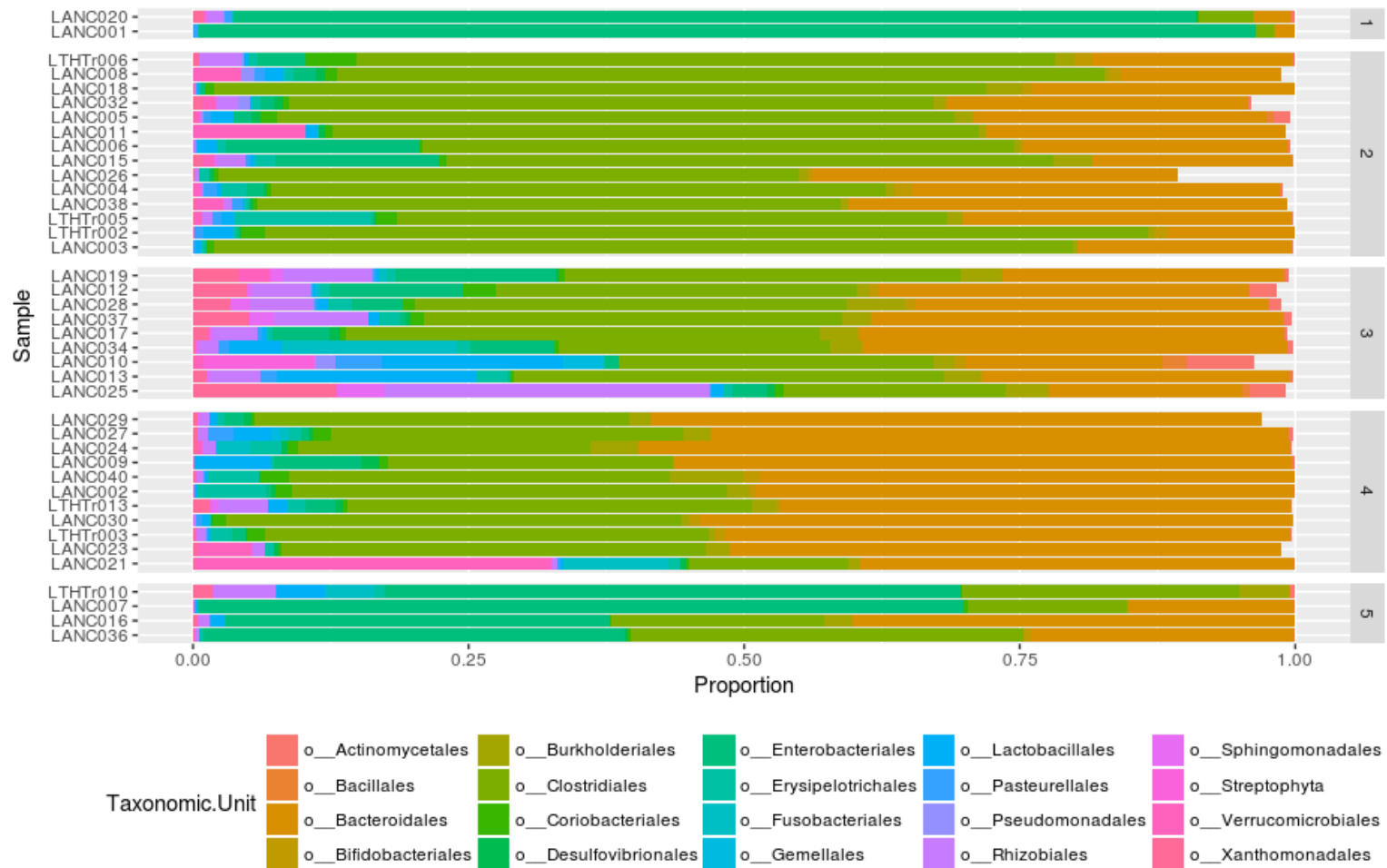


**Figure 5.3** – Relative taxonomic composition of 16S rRNA amplicon sequences in human intestinal biopsy samples, at order level, depicting 5 hierarchical clusters in Figure 5.2B. O, order. Relative proportions do not always total 1 as order lower than 25% in abundance were excluded from analysis.

Fusobacteriales and Actinomycetales, with a consequential overall increased microbiota diversity compared to the other groups. Proportions of Bacteroidales are relatively average within this group. On the other hand, group 4 is defined by Bacteroidales predomination with reduced Clostridiales and limited microbiota diversity across less predominant order such as Enterobacteriales. Group 5 is distinguished by an almost equivalent abundance of Enterobacteriales with combined Clostridiales and Bacteroidales, and a depletion of other less predominant bacterial taxa to very low and in some cases almost non-existent levels.

#### **5.4.2 – Substantial interpatient variation observed in human urinary metabolite profiles.**

<sup>1</sup>H NMR spectroscopy and subsequent metabolite annotation was employed to determine urinary metabolite profiles in the patient cohort. A representative urine NMR spectra is presented and annotated in figure 5.4 using TameNMR within the Galaxy framework (available at [www.galaxy.liv.ac.uk](http://www.galaxy.liv.ac.uk)). The highly overlapped nature of urine NMR spectra is visible, particularly in the aromatic signals region between 6 and 9 ppm. A total of 237 metabolites were identified across 41 urine NMR spectra in the patient cohort (appendix 8).

As with Illumina sequencing data, hierarchical cluster analysis, which assigns a Euclidean pairwise distance measure to samples to denote similarity or singularity, was performed on normalised and scaled relative metabolite concentrations to assess similarity of urinary metabolite profiles (figure 5.5A). No distinct grouping was observable in profiles across the cohort as the dendrogram is predominated by small and highly dissimilar clusters.

To gain initial insights into the relationship between the microbiota groups and metabolites, the microbiota group assignments for each participant were transposed onto the paired metabolite dendrogram labels (figure 5.5B). On the whole the microbiota groups are broadly distributed throughout the metabolite dendrogram with no immediate observable trend. However, group 2 (red) and group 3 (green) appear to cluster with themselves and each other more frequently than any other group. Groups 3 and 5 (turquoise) are most distinct from each other whilst group 4 (blue) has similarities with all other groups except group 3 (figure 5.5B). Samples LHTTr013 and LANCO12 are highly distinct to all other samples as they cluster individually with a distance measure of 30+, likely due to confounding interpatient variables affecting metabolite composition.

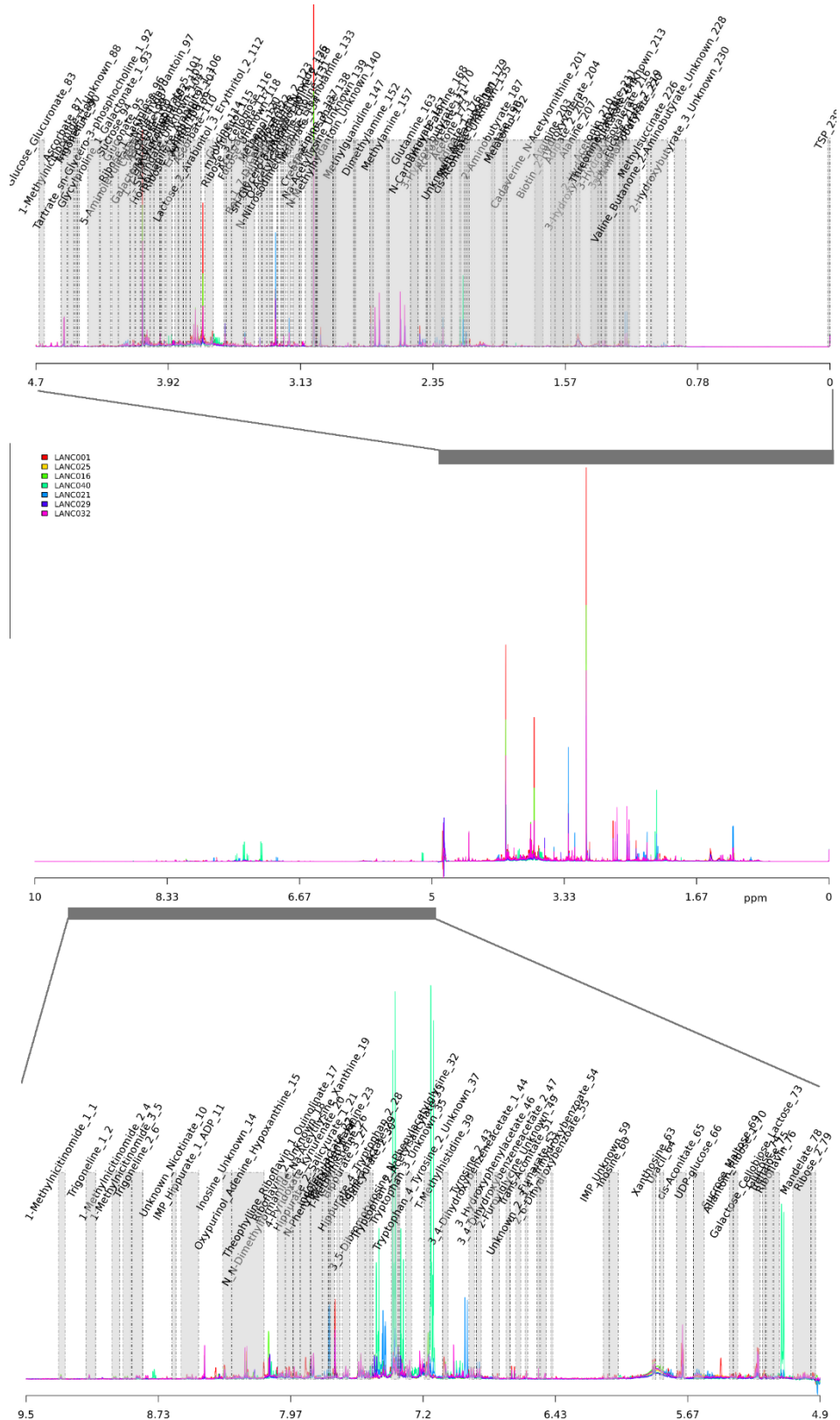


**Figure 5.4 – Representative <sup>1</sup>H NMR spectra of patient urine samples with respective metabolite annotations of manually defined buckets. TSP is utilised as a reference for 0 ppm. For purposes of clarity, buckets labelled as ‘Unknown’ have been excluded. Annotated metabolite bucket pattern file is presented in Appendix 7.**

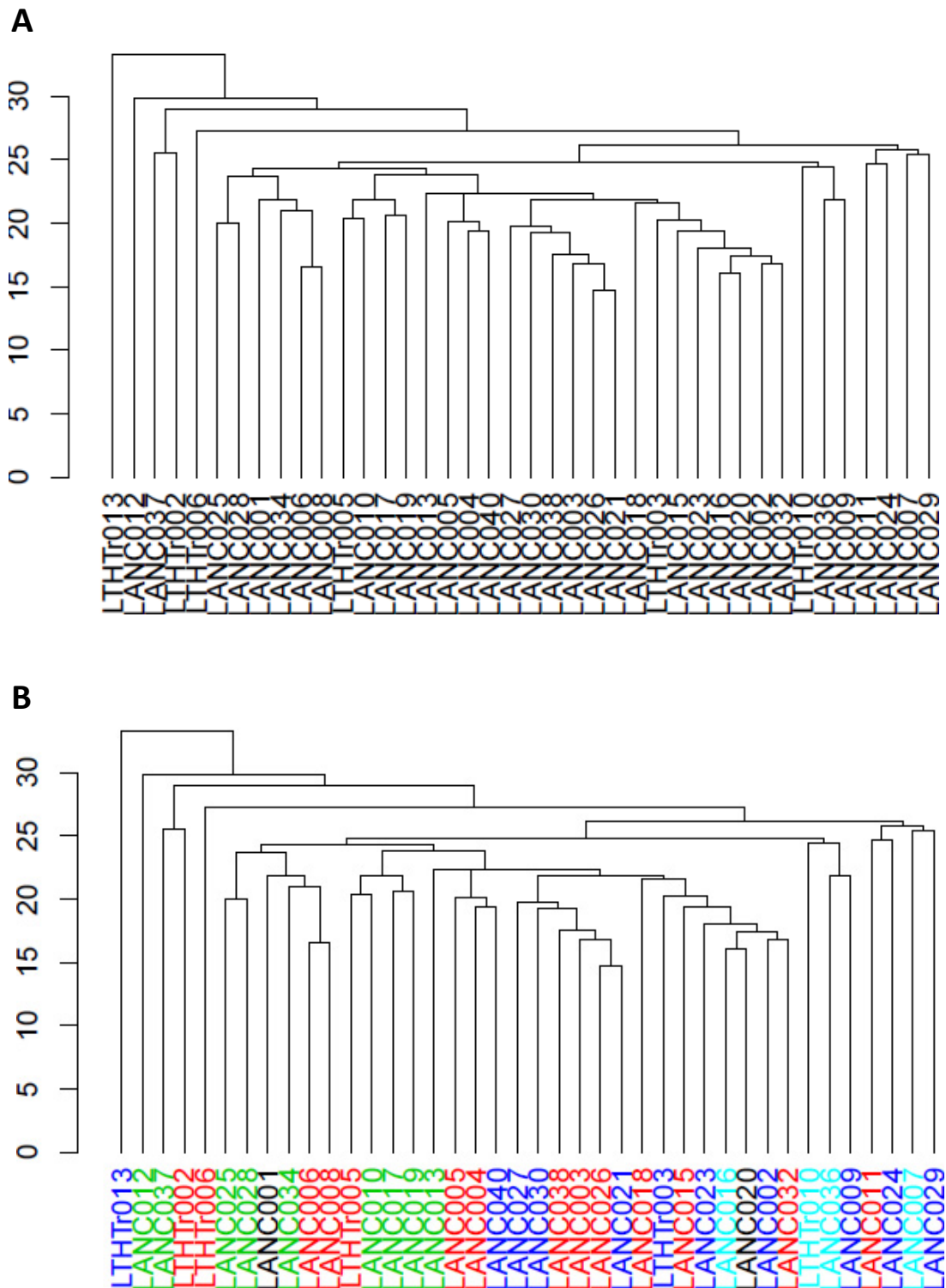


**Figure 5.5 – Hierarchical cluster analysis of (A)  $^1\text{H}$  NMR urinary metabolite NMR profiles. (B) Patient labels are coloured according to intestinal microbiota clustering groups at order level (figure 5.2B). Black, group 1; red, 2; green, 3; blue, 4 and turquoise,**

### 5.4.3 – Various urinary metabolites are correlated with intestinal microbiota profiles in humans.

Regression analysis of urinary metabolites was performed against the composition of four intestinal microbiota clusters identified at taxonomic level order to investigate the potential relationship between microbiota profiles and urinary metabolites in humans (figure 5.6). On the whole the effect sizes, indicating extent of association between the two variables, were small, likely as a result of large variability in metabolite profiles between patients. Despite this, several candidate metabolites were identified; carnosine was positively correlated with group 2 whilst negatively correlated with group 5. Epicatechin was positively associated with groups 3 and 5 whilst inversely associated with groups 2 and 4. In addition, urocanate and hydroxytryptophan were positively correlated with groups 3 and 4 respectively. Interestingly, no SCFA metabolites were identified to be associated with intestinal microbiota profiles.



**Figure 5.6 – Penalised multinomial regression analysis of urinary metabolites against enterotype-like microbiota profiles.** Metabolites with a positive effect size are positively correlated with microbiota profile whilst a negative effect size indicates negative correlation with corresponding microbiota profile. (Intercept) represents the bias of the model, i.e. the odds of choosing a cluster if the metabolite levels were all 0. Group 1 was omitted from analysis due to limited sample numbers.

#### **5.4.4 – Urinary metabolites are also associated with specific microbial populations.**

Considering the observed interpatient limitations related to study participant numbers in identifying associations between intestinal microbiota profiles and urinary metabolites, regression analysis of urinary metabolites against specific microbiota classifications at phylum and order taxonomic levels was also performed (figure 5.7).

As was observed with the results of the microbiota group regression in figure 5.6, epicatechin was identified to be the metabolite most strongly correlated with intestinal microbiota populations. At order level, epicatechin was identified to be negatively correlated with Bacteroidales and Clostridiales with an effect size of -0.35 and -0.2 respectively and inversely correlated with Enterobacteriales, Lactobacillales and Rhizobiales (figure 5.7). Also observed, uridine monophosphate (UMP) negatively correlated with Clostridiales but strongly correlated with Enterobacteriales whilst trigonelline was found to have inverse correlative trends to UMP. In addition, N-Carbamoyl-beta-alanine and 2-Hydroxyisovalerate were identified to have small effect sizes in positive and negative correlation with Enterobacteriales and Clostridiales, respectively. Cytidine was identified to have a similar correlation profile to epicatechin as it was found to negatively correlate with Bacteroides and Clostridiales and positively correlate with Enterobacteriales. However, the overall effect sizes, indicating extent of association between the two variables, were small, suggesting that the representativeness of the microbial populations may be limited due to large interpatient variation in urinary metabolites.

These findings phylogenetically translate to that presented in figure 5.8, with epicatechin, cytidine, N-Carbamoyl-beta-alanine and UMP identified to negatively correlate with Bacteroidetes and Firmicutes phyla and positively correlate with Proteobacteria phylum. Trigonelline was identified to be negatively correlated with Proteobacteria and positively correlated with Firmicutes.

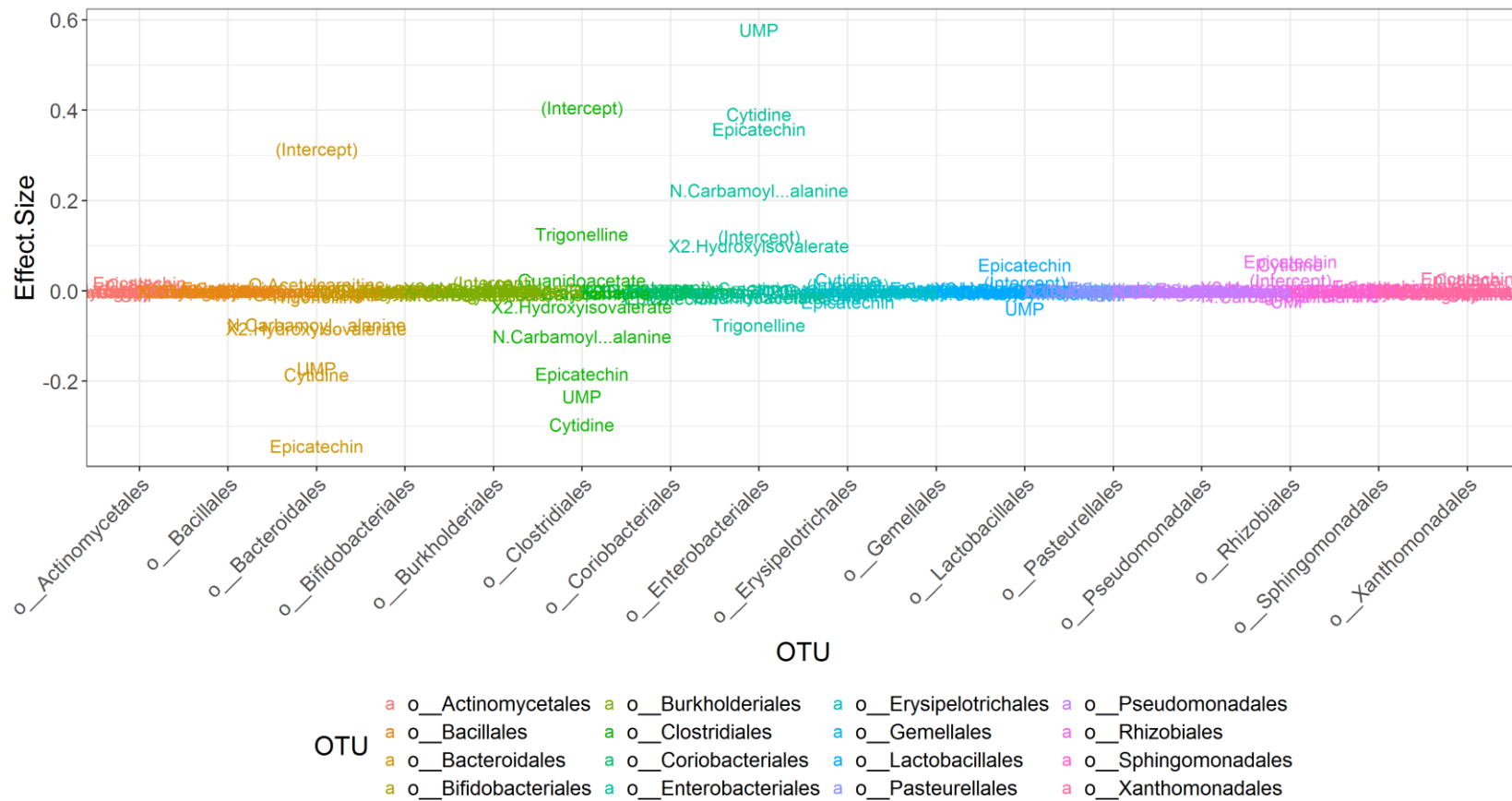


**Figure 5.7 – Penalised linear regression analysis of urinary metabolites against intestinal microbiota taxa at order taxonomic level.** Metabolites with a positive effect size are positively correlated with microbiota taxa whilst a negative effect size indicates negative correlation with corresponding microbial taxa. (Intercept) represents the bias of the model, i.e. the odds of choosing a cluster if the metabolite levels were all 0. Abbreviations: o, order; UMP, Uridine monophosphate; N.Carbamol...alanine, N-Carbamoyl-beta-alanine.

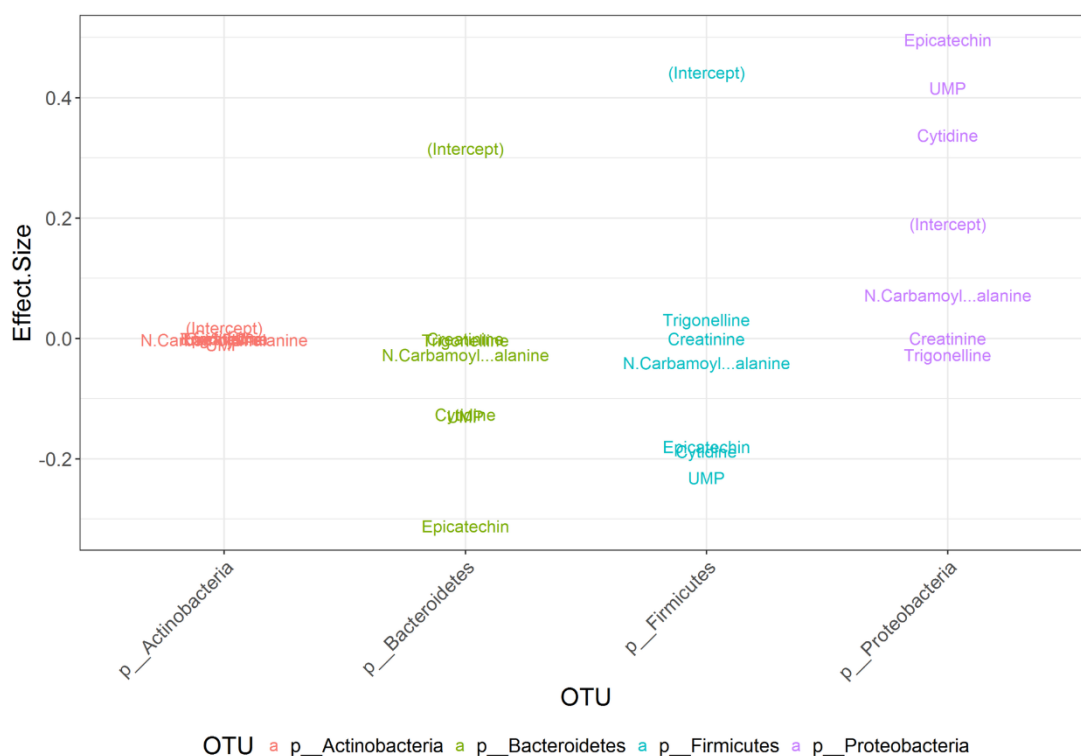


**Figure 5.8 – Penalised linear regression analysis of urinary metabolites against intestinal microbiota taxa at phyla taxonomic level.** Metabolites with a positive effect size are positively correlated with microbiota taxa whilst a negative effect size indicates negative correlation with corresponding microbial taxa. (Intercept) represents the bias of the model, i.e. the odds of choosing a cluster if the metabolite levels were all 0.

Abbreviations: p, phylum; UMP, Uridine monophosphate; N.Carbamol...alanine, N-Carbamoyl-beta-alanine.



## 5.5 – Discussion:

This chapter aimed to explore the potential relationship between intestinal microbiota composition and urinary metabolites in humans, with the long-term goal of utilising urinary metabolite analysis as a potential rapid and convenient indicator of health and disease. To do this intestinal microbiota profiles and urinary metabolites were determined for 42 patients utilising Illumina® 16S sequencing and <sup>1</sup>H NMR spectroscopy, respectively then compared via hierarchical and regression analyses.

First, hierarchical cluster analysis of intestinal microbiota profiles at taxonomic level order identified 5 distinct enterotype-like groups within the study cohort, each predominated by a different bacterial taxa. Interestingly, none of these profiles were unique to this study and have all been previously reported in the literature as associated with health or disease phenotypes. Groups 1 and 5 were predominated by Enterobacteriales belonging to the phylum, Proteobacteria, with significant reductions observed in the proportion of all other microbial orders, particularly Bacteroidales and Clostridales. Such microbiota composition is often reported in cases of active IBD and CRC, which are primarily defined by an outgrowth of Enterobacteriales (Frank et al., 2007, Sobhani et al., 2011). Group 2 was identified to be largely predominated by Clostridales and Bacteroidales, then harbour a small proportion of order such as, Enterobacteriales, Verrucomicrobiales and Actinomycetales. Such microbiota is considered to be 'normal' and associated with maintenance of intestinal homeostasis, host-microbiota tolerance and promoting overall host health (The Human Microbiome Consortium (2012) and as discussed in literature review). However it is also observable within this group that several patients are largely predominated by Clostridales. Such vast expansion of Clostridales has also been reported in cases of obesity, with a disrupted Bacteroidetes to Firmicutes ratio and reduced overall microbial diversity (Turnbaugh et al., 2009). Group 3 was defined by reduced proportions of Clostridales to create an even Bacteroidetes to Firmicutes ratio. A reduction in the Firmicutes phylum is often linked to carbohydrate-reduced diets and so may be a reflection of host dietary preferences (De Filippo et al., 2010). Group 3 also appeared to have increased proportions of typically less predominant microbial populations. This may be a reflection of pathobiont expansion in consequence to a loss of predominant microbial populations and reduced niche competition. Group 4 was identified to have a shift in microbiota predominance to Bacteroidales with reduced Clostridales and overall bacterial diversity in less predominant order. Expansion of the Bacteroidetes phylum has been

previously correlated with diets that are protein rich but reduced in calories (Russell et al., 2011, Monira et al., 2011). Such diets and their associated microbiota-enterotype have been suggested to be detrimental to intestinal health due a reduction in protective microbiota-mediated SCFA synthesis and a concomitant increase in cancer-associated metabolites (Russell et al., 2011).

The four predominant enterotype-like groups identified within this study somewhat conform to those suggested in the literature to be defined by *Bacteroides*, *Prevotella*, *Ruminococcus* and Enterobacteriaceae abundance (Arumugam et al., 2011, Harmsen and C., 2016). *Bacteroides* and *Prevotella* are genus classifications within the order Bacteroidales whilst *Ruminococcus* and Enterobacteriaceae are classifications belonging to Clostridiales and Enterobacteriales respectively, thus fitting with 3 of the microbiota groups identified in the cohort within this study. This trend also indicated that the data presented fits into different categories of dysbiosis with group 2 typically representing health and the other groups signifying distinct profiles of dysbiosis that may be associated with various diseases. However, long-term participant follow up and assimilation of medical history would be required in future studies to confirm whether such profiles are retained over time and identify any connections to clinical complications.

It is known that various intestinal microbes contribute to host metabolism, but it is likely that the full breadth of such interactions will not become apparent for many years, as the contents of table 5.1 continues to expand. For example, it is not currently understood which microbes are involved in the conjugation of glycine and benzoic acid to form hippurate, despite it being one of the most frequently detected urinary metabolites (Bouatra et al., 2013). This study aimed to perform broad functional characterisation of the intestinal microbiota relationship with urinary metabolites and several associations were identified. Epicatechin was observed to be positively correlated with groups 3 and 5 but negatively correlated with groups 2 and 4, thus suggesting a negative association with potentially cancer and obesity-linked dysbiotic profiles. Epicatechin (KEGG ID: C09727) is a polyphenolic flavonoid present in abundance in plants, cocoa, tea and grapes which is known to have strong antioxidant properties and has been shown to mimic the effects of insulin, offering protection against diabetes (KEGG pathway; Kanehisa and Goto (2000); Samarghandian et

al. (2017)). Furthermore, epicatechin and associated metabolites have recently been identified to harbour protective effects in cervical cancer by attenuating proliferation *in vitro* in HeLa cells (Hara-Terawaki et al., 2017). The mechanisms underpinning such observations remain speculative but the health benefit of this metabolite is undoubted. The negative association observed in this study between epicatechin abundance and groups 2 and 4 microbiota enterotypes indicates a potential role for epicatechin as a non-invasive predictor of dysbiosis and associated complications including obesity, type II diabetes and cancer.

Urocanate (KEGG ID: C0785) is a metabolic intermediate derived from host- and microbiota-mediated metabolism of histidine to glutamate (KEGG pathway; Kanehisa and Goto (2000)). This metabolite was found to be associated with group 3 microbiota, defined by an increase in proportions of usually less predominant microbial populations and a reduction in Clostridiales. Whilst this profile is not readily associated with a host clinical phenotype it may be a reflection of increased microbial diversity. Predominant metabolic functions are usually attributed to the most abundant microbiota, but microbes present in minor abundances can share metabolic functionality, promoting their survival and collectively inducing functional changes in the host (discussed in Arumugam et al. (2011)). It is therefore plausible that low abundant microbes with combined metabolic activity can substantially influence the human urine metabolome. It is also generally accepted that a microbiota rich in diversity promotes host health therefore, metabolites such as urocanate may be a reflection of a diverse microbiota, rich in low abundance species.

Carnosine (KEGG ID: C00386) is a dipeptide composed of alanine and histidine amino acids that is abundant in muscle tissue (KEGG pathway; Kanehisa and Goto (2000)). Increased carnosine levels have previously been associated with diets high in meat and fish intake (Cheung et al., 2017). Such protein rich diets have been associated with colorectal cancer development due to production of harmful metabolites such as nitrosamine and concomitant losses of SCFAs (Russell et al., 2011). However, a diet well balanced with protein and carbohydrate intake has been shown to promote microbiota diversity and have sufficient SCFA to counteract effects of such harmful metabolites and promote host health (Russell et al., 2011). The observation that carnosine is associated with group 2 microbiota profile

typically representative of health, presents itself as a potential biomarker of intestinal health if present with a definable physiological range.

Linear regression analysis was also performed against predominant microbial taxa in the intestine to investigate the relationship between metabolites and different microbial populations. The metabolites identified to be correlated with the enterotype-like microbiota groups were also reflected in the microbial taxa-associated analysis. For instance, epicatechin, that was identified to be negatively associated with a Firmicutes dominant, obesity-like profile, was observed to negatively correlate with Clostridiales and Bacteroidales and positively correlate with Enterobacteriales. The strong association between epicatechin and Proteobacteria abundance may potentially prove to be useful in prediction of localised pathologies associated with Proteobacteria predominance, such as IBD.

Numerous studies report significant alterations in the abundance of microbiota derived metabolites in the urine of patients with various dysbiosis-associated diseases (Williams et al., 2009, Stephens et al., 2013). This indicates that different populations of microbiota produce different end products of metabolism that are detectable in host urine. To our surprise, none of the metabolites identified to be associated with the four microbiota profiles observed in the study cohort were derived from the intestinal microbiota. This is likely due to the limited study numbers, especially within each microbiota group, meaning that any consequential changes observed in the bacterial derived metabolites were not significant enough to outweigh the variations in endogenous and diet-associated metabolites between the same groups. For example, N-Carbamoyl-beta-alanine (also referred to as Ureidopropionic acid; KEGG ID: C02642) and UMP (KEGG ID: C00105) detected in our analyses, are intermediates in the endogenous metabolism of uracil and are indicative of the chemical complexity of urine (The human metabolome database: Wishart et al. (2009)). To overcome this, future work should increase participant numbers and also employ targeted profiling of bacterial derived metabolites to extract this potentially important information from the dataset. Furthermore, former studies have concluded that urinary metabolites are influenced by environmental factors more significantly than serum metabolites (Walsh et al., 2006). Considering this, it may be more feasible in future work to first apply our study

rationale and methodology to blood samples as serum is relatively easy to obtain, chemically less complex and subject to less environmental variation than urine.

The majority of metabolites identified in this study, including epicatechin, 2-Hydroxyisovalerate (KEGG ID: C04181) and carnosine, originate from food present in the host diet (The human metabolome database: Wishart et al. (2009)). Although such metabolites exist mainly as a result of endogenous metabolism, they may have potential to reflect intestinal microbiota composition. The influence of host diet on shaping the composition of the intestinal microbiota is well documented and this study has shown correlations between host-metabolised compounds and different microbiota profiles. It is therefore possible that dietary metabolites present in the urine may reflect a specific type of host diet, such as carnosine in omnivorous diets, which is indirectly indicative of the intestinal microbiota profile of that individual.

The methods utilised for metabolite identification of NMR peaks are based entirely on annotation via fitting to a reference spectral library of purified metabolites. To confirm metabolite identification, future experiments should spike urine aliquots with purified and quantified metabolites of interest, to determine the affected NMR peaks as well as enabling absolute quantification (Stephens et al., 2013). Furthermore, the microbiota sequencing data are presented as relative proportions of total bacteria and may result in misinterpretation of microbiota predominance. For example, the increase in proportions of typically less predominant microbiota observed in group 3 of this study may actually be a reflection of a loss of predominant populations and thus a decreased overall bacterial load. It would be beneficial in future analyses to determine the OTU counts for each microbial taxa to enable direct comparison.

This research has suggested associations between gut microbiota profiles and various urinary metabolites which may potentially be implicated in health and disease. To fully evaluate their potential as predictive clinical biomarkers for various dysbiosis-associated diseases, long-term follow up studies should be conducted in future to assess progressive incidence rates for each disease-associated metabolite or metabolite profile. Although this study has

identified correlations between microbiota profiles and various metabolites, long-term data detailing clinical outcomes of these patients was not obtained, due to the nature of the original research aims, therefore such analyses were not possible.

In addition, this study ambitiously attempted integrative analysis of two “omics” datasets and successfully identified potential urinary metabolites associated with defined intestinal microbiota profiles via combined analysis of microbiomics and metabolomics datasets. Such multi-omics approaches are relatively novel and are said to require large sample numbers, tailored statistical analyses and considerable time investment from skilled researchers (Hasin et al., 2017). This study was primarily hindered by substantial interpatient variability in urinary metabolite profiles that is likely to be diet-associated variation. Future work to significantly increase study participants will aid in achieving statistical power for urinary metabolite analysis and downstream integration of different omics datasets. Furthermore, collection of qualitative data concerning participant lifestyle and diet with particular focus on macronutrient intake, BMI, use of medicines and any additional pathologies will further assist in elucidating the relationship between the intestinal microbiota and urinary metabolites.

## **Chapter 6:**

# **Investigating the Potential Application of Diagnosing Dysbiosis via Urinary NMR Metabolomics for Detection of Disease Susceptibility.**

## 6.1 – Rationale:

Intestinal dysbiosis is associated with numerous localised and systemic pathologies and research presented in chapter 5 demonstrated various urinary metabolites that are putatively associated with intestinal microbiota composition and thus health or disease. Utilising IBD as an example of a localised dysbiosis-associated disease, this study aimed to apply such principle to prediction of microbiota composition in health and disease states, which may in time be utilised to aid diagnosis via rapid, inexpensive and non-invasive methods.

CD and UC are the two predominant classifications of IBD which are thought to manifest as a consequence of a disrupted immunological response to a dysbiotic gut microbiota. However, despite extensive efforts to elucidate the complexities of these diseases, the precise aetiology and pathophysiology remain uncertain. Current diagnostic strategies for IBD involve combined analysis of historical clinical data, endoscopy examination and histological assessment of mucosal biopsies. Collectively, such techniques are disadvantageous due to their highly invasive and time-consuming nature. Prompt and accurate diagnosis of IBD has proven crucial for improved patient quality of life and effective clinical management as it enables timely administration of appropriate therapeutics. For example, newly diagnosed CD patients promptly given immunosuppressants such as azathioprine, were observed over a period of 26 weeks and found to enter remission earlier and more frequently than those initially given therapeutics considered to be less efficacious (Ricart et al., 2008). Furthermore, the study also reported that timely administration of appropriate therapeutics almost doubled the median time to relapse between the two cohorts (Ricart et al., 2008). At present, no adequate method for detection of IBD exists prior to clinical presentation and so there remains an urgent requirement for novel, non-invasive pre-screening and early diagnostic techniques for IBD.

In recent years research has begun to investigate the role of metabolites in the onset and progression of various diseases, including IBD. Current studies have utilised both animal models, with IL-10 gene deficient mice (Murdoch et al., 2008) and serum, faecal and urine sampling of IBD patients, in an attempt to identify clinical metabolic biomarkers of disease. Several studies investigating faecal metabolomics reported significant differences in the



metabolite profiles of IBD and controls as well as between IBD subsets, CD and UC. Notably, decreased levels of butyrate, acetate and methylamine were found in faecal samples of IBD patients compared to those of healthy controls (Marchesi et al., 2007, Le Gall et al., 2011). Similar metabolomics studies have also investigated the profiles of urine obtained from IBD patients and controls, primarily due to the more convenient nature of sample collection within a clinical environment. Reported results were largely analogous to those obtained from faecal samples, with considerable separation of the two groups utilising PLS-DA models. Determinative urine metabolites include increases in amino acids such as leucine and creatinine, as well as decreases in concentrations of hippurate, acetate and 2-hydroxyisobutyrate (Stephens et al., 2013, Dawiskiba et al., 2014).

There is evidence to suggest that the gut microbiome of IBD patients is distinctive from controls with significant shifts observed in microbial predominance (as discussed in the literature review; Frank et al. (2007)). However, despite repeated conclusive evidence presented in the literature that IBD patients can be distinguished from healthy based on either metabolite or microbiota profile analyses, research has not yet comprehensively explored whether such findings are linked. It may be that dysbiosis of the gut microbiota is accountable for changes observed in the urinary metabolome of IBD patients as a consequence of altered metabolism in a dysbiotic gut. Evidence to support this theory is provided by the fact that the key metabolites identified to hold distinctive power between IBD and controls are primarily amino acids and SCFAs (Bjerrum et al., 2015). SCFA metabolites, including acetate, butyrate and propionate are produced by the activity of the gut microbiota during fermentation of indigestible complex carbohydrates (Reviewed in Rios-Covian et al. (2016)). It is therefore feasible that IBD-associated fluctuations in the composition of the gut microbiota alters synthesis of SCFAs to an extent detectable in patient's urine. This thesis proposes that intestinal dysbiosis observed in IBD leads to distinct variations in the urinary metabolite profiles which may be harnessed for non-invasive diagnostic tests.

## **6.2 – Research Aims:**

- To validate literature reporting distinct microbial and urinary metabolome profiles between IBD and control cohorts.
- To investigate potential relationship between dysbiotic gut microbiota and altered urinary metabolite profiles in IBD patients.

## **6.3 – Methods Summary:**

Illumina® 16S sequencing microbiota and urinary metabolite profile datasets, generated as described in sections 2.2.13, 2.2.14 and 2.2.15, and analysed in chapter 5, were retrospectively assigned into IBD or Control groups according to their diagnosis following endoscopy and histological examination. Multivariate statistical analyses, including hierarchical cluster, PCA and OPLS-DA were employed to investigate potential differences in microbiota and metabolite profiles in IBD and control participants.

## **6.4 – Results:**

### **6.4.1 – Partial separation observed between IBD and control intestinal microbiota profiles.**

Intestinal microbiota profiles of IBD and control individuals were generated utilising Illumina 16S sequencing and are presented at phyla, order level in figures 6.1 and 6.2 respectively. Whilst no immediate trends are apparent between the two groups in these figures, the vast interpatient variability in microbiota composition is obvious, particularly at order level.

Hierarchical clustering analysis of the proportionate microbiota data at phylum, order and genus level, was performed to assess the relationship of microbiota profiles within the two groups (figure 6.3). At phylum level, four distinct groups are apparent with the majority of IBD patients clustering within the rightmost group, although this trend is not exclusive to IBD patients (Figure 6.3A). The same pattern is observed in the clustering of IBD and control patients at order level, with no distinct clusters observed between the two groups (Figure 6.3B). At genus level there are no distinctive trends in clustering between IBD and control patients with an almost even distribution of the patients observed throughout three main clusters, thus indicating that interpatient diversity is more substantial than disease-control group variation (Figure 6.3C).

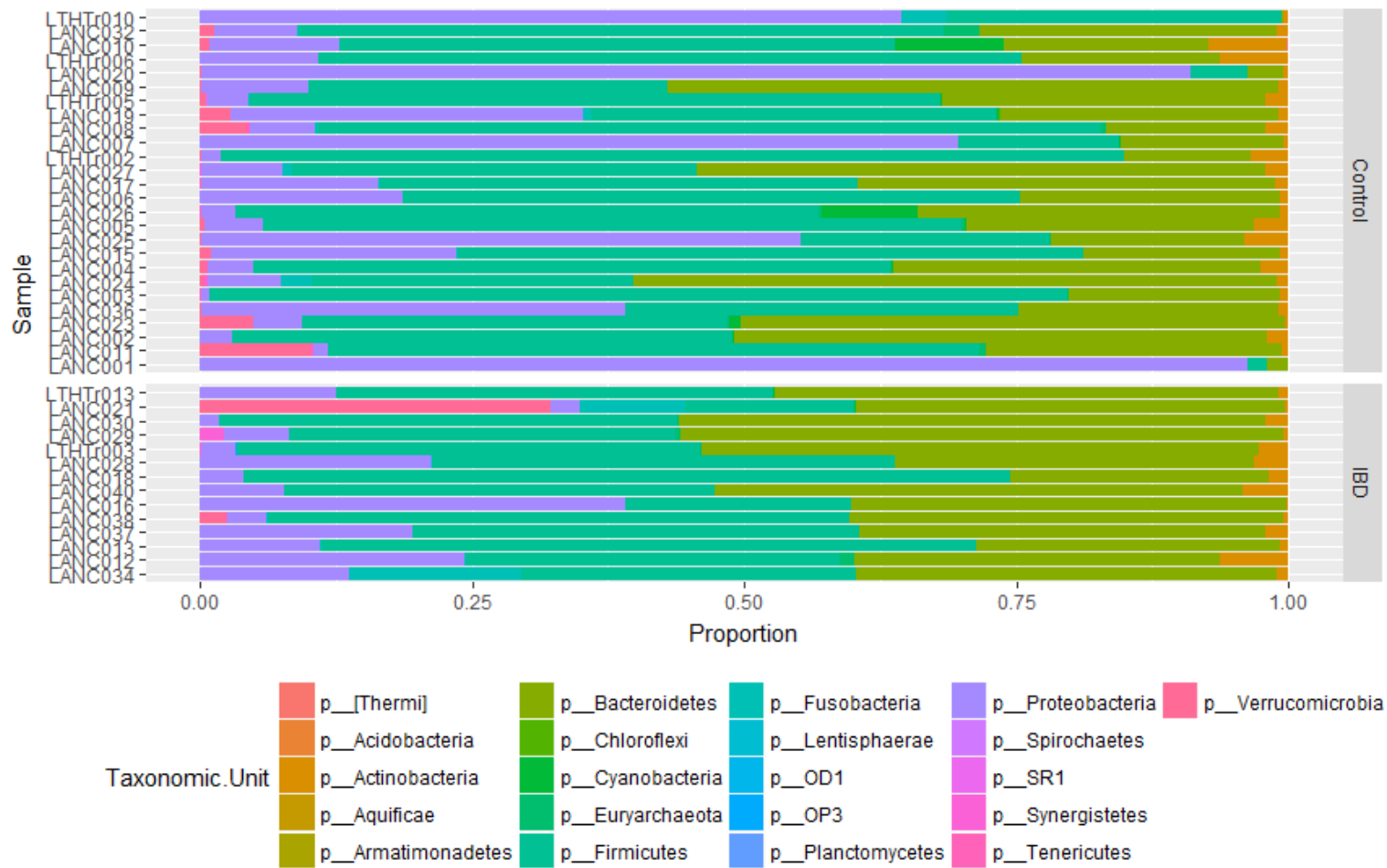


**Figure 6.1** – Relative taxonomic composition of 16S rRNA amplicon sequences from human intestinal biopsy samples, at phylum level, in IBD and control patients. p, Phylum.

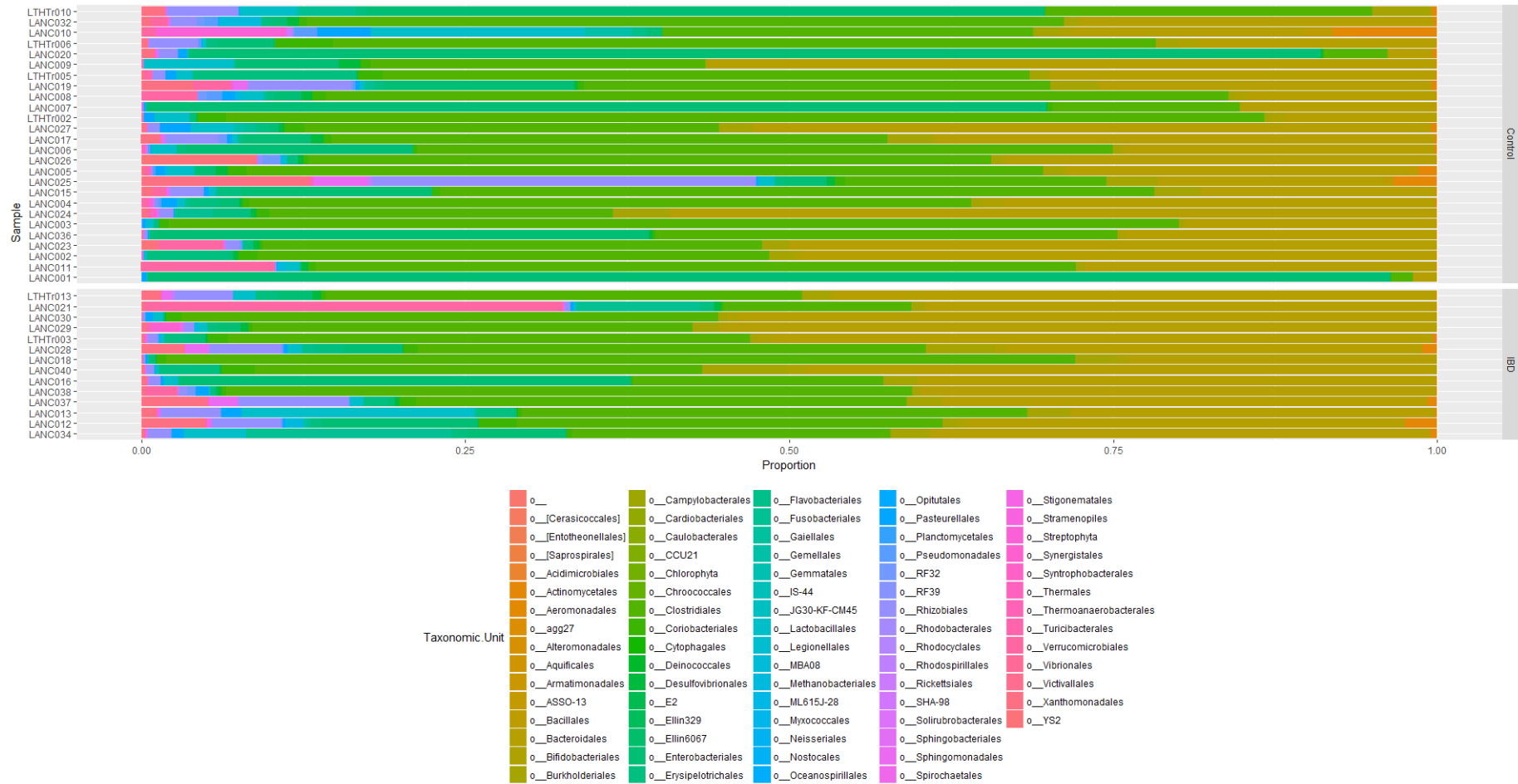


**Figure 6.2** – Relative taxonomic composition of 16S rRNA amplicon sequences from human intestinal biopsy samples, at order level, in IBD and control patients. o, order.



Comparison of control and IBD intestinal microbiota profiles was conducted using PCA. Figure 6.4A demonstrates little separation between the two groups with entirely overlapping clusters. However, the plot also indicates that IBD patients appear to harbour a more consistent microbiota profile as they are observed to be gathered in a tighter cluster than that of the control cohort. Furthermore the PCA biplot which represents the relationship between PC scores and variables as vectors, demonstrates that the variability observed across the control cohort is accountable to proportionate difference in the three predominant order, *Clostridiales*, *Bacteroidales* and *Enterobacteriales* (figure 6.4B).

Supervised multivariate statistical modelling utilising OPLS-DA revealed greater separation between IBD and control microbiota profiles with little overlap observed (figure 6.5A). However, figure 6.5B presents the model overview and it can be seen that although the model explains a large amount of the variance observed across cohorts, as evidenced by  $R^2$  values of 0.509 and 0.159 for X and Y axis respectively, the model has a negative  $Q^2$  value of -0.0421 and therefore does not predict disease state when applied to new data. In addition, orthogonal variation  $R^2$  values were identified to be 0.134 and 0.159 for X and Y axis, indicating that a considerable amount of variation in the microbiota of the study cohort is not related to disease groups.

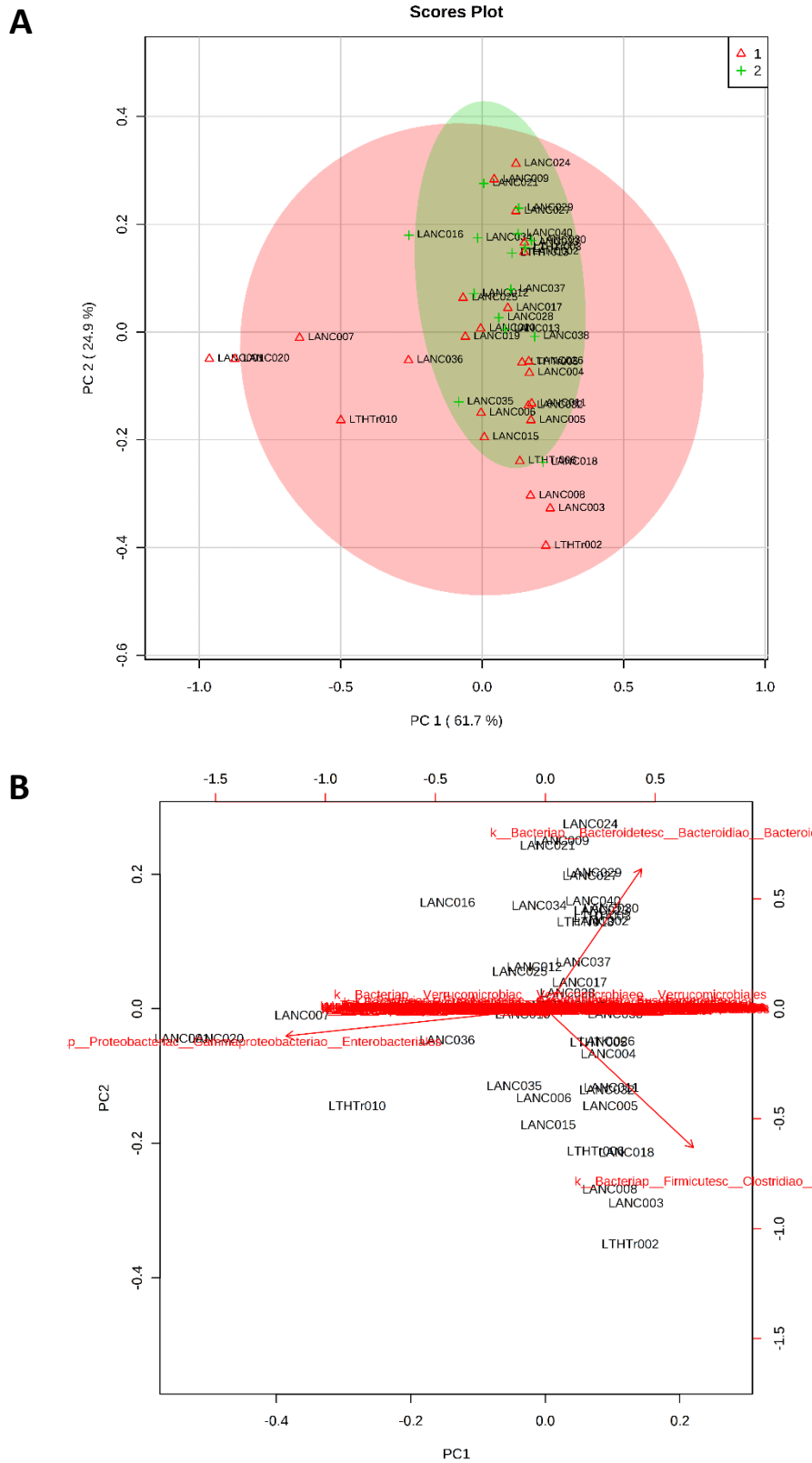


**Figure 6.4 – PCA of intestinal microbiota profiles from IBD and control patients. (A)** PCA scores plot and **(B)** corresponding biplot of proportionate microbiota data, at taxonomic level order, from IBD (green) and control (red) cohorts.



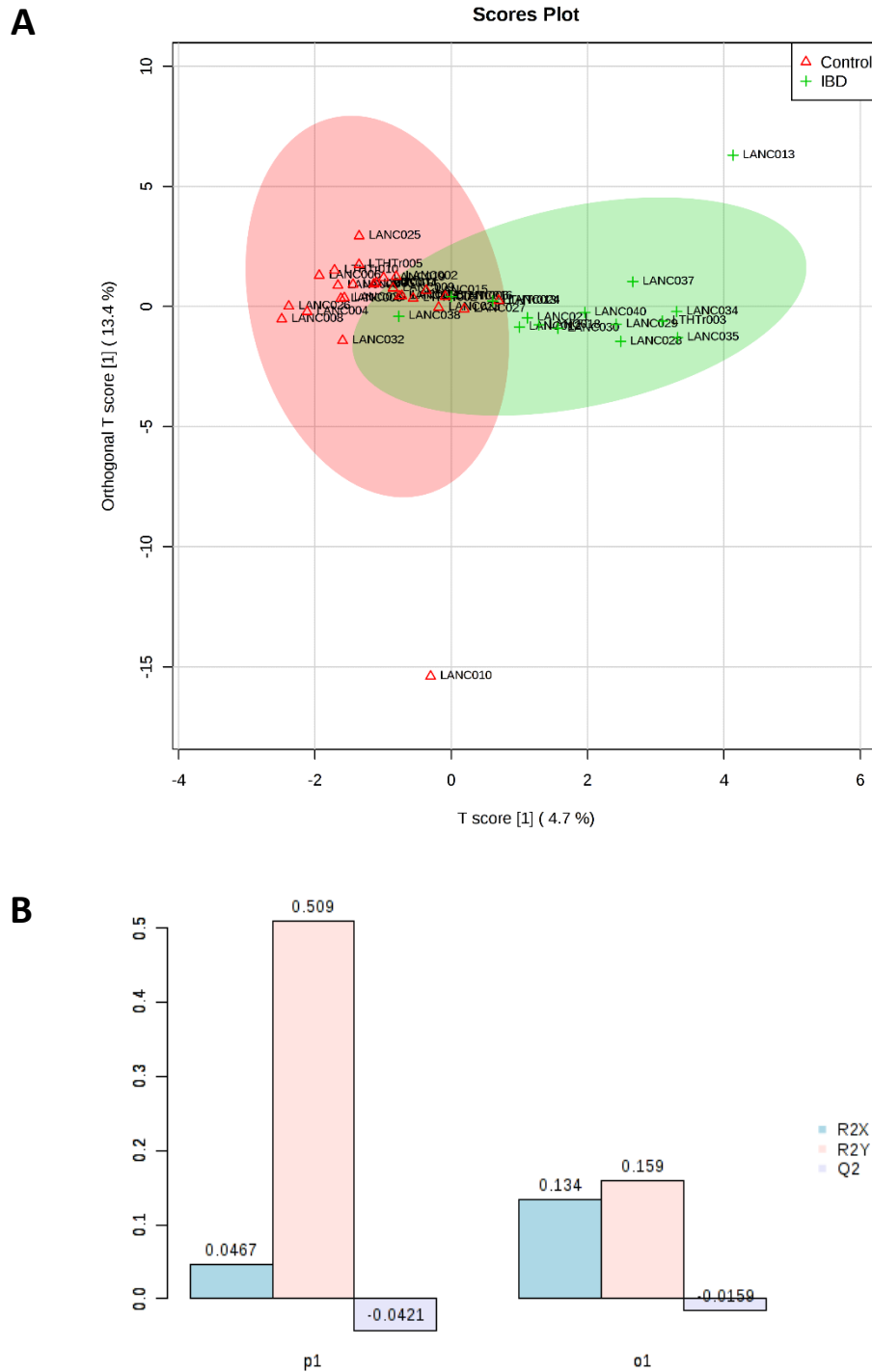


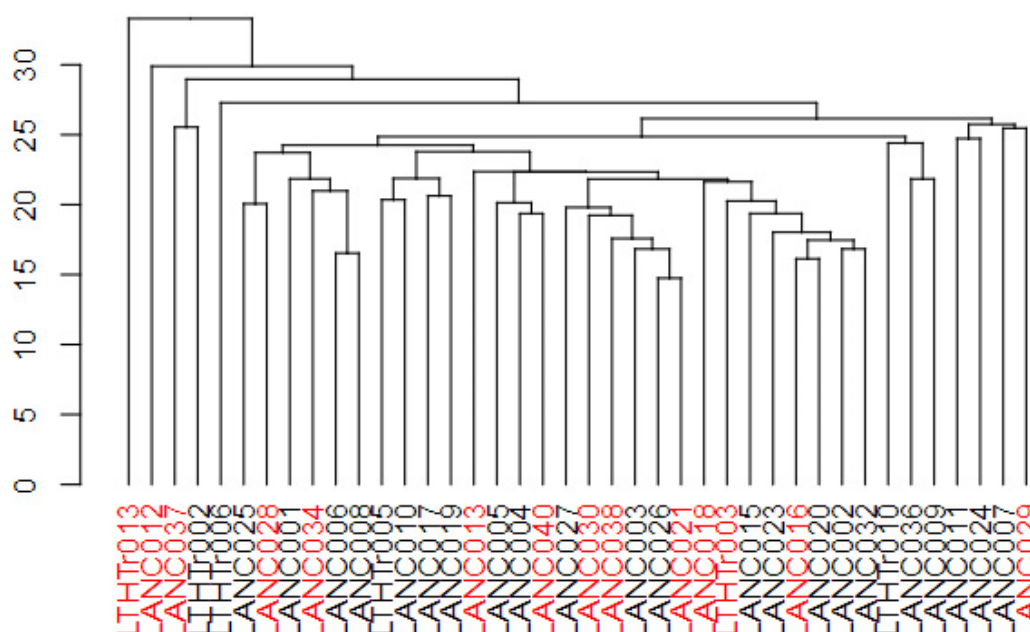
**Figure 6.5 – OPLS-DA of intestinal microbiota profiles from IBD and control patients.**

(A) OPLS-DA scores plot and (B) model overview of proportionate microbiota data, at taxonomic level order, from IBD (green) and control (red) cohorts.  $R^2X$  and  $R^2Y$  are the explained variance of X and Y matrix, respectively and  $Q^2$  is the predictive accuracy of the model. p1, Predictive variation, is the variation of X (microbiota) correlated to Y (groups); o1, orthogonal variation, is the variation in X that is uncorrelated to Y.

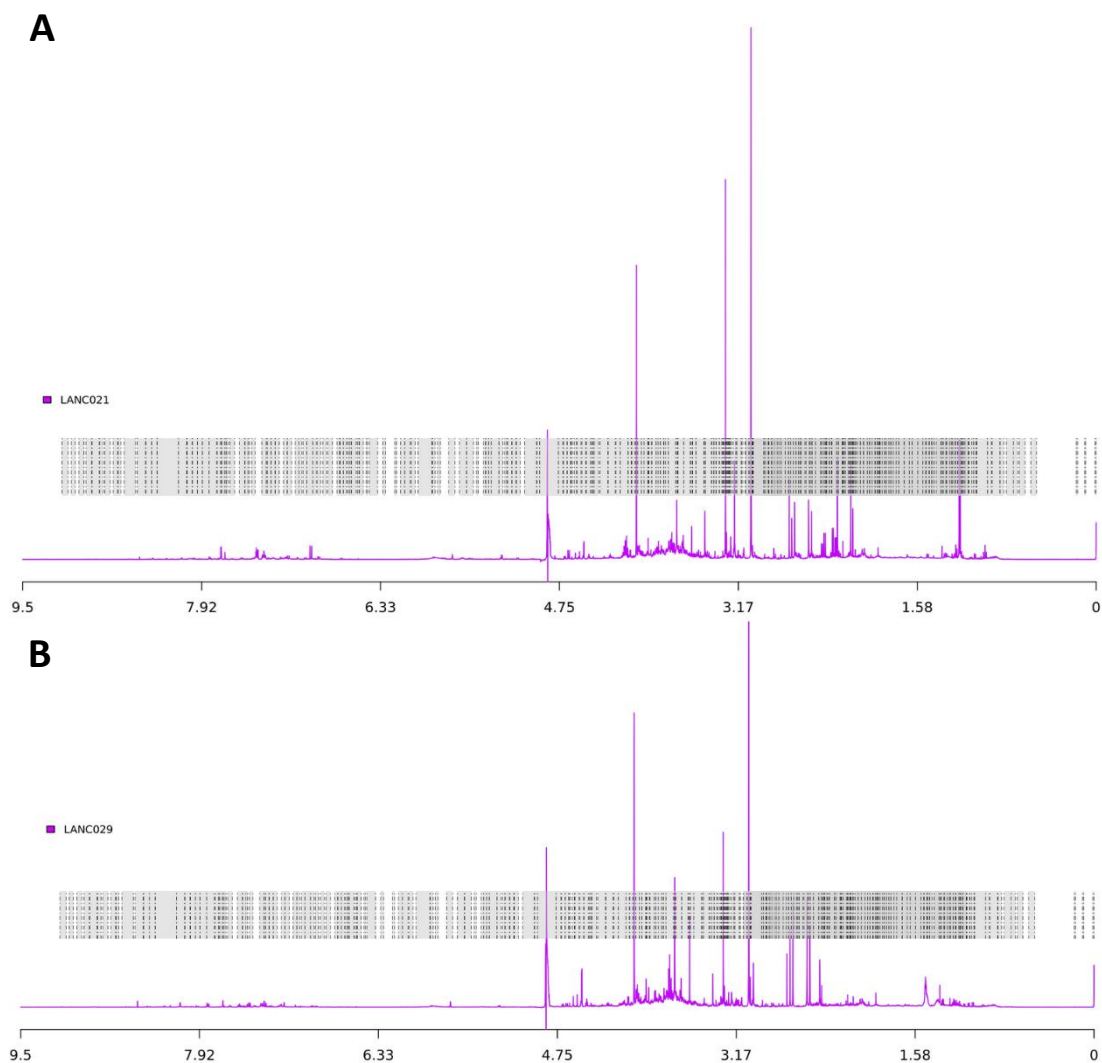
#### 6.4.2 – No distinct differences observed in urinary metabolite profiles of IBD and control cohorts.

Representative  $^1\text{H}$  NMR spectra of urinary metabolites from IBD and control participants are presented in figure 6.7. Distinct differences in peaks and peak intensities are apparent in IBD and control spectra, particularly in the region of 2-3ppm.

Hierarchical clustering analysis revealed that all metabolite profiles are largely dissimilar, as evidenced by an absence of distinct clusters present on the dendrogram (figure 6.6). In addition a minimum branch height of 15 on a relative scale of closeness for all samples is substantially larger than that of the microbiota clustering dendrograms indicating greater variation in metabolite profiles than in the microbiota across the cohort. There is no apparent similarity within the metabolome profiles of IBD and control groups evidenced with cluster analysis, but interestingly, the three most unique profiles, individually branched on the leftmost side of the dendrogram, are those of IBD patients.



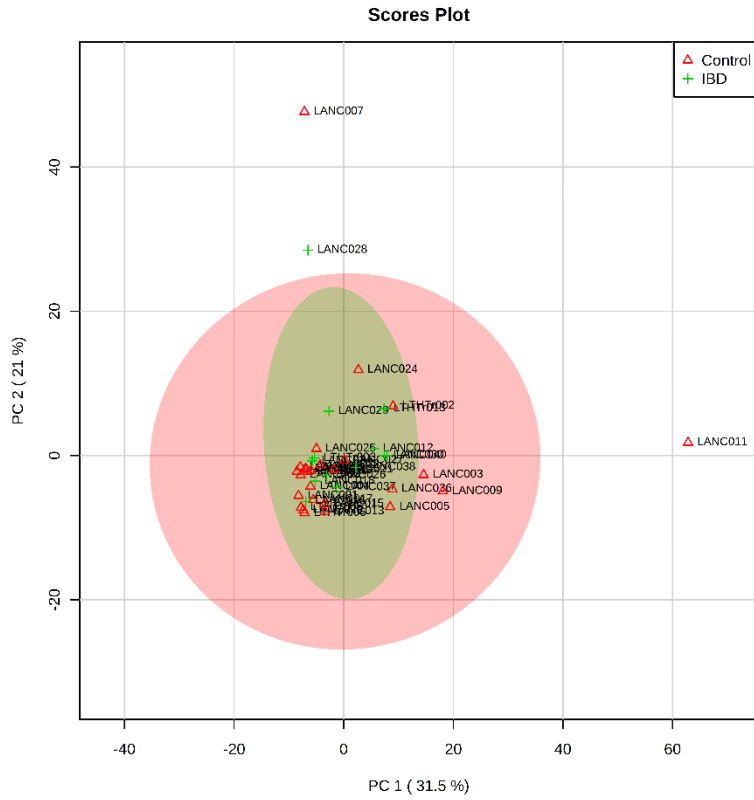
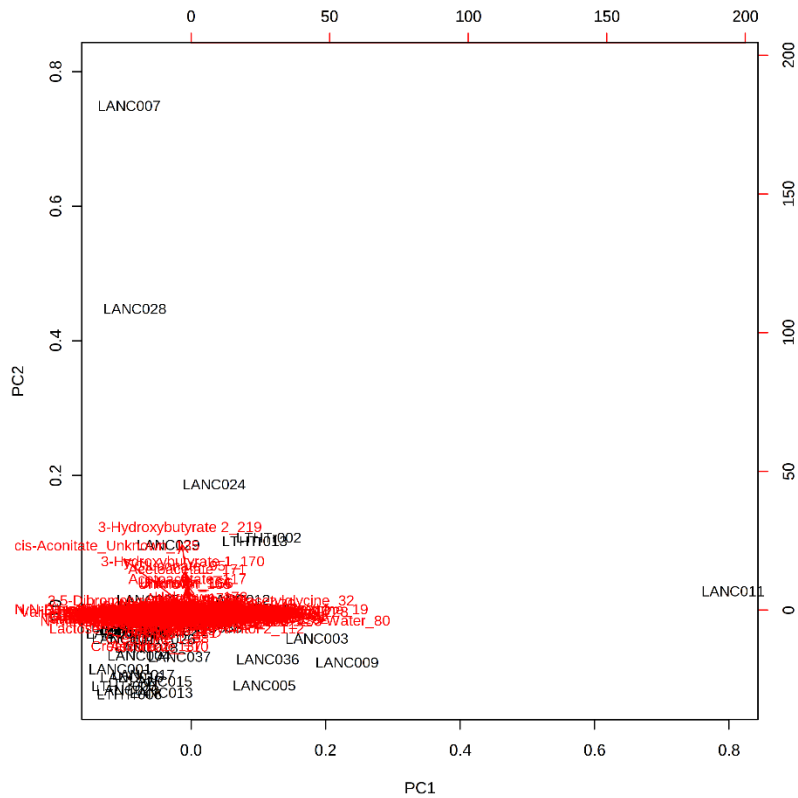
**Figure 6.6 – Hierarchical cluster analysis of  $^1\text{H}$  NMR urinary metabolite NMR profiles from IBD (red) and control (black) cohorts.**



**Figure 6.7 – Representative <sup>1</sup>H NMR spectra of (A) IBD and (B) Control urine samples** with defined bucket boundaries. Metabolite annotations have been omitted for clarity, bucket identities are reported in appendix 8.

Comparison of urinary metabolite profiles of IBD patients and controls utilising PCA revealed no differences between the two cohorts as no segregation was observed in the PCA clusters (figure 6.8A). Additionally, the associated PCA biplot revealed that there are no metabolites that hold importance as evidenced by the equivalent magnitude of vectors present on the biplot (figure 6.8B). Of all metabolites analysed, the 3-hydroxybutyrate vector was observed to have the largest magnitude and therefore may hold potential importance in distinguishing urinary metabolite profiles.

OPLS-DA supervised modelling of urine metabolite data revealed greater segregation of IBD and control metabolite profiles (figure 6.9A). However, as was observed with the microbiota data, the model explained a reasonable amount of variance with  $R^2$  values of 0.0762 and 0.228 for X and Y axis respectively, but the model has no predictive power for disease group with a  $Q^2$  of -0.331 and is therefore invalid (figure 6.9B). Furthermore, orthogonal variation was identified to be higher than predictive variation with  $R^2$  values of 0.0762 and 0.228 for X and Y axis, respectively, indicating that the interpatient variation in metabolite profiles is greater than intergroup variation.

**A****B**

**Figure 6.8 – PCA of urine metabolite profiles from IBD and control patients. (A)** PCA scores plot and **(B)** corresponding biplot of relative  $^1\text{H}$  NMR metabolite concentrations, from IBD (green) and control (red) cohorts.

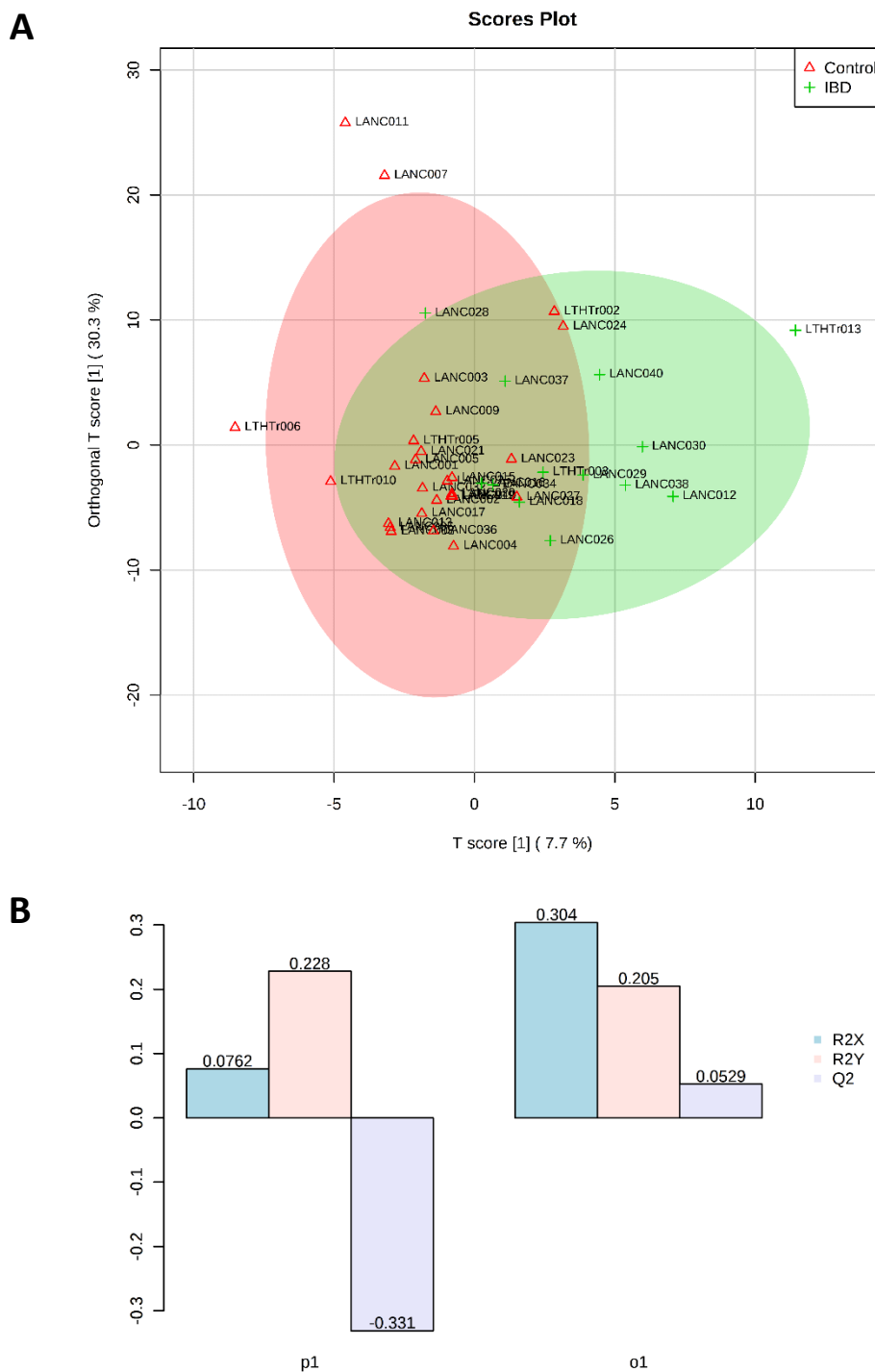


**Figure 6.9 – OPLS-DA of urine metabolite profiles from IBD and control patients.**

(A) OPLS-DA scores plot and (B) model overview of relative <sup>1</sup>H NMR metabolite concentrations, from IBD (green) and control (red) cohorts. R<sup>2</sup>X and R<sup>2</sup>Y are the explained variance of X and Y matrix, respectively and Q<sup>2</sup> is the predictive accuracy of the model. p1, Predictive variation, is the variation of X (metabolites) correlated to Y (groups); o1, orthogonal variation, is the variation in X that is uncorrelated to Y.

**6.4.3 – Participant demographics demonstrated well matched study cohorts but a variety of confounding variables exist between IBD patients.**

Considering the lack of differences observed in the intestinal microbiota and metabolite profiles observed thus far, subsequent attempts to perform integrated analysis of the two datasets was not feasible or worthwhile. Instead review of participant demographics and clinical characteristics was performed to assess suitability of the study cohort and the relevant collected data are presented in table 6.1.

	<b>IBD</b>	<b>Control</b>	<b>Excluded</b>
Number (male/female)	15 (8/7)	26 (13/13)	12
Average age in years ( $\pm$ StDev)	55 ( $\pm$ 16)	56 ( $\pm$ 16)	-
Average disease duration in years (Range)	16 (0-42)	-	-
Disease Classification:			
Crohn's disease	8	-	-
Ulcerative Colitis	5	-	-
Other	2	-	-
Disease state:			
Active IBD	10	-	-
Remission	1	-	-
Untreated - new diagnosis	4	-	-
Medication/treatments:			
Surgical resection	2	-	-
Asacol	3	-	-
5-ASA	4	-	-
Azathioprine	4	-	-
Methotrexate	2	-	-
Budesonide	1	-	-
Sulfasalazine	1	-	-

A total of 53 patients consented to participation in the study, fifteen of whom were confirmed IBD cases based on a combined review of historical, endoscopic and histological data, whilst 26 were classified as controls as defined in the study inclusion and exclusion criteria, resulting in largely unbalanced study groups. A variety of factors including retrospective IBS diagnosis and complications preventing sample collection led to the exclusion of 12 participants. The male to female ratio was well matched with 47% females in the IBD group and a 50% even split in the controls. In addition the average age was almost identical at 55 and 56 ( $\pm$ 16) years in both groups.

Within the IBD group 8 patients were confirmed as Crohn's disease diagnosis and 5 were Ulcerative colitis. In addition 2 patients were classified as other following diagnosis of ischaemic colitis and collagenous colitis respectively. Furthermore, substantial variation was observed in disease state with two thirds of IBD patients classified as active IBD whilst receiving treatment, whilst 1 patient was in remission and 4 others were retrospectively diagnosed and had not yet received any treatment. Finally the range of treatments received was highly variable with administration of various combinations and doses of therapeutics and 2 bowel resections.



## 6.5 – Discussion:

This chapter aimed to explore the relationship between the gut microbiota and urinary metabolite profiles in IBD and Control patients, with an anticipation of identifying a novel non-invasive diagnostic tool for IBD, with potential future application to other dysbiosis-associated pathologies. First, the gut microbiota profiles of IBD and control patients were compared and no difference was observed between the two groups utilising both supervised and supervised statistical methods. This observation is inconsistent with findings presented in the literature as previous studies have reported substantial difference in intestinal microbiota profiles (Frank et al., 2007). Next the urinary metabolite profiles of IBD and controls were compared however, little separation was observed between the two cohorts utilising hierarchical, PCA and OPLS-DA models. Again, this finding contrasts with that reported in the literature, with distinct differentiation identified in the urinary metabolite profiles of IBD and controls (Stephens et al., 2013, Williams et al., 2009). The OPLS-DA statistical modelling employed in this study generated highly disparate  $R^2$  and  $Q^2$  values whilst well matched values of  $R_2 = 0.811$ ;  $Q_2 = 0.698$  were reported in the Stephens *et al.* study, indicating that the data presented in this thesis is subject to model overfitting (Worley and Powers, 2013). Overfitting occurs in supervised statistical methods when the model is highly dependent on the training data, usually as a result of a large number of variables compared with the number of observations (Worley and Powers, 2013). Alternatively, such discrepancies in the data presented with that in the literature may in fact be a result of differences in study design and implementation. For instance, the control cohort in Stephens *et al.* study were self-identified healthy individuals, whereas we recruited outpatients at endoscopy clinics and retrospectively assigned patients to study groups following diagnosis (Stephens et al., 2013). In addition, different  $^1\text{H}$  NMR acquisition parameters were employed in both studies as well as different data processing methods; targeted vs exploratory metabolomics. Such variability in study methodologies can cause data discrepancies and reinforces the requirement for wide-scale method standardisation.

Interestingly, hierarchical clustering of the metabolome profiles identified that the most dissimilar and therefore unique samples were obtained from IBD patients. IBD is defined by development of a 'leaky gut' due to an extensive breakdown in EBF following a loss of tight junction expression, increased apoptosis and chronic inflammation (Su et al., 2013). Such physiology leads to increased intestinal permeability and has been shown to result in

escalated translocation of bacteria and derived products across the epithelial barrier and into the periphery of the host (Demehri et al., 2013). This process is considered crucial in disease progression and severity, and has induced debates to whether dysbiosis is a cause or consequence of IBD (reviewed in Butto and Haller (2016)). It is therefore also plausible that a breakdown of EBF results in an uncontrolled influx of host and bacterial derived metabolites following a loss of absorptive selection mechanisms. This would manifest substantial alterations in the host urinary metabolite profile and abundances and may explain the highly dissimilar profiles observed in three of the study cohort.

The lack of separation between intestinal microbiota and metabolite profiles observed in this study may be a consequence of limited sample size, with only 41 participants in total; 15 in the IBD group and 26 controls. Previous studies successfully demonstrating separation between the groups have been conducted on 100+ participants, likely providing sufficient statistical power to outweigh interpatient genetic and environmental confounding variables to accurately reject the null hypothesis (Stephens et al., 2013, Williams et al., 2009). In addition, the control population within this study is not without limitations; control participants were recruited from endoscopy waiting lists and were categorised retrospectively based on inclusion criteria of no IBD, IBS or colon cancer diagnosis. However, it should not be ignored that the majority of such patients were referred to endoscopy following presentation of concerning clinical symptoms, such as chronic diarrhoea. Such clinical features have been associated with altered intestinal microbiota composition and could consequently attenuate distinction between IBD and control populations. The NHS is now gradually implementing a new CRC screening programme available to all men and women over 55, inviting individuals for endoscope examination in addition to the faecal occult blood test routinely utilised for screening (WWW, NHS Bowel Cancer Screening). This programme will benefit future studies as it will facilitate access to more ideal control patients that are better representations of the general population and healthy individuals.

The reliability of the IBD test group may also be scrutinised as collated participant demographics detail substantial variations between IBD participants particularly in the case of treatments. It was found that one third of the participants were not receiving treatment, either due to remission or new diagnosis, whilst 2 participants had previously undergone

surgical bowel resection and the remaining individuals were in receipt of a variety of medications. Previous research has demonstrated that various forms of prescribed medication and treatments can attenuate metabolic discrimination of IBD patients, particularly between disease subsets. Two studies reported differing metabolite profiles in patients on TNF- $\alpha$  antibody therapy to those on alternative forms of treatment (Stephens et al., 2013, Bjerrum et al., 2015). In addition, the same studies demonstrated that IBD patients who have previously undergone surgical bowel resection may also confound statistical outcome of urinary metabolite analyses, which is logical as a shorter colon is likely to result in reduced or altered metabolite absorption (Stephens et al., 2013, Bjerrum et al., 2015). Furthermore, it has been previously reported that urinary metabolite profiles differ in patient with active IBD and those in remission (Dawiskiba et al., 2014). Considering this study was conducted with the long term goal of developing a potential novel diagnostic or pre-screening test for IBD in addition to other dysbiosis-associated diseases, future research should aim to obtain samples from newly diagnosed and untreated IBD patients to remove confounding variables and ensure representativeness, although such rigorous recruitment criteria would have been infeasible within the time frame of this study. Longitudinal studies that investigate participants at diagnosis and after 'X' weeks of treatment would also be useful to eliminate confounding variables and thus facilitate monitoring of intestinal microbiota and host metabolite responses to either drug or dietary-associated therapeutics.

Overall, this study aimed to first confirm reports of distinct urinary metabolite and intestinal microbiota profiles in IBD and healthy individuals and then perform integrated omics analyses, analogous to that applied in chapter 5, to investigate the potential relationship between bacterial derived metabolites and health or disease state. However, due to limited patient recruitment and subsequent sample size, statistical power was not reached with the initial aim of this study meaning the latter could not be conducted. Further research, implementing the improvements suggested herein, is therefore required to establish whether specific urinary metabolites or metabolite profiles can predict inflammatory bowel disease, as an example of a dysbiosis-associated disease.

## **Chapter 7:**

### **Discussion and Future Directions**

## **7.1 – Discussion and Future Directions**

The intestinal microbiota is a highly diverse microbial ecosystem that holds vast health implications for the human host. From promoting metabolic capabilities and mediating inflammatory responses through to potentially influencing host behaviour via the gut-brain axis, the intestinal microbiota is undoubtedly a super organism that is pivotal in most aspects of health and disease. Decades of research has methodically unravelled the complex cellular and biochemical mechanisms facilitating host-microbiota coevolution as well as factors such as dysbiosis that underpin the breakdown of homeostasis and onset of intestinal disease. However despite such advances, caveats in this literature persist, most notably regarding characterisation of dysbiosis and translation of research into clinical diagnostic and therapeutic applications.

In relation to this project, our research area of interest concerned dysbiosis of the intestinal microbiota and its role in the onset and as a potential predictor of associated pathologies. We first employed a novel human model utilising loop ileostomy patients to study intestinal microbiota profiles in distinct nutritional environments, controlling for confounding interpatient genetic and environment variability. From here we next assessed the consequences of dysbiosis in patients undergoing ileostomy reversal surgery with consideration to post-operative clinical outcome. Finally we attempted multi-omics integration of NMR and Illumina sequencing data to assess the relationship between intestinal microbiota profiles and urinary metabolites as a potential clinical indicator of dysbiosis. Collectively, the results generated advance our understanding of intestinal dysbiosis and provide promise for further development in future studies.

## **7.2 – Dysbiosis as a Cause of Intestinal Pathology.**

A long standing debate exists in the field of intestinal microbiota research as to the cause or consequential role of dysbiosis in pathogenesis of associated diseases (reviewed in Butto and Haller (2016)). One side of the argument proposes that dysbiosis occurs in consequence to disease as localised inflammation-associated changes in epithelial integrity may select for a dysbiotic microbiota and perpetuate disease phenotype. Alternatively, it is also suggested that the acquisition of a dysbiotic microbiota induces inflammation and causes breakdown

of EBF resulting in disease pathology. Both theories are plausible but the latter, if proven accurate, would influence the clinical management and diagnosis of associated diseases considerably.

Our investigations into microbiota composition exploiting a novel human model in loop ileostomy patients identified that intestinal dysbiosis caused substantial distortion of mucosal architecture, with considerable villous atrophy, as a result of reduced IEC proliferation which is likely due to altered host-microbiota interactions at the epithelial surface. The use of our novel human model was advantageous as it enabled inpatient comparisons of microbiota profiles and associated intestinal physiology whilst controlling for interpatient genetic and environmental variables that often confound such clinical studies. Functional ileostomy limbs served as paired controls due to receipt of enteral nutrition and these samples were found to maintain healthy intestinal environment when compared to the respective defunctioned ileum. Such findings support a causal role for perturbations in the intestinal microbiota in localised disease pathologies as the experimental model controlled for all confounding variables thus demonstrating capacity for a dysbiotic microbiota to instigate disease pathology.

The aetiology of dysbiosis is regarded as multifactorial since no contributory genetic or environmental factor is independently sufficient to instigate dysbiosis associated disease. Considering our human model, the intestinal microbiota was subject to extreme insult in the form of complete nutritional deprivation which induced dysbiosis and intestinal injury. However, it is unlikely that natural variation in host diet is substantial enough to cause such profound and detrimental dysbiosis, meaning host genetic and environmental influences are also required for disease onset. Interestingly, the aetiology of cancer has been defined by a 'multi-hit' hypothesis which states that multiple mutations acquired in tumour suppressor genes are required to instigate tumour growth, particularly in CRC (Segditsas et al., 2009). Furthermore, this same principle has been suggested for two recognised dysbiosis associated pathologies, schizophrenia and NAFLD, with a combination of genetic susceptibility and various determinative environmental factors that are encountered at different stages through life resulting in full clinical onset (Feigenson et al., 2014, Buzzetti et al., 2016). Intestinal dysbiosis also fits this hypothesis, with genetic and environmental factors, such as

NOD mutations and postpartum colonisation, underpinning predisposition, then subsequent lifestyle practices such as diet and antibiotic use which pivotally lead to dysbiosis. Essentially, the more 'hits' an individual has with predisposing factors the more susceptible they are to developing dysbiosis and associated diseases.

Current treatments for dysbiosis associated diseases function to reverse a 'hit' in disease susceptibility by disrupting functional interactions that promote disease onset. These therapeutics usually target either the aberrant immune response or the dysbiotic microbiota to attenuate disease pathology. For example, inflammatory cytokines have been targeted with antibody therapies such as anti-TNF- $\alpha$  antibody, Infliximab for treatment of IBD (De Bie et al., 2011). Alternatively, FMT which involves transplanting a healthy microbiota into a diseased host to eliminate dysbiosis has also been explored in IBD therapy and is considered to be more efficacious than immunomodulatory techniques which may be counteracted by compensatory immune pathways (Moayyedi et al., 2015, Paramsothy et al., 2017).

A novel opportunity for microbiota-targeted therapeutic intervention which may provide an interesting avenue for further research involves the use of prebiotic preparations in loop ileostomy patients. Direct administration of prebiotics to the defunctioned intestine in the weeks prior to reversal surgery could restore the microbiota and reinstate intestinal homeostasis, offering an improved microbial and physiological environment better able to promote intestinal health and repair following reanastomosis. This could potentially reduce morbidity rates associated with reversal procedure as the risk of developing complications such as post-operative ileus may be consequently reduced. Furthermore, the application of probiotics to the defunctioned intestine should be considered inappropriate as artificial increases in bacterial load within a dysbiotic and unstable physiological environment is likely to trigger chronic inflammation and perpetuate breakdown of EBF, increasing potential of clinical complications.

Finally, one overarching conclusion from this research is that the future direction of therapeutics is likely to progress into personalised treatment strategies to accommodate individual variability in the functional composition of the intestinal microbiota. The principle

of personalised medicine to make such accommodations has recently been explored in type II diabetic patients. Zeevi *et al.* developed a clinical model which successfully utilised 16S rRNA intestinal microbiota, clinical and postprandial glucose data of 800 individuals to predict glucose response to 'real-life' meals for a validation cohort (Zeevi *et al.*, 2015). This research then enabled personalisation of meal choices based on intestinal microbiota profiles which consequently reduced the risk of diabetes via microbiota-mediated indirect control postprandial glucose levels.

### **7.3 – Dysbiosis as a Predictor of Disease.**

Previous studies have defined intestinal microbiota 'enterotypes' that are predominated by a different microbial phyla and exist independent of cultural differences within the human race (Arumugam *et al.*, 2011, Harmsen and C., 2016). These four enterotypes are suggested to share common functionality and have been inferred with either health or disease. In our research five distinct enterotype-like profiles were identified within the study cohort via hierarchical cluster analysis of proportionate microbiota data. These profiles were analogous to enterotypes described in the literature, with each predominated by distinct microbiota populations that have previously been associated with health or disease status such as IBD and obesity. This suggests that the substantial inter-individual variation observed in intestinal microbiota profiles, at genus and species taxonomic levels, may not hinder clinical advancements as much as is currently anticipated because such rationale endorses stratification of patients into defined microbiota subgroups. This principle is fortified with the observation that different microbial species share common metabolic functionality and so exert significant influences on host phenotype through combined biochemical and enzymatic capabilities despite presence in low abundances. Ultimately, this may render microbiota variation at species level insignificant when concerning the functional consequences of dysbiosis in the onset of associated diseases.

The current diagnosis of dysbiosis associated diseases relies solely on combined assessment of clinical presentations and historical patient data, largely due to the multifactorial nature of such diseases which makes their prediction difficult. However, considering the proposed pivotal role of dysbiosis as a determinative 'hit' factor in the onset of various associated



diseases, and the association of specific enterotypes with various diseases, it may be possible to predict host disease susceptibility based on analysis of intestinal microbiota composition. To test this theory we investigated the potential prospect that host urinary metabolites reflect functional enterotypes. The rationale for this connection was supported by the understanding that different microbial fermentation pathways produce distinct SCFA end-products, that when in excess, are excreted through urination (Tremaroli and Backhed, 2012). Several urinary metabolites were identified to be associated with the enterotypes defined in our study cohort, however such metabolites tended to be dietary-associated, such as flavonoids, rather than metabolites directly associated with bacterial activity, such as SCFA. This is not entirely surprising as it may be a reflection of a diet that is supportive of a particular enterotype, rather than a reflection of enterotype metabolism. We found such dietary metabolite associations were replicated when correlated with four predominant microbiota phyla. Such findings may hold potential to manipulate an individual's enterotype through dietary means. In addition, these findings do not discount the distinguishing potential of SCFA metabolites for intestinal microbiota prediction as the enriched and chemically-complex nature of urine as a waste product of metabolism is likely to have overshadowed fluctuations in less abundant metabolites. Targeted metabolite analyses can be employed in future to investigate specific metabolites of interest.

Future research should also undertake application of this theory to detect dysbiosis associated diseases by investigating the predictive capacity of the intestinal microbiota for IBD (or another example disease) through urinary metabolite analysis. Previous research has demonstrated an ability to distinguish IBD from healthy via discriminant analysis of urinary NMR metabolite profiles, with significant differences observed in host- and bacterial-derived metabolites (Stephens et al., 2013, Williams et al., 2009). Still, research had not yet correlated such metabolite profiles with intestinal microbiota composition and health and disease status within the same individual. Unfortunately our attempts were hindered by limited sample numbers and flawed participant cohorts resulting in no distinction between IBD and controls using metabolite or microbiota analysis. In future, particular consideration should be paid to ensure the representative nature of study cohorts to undiagnosed IBD and healthy populations, for example. This will offer better predictive capacity to first replicate the findings of previous studies and subsequently enable integration of the microbiota and

metabolomic datasets to determine predictive capacity of host urinary metabolites for health and disease.

One significant issue surrounding application of novel diagnostic or screening techniques is the feasibility of biomarker detection. To ensure downstream compatibility of this theory and practise to clinical implementation, a convenient and non-invasive test to detect dysbiosis would be required. Current NMR spectrometry based analysis of urinary metabolites would be costly, time consuming and thus infeasible on a broad scale. Following comprehensive identification of characteristic metabolite profiles, associated with intestinal enterotypes, a set of reagent strips could be developed to enable rapid and low-cost quantification of metabolites, in the form of a urine dipstick test, analogous to that routinely utilised to estimate glucose levels during diagnosis of type II diabetes.

In conclusion, this thesis supports the growing body of evidence suggesting that the microbiota is paramount in intestinal (and organismal) health. Determination of intestinal microbiota composition, ideally via rapid, inexpensive and non-invasive techniques such as analysis of urinary metabolites, could theoretically be utilised to predict patient disease susceptibility and stratify patients to appropriate therapeutics. Such a pre-screening technique lends itself well to the probable forthcoming application of personalised medicine, as a convenient detector of microbiota composition that could be utilised to make informed decisions with drug prescriptions and disease diagnoses.

# **Bibliography**

## References

- ABRAMS, G. D., BAUER, H. & SPRINZ, H. 1963. Influence of the normal flora on mucosal morphology and cellular renewal in the ileum. A comparison of germ-free and conventional mice. *Lab Invest*, 12, 355-64.
- ABREU, M. T. 2010. Toll-like receptor signalling in the intestinal epithelium: how bacterial recognition shapes intestinal function. *Nat Rev Immunol*. England.
- ABRISQUETA, J., ABELLAN, I., FRUTOS, M. D., LUJAN, J. & PARRILLA, P. 2013. [Afferent loop stimulation prior to ileostomy closure]. *Cir Esp*, 91, 50-2.
- ABRISQUETA, J., ABELLAN, I., LUJAN, J., HERNANDEZ, Q. & PARRILLA, P. 2014. Stimulation of the efferent limb before ileostomy closure: a randomized clinical trial. *Dis Colon Rectum*, 57, 1391-6.
- ALAM, M., MIDTVEDT, T. & URIBE, A. 1994. Differential cell kinetics in the ileum and colon of germfree rats. *Scand J Gastroenterol*, 29, 445-51.
- ALTSCHUL, S. F., GISH, W., MILLER, W., MYERS, E. W. & LIPMAN, D. J. 1990. Basic local alignment search tool. *J Mol Biol*, 215, 403-10.
- ARRIETA, M. C., STIEMSMA, L. T., DIMITRIU, P. A., THORSON, L., RUSSELL, S., YURIST-DOUTSCH, S., KUZELJEVIC, B., GOLD, M. J., BRITTON, H. M., LEFEBVRE, D. L., SUBBARAO, P., MANDHANE, P., BECKER, A., MCNAGNY, K. M., SEARS, M. R., KOLLMANN, T., MOHN, W. W., TURVEY, S. E. & FINLAY, B. B. 2015. Early infancy microbial and metabolic alterations affect risk of childhood asthma. *Sci Transl Med*, 7, 307ra152.
- ARUMUGAM, M., RAES, J., PELLETIER, E., LE PASLIER, D., YAMADA, T., MENDE, D. R., FERNANDES, G. R., TAP, J., BRULS, T., BATTO, J.-M., BERTALAN, M., BORRUEL, N., CASELLAS, F., FERNANDEZ, L., GAUTIER, L., HANSEN, T., HATTORI, M., HAYASHI, T., KLEEREBEZEM, M., KUROKAWA, K., LECLERC, M., LEVENEZ, F., MANICHANH, C., NIELSEN, H. B., NIELSEN, T., PONS, N., POULAIN, J., QIN, J., SICHERITZ-PONTEN, T., TIMS, S., TORRENTS, D., UGARTE, E., ZOETENDAL, E. G., WANG, J., GUARNER, F., PEDERSEN, O., DE VOS, W. M., BRUNAK, S., DORE, J., WEISSENBACH, J., EHRLICH, S. D. & BORK, P. 2011. Enterotypes of the human gut microbiome. *Nature*, 473, 174-180.
- ATARASHI, K., TANOUE, T., OSHIMA, K., SUDA, W., NAGANO, Y., NISHIKAWA, H., FUKUDA, S., SAITO, T., NARUSHIMA, S., HASE, K., KIM, S., FRITZ, J. V., WILMES, P., UEHA, S., MATSUSHIMA, K., OHNO, H., OLLE, B., SAKAGUCHI, S., TANIGUCHI, T., MORITA, H., HATTORI, M. & HONDA, K. 2013. Treg induction by a rationally selected mixture of Clostridia strains from the human microbiota. *Nature*, 500, 232-6.
- AVERSHINA, E. & RUDI, K. 2015. Confusion about the species richness of human gut microbiota. *Benef Microbes*, 6, 657-9.
- BACCHETTI DE GREGORIS, T., ALDRED, N., CLARE, A. S. & BURGESS, J. G. 2011. Improvement of phylum- and class-specific primers for real-time PCR quantification of bacterial taxa. *J Microbiol Methods*, 86, 351-6.
- BAILEY, C. M., WHEELER, J. M., BIRKS, M. & FAROUK, R. 2003. The incidence and causes of permanent stoma after anterior resection. *Colorectal Dis*, 5, 331-4.
- BARKER, N., VAN DE WETERING, M. & CLEVERS, H. 2008. The Intestinal Stem Cell. *Genes & Development* 22, 1856-1864.
- BAUMGART, M., DOGAN, B., RISHNIW, M., WEITZMAN, G., BOSWORTH, B., YANTISS, R., ORSI, R. H., WIEDMANN, M., MCDONOUGH, P., KIM, S. G., BERG, D., SCHUKKEN, Y., SCHERL, E. & SIMPSON, K. W. 2007. Culture independent analysis of ileal mucosa reveals a selective increase in invasive Escherichia coli of novel phylogeny relative to depletion of Clostridiales in Crohn's disease involving the ileum. *Isme j*, 1, 403-18.

- BEAMISH, E. L., JOHNSON, J., SHAW, E. J., SCOTT, N. A., BHOWMICK, A. & RIGBY, R. J. 2017. Loop ileostomy-mediated fecal stream diversion is associated with microbial dysbiosis. *Gut Microbes*, 1-12.
- BECKONERT, O., KEUN, H. C., EBBELS, T. M., BUNDY, J., HOLMES, E., LINDON, J. C. & NICHOLSON, J. K. 2007. Metabolic profiling, metabolomic and metabonomic procedures for NMR spectroscopy of urine, plasma, serum and tissue extracts. *Nat Protoc*, 2, 2692-703.
- BENNETT, B. J., DE AGUIAR VALLIM, T. Q., WANG, Z., SHIH, D. M., MENG, Y., GREGORY, J., ALLAYEE, H., LEE, R., GRAHAM, M., CROOKE, R., EDWARDS, P. A., HAZEN, S. L. & LUSIS, A. J. 2013. Trimethylamine-N-oxide, a metabolite associated with atherosclerosis, exhibits complex genetic and dietary regulation. *Cell Metab*, 17, 49-60.
- BERG, R. D. 1996. The indigenous gastrointestinal microflora. *Trends Microbiol*, 4, 430-5.
- BIASUCCI, G., BENENATI, B., MORELLI, L., BESSI, E. & BOEHM, G. 2008. Cesarean delivery may affect the early biodiversity of intestinal bacteria. *J Nutr*, 138, 1796s-1800s.
- BIEDERMANN, L., BRULISAUER, K., ZEITZ, J., FREI, P., SCHARL, M., VAVRICKA, S. R., FRIED, M., LOESSNER, M. J., ROGLER, G. & SCHUPPLER, M. 2014. Smoking cessation alters intestinal microbiota: insights from quantitative investigations on human fecal samples using FISH. *Inflamm Bowel Dis*, 20, 1496-501.
- BIRRENBACH, T. & BOCKER, U. 2004. Inflammatory bowel disease and smoking: a review of epidemiology, pathophysiology, and therapeutic implications. *Inflamm Bowel Dis*, 10, 848-59.
- BJERRUM, J. T., WANG, Y., HAO, F., COSKUN, M., LUDWIG, C., GUNTHER, U. & NIELSEN, O. H. 2015. Metabonomics of human fecal extracts characterize ulcerative colitis, Crohn's disease and healthy individuals. *Metabolomics*, 11, 122-133.
- BONEN, D. K., OGUURA, Y., NICOLAE, D. L., INOHARA, N., SAAB, L., TANABE, T., CHEN, F. F., FOSTER, S. J., DUERR, R. H., BRANT, S. R., CHO, J. H. & NUNEZ, G. 2003. Crohn's disease-associated NOD2 variants share a signaling defect in response to lipopolysaccharide and peptidoglycan. *Gastroenterology*, 124, 140-6.
- BOUATRA, S., AZIAT, F., MANDAL, R., GUO, A. C., WILSON, M. R., KNOX, C., BJORND AHL, T. C., KRISHNAMURTHY, R., SALEEM, F., LIU, P., DAME, Z. T., POELZER, J., HUYNH, J., YALLOU, F. S., PSYCHOGIOS, N., DONG, E., BOGUMIL, R., ROEHRING, C. & WISHART, D. S. 2013. The human urine metabolome. *PLoS One*, 8, e73076.
- BOUSKRA, D., BREZILLON, C., BERARD, M., WERTS, C., VARONA, R., BONECA, I. G. & EBERL, G. 2008. Lymphoid tissue genesis induced by commensals through NOD1 regulates intestinal homeostasis. *Nature*, 456, 507-10.
- BRANDL, K., SUN, L., NEPPL, C., SIGGS, O. M., LE GALL, S. M., TOMISATO, W., LI, X., DU, X., MAENNEL, D. N., BLOBEL, C. P. & BEUTLER, B. 2010. MyD88 signaling in nonhematopoietic cells protects mice against induced colitis by regulating specific EGF receptor ligands. *Proc Natl Acad Sci U S A*, 107, 19967-72.
- BROGDEN, K. A. 2005. Antimicrobial peptides: pore formers or metabolic inhibitors in bacteria? *Nat Rev Microbiol*, 3, 238-50.
- BUTTO, L. F. & HALLER, D. 2016. Dysbiosis in intestinal inflammation: Cause or consequence. *Int J Med Microbiol*, 306, 302-9.
- BUZZETTI, E., PINZANI, M. & TSOCHATZIS, E. A. 2016. The multiple-hit pathogenesis of non-alcoholic fatty liver disease (NAFLD). *Metabolism*, 65, 1038-48.
- CAMILLERI, M., VAZQUEZ-ROQUE, M., ITURRINO, J., BOLDINGH, A., BURTON, D., MCKINZIE, S., WONG, B. S., RAO, A. S., KENNY, E., MANSSON, M. & ZINSMEISTER, A. R. 2012. Effect of a glucagon-like peptide 1 analog, ROSE-010, on GI motor functions in female patients with constipation-predominant irritable bowel syndrome. *Am J Physiol Gastrointest Liver Physiol*, 303, G120-8.

- CANI, P. D., AMAR, J., IGLESIAS, M. A., POGGI, M., KNAUF, C., BASTELICA, D., NEYRINCK, A. M., FAVA, F., TUOHY, K. M., CHABO, C., WAGET, A., DELMEE, E., COUSIN, B., SULPICE, T., CHAMONTIN, B., FERRIERES, J., TANTI, J. F., GIBSON, G. R., CASTEILLA, L., DELZENNE, N. M., ALESSI, M. C. & BURCELIN, R. 2007. Metabolic endotoxemia initiates obesity and insulin resistance. *Diabetes*, 56, 1761-72.
- CANI, P. D., POSSEMIERS, S., VAN DE WIELE, T., GUIOT, Y., EVERARD, A., ROTTIER, O., GEURTS, L., NASLAIN, D., NEYRINCK, A., LAMBERT, D. M., MUCCIOLI, G. G. & DELZENNE, N. M. 2009. Changes in gut microbiota control inflammation in obese mice through a mechanism involving GLP-2-driven improvement of gut permeability. *Gut*, 58, 1091-103.
- CAPORASO, J. G., KUCZYNSKI, J., STOMBAUGH, J., BITTINGER, K., BUSHMAN, F. D., COSTELLO, E. K., FIERER, N., PENA, A. G., GOODRICH, J. K., GORDON, J. I., HUTTLEY, G. A., KELLEY, S. T., KNIGHTS, D., KOENIG, J. E., LEY, R. E., LOZUPONE, C. A., MCDONALD, D., MUEGGE, B. D., PIRRUNG, M., REEDER, J., SEVINSKY, J. R., TURNBAUGH, P. J., WALTERS, W. A., WIDMANN, J., YATSUNENKO, T., ZANEVELD, J. & KNIGHT, R. 2010. QIIME allows analysis of high-throughput community sequencing data. *Nat Methods*. United States.
- CARD, T., LOGAN, R. F., RODRIGUES, L. C. & WHEELER, J. G. 2004. Antibiotic use and the development of Crohn's disease. *Gut*, 53, 246-50.
- CENTER, M. M., JEMAL, A. & WARD, E. 2009. International trends in colorectal cancer incidence rates. *Cancer Epidemiol Biomarkers Prev*, 18, 1688-94.
- CHEUNG, W., KESKI-RAHKONEN, P., ASSI, N., FERRARI, P., FREISLING, H., RINALDI, S., SLIMANI, N., ZAMORA-ROS, R., RUNDLE, M., FROST, G., GIBBONS, H., CARR, E., BRENNAN, L., CROSS, A. J., PALA, V., PANICO, S., SACERDOTE, C., PALLI, D., TUMINO, R., KUHN, T., KAAKS, R., BOEING, H., FLOEGEL, A., MANCINI, F., BOUTRON-ROUAULT, M. C., BAGLIETTO, L., TRICHOPOULOU, A., NASKA, A., ORFANOS, P. & SCALBERT, A. 2017. A metabolomic study of biomarkers of meat and fish intake. *Am J Clin Nutr*, 105, 600-608.
- CLAYTON, E. M., REA, M. C., SHANAHAN, F., QUIGLEY, E. M., KIELY, B., HILL, C. & ROSS, R. P. 2009. The vexed relationship between *Clostridium difficile* and inflammatory bowel disease: an assessment of carriage in an outpatient setting among patients in remission. *Am J Gastroenterol*, 104, 1162-9.
- COLLADO, M. C., RAUTAVA, S., AAKKO, J., ISOLAURI, E. & SALMINEN, S. 2016. Human gut colonisation may be initiated in utero by distinct microbial communities in the placenta and amniotic fluid. *Sci Rep*, 6, 23129.
- CONSORTIUM, T. H. M. 2012. Structure, function and diversity of the healthy human microbiome. *Nature*, 486, 207-14.
- CORPET, D. E. 2000. Model Systems of Human Intestinal Flora, to Set Acceptable Daily Intakes of Antimicrobial Residues. *Microb Ecol Health Dis*, 12, 37-41.
- CRAIG, A., CLOAREC, O., HOLMES, E., NICHOLSON, J. K. & LINDON, J. C. 2006. Scaling and normalization effects in NMR spectroscopic metabolomic data sets. *Anal Chem*, 78, 2262-7.
- CSORDAS, A. 1996. Butyrate, aspirin and colorectal cancer. *Eur J Cancer Prev*, 5, 221-31.
- DAI, Z. L., WU, G. & ZHU, W. Y. 2011. Amino acid metabolism in intestinal bacteria: links between gut ecology and host health. *Front Biosci (Landmark Ed)*, 16, 1768-86.
- DAWISKIBA, T., DEJA, S., MULAK, A., ZABEK, A., JAWIEN, E., PAWELKA, D., BANASIK, M., MASTALERZ-MIGAS, A., BALCERZAK, W., KALISZEWSKI, K., SKORA, J., BARC, P., KORTA, K., PORMANCZUK, K., SZYBER, P., LITARSKI, A. & MLYNARZ, P. 2014. Serum and urine metabolomic fingerprinting in diagnostics of inflammatory bowel diseases. *World J Gastroenterol*, 20, 163-74.

- DE BIE, C. I., HUMMEL, T. Z., KINDERMANN, A., KOKKE, F. T., DAMEN, G. M., KNEEPKENS, C. M., VAN RHEENEN, P. F., SCHWEIZER, J. J., HOEKSTRA, J. H., NORBRUIS, O. F., TJON, A. T. W. E., VREUGDENHIL, A. C., DECKERS-KOCKEN, J. M., GIJSBERS, C. F., ESCHER, J. C. & DE RIDDER, L. 2011. The duration of effect of infliximab maintenance treatment in paediatric Crohn's disease is limited. *Aliment Pharmacol Ther*, 33, 243-50.
- DE BOER, W., OTTEN, M. H., MAN, W. K. & HING, A. 2012. Sa2070 VSL#3<sup>®</sup>, a Probiotic Combination, Reduces the Severity of Abdominal Pain and Bloating and Improves Quality of Life in Irritable Bowel Syndrome (IBS): Data From a Multi-Centre, Prospective, Observational Study. *Gastroenterology*, 142, S-394.
- DE FILIPPO, C., CAVALIERI, D., DI PAOLA, M., RAMAZZOTTI, M., POULLET, J. B., MASSART, S., COLLINI, S., PIERACCINI, G. & LIONETTI, P. 2010. Impact of diet in shaping gut microbiota revealed by a comparative study in children from Europe and rural Africa. *Proc Natl Acad Sci U S A*, 107, 14691-6.
- DE LA COCHETIERE, M. F., DURAND, T., LEPAGE, P., BOURREILLE, A., GALMICHE, J. P. & DORE, J. 2005. Resilience of the dominant human fecal microbiota upon short-course antibiotic challenge. *J Clin Microbiol*, 43, 5588-92.
- DEMEHRI, F. R., BARRETT, M., RALLS, M. W., MIYASAKA, E. A., FENG, Y. & TEITELBAUM, D. H. 2013. Intestinal epithelial cell apoptosis and loss of barrier function in the setting of altered microbiota with enteral nutrient deprivation. *Front Cell Infect Microbiol*, 3, 105.
- DEN BESTEN, G., LANGE, K., HAVINGA, R., VAN DIJK, T. H., GERDING, A., VAN EUNEN, K., MULLER, M., GROEN, A. K., HOOVELD, G. J., BAKKER, B. M. & REIJNGOUD, D. J. 2013. Gut-derived short-chain fatty acids are vividly assimilated into host carbohydrates and lipids. *Am J Physiol Gastrointest Liver Physiol*, 305, G900-10.
- DESAI, M. S., SEEKATZ, A. M., KOROPATKIN, N. M., KAMADA, N., HICKEY, C. A., WOLTER, M., PUDLO, N. A., KITAMOTO, S., TERRAPON, N., MULLER, A., YOUNG, V. B., HENRISSAT, B., WILMES, P., STAPPENBECK, T. S., NUNEZ, G. & MARTENS, E. C. 2016. A Dietary Fiber-Deprived Gut Microbiota Degrades the Colonic Mucus Barrier and Enhances Pathogen Susceptibility. *Cell*, 167, 1339-1353.e21.
- DICKSVED, J., HALFVARSON, J., ROSENQUIST, M., JARNEROT, G., TYSK, C., APAJALAHTI, J., ENGSTRAND, L. & JANSSON, J. K. 2008. Molecular analysis of the gut microbiota of identical twins with Crohn's disease. *Isme j*, 2, 716-27.
- DIETERLE, F., ROSS, A., SCHLOTTERBECK, G. & SENN, H. 2006. Probabilistic quotient normalization as robust method to account for dilution of complex biological mixtures. Application in 1H NMR metabolomics. *Anal Chem*, 78, 4281-90.
- DRUMMOND, P. D. & HEWSON-BOWER, B. 1997. Increased psychosocial stress and decreased mucosal immunity in children with recurrent upper respiratory tract infections. *J Psychosom Res*, 43, 271-8.
- DUMAS, M. E., BARTON, R. H., TOYE, A., CLOAREC, O., BLANCHER, C., ROTHWELL, A., FEARNSIDE, J., TATOUD, R., BLANC, V., LINDON, J. C., MITCHELL, S. C., HOLMES, E., MCCARTHY, M. I., SCOTT, J., GAUGUIER, D. & NICHOLSON, J. K. 2006. Metabolic profiling reveals a contribution of gut microbiota to fatty liver phenotype in insulin-resistant mice. *Proc Natl Acad Sci U S A*, 103, 12511-6.
- DURBAN, A., ABELLAN, J. J., JIMENEZ-HERNANDEZ, N., PONCE, M., PONCE, J., SALA, T., D'AURIA, G., LATORRE, A. & MOYA, A. 2011. Assessing gut microbial diversity from feces and rectal mucosa. *Microb Ecol*, 61, 123-33.
- ECKBURG, P. B., BIK, E. M., BERNSTEIN, C. N., PURDOM, E., DETHLEFSEN, L., SARGENT, M., GILL, S. R., NELSON, K. E. & RELMAN, D. A. 2005. Diversity of the human intestinal microbial flora. *Science*, 308, 1635-8.

- ECONOMOU, M., TRIKALINOS, T. A., LOIZOU, K. T., TSIANOS, E. V. & IOANNIDIS, J. P. 2004. Differential effects of NOD2 variants on Crohn's disease risk and phenotype in diverse populations: a metaanalysis. *Am J Gastroenterol*, 99, 2393-404.
- EKELUND, M., KRISTENSSON, E. & EKBLAD, E. 2007. Total parenteral nutrition causes circumferential intestinal atrophy, remodeling of the intestinal wall, and redistribution of eosinophils in the rat gastrointestinal tract. *Dig Dis Sci*, 52, 1833-9.
- EL-HUSSUNA, A., LAURITSEN, M. & BULOW, S. 2012. Relatively high incidence of complications after loop ileostomy reversal. *Dan Med J*, 59, A4517.
- ENGSTRAND LILJA, H., WEFER, H., NYSTROM, N., FINKEL, Y. & ENGSTRAND, L. 2015. Intestinal dysbiosis in children with short bowel syndrome is associated with impaired outcome. *Microbiome*, 3, 18.
- ESCHERICH, T. 1988. The intestinal bacteria of the neonate and breast-fed infant. 1884. *Rev Infect Dis*, 10, 1220-5.
- FAO/WHO 2002. Guidelines for the Evaluation of Probiotics in Food. *London Ontario, Canada*, 30, 1-11.
- FEIGENSON, K. A., KUSNECOV, A. W. & SILVERSTEIN, S. M. 2014. Inflammation and the two-hit hypothesis of schizophrenia. *Neurosci Biobehav Rev*, 38, 72-93.
- FRANK, D. N., ST AMAND, A. L., FELDMAN, R. A., BOEDEKER, E. C., HARPAZ, N. & PACE, N. R. 2007. Molecular-phylogenetic characterization of microbial community imbalances in human inflammatory bowel diseases. *Proc Natl Acad Sci U S A*, 104, 13780-5.
- FRIEDMAN, J., HASTIE, T. & TIBSHIRANI, R. 2010. Regularization Paths for Generalized Linear Models via Coordinate Descent. *J Stat Softw*, 33, 1-22.
- FRISCH, S. M. & FRANCIS, H. 1994. Disruption of epithelial cell-matrix interactions induces apoptosis. *J Cell Biol*, 124, 619-26.
- GARRITY, G., BRENNER, D. J., KRIEG, N. R. & STALEY, J. T. 2005. *Bergey's Manual of Systematic Bacteriology. Volume Two: The Proteobacteria (Part C)*. Springer US.
- GASSER, E. & PAREKH, N. 2005. Parenteral Nutrition: Macronutrient Composition and Requirements. *Support Line*, 27, 6-12.
- GIBSON, G. R., BEATTY, E. R., WANG, X. & CUMMINGS, J. H. 1995. Selective stimulation of bifidobacteria in the human colon by oligofructose and inulin. *Gastroenterology*, 108, 975-82.
- GOPHNA, U., SOMMERFELD, K., GOPHNA, S., DOOLITTLE, W. F. & VELDHIJZEN VAN ZANTEN, S. J. 2006. Differences between tissue-associated intestinal microfloras of patients with Crohn's disease and ulcerative colitis. *J Clin Microbiol*, 44, 4136-41.
- GORDON, H. A. & BRUCKNER-KARDOSS, E. 1961. Effect of normal microbial flora on intestinal surface area. *Am J Physiol*, 201, 175-8.
- GRAF, D., DI CAGNO, R., FAK, F., FLINT, H. J., NYMAN, M., SAARELA, M. & WATZL, B. 2015. Contribution of diet to the composition of the human gut microbiota. *Microb Ecol Health Dis*, 26, 26164.
- GRIBBLE, F. M. & REIMANN, F. 2016. Enteroendocrine Cells: Chemosensors in the Intestinal Epithelium. *Annu Rev Physiol*, 78, 277-99.
- GRIFFITHS, B. S., HALLETT, P. D., KUAN, H. L., PITKIN, Y. & AITKEN, M. N. 2005. Biological and physical resilience of soil amended with heavy metal-contaminated sewage sludge.
- GRONLUND, M. M., LEHTONEN, O. P., EEROLA, E. & KERO, P. 1999. Fecal microflora in healthy infants born by different methods of delivery: permanent changes in intestinal flora after cesarean delivery. *J Pediatr Gastroenterol Nutr*, 28, 19-25.
- HARA-TERAWAKI, A., TAKAGAKI, A., KOBAYASHI, H. & NANJO, F. 2017. Inhibitory Activity of Catechin Metabolites Produced by Intestinal Microbiota on Proliferation of HeLa Cells. *Biol Pharm Bull*, 40, 1331-1335.
- HARMSSEN, H. J. & C., G. M. 2016. *Microbiota of the Human Body: The Human Gut Microbiota*. , Springer International Publishing.



- HARMSSEN, H. J., WILDEBOER-VELOO, A. C., RAANGS, G. C., WAGENDORP, A. A., KLIJN, N., BINDELS, J. G. & WELLING, G. W. 2000. Analysis of intestinal flora development in breast-fed and formula-fed infants by using molecular identification and detection methods. *J Pediatr Gastroenterol Nutr*, 30, 61-7.
- HARTMAN, A. L., LOUGH, D. M., BARUPAL, D. K., FIEHN, O., FISHBEIN, T., ZASLOFF, M. & EISEN, J. A. 2009. Human gut microbiome adopts an alternative state following small bowel transplantation. *Proc Natl Acad Sci U S A*, 106, 17187-92.
- HASIN, Y., SELDIN, M. & LUSIS, A. 2017. Multi-omics approaches to disease. *Genome Biol*, 18, 83.
- HELMUS, D. S., THOMPSON, C. L., ZELENSKIY, S., TUCKER, T. C. & LI, L. 2013. Red meat-derived heterocyclic amines increase risk of colon cancer: a population-based case-control study. *Nutr Cancer*, 65, 1141-50.
- HILL, D. A., HOFFMANN, C., ABT, M. C., DU, Y., KOBULEY, D., KIRN, T. J., BUSHMAN, F. D. & ARTIS, D. 2010. Metagenomic analyses reveal antibiotic-induced temporal and spatial changes in intestinal microbiota with associated alterations in immune cell homeostasis. *Mucosal Immunol*, 3, 148-58.
- HILL, M. J. 1997. Intestinal flora and endogenous vitamin synthesis. *Eur J Cancer Prev*, 6 Suppl 1, S43-5.
- HIRAYAMA, K. & ITOH, K. 2005. Human flora-associated (HFA) animals as a model for studying the role of intestinal flora in human health and disease. *Curr Issues Intest Microbiol*, 6, 69-75.
- HIROTA, S. A., NG, J., LUENG, A., KHAJAH, M., PARHAR, K., LI, Y., LAM, V., POTENTIER, M. S., NG, K., BAWA, M., MCCAFFERTY, D. M., RIOUX, K. P., GHOSH, S., XAVIER, R. J., COLGAN, S. P., TSCHOPP, J., MURUVE, D., MACDONALD, J. A. & BECK, P. L. 2011. NLRP3 inflammasome plays a key role in the regulation of intestinal homeostasis. *Inflamm Bowel Dis*, 17, 1359-72.
- HODIN, C. M., VISSCHERS, R. G., RENSEN, S. S., BOONEN, B., OLDE DAMINK, S. W., LENAERTS, K. & BUURMAN, W. A. 2012. Total parenteral nutrition induces a shift in the Firmicutes to Bacteroidetes ratio in association with Paneth cell activation in rats. *J Nutr*, 142, 2141-7.
- HOFFMANN, C., DOLLIVE, S., GRUNBERG, S., CHEN, J., LI, H., WU, G. D., LEWIS, J. D. & BUSHMAN, F. D. 2013. Archaea and fungi of the human gut microbiome: correlations with diet and bacterial residents. *PLoS One*, 8, e66019.
- HUBNER, M., MANTZIARI, S., DEMARTINES, N., PRALONG, F., COTI-BERTRAND, P. & SCHAFER, M. 2016. Postoperative Albumin Drop Is a Marker for Surgical Stress and a Predictor for Clinical Outcome: A Pilot Study. *Gastroenterol Res Pract*, 2016, 8743187.
- HUGHES, J. R. & HATSUKAMI, D. 1986. Signs and symptoms of tobacco withdrawal. *Arch Gen Psychiatry*, 43, 289-94.
- ISLAM, K. B., FUKIYA, S., HAGIO, M., FUJII, N., ISHIZUKA, S., OOKA, T., OGURA, Y., HAYASHI, T. & YOKOTA, A. 2011. Bile acid is a host factor that regulates the composition of the cecal microbiota in rats. *Gastroenterology*, 141, 1773-81.
- JIANG, H., LEI, R., DING, S. W. & ZHU, S. 2014. Skewer: a fast and accurate adapter trimmer for next-generation sequencing paired-end reads. *BMC Bioinformatics*, 15, 182.
- JOHANSSON, M. E., PHILLIPSON, M., PETERSSON, J., VELCICH, A., HOLM, L. & HANSSON, G. C. 2008. The inner of the two Muc2 mucin-dependent mucus layers in colon is devoid of bacteria. *Proc Natl Acad Sci U S A*, 105, 15064-9.
- JOOSSENS, M., HUYS, G., CNOCKAERT, M., DE PRETER, V., VERBEKE, K., RUTGEERTS, P., VANDAMME, P. & VERMEIRE, S. 2011. Dysbiosis of the faecal microbiota in patients with Crohn's disease and their unaffected relatives. *Gut*, 60, 631-7.

- KALLIOMAKI, M., COLLADO, M. C., SALMINEN, S. & ISOLAURI, E. 2008. Early differences in fecal microbiota composition in children may predict overweight. *Am J Clin Nutr*, 87, 534-8.
- KANEHISA, M. & GOTO, S. 2000. KEGG: kyoto encyclopedia of genes and genomes. *Nucleic Acids Res*, 28, 27-30.
- KAWAMOTO, S., MARUYA, M., KATO, L. M., SUDA, W., ATARASHI, K., DOI, Y., TSUTSUI, Y., QIN, H., HONDA, K., OKADA, T., HATTORI, M. & FAGARASAN, S. 2014. Foxp3(+) T cells regulate immunoglobulin a selection and facilitate diversification of bacterial species responsible for immune homeostasis. *Immunity*, 41, 152-65.
- KLAPPENBACH, J. A., SAXMAN, P. R., COLE, J. R. & SCHMIDT, T. M. 2001. rrndb: the Ribosomal RNA Operon Copy Number Database. *Nucleic Acids Res*, 29, 181-4.
- KLINDWORTH, A., PRUESSE, E., SCHWEER, T., PEPLIES, J., QUAST, C., HORN, M. & GLOCKNER, F. O. 2013. Evaluation of general 16S ribosomal RNA gene PCR primers for classical and next-generation sequencing-based diversity studies. *Nucleic Acids Res*, 41, e1.
- KNIGHTS, D., WARD, T. L., MCKINLAY, C. E., MILLER, H., GONZALEZ, A., MCDONALD, D. & KNIGHT, R. 2014. Rethinking "enterotypes". *Cell Host Microbe*, 16, 433-7.
- KOREN, O., KNIGHTS, D., GONZALEZ, A., WALDRON, L., SEGATA, N., KNIGHT, R., HUTTENHOWER, C. & LEY, R. E. 2013. A guide to enterotypes across the human body: meta-analysis of microbial community structures in human microbiome datasets. *PLoS Comput Biol*, 9, e1002863.
- KOVALENKO, P. L. & BASSON, M. D. 2012. Changes in morphology and function in small intestinal mucosa after Roux-en-Y surgery in a rat model. *J Surg Res*, 177, 63-9.
- KRYCH, L., HANSEN, C. H., HANSEN, A. K., VAN DEN BERG, F. W. & NIELSEN, D. S. 2013. Quantitatively different, yet qualitatively alike: a meta-analysis of the mouse core gut microbiome with a view towards the human gut microbiome. *PLoS One*, 8, e62578.
- KUCHARZIK, T., LUGERING, A., LUGERING, N., RAUTENBERG, K., LINNEPE, M., CICHON, C., REICHEL, R., STOLL, R., SCHMIDT, M. A. & DOMSCHKE, W. 2000. Characterization of M cell development during indomethacin-induced ileitis in rats. *Aliment Pharmacol Ther*, 14, 247-56.
- KUDSK, K. A., CROCE, M. A., FABIAN, T. C., MINARD, G., TOLLEY, E. A., PORET, H. A., KUHL, M. R. & BROWN, R. O. 1992. Enteral versus parenteral feeding. Effects on septic morbidity after blunt and penetrating abdominal trauma. *Ann Surg*, 215, 503-11; discussion 511-3.
- KURITA, M., HOLLOWAY, T., GARCIA-BEA, A., KOZLENKOV, A., FRIEDMAN, A. K., MORENO, J. L., HESHMATI, M., GOLDEN, S. A., KENNEDY, P. J., TAKAHASHI, N., DIETZ, D. M., MOCCI, G., GABILONDO, A. M., HANKS, J., UMALI, A., CALLADO, L. F., GALLITANO, A. L., NEVE, R. L., SHEN, L., BUXBAUM, J. D., HAN, M. H., NESTLER, E. J., MEANA, J. J., RUSSO, S. J. & GONZALEZ-MAESO, J. 2012. HDAC2 regulates atypical antipsychotic responses through the modulation of mGlu2 promoter activity. *Nat Neurosci*, 15, 1245-54.
- LATHROP, S. K., BLOOM, S. M., RAO, S. M., NUTSCH, K., LIO, C. W., SANTACRUZ, N., PETERSON, D. A., STAPPENBECK, T. S. & HSIEH, C. S. 2011. Peripheral education of the immune system by colonic commensal microbiota. *Nature*, 478, 250-4.
- LAWLEY, T. D., CLARE, S., WALKER, A. W., GOULDING, D., STABLER, R. A., CROUCHER, N., MASTROENI, P., SCOTT, P., RAISEN, C., MOTTRAM, L., FAIRWEATHER, N. F., WREN, B. W., PARKHILL, J. & DOUGAN, G. 2009. Antibiotic treatment of clostridium difficile carrier mice triggers a supershedder state, spore-mediated transmission, and severe disease in immunocompromised hosts. *Infect Immun*, 77, 3661-9.

- LE GALL, G., NOOR, S. O., RIDGWAY, K., SCOVELL, L., JAMIESON, C., JOHNSON, I. T., COLQUHOUN, I. J., KEMSLEY, E. K. & NARBAD, A. 2011. Metabolomics of fecal extracts detects altered metabolic activity of gut microbiota in ulcerative colitis and irritable bowel syndrome. *J Proteome Res*, 10, 4208-18.
- LEE, S., SUNG, J., LEE, J. & KO, G. 2011. Comparison of the gut microbiotas of healthy adult twins living in South Korea and the United States. *Appl Environ Microbiol*, 77, 7433-7.
- LEHOURITIS, P., CUMMINS, J., STANTON, M., MURPHY, C. T., MCCARTHY, F. O., REID, G., URBANIAK, C., BYRNE, W. L. & TANGNEY, M. 2015. Local bacteria affect the efficacy of chemotherapeutic drugs. *Sci Rep*, 5, 14554.
- LELOUARD, H., FALLET, M., DE BOVIS, B., MERESSE, S. & GORVEL, J. P. 2012. Peyer's patch dendritic cells sample antigens by extending dendrites through M cell-specific transcellular pores. *Gastroenterology*, 142, 592-601.e3.
- LEY, R. E., TURNBAUGH, P. J., KLEIN, S. & GORDON, J. I. 2006. Microbial ecology: human gut microbes associated with obesity. *Nature*, 444, 1022-3.
- LI, M., WANG, B., ZHANG, M., RANTALAINEN, M., WANG, S., ZHOU, H., ZHANG, Y., SHEN, J., PANG, X., WEI, H., CHEN, Y., LU, H., ZUO, J., SU, M., QIU, Y., JIA, W., XIAO, C., SMITH, L. M., YANG, S., HOLMES, E., TANG, H., ZHAO, G., NICHOLSON, J. K., LI, L. & ZHAO, L. 2008. Symbiotic gut microbes modulate human metabolic phenotypes. *Proc Natl Acad Sci U S A*, 105, 2117-22.
- LIANG, P. S., CHEN, T. Y. & GIOVANNUCCI, E. 2009. Cigarette smoking and colorectal cancer incidence and mortality: systematic review and meta-analysis. *Int J Cancer*, 124, 2406-15.
- LIMAYE, A. P., TURGEON, D. K., COOKSON, B. T. & FRITSCH, T. R. 2000. Pseudomembranous Colitis Caused by a Toxin A- B+ Strain of Clostridium difficile. *Journal of Clinical Microbiology*, 38, 1696-1697.
- LIN, H. C., ZAIDEL, O. & HUM, S. 2002. Intestinal transit of fat depends on accelerating effect of cholecystokinin and slowing effect of an opioid pathway. *Dig Dis Sci*, 47, 2217-21.
- LIN, M. Y., DE ZOETE, M. R., VAN PUTTEN, J. P. & STRIJBIS, K. 2015. Redirection of Epithelial Immune Responses by Short-Chain Fatty Acids through Inhibition of Histone Deacetylases. *Front Immunol*, 6, 554.
- LISZT, K., ZWIELEHNER, J., HANDSCHUR, M., HIPPE, B., THALER, R. & HASLBERGER, A. G. 2009. Characterization of bacteria, clostridia and Bacteroides in faeces of vegetarians using qPCR and PCR-DGGE fingerprinting. *Ann Nutr Metab*, 54, 253-7.
- LIVAK, K. J. & SCHMITTGEN, T. D. 2001. Analysis of relative gene expression data using real-time quantitative PCR and the 2(-Delta Delta C(T)) Method. *Methods*, 25, 402-8.
- LIZKO, N. N. 1987. Stress and intestinal microflora. *Nahrung*, 31, 443-7.
- MACFABE, D. F., CAIN, N. E., BOON, F., OSSENKOPP, K. P. & CAIN, D. P. 2011. Effects of the enteric bacterial metabolic product propionic acid on object-directed behavior, social behavior, cognition, and neuroinflammation in adolescent rats: Relevance to autism spectrum disorder. *Behav Brain Res*, 217, 47-54.
- MACIA, L., THORBURN, A. N., BINGE, L. C., MARINO, E., ROGERS, K. E., MASLOWSKI, K. M., VIEIRA, A. T., KRANICH, J. & MACKAY, C. R. 2012. Microbial influences on epithelial integrity and immune function as a basis for inflammatory diseases. *Immunol Rev*, 245, 164-76.
- MAGOC, T. & SALZBERG, S. L. 2011. FLASH: fast length adjustment of short reads to improve genome assemblies. *Bioinformatics*, 27, 2957-63.
- MARCHESI, J. R., HOLMES, E., KHAN, F., KOCHHAR, S., SCANLAN, P., SHANAHAN, F., WILSON, I. D. & WANG, Y. 2007. Rapid and noninvasive metabonomic characterization of inflammatory bowel disease. *J Proteome Res*, 6, 546-51.

- MARCOBAL, A., KASHYAP, P. C., NELSON, T. A., ARONOV, P. A., DONIA, M. S., SPORMANN, A., FISCHBACH, M. A. & SONNENBURG, J. L. 2013. A metabolomic view of how the human gut microbiota impacts the host metabolome using humanized and gnotobiotic mice. *Isme j*, 7, 1933-43.
- MAUKONEN, J., SATOKARI, R., MATTO, J., SODERLUND, H., MATTILA-SANDHOLM, T. & SAARELA, M. 2006. Prevalence and temporal stability of selected clostridial groups in irritable bowel syndrome in relation to predominant faecal bacteria. *J Med Microbiol*, 55, 625-33.
- MAZMANIAN, S. K., ROUND, J. L. & KASPER, D. L. 2008. A microbial symbiosis factor prevents intestinal inflammatory disease. *Nature*, 453, 620-5.
- MENCARELLI, A. & FIORUCCI, S. 2010. FXR an emerging therapeutic target for the treatment of atherosclerosis. *J Cell Mol Med*, 14, 79-92.
- METGES, C. C. 2000. Contribution of microbial amino acids to amino acid homeostasis of the host. *J Nutr*, 130, 1857s-64s.
- MIEDEMA, B. W., KOHLER, L., SMITH, C. D., PHILLIPS, S. F. & KELLY, K. A. 1998. Preoperative perfusion of bypassed ileum does not improve postoperative function. *Dig Dis Sci*, 43, 429-35.
- MIYASAKA, E. A., FENG, Y., POROYKO, V., FALKOWSKI, N. R., ERB-DOWNWARD, J., GILLILLAND, M. G., 3RD, MASON, K. L., HUFFNAGLE, G. B. & TEITELBAUM, D. H. 2013. Total parenteral nutrition-associated lamina propria inflammation in mice is mediated by a MyD88-dependent mechanism. *J Immunol*, 190, 6607-15.
- MOAYYEDI, P., SURETTE, M. G., KIM, P. T., LIBERTUCCI, J., WOLFE, M., ONISCHI, C., ARMSTRONG, D., MARSHALL, J. K., KASSAM, Z., REINISCH, W. & LEE, C. H. 2015. Fecal Microbiota Transplantation Induces Remission in Patients With Active Ulcerative Colitis in a Randomized Controlled Trial. *Gastroenterology*, 149, 102-109.e6.
- MONIRA, S., NAKAMURA, S., GOTOH, K., IZUTSU, K., WATANABE, H., ALAM, N. H., ENDTZ, H. P., CRAVIOTO, A., ALI, S. I., NAKAYA, T., HORII, T., IIDA, T. & ALAM, M. 2011. Gut microbiota of healthy and malnourished children in bangladesh. *Front Microbiol*, 2, 228.
- MORITA, C., TSUJI, H., HATA, T., GONDO, M., TAKAKURA, S., KAWAI, K., YOSHIHARA, K., OGATA, K., NOMOTO, K., MIYAZAKI, K. & SUDO, N. 2015. Gut Dysbiosis in Patients with Anorexia Nervosa. *PLoS One*, 10, e0145274.
- MURDOCH, T. B., FU, H., MACFARLANE, S., SYDORA, B. C., FEDORAK, R. N. & SLUPSKY, C. M. 2008. Urinary metabolic profiles of inflammatory bowel disease in interleukin-10 gene-deficient mice. *Anal Chem*, 80, 5524-31.
- MUYZER, G., DE WAAL, E. C. & UITTERLINDEN, A. G. 1993. Profiling of complex microbial populations by denaturing gradient gel electrophoresis analysis of polymerase chain reaction-amplified genes coding for 16S rRNA. *Appl Environ Microbiol*, 59, 695-700.
- NAEEM, S., KNOPS, J. M. H., TILMAN, D., HOWE, K. M., KENNEDY, T. & GALE, S. 2000. Plant diversity increases resistance to invasion in the absence of covarying extrinsic factors.
- NAKADE, Y., FUKUDA, H., IWA, M., TSUKAMOTO, K., YANAGI, H., YAMAMURA, T., MANTYH, C., PAPPAS, T. N. & TAKAHASHI, T. 2007. Restraint stress stimulates colonic motility via central corticotropin-releasing factor and peripheral 5-HT3 receptors in conscious rats. *Am J Physiol Gastrointest Liver Physiol*, 292, G1037-44.
- NICHOLSON, J. K., HOLMES, E., KINROSS, J., BURCELIN, R., GIBSON, G., JIA, W. & PETERSSON, S. 2012. Host-gut microbiota metabolic interactions. *Science*, 336, 1262-7.

- OKUMURA, R., KURAKAWA, T., NAKANO, T., KAYAMA, H., KINOSHITA, M., MOTOOKA, D., GOTOH, K., KIMURA, T., KAMIYAMA, N., KUSU, T., UEDA, Y., WU, H., IJIMA, H., BARMAN, S., OSAWA, H., MATSUNO, H., NISHIMURA, J., OHBA, Y., NAKAMURA, S., IIDA, T., YAMAMOTO, M., UMEMOTO, E., SANO, K. & TAKEDA, K. 2016. Lypd8 promotes the segregation of flagellated microbiota and colonic epithelia. *Nature*, 532, 117-21.
- ORTEGA-DEBALLON, P., RADAIS, F., FACY, O., D'ATHIS, P., MASSON, D., CHARLES, P. E., CHEYNEL, N., FAVRE, J. P. & RAT, P. 2010. C-reactive protein is an early predictor of septic complications after elective colorectal surgery. *World J Surg*, 34, 808-14.
- OSAWA, N. & MITSUHASHI, S. 1964. Infection of Germfree Mice with Shigella Flexneri 3A. *Jpn J Exp Med*, 34, 77-80.
- PALMER, C., BIK, E. M., DIGIULIO, D. B., RELMAN, D. A. & BROWN, P. O. 2007. Development of the human infant intestinal microbiota. *PLoS Biol*, 5, e177.
- PARAMSOTHY, S., KAMM, M. A., KAAKOUSH, N. O., WALSH, A. J., VAN DEN BOGAERDE, J., SAMUEL, D., LEONG, R. W. L., CONNOR, S., NG, W., PARAMSOTHY, R., XUAN, W., LIN, E., MITCHELL, H. M. & BORODY, T. J. 2017. Multidonor intensive faecal microbiota transplantation for active ulcerative colitis: a randomised placebo-controlled trial. *Lancet*, 389, 1218-1228.
- PARK, J. H., KOTANI, T., KONNO, T., SETIAWAN, J., KITAMURA, Y., IMADA, S., USUI, Y., HATANO, N., SHINOHARA, M., SAITO, Y., MURATA, Y. & MATOZAKI, T. 2016. Promotion of Intestinal Epithelial Cell Turnover by Commensal Bacteria: Role of Short-Chain Fatty Acids. *PLoS One*, 11, e0156334.
- PEMBERTON, J. H., KELLY, K. A., BEART, R. W., JR., DOZOIS, R. R., WOLFF, B. G. & ILSTRUP, D. M. 1987. Ileal pouch-anal anastomosis for chronic ulcerative colitis. Long-term results. *Ann Surg*, 206, 504-13.
- PENDERS, J., THIJIS, C., VINK, C., STELMA, F. F., SNIJDERS, B., KUMMELING, I., VAN DEN BRANDT, P. A. & STOBBERINGH, E. E. 2006. Factors influencing the composition of the intestinal microbiota in early infancy. *Pediatrics*, 118, 511-21.
- PETERSON, L. W. & ARTIS, D. 2014. Intestinal epithelial cells: regulators of barrier function and immune homeostasis. *Nat Rev Immunol*, 14, 141-53.
- PEYRET, B., COLLARDEAU, S., TOUZET, S., LORAS-DUCLAUX, I., YANTREN, H., MICHALSKI, M. C., CHAIX, J., RESTIER-MIRON, L., BOUVIER, R., LACHAUX, A. & PERETTI, N. 2011. Prevalence of liver complications in children receiving long-term parenteral nutrition. *Eur J Clin Nutr*, 65, 743-9.
- PHANG, P. T., HAIN, J. M., PEREZ-RAMIREZ, J. J., MADOFF, R. D. & GEMLO, B. T. 1999. Techniques and complications of ileostomy takedown. *Am J Surg*, 177, 463-6.
- PIERCE, E. S. 2010. Ulcerative colitis and Crohn's disease: is Mycobacterium avium subspecies paratuberculosis the common villain? *Gut Pathog*. England.
- PINSK, V., LEMBERG, D. A., GREWAL, K., BARKER, C. C., SCHREIBER, R. A. & JACOBSON, K. 2007. Inflammatory bowel disease in the South Asian pediatric population of British Columbia. *Am J Gastroenterol*, 102, 1077-83.
- PRASAD, S., DHIMAN, R. K., DUSEJA, A., CHAWLA, Y. K., SHARMA, A. & AGARWAL, R. 2007. Lactulose improves cognitive functions and health-related quality of life in patients with cirrhosis who have minimal hepatic encephalopathy. *Hepatology*, 45, 549-59.
- QIN, J., LI, R., RAES, J., ARUMUGAM, M., BURGDORF, K. S., MANICHANH, C., NIELSEN, T., PONS, N., LEVENEZ, F., YAMADA, T., MENDE, D. R., LI, J., XU, J., LI, S., LI, D., CAO, J., WANG, B., LIANG, H., ZHENG, H., XIE, Y., TAP, J., LEPAGE, P., BERTALAN, M., BATTO, J. M., HANSEN, T., LE PASLIER, D., LINNEBERG, A., NIELSEN, H. B., PELLETIER, E., RENAULT, P., SICHERITZ-PONTEN, T., TURNER, K., ZHU, H., YU, C., JIAN, M., ZHOU, Y., LI, Y., ZHANG, X., QIN, N., YANG, H., WANG, J., BRUNAK, S., DORE, J., GUARNER, F., KRISTIANSEN, K., PEDERSEN, O., PARKHILL, J., WEISSENBACH, J., BORK, P. &

- EHRlich, S. D. 2010. A human gut microbial gene catalogue established by metagenomic sequencing. *Nature*, 464, 59-65.
- RAJ, T., DILEEP, U., VAZ, M., FULLER, M. F. & KURPAD, A. V. 2008. Intestinal microbial contribution to metabolic leucine input in adult men. *J Nutr*, 138, 2217-21.
- RAKOFF-NAHOUM, S., PAGLINO, J., ESLAMI-VARZANEH, F., EDBERG, S. & MEDZHITOV, R. 2004. Recognition of commensal microflora by toll-like receptors is required for intestinal homeostasis. *Cell*, 118, 229-41.
- RALLS, M. W., MIYASAKA, E. & TEITELBAUM, D. H. 2014. Intestinal microbial diversity and perioperative complications. *JPEN J Parenter Enteral Nutr*, 38, 392-9.
- RATH, H. C., HERFARTH, H. H., IKEDA, J. S., GRENTHER, W. B., HAMM, T. E., JR., BALISH, E., TAUROG, J. D., HAMMER, R. E., WILSON, K. H. & SARTOR, R. B. 1996. Normal luminal bacteria, especially Bacteroides species, mediate chronic colitis, gastritis, and arthritis in HLA-B27/human beta2 microglobulin transgenic rats. *J Clin Invest*, 98, 945-53.
- RESCIGNO, M., URBANO, M., VALZASINA, B., FRANCOLINI, M., ROTTA, G., BONASIO, R., GRANUCCI, F., KRAEHENBUHL, J. P. & RICCIARDI-CASTAGNOLI, P. 2001. Dendritic cells express tight junction proteins and penetrate gut epithelial monolayers to sample bacteria. *Nat Immunol*, 2, 361-7.
- REYES, A., HAYNES, M., HANSON, N., ANGLY, F. E., HEATH, A. C., ROHWER, F. & GORDON, J. I. 2010. Viruses in the fecal microbiota of monozygotic twins and their mothers. *Nature*, 466, 334-338.
- RICART, E., GARCIA-BOSCH, O., ORDAS, I. & PANES, J. 2008. Are we giving biologics too late? The case for early versus late use. *World J Gastroenterol*, 14, 5523-7.
- RIOS-COVIAN, D., RUAS-MADIEDO, P., MARGOLLES, A., GUEIMONDE, M., DE LOS REYES-GAVILAN, C. G. & SALAZAR, N. 2016. Intestinal Short Chain Fatty Acids and their Link with Diet and Human Health. *Front Microbiol*, 7, 185.
- ROBERFROID, M., GIBSON, G. R., HOYLES, L., MCCARTNEY, A. L., RASTALL, R., ROWLAND, I., WOLVERS, D., WATZL, B., SZAJEWSKA, H., STAHL, B., GUARNER, F., RESPONDEK, F., WHELAN, K., COXAM, V., DAVICCO, M. J., LEOTOING, L., WITTRANT, Y., DELZENNE, N. M., CANI, P. D., NEYRINCK, A. M. & MEHEUST, A. 2010. Prebiotic effects: metabolic and health benefits. *Br J Nutr*, 104 Suppl 2, S1-63.
- RUSSELL, W. R., GRATZ, S. W., DUNCAN, S. H., HOLTROP, G., INCE, J., SCOBIE, L., DUNCAN, G., JOHNSTONE, A. M., LOBLEY, G. E., WALLACE, R. J., DUTHIE, G. G. & FLINT, H. J. 2011. High-protein, reduced-carbohydrate weight-loss diets promote metabolite profiles likely to be detrimental to colonic health. *Am J Clin Nutr*, 93, 1062-72.
- SAMARGHANDIAN, S., AZIMI-NEZHAD, M. & FARKHONDEH, T. 2017. Catechin Treatment Ameliorates Diabetes and Its Complications in Streptozotocin-Induced Diabetic Rats. *Dose Response*, 15, 1559325817691158.
- SAVAGE, D. C., SIEGEL, J. E., SNELLEN, J. E. & WHITT, D. D. 1981. Transit time of epithelial cells in the small intestines of germfree mice and ex-germfree mice associated with indigenous microorganisms. *Appl Environ Microbiol*, 42, 996-1001.
- SCHNEIDER, C. A., RASBAND, W. S. & ELICEIRI, K. W. 2012. NIH Image to ImageJ: 25 years of image analysis. *Nat Methods*, 9, 671-5.
- SCHULZ, M. D., ATAY, C., HERINGER, J., ROMRIG, F. K., SCHWITALLA, S., AYDIN, B., ZIEGLER, P. K., VARGA, J., REINDL, W., POMMERENKE, C., SALINAS-RIESTER, G., BOCK, A., ALPERT, C., BLAUT, M., POLSON, S. C., BRANDL, L., KIRCHNER, T., GRETEN, F. R., POLSON, S. W. & ARKAN, M. C. 2014. High-fat-diet-mediated dysbiosis promotes intestinal carcinogenesis independently of obesity. *Nature*, 514, 508-12.
- SEGDIRSAS, S., ROWAN, A. J., HOWARTH, K., JONES, A., LEEDHAM, S., WRIGHT, N. A., GORMAN, P., CHAMBERS, W., DOMINGO, E., ROYLANCE, R. R., SAWYER, E. J.,

- SIEBER, O. M. & TOMLINSON, I. P. 2009. APC and the three-hit hypothesis. *Oncogene*, 28, 146-55.
- SHABBIR, J. & BRITTON, D. C. 2010. Stoma complications: a literature overview. *Colorectal Dis*, 12, 958-64.
- SHIMOTOYODOME, A., MEGURO, S., HASE, T., TOKIMITSU, I. & SAKATA, T. 2000. Short chain fatty acids but not lactate or succinate stimulate mucus release in the rat colon. *Comp Biochem Physiol A Mol Integr Physiol*, 125, 525-31.
- SHIN, R., SUZUKI, M. & MORISHITA, Y. 2002. Influence of intestinal anaerobes and organic acids on the growth of enterohaemorrhagic *Escherichia coli* O157:H7. *J Med Microbiol*, 51, 201-6.
- SINAL, C. J., TOHKIN, M., MIYATA, M., WARD, J. M., LAMBERT, G. & GONZALEZ, F. J. 2000. Targeted disruption of the nuclear receptor FXR/BAR impairs bile acid and lipid homeostasis. *Cell*, 102, 731-44.
- SINCLAIR, J. L. & ALEXANDER, M. 1984. Role of resistance to starvation in bacterial survival in sewage and lake water. *Appl Environ Microbiol*, 48, 410-5.
- SINHA, R. & JASTREBOFF, A. M. 2013. Stress as a common risk factor for obesity and addiction. *Biol Psychiatry*, 73, 827-35.
- SLUPSKY, C. M., RANKIN, K. N., WAGNER, J., FU, H., CHANG, D., WELJIE, A. M., SAUDE, E. J., LIX, B., ADAMKO, D. J., SHAH, S., GREINER, R., SYKES, B. D. & MARRIE, T. J. 2007. Investigations of the effects of gender, diurnal variation, and age in human urinary metabolomic profiles. *Anal Chem*, 79, 6995-7004.
- SOBHANI, I., TAP, J., ROUDOT-THORAVALL, F., ROPERCH, J. P., LETULLE, S., LANGELLA, P., CORTHIER, G., TRAN VAN NHIEU, J. & FURET, J. P. 2011. Microbial dysbiosis in colorectal cancer (CRC) patients. *PLoS One*, 6, e16393.
- SOKOL, H., PIGNEUR, B., WATTERLOT, L., LAKHDARI, O., BERMUDEZ-HUMARAN, L. G., GRATADOUX, J. J., BLUGEON, S., BRIDONNEAU, C., FURET, J. P., CORTHIER, G., GRANGETTE, C., VASQUEZ, N., POCHART, P., TRUGNAN, G., THOMAS, G., BLOTTIERE, H. M., DORE, J., MARTEAU, P., SEKSIK, P. & LANGELLA, P. 2008. Faecalibacterium prausnitzii is an anti-inflammatory commensal bacterium identified by gut microbiota analysis of Crohn disease patients. *Proc Natl Acad Sci U S A*, 105, 16731-6.
- STEPHENS, N. S., SIFFLEDEEN, J., SU, X., MURDOCH, T. B., FEDORAK, R. N. & SLUPSKY, C. M. 2013. Urinary NMR metabolomic profiles discriminate inflammatory bowel disease from healthy. *J Crohns Colitis*, 7, e42-8.
- STIDL, R., SONTAG, G., KOLLER, V. & KNASMULLER, S. 2008. Binding of heterocyclic aromatic amines by lactic acid bacteria: results of a comprehensive screening trial. *Mol Nutr Food Res*, 52, 322-9.
- SU, L., NALLE, S. C., SHEN, L., TURNER, E. S., SINGH, G., BRESKIN, L. A., KHRAMTSOVA, E. A., KHRAMTSOVA, G., TSAI, P. Y., FU, Y. X., ABRAHAM, C. & TURNER, J. R. 2013. TNFR2 activates MLCK-dependent tight junction dysregulation to cause apoptosis-mediated barrier loss and experimental colitis. *Gastroenterology*, 145, 407-15.
- TANA, C., UMESAKI, Y., IMAOKA, A., HANDA, T., KANAZAWA, M. & FUKUDO, S. 2010. Altered profiles of intestinal microbiota and organic acids may be the origin of symptoms in irritable bowel syndrome. *Neurogastroenterol Motil*, 22, 512-9, e114-5.
- TAP, J., MONDOT, S., LEVENEZ, F., PELLETIER, E., CARON, C., FURET, J. P., UGARTE, E., MUNOZ-TAMAYO, R., PASLIER, D. L., NALIN, R., DORE, J. & LECLERC, M. 2009. Towards the human intestinal microbiota phylogenetic core. *Environ Microbiol*, 11, 2574-84.
- TAUPIN, D. R., KINOSHITA, K. & PODOLSKY, D. K. 2000. Intestinal trefoil factor confers colonic epithelial resistance to apoptosis. *Proc Natl Acad Sci U S A*, 97, 799-804.

- THOMAS, C., GIOIELLO, A., NORIEGA, L., STREHLE, A., OURY, J., RIZZO, G., MACCHIARULO, A., YAMAMOTO, H., MATAKI, C., PRUZANSKI, M., PELLICCIARI, R., AUWERX, J. & SCHOONJANS, K. 2009. TGR5-mediated bile acid sensing controls glucose homeostasis. *Cell Metab*, 10, 167-77.
- TOLHURST, G., HEFFRON, H., LAM, Y. S., PARKER, H. E., HABIB, A. M., DIAKOIANNAKI, E., CAMERON, J., GROSSE, J., REIMANN, F. & GRIBBLE, F. M. 2012. Short-chain fatty acids stimulate glucagon-like peptide-1 secretion via the G-protein-coupled receptor FFAR2. *Diabetes*, 61, 364-71.
- TREMAROLI, V. & BACKHED, F. 2012. Functional interactions between the gut microbiota and host metabolism. *Nature*, 489, 242-9.
- TSABOURI, S., PRIFTIS, K. N., CHALIASOS, N. & SIAMOPOULOU, A. 2014. Modulation of gut microbiota downregulates the development of food allergy in infancy. *Allergol Immunopathol (Madr)*, 42, 69-77.
- TURNBAUGH, P. J., HAMADY, M., YATSUNENKO, T., CANTAREL, B. L., DUNCAN, A., LEY, R. E., SOGIN, M. L., JONES, W. J., ROE, B. A., AFFOURTIT, J. P., EGHOLM, M., HENRISSAT, B., HEATH, A. C., KNIGHT, R. & GORDON, J. I. 2009. A core gut microbiome in obese and lean twins. *Nature*, 457, 480-4.
- TURNBAUGH, P. J., LEY, R. E., MAHOWALD, M. A., MAGRINI, V., MARDIS, E. R. & GORDON, J. I. 2006. An obesity-associated gut microbiome with increased capacity for energy harvest. *Nature*, 444, 1027-31.
- TURSI, A., BRANDIMARTE, G., GIORGETTI, G. M., FORTI, G., MODEO, M. E. & GIGLIOBIANCO, A. 2004. Low-dose balsalazide plus a high-potency probiotic preparation is more effective than balsalazide alone or mesalazine in the treatment of acute mild-to-moderate ulcerative colitis. *Med Sci Monit*, 10, Pi126-31.
- VAN DEN BERG, R. A., HOEFSLOOT, H. C., WESTERHUIS, J. A., SMILDE, A. K. & VAN DER WERF, M. J. 2006. Centering, scaling, and transformations: improving the biological information content of metabolomics data. *BMC Genomics*, 7, 142.
- VAN NOOD, E., VRIEZE, A., NIEUWDORP, M., FUENTES, S., ZOETENDAL, E. G., DE VOS, W. M., VISSER, C. E., KUIJPER, E. J., BARTELSMAN, J. F., TIJSSEN, J. G., SPEELMAN, P., DIJKGRAAF, M. G. & KELLER, J. J. 2013. Duodenal infusion of donor feces for recurrent *Clostridium difficile*. *N Engl J Med*, 368, 407-15.
- VELAGAPUDI, V. R., HEZAVEH, R., REIGSTAD, C. S., GOPALACHARYULU, P., YETUKURI, L., ISLAM, S., FELIN, J., PERKINS, R., BOREN, J., ORESIC, M. & BACKHED, F. 2010. The gut microbiota modulates host energy and lipid metabolism in mice. *J Lipid Res*, 51, 1101-12.
- VON SCHILLDE, M. A., HORMANNSPERGER, G., WEIHER, M., ALPERT, C. A., HAHNE, H., BAUERL, C., VAN HUYNEGEM, K., STEIDLER, L., HRNCIR, T., PEREZ-MARTINEZ, G., KUSTER, B. & HALLER, D. 2012. Lactocepin secreted by *Lactobacillus* exerts anti-inflammatory effects by selectively degrading proinflammatory chemokines. *Cell Host Microbe*, 11, 387-96.
- VOS, P., GARRITY, G., JONES, D., KRIEG, N. R., LUDWIG, W., RAINEY, F. A., SCHLEIFER, K. H. & WHITMAN, W. 2009. *Bergey's Manual of Systematic Bacteriology. Volume 3: The Firmicutes*, Springer-Verlag New York.
- WALLACE, R. J. 1996. Ruminal microbial metabolism of peptides and amino acids. *J Nutr*, 126, 1326s-34s.
- WALSH, M. C., BRENNAN, L., MALTHOUSE, J. P., ROCHE, H. M. & GIBNEY, M. J. 2006. Effect of acute dietary standardization on the urinary, plasma, and salivary metabolomic profiles of healthy humans. *Am J Clin Nutr*, 84, 531-9.
- WANG, M., KARLSSON, C., OLSSON, C., ADLERBERTH, I., WOLD, A. E., STRACHAN, D. P., MARTRICARDI, P. M., ABERG, N., PERKIN, M. R., TRIPODI, S., COATES, A. R., HESSELMAR, B., SAALMAN, R., MOLIN, G. & AHRNE, S. 2008. Reduced diversity in



- the early fecal microbiota of infants with atopic eczema. *J Allergy Clin Immunol*, 121, 129-34.
- WANG, Q., GARRITY, G. M., TIEDJE, J. M. & COLE, J. R. 2007. Naive Bayesian classifier for rapid assignment of rRNA sequences into the new bacterial taxonomy. *Appl Environ Microbiol*, 73, 5261-7.
- WEXLER, H. M. 2007. Bacteroides: the good, the bad, and the nitty-gritty. *Clin Microbiol Rev*, 20, 593-621.
- WHITMAN, W., GOODFELLOW, M., KÄMPFER, P., BUSSE, H., TRUJILLO, M., LUDWIG, W., SUZUKI, K. & PARTE, A. 2012. *Bergey's Manual of Systematic Bacteriology. Volume 5: The Actinobacteria.*, Springer-Verlag New York.
- WICKHAM, H. 2009. *ggplot2. Elegant Graphics for Data Analysis.*, Springer-Verlag New York.
- WILLIAMS, H. R., COX, I. J., WALKER, D. G., NORTH, B. V., PATEL, V. M., MARSHALL, S. E., JEWELL, D. P., GHOSH, S., THOMAS, H. J., TEARE, J. P., JAKOBOVITS, S., ZEKI, S., WELSH, K. I., TAYLOR-ROBINSON, S. D. & ORCHARD, T. R. 2009. Characterization of inflammatory bowel disease with urinary metabolic profiling. *Am J Gastroenterol*, 104, 1435-44.
- WILLING, B. P., DICKSVED, J., HALFVARSON, J., ANDERSSON, A. F., LUCIO, M., ZHENG, Z., JARNEROT, G., TYSK, C., JANSSON, J. K. & ENGSTRAND, L. 2010. A pyrosequencing study in twins shows that gastrointestinal microbial profiles vary with inflammatory bowel disease phenotypes. *Gastroenterology*, 139, 1844-1854.e1.
- WISHART, D. S., KNOX, C., GUO, A. C., EISNER, R., YOUNG, N., GAUTAM, B., HAU, D. D., PSYCHOGIOS, N., DONG, E., BOUATRA, S., MANDAL, R., SINELNIKOV, I., XIA, J., JIA, L., CRUZ, J. A., LIM, E., SOBSEY, C. A., SHRIVASTAVA, S., HUANG, P., LIU, P., FANG, L., PENG, J., FRADETTE, R., CHENG, D., TZUR, D., CLEMENTS, M., LEWIS, A., DE SOUZA, A., ZUNIGA, A., DAWE, M., XIONG, Y., CLIVE, D., GREINER, R., NAZYROVA, A., SHAYKHUTDINOV, R., LI, L., VOGEL, H. J. & FORSYTHE, I. 2009. HMDB: a knowledgebase for the human metabolome. *Nucleic Acids Res*, 37, D603-10.
- WORLEY, B. & POWERS, R. 2013. Multivariate Analysis in Metabolomics. *Curr Metabolomics*, 1, 92-107.
- XIA, J., SINELNIKOV, I. V., HAN, B. & WISHART, D. S. 2015. MetaboAnalyst 3.0--making metabolomics more meaningful. *Nucleic Acids Res*, 43, W251-7.
- XU, W., HE, B., CHIU, A., CHADBURN, A., SHAN, M., BULDYS, M., DING, A., KNOWLES, D. M., SANTINI, P. A. & CERUTTI, A. 2007. Epithelial cells trigger frontline immunoglobulin class switching through a pathway regulated by the inhibitor SLPI. *Nat Immunol*, 8, 294-303.
- ZEEVI, D., KOREM, T., ZMORA, N., ISRAELI, D., ROTHSCHILD, D., WEINBERGER, A., BEN-YACOV, O., LADOR, D., AVNIT-SAGI, T., LOTAN-POMPAN, M., SUEZ, J., MAHDI, J. A., MATOT, E., MALKA, G., KOSOWER, N., REIN, M., ZILBERMAN-SCHAPIRA, G., DOHNALOVA, L., PEVSNER-FISCHER, M., BIKOVSKY, R., HALPERN, Z., ELINAV, E. & SEGAL, E. 2015. Personalized Nutrition by Prediction of Glycemic Responses. *Cell*, 163, 1079-94.
- ZEUTHEN, L. H., FINK, L. N. & FROKIAER, H. 2008. Epithelial cells prime the immune response to an array of gut-derived commensals towards a tolerogenic phenotype through distinct actions of thymic stromal lymphopoietin and transforming growth factor-beta. *Immunology*, 123, 197-208.
- ZHANG, C., ZHANG, M., WANG, S., HAN, R., CAO, Y., HUA, W., MAO, Y., ZHANG, X., PANG, X., WEI, C., ZHAO, G., CHEN, Y. & ZHAO, L. 2010. Interactions between gut microbiota, host genetics and diet relevant to development of metabolic syndromes in mice. *Isme j*, 4, 232-41.
- ZHU, B., WANG, X. & LI, L. 2010. Human gut microbiome: the second genome of human body. *Protein Cell*, 1, 718-25.

## Websites

BioEdit Software

[www.mbio.ncsu.edu/BioEdit/bioedit.html](http://www.mbio.ncsu.edu/BioEdit/bioedit.html)

Colostomy Association

<http://www.colostomyassociation.org.uk/index.php?p=199&pp=3&page=Stoma%20Reversal>

Illumina Inc® 2012

<https://www.illumina.com/company/video-hub/JA6mofeuntk.html>

ImageJ Software

<https://imagej.nih.gov/ij/>

KEGG Pathway Database

<http://www.genome.jp/kegg/pathway.html>

MetaboAnalyst

<http://www.metaboanalyst.ca/faces/home.xhtml>

NCBI BLASTn

<https://blast.ncbi.nlm.nih.gov/Blast.cgi>

NHS Bowel Cancer Screening

<http://www.nhs.uk/Conditions/bowel-cancer-screening/Pages/Introduction.aspx>

RStudio Software

<https://www.rstudio.com/>

TameNMR Software



[www.galaxy.liv.ac.uk](http://www.galaxy.liv.ac.uk) from autumn 2017

VSL#3 Polybiotic Food Supplement

<https://www.vsl3.co.uk/index.php>

# Publication

## Loop ileostomy-mediated fecal stream diversion is associated with microbial dysbiosis

Emma L. Beamish<sup>a</sup>, Judith Johnson<sup>b</sup>, Elisabeth J. Shaw <sup>a</sup>, Nigel A. Scott<sup>b</sup>, Arnab Bhowmick<sup>b</sup>, and Rachael J. Rigby <sup>a</sup>

<sup>a</sup>Division of Biomedical and Life Sciences, Lancaster University, Lancaster, UK; <sup>b</sup>Lancashire Teaching Hospitals NHS Foundation Trust, Preston, UK

### ABSTRACT

Loop ileostomy is an effective procedure to protect downstream intestinal anastomoses. Ileostomy reversal surgery is often performed within 12 months of formation but is associated with substantial morbidity due to severe post-surgical complications. Distal ileum is deprived of enteral nutrition and rendered inactive, often becoming atrophied and fibrotic. This study aimed to investigate the microbial and morphological changes that occur in the defunctioned ileum following loop ileostomy-mediated fecal stream diversion. Functional and defunctioned ileal resection tissue was obtained at the time of loop-ileostomy closure. Inpatient comparisons, including histological assessment of morphology and epithelial cell proliferation, were performed on paired samples using the functional limb as control. Mucosal-associated microflora was quantified via determination of 16S rRNA gene copy number using qPCR analysis. DGGE with Sanger sequencing and qPCR methods profiled microflora to genus and phylum level, respectively. Reduced villous height and proliferation confirmed atrophy of the defunctioned ileum. DGGE analysis revealed that the microflora within defunctioned ileum is less diverse and convergence between defunctioned microbiota profiles was observed. Candidate Genera, notably Clostridia and Streptococcus, reduced in relative terms in defunctioned ileum. We conclude that ileostomy-associated nutrient deprivation results in dysbiosis and impaired intestinal renewal in the defunctioned ileum. Altered host-microbial interactions at the mucosal surface likely contribute to the deterioration in homeostasis and thus may underpin numerous postoperative complications. Strategies to sustain the microflora before reanastomosis should be investigated.

### ARTICLE HISTORY

Received 11 November 2016

Revised 17 May 2017

Accepted 2 June 2017

### KEYWORDS


atrophy; dysbiosis; enteral nutrition; Loop ileostomy; microbiota; morphology; small intestine


### Introduction

Loop ileostomy formation is often performed to reduce septic complications in patients who have undergone extensive bowel surgery. It is most frequently formed following surgical resection in colorectal carcinoma patients to prevent leakage of distal anastomosis, sepsis and the requirement for urgent repeat operation. It functions to protect downstream anastomoses via temporary fecal stream diversion through the abdominal wall. Despite its precautionary therapeutic benefits, the use of fecal stream diversion continues to be debated due to complications associated with ileostomy formation and reversal.

Previous studies have highlighted the effectiveness of a well-formed loop ileostomy at defunctioning

downstream intestine following surgery.<sup>1</sup> Loop ileostomy formation gives rise to 2 contrasting nutritional environments; the proximal ileum remains functional with nutrient and water absorption occurring at the mucosal surface from peristaltic-motiled chyme, while the distal ileum is deprived of luminal contents and thus rendered inactive. A defunctioned loop ileostomy is usually reversed within 12 months, reinstating luminal flow through the entire intestine. In addition to the inconvenience of a second operation for loop closure, the reversal procedure is associated with a substantial morbidity of around 20%.<sup>2–5</sup> Small bowel obstruction and anastomotic leakage are the most common post-surgical complications with respective incidence rates up to 22% and 10%.<sup>2,6</sup>

**CONTACT** Dr. Rachael J. Rigby  rachael.rigby@lancaster.ac.uk  Faculty of Health and Medicine, Furness College, Lancaster University, Lancaster, LA1 4YG, United Kingdom.

 Supplemental data for this article can be accessed on the publisher's website.

© 2017 Emma L. Beamish, Judith Johnson, Elisabeth J. Shaw, Nigel A. Scott, Arnab Bhowmick, and Rachael J. Rigby. Published with license by Taylor & Francis  
This is an Open Access article distributed under the terms of the Creative Commons Attribution License (<http://creativecommons.org/licenses/by/4.0/>), which permits unrestricted use, distribution, and reproduction in any medium, provided the original work is properly cited.

Further complications include prolonged postoperative ileus and fecal incontinence, as well as incisional hernia and wound infections at the site of stoma formation.<sup>6-8</sup> Due to such complications, around 5% of cases prove to be irreversible, leaving patients with a permanent stoma and a reduced quality of life.<sup>9</sup>

Intestinal structure and function are directly related and hence research has thus far focused on the pathophysiology of the defunctioned intestine. Both animal models and human studies have documented the atrophic nature of the defunctioned intestine before closure.<sup>10,11</sup> In addition, previous research has demonstrated a significant loss of motility and muscle volume in the defunctioned intestine.<sup>11</sup> Collectively, these physiologic factors are likely to contribute to the post-surgical complications associated with reversal surgery. However, the mechanisms underlying such physiologic changes remain yet to be explored. Clinical studies have reported attempts to stimulate the defunctioned intestine before reanastomosis and loop closure.<sup>12-14</sup> Thus far, there have been varied reports of success at reducing post-surgical complications, with particular focus placed on postoperative ileus. Such studies were conducted with the aim of gradually activating cellular mechanisms of absorption and motility to restore functionality to the intestine before reversal surgery. However, such rationale and practice vastly disregards the importance of a healthy gut microbiome for proficient intestinal function.

The intestinal microbiota has received considerable interest in recent years and research is beginning to uncover the pivotal role gut microflora play in the complex homeostatic host-microbial interactions essential for maintaining intestinal health (reviewed in ref.<sup>15</sup>). Germ free animal studies revealed substantial defects in the development of various gut-associated lymphoid tissues as well as reduced intestinal epithelial cell (IEC) turnover when compared with specific pathogen free controls.<sup>16,17</sup> In addition, mice lacking MyD88 adaptor protein, essential for Toll-like receptor signaling, demonstrated that recognition of commensal bacteria by TLR on the apical surface of IEC is fundamental for both maintenance of intestinal homeostasis and repair in response to injury.<sup>18</sup> The composition of the intestinal microbiota is modulated by various host genetic and environmental factors including medical practices such as antibiotic use, method of childbirth and most

significantly, host diet.<sup>19-21</sup> A plethora of literature now exists detailing the effects of diet modulation on the intestinal microbiota (Reviewed in ref.<sup>22</sup>). Notably, a recent mouse model of total parenteral nutrition (TPN) demonstrated that enteral nutrient deprivation leads to significant shifts in microbial dominance with associated reduced epithelial turnover and intestinal atrophy.<sup>23,24</sup>

We propose that loop ileostomy-mediated fecal stream diversion and the resultant loss of enteral nutrition in the downstream intestine alters microbiota composition, which in turn affects IEC turnover and consequently impacts on intestinal structure and function. This study aimed to investigate microbial and physiologic changes that occur in the defunctioned ileum following fecal stream diversion.

## Materials and methods

### Study inclusion criteria

Research was conducted in accordance with North West Research Ethics Committee guidelines (ref: 13/NW/0695). Patients undergoing loop ileostomy reversal surgery were recruited at Lancashire Teaching Hospitals NHS Trust (Lancashire, UK). Patients who had ongoing bowel pathologies, such as inflammatory bowel disease, or had antibiotic treatments within the last 3 months, were deemed ineligible. Tissue was obtained from 34 patients and all recruited participants had loop ileostomy to protect downstream anastomoses following resection of colorectal cancer tumors. Participant demographics and post-surgical clinical data are presented in Table 1.

### Sample acquisition and handling

Loop ileostomy reversal surgery involves reanastomosis of functional and defunctioned ileum using a

**Table 1.** Participant Demographics and Post-surgical Clinical Data.

Participant Demographics and Post-surgical Clinical Data	
Age (years)*	58 (± 16)
BMI†	26.0 (± 2.4)
Days since ileostomy formation*	392 (± 264)
Gender (% females)	51
CRP (mg/L)*	87.9 (± 54.8)
Albumin (g/L)*	38.1 (± 3.4)
WBC (x10 <sup>9</sup> /L)*	9.4 (± 1.7)

Note. \*The mean is given with standard deviation in parentheses.



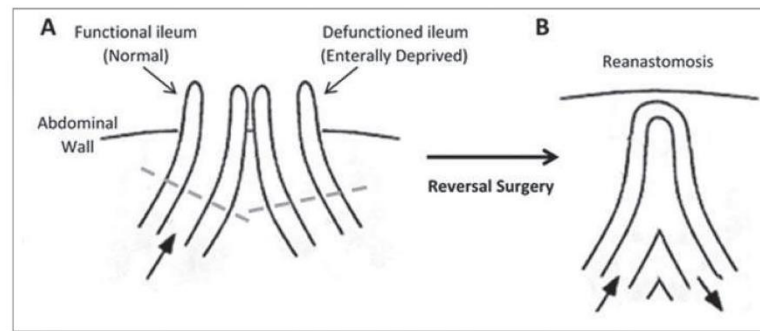


**Figure 1.** Structure of the intestine. (A) Loop ileostomy and (B) following reanastomosis. Block arrows denote presence and direction of luminal contents flow. Tissue located above dashed lines represent areas of intestine removed before reanastomosis and form the specimen acquired for our research.

linear stapler. A short region of the intestine is routinely removed from the end of each limb before reanastomosis and these are the specimen acquired for this study (see Fig. 1). All specimen were maintained in Minimal Essential Media (Sigma-Aldrich), on ice and were processed within 2 hours of collection. Luminal-associated microflora were pelleted from media. Mucosal-associated microflora were obtained from mucosal biopsies of equal mass from each specimen.

#### **Histological analyses**

Full thickness tissue sections were fixed in 4% paraformaldehyde solution for 24 hours. Morphological analysis was performed on haematoxylin and eosin (H&E) stained sections. Villous height was measured using ImageJ software.<sup>25</sup> Coded H & E sections were scored for inflammation by a blinded observer. Scoring applied a well-validated system which assigns a score of 0 – 4 for inflammation and mucosal damage based on degree and extent of transmural inflammation, goblet cell depletion, immune infiltrate and architecture distortion.<sup>26</sup>

#### **Immunofluorescence PCNA analysis**

Paraffin sections were dewaxed, rehydrated and subjected to antigen retrieval, by boiling in Sodium Citrate Buffer (10mM Sodium Citrate, 0.05% Tween 20, pH 6.0), using a microwave oven, for 15 minutes. Slides were stained with mouse anti-PCNA (PC10) primary antibody and goat anti-mouse Alexa-Fluor<sup>®</sup> 488 antibody (ThermoFisher Scientific). Slides were counterstained with

Hoescht33342 trihydrochloride nucleic acid stain (Life Technologies) and mounted using VectaShield mounting medium (Vector Laboratories). Number of PCNA-positive IEC per crypt was counted by a blinded observer and the percent of proliferative cells/all nucleated cells was calculated.

#### **TUNEL assay**

TUNEL assay was performed on tissue sections using Click-iT Plus TUNEL Alexa Flour 594 kit, according to manufacturer's protocol (ThermoFisher Scientific). Tissue sections were subjected to antigen retrieval, by boiling in Sodium Citrate Buffer (10mM Sodium Citrate, 0.05% Tween 20, pH 6.0), using a microwave oven, for 15 minutes. Following TUNEL assay, slides were counterstained with Hoescht33342 trihydrochloride nucleic acid stain (Life Technologies) and mounted using VectaShield mounting medium (Vector Laboratories). Total number of apoptotic cells per villous was quantified by a blinded observer.

#### **Mucosal bacterial DNA extraction**

Mucosal biopsies were finely sliced to aid release of associated microflora. Total genomic DNA was extracted using QIAamp Cador pathogen lysis minikit (Qiagen), according to the manufacturer's protocol.

#### **Luminal bacterial DNA extraction**

Media samples were centrifuged at 6000xg to pellet bacteria and resuspended in 500 $\mu$ L buffer ATL (Qiagen). Pellets were subjected to mechanical lysis at

maximum speed for 10 minutes in Pathogen lysis tubes (Qiagen), before DNA extraction using QIAamp UCP Pathogen Mini Kit (Qiagen), according to the manufacturer's protocol.

#### **Denaturation gradient gel electrophoresis (DGGE) profiling**

A highly conserved 200bp sequence, neighboring the V3 hypervariable region of the 16S rRNA gene, was amplified using universal 16S rRNA primers, 341F\_GC and 518R (Table S1).<sup>27</sup> Gels were post-stained using SYBR Gold Nucleic Acid Gel Stain and visualized using Image Lab software with 4 seconds exposure. On each DGGE gel, a standard marker, composed of pooled fecal microbial DNA from 5 healthy individuals, was included to allow comparison between gels. DGGE profiles were processed digitally using BioNumerics software (version 7.5; Applied Maths), following the manufacturer's guidelines.

#### **DGGE band excision and sequencing analysis**

Amplicons from DGGE bands of interest were reamplified directly from the gel, via inoculation using a sterile pipette tip. The purity of the PCR products was confirmed via repeat DGGE analysis and extraction until a single band was obtained. Purification was confirmed by running extracted band, neighboring the original sample (Figure S1). Following matched confirmation of target bands with original sample profiles, amplicons were subjected to Sanger sequencing (Source Bioscience), using primers 341F+GC Clamp and 518r. Consensus sequences were generated using BioEdit software (available at [www.mbio.ncsu.edu/BioEdit/bioedit.html](http://www.mbio.ncsu.edu/BioEdit/bioedit.html)) and sequences were then classified using nucleotide Basic Local Alignment Search Tool (BLASTn; available online at [www.blast.ncbi.nlm.nih.gov.uk](http://www.blast.ncbi.nlm.nih.gov.uk)). Sequences with complete query coverage and max ident. >99% were classified to genus level. This method of classification was validated first with DNA extracted from known bacterial samples.

#### **16SrDNA qRT-PCR**

Predominant microbial phyla were compared using phylum-specific and universal 16S rRNA primers (Table S1). 30–50ng of template DNA was added

to each PCR reaction. PCR parameters were as follows: 1 cycle of 95°C for 5 min, 35 cycles of 95°C for 20 sec, 61.5°C for 10 sec, annealing, 72°C for 30 sec and 1 cycle of 72°C for 5 min. Data was normalized to total bacteria, using universal primers, and the relative abundances of each phylum determined using the delta delta Ct ( $2^{-\Delta\Delta Ct}$ ) algorithm method.<sup>28</sup>

#### **Determination of total bacterial load**

Total bacterial load in the functional and defunctioned intestine was measured via qPCR, using universal eubacterial 16S rRNA primers, Uni334F and Uni514R (Table S1)<sup>29</sup> and Sybr Green ReadyMix (Sigma-Aldrich). A standard curve constructed for bacterial enumeration using pCR2.1 Topo-TA plasmid vector, containing a cloned portion of the 16S rRNA gene. Bacterial quantification relates to total 16S rRNA gene copy number and not colony forming units or cell counts.

#### **Statistical analyses**

All statistical analyses were performed using SPSS Statistics Desktop (IBM).  $p \leq 0.05$  was deemed statistically significant (\*  $p \leq 0.05$ ; \*\*  $p \leq 0.01$ ; \*\*\*  $p \leq 0.001$ ).

## **Results**

### **Defunctioned intestine is atrophied, but not inflamed**

We confirmed that intestinal atrophy occurs following loop ileostomy-mediated defunctioning (Fig. 2A). A  $47\% \pm 15\%$  reduction in average villous height was observed in defunctioned ileum of all patients, compared with functional tissue (Fig. 2B). Despite significant atrophy and apparent structural remodeling in defunctioned tissue (Fig. 2A), no significant difference in inflammation was observed compared with functional tissue (Figure S2;  $n = 9$ ,  $p \geq 0.05$ ), suggestive of an absence of chronic inflammation at time of reversal surgery.

### **Total bacterial load is reduced in response to defunctioning**

Determination of total mucosal bacterial load was performed via quantification of 16S rRNA gene copy number. Small intestinal bacterial load is



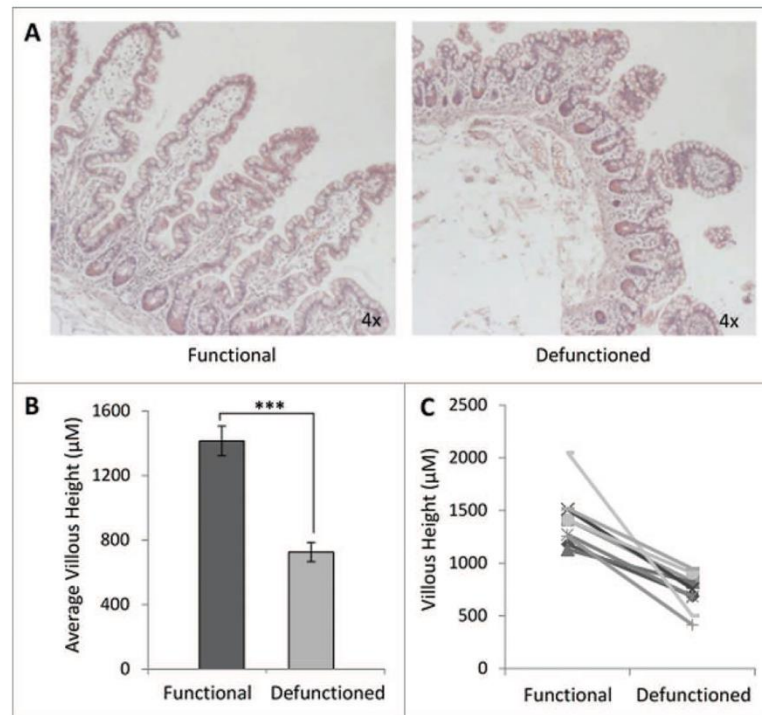


**Figure 2.** Histological analyses of function and defunctioned ileum. (A) Representative H&E stained sections, magnification 4x. (B) Average villous height  $\pm$  SEM ( $n = 9$ ,  $p = 0.0004$ ) (C) Paired villous height.

considered to be around 108 cells per ml of luminal content.<sup>30</sup> In accordance with this, the average mucosa-associated bacterial load in functional ileum was determined to be  $2.63 \times 10^8$  gene copies per gram of tissue, compared with  $9.89 \times 10^7$  in the defunctioned (Fig. 3A). This constituted a 62.4%

decrease in bacterial load (Fig. 3A;  $n = 27$ ,  $p = 0.0003$ ). A reduction occurred consistently across all paired samples tested (Fig. 3B), suggesting that fecal stream diversion and consequential microbial enteral nutrient deprivation leads to a substantial reduction in total bacterial load.

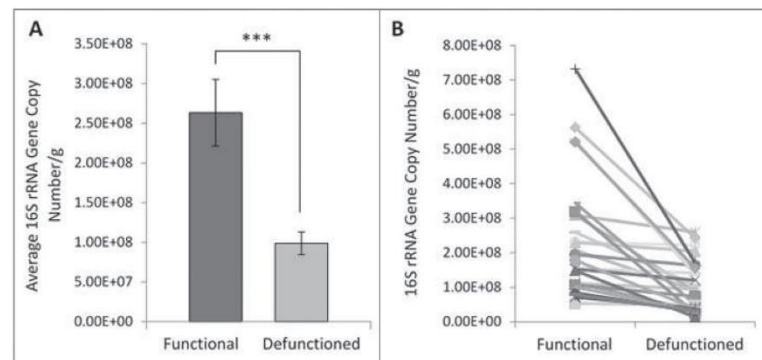


**Figure 3.** Bacterial enumeration of (A) average- and (B) absolute-16S rRNA gene copy numbers per gram of mucosal tissue in functional and defunctioned intestine ( $n = 27$ ;  $p = 0.0003$ ).

**Loss of microbial diversity and convergence toward a similar bacterial profile occurs in defunctioned intestine**

Considering the decrease total bacterial load in defunctioned intestine, microbial composition was investigated using DGGE. Digital processing of DGGE gel image enabled standardized identification of bands across all profiles and generation of a binary presence or absence banding profile for each sample (Fig. 4A). Each band on a DGGE gel represents one or more closely bacterial species therefore the number of bands in each profile reflects the number of different bacterial species and thus overall microbial diversity. On average, the total number of bands in the defunctioned profiles was lower than the number observed in the functional profiles (average of 16 bands to 11 bands, respectively; Fig. 4B), indicating that fecal stream diversion reduces diversity of the intestinal microbiota.

Hierarchical cluster analysis of binary DGGE banding profiles revealed considerable similarity between

the defunctioned profiles, as they cluster together rather than with their paired functional counterparts (Fig. 5). Profiles from functional ileum also clustered together (Fig. 5) demonstrating that, irrespective of interpatient variability, distinct microbial populations exist within the 2 different nutritional environments.

**Dysbiosis is apparent at phylum and genus level in defunctioned bowel**

To characterize the apparent disparity in microbial profiles between functional and defunctioned intestine, sequencing analysis was performed on extracted bands classes of interest. In total, 73 distinct band classes were identified across 22 DGGE profiles (11 functional and 11 defunctioned paired samples). A total of 10 band classes, differing in percent presence between functional and defunctioned profiles, were selected and of these, 8 were successfully extracted, purified and sequenced (Fig. S1; Fig. 4C). Subsequent BLAST analysis revealed the

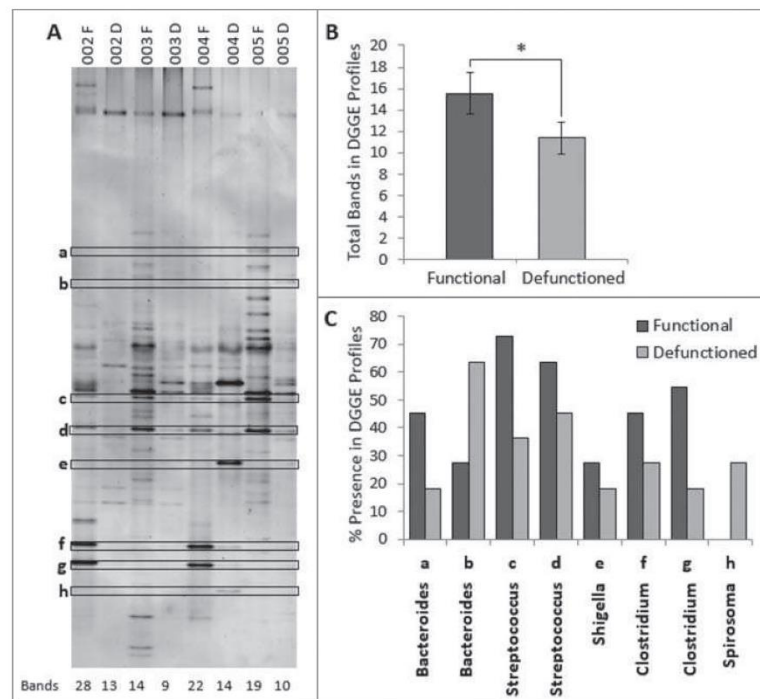


**Figure 4.** (A) Example of denaturation gradient gel electrophoresis (DGGE) profiles. Band classes are depicted using characters a through h and corresponding bands are enclosed. F, functional ileum; D, defunctioned ileum. (B) Microbial diversity in functional and defunctioned ileum expressed as total number of bands in DGGE profiles ( $n = 11$ ;  $P = 0.04$ ). (C) Purified and sequenced band classes expressed as a percentage presence in DGGE profiles across all patients. Characters a-h correspond to the band classes highlighted in A. Inclined, corresponding assigned bacterial genus per band class.

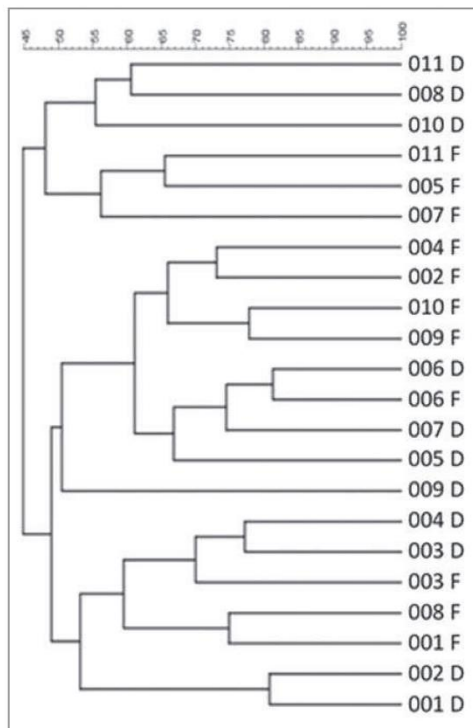


**Figure 5.** Hierarchical cluster analysis of DGGE profiles represented in graphical form as an UPGMA dendrogram. F: functional ileum, D: defunctioned ileum ( $n = 11$ ).

highest matched identities from NCBI nucleotide databases for each band class and the highest sequence similarity (99–100%) match was assigned at genus level. Band classes a and b were assigned to the *Bacteroides* genus, band class c and d to *Streptococcus*, band class e to *Shigella*, band class f and g to *Clostridium* and band class h to *Spirosoma* (Fig. 4C). Figure 4C also demonstrates percent reductions in *Clostridium* (18.2% and 36.3% band class f and g, respectively), *Shigella/Escherichia* (9%, band e) and *Streptococcus* (36.3% and 18.2%, band c and d) genera across defunctioned, compared with functional profiles. Conversely, an increase in the percentage presence of *Spirosoma* (27% increase, band h) was observed in the defunctioned profiles. Interestingly, members of the *Bacteroides* genus were observed to increase or decrease in percent presence across the functional and defunctioned profiles (27.3% reduction and 36% increase, band a and b, respectively; Fig. 4C).

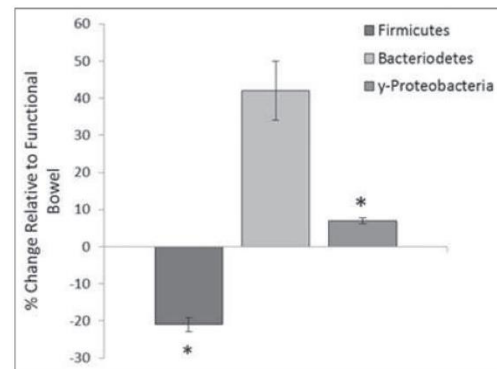


**Figure 6.** Percentage change of phyla abundance in defunctioned ileum relative to functional. Data normalized to universal 16S rDNA primers (Firmicutes ( $n = 18$ ,  $p = 0.02$ ), Bacteroidetes ( $n = 18$ , NS),  $\gamma$ -Proteobacteria ( $n = 9$ ,  $p \leq 0.05$ )).

Furthermore, relative quantification of 3 bacterial phyla, Bacteroidetes, Firmicutes and  $\gamma$ -Proteobacteria, was performed on the functional and defunctioned intestine using qRT-PCR. We identified a significant reduction in the relative abundance of the Firmicutes phylum (21% reduction,  $n = 18$ ;  $p = 0.02$ ) and a small but significant increase in the  $\gamma$ -Proteobacteria phylum (6.9% increase,  $n = 9$ ,  $p = 0.05$ ) in the defunctioned intestine compared with the paired functional controls (Fig. 6). Consistent with DGGE results, the relative abundance of Bacteroidetes varied considerably across our patient cohort (Fig. 6).

#### **Reduced IEC proliferation was observed in defunctioned crypts**

To assess potential functional impact of dysbiosis upon epithelial replenishment, the proportion of proliferative cells per crypt were determined. Loop ileostomy-mediated defunctioning resulted in a decline in the percent of PCNA-positive IECs per crypt ( $38.1\% \pm 8.3\%$ ; Fig. 7) compared with that observed in the functional controls ( $61.8\% \pm 11.9\%$ ; Fig. 7). This represents an overall average reduction of  $23.7\% \pm 4\%$  ( $n = 5$ ,  $p = 0.01$ ), supporting evidence that microbial changes influence IEC proliferation. Furthermore, TUNEL staining revealed no difference in rates of apoptosis between the functional and defunctioned ileum (data not shown). This suggests that reduction in villous height is due to decreased proliferation of IEC



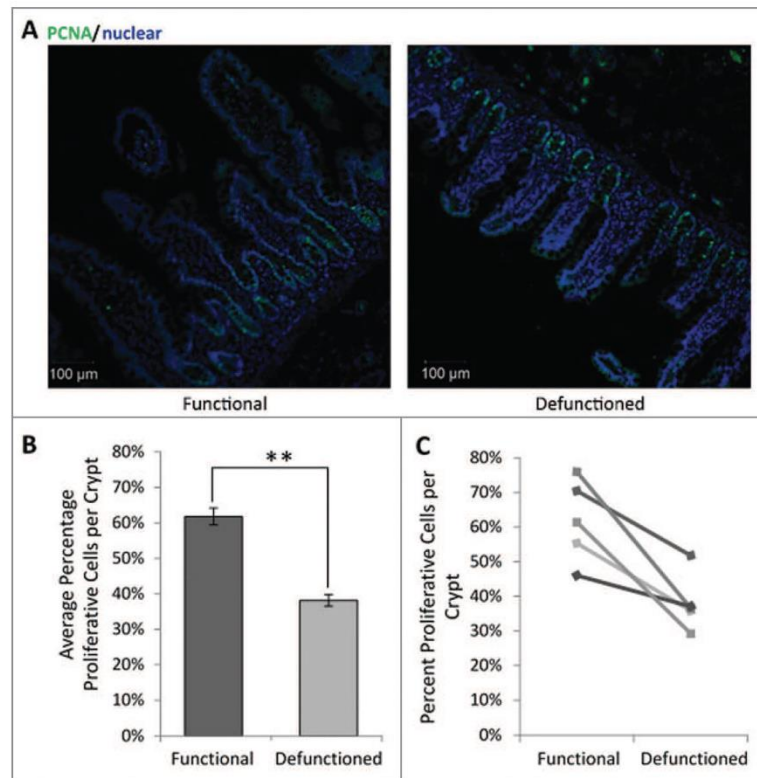


**Figure 7.** (A) Representative immunofluorescent PCNA labeling (green) to measure proliferation. All nucleated cells, counterstained using Hoechst 33342, are colored blue. Magnification 10x. (B) Average percent proliferating PCNA positive cells/crypt  $\pm$  SEM ( $n = 5$ ;  $p = 0.01$ ). (C) Paired percent PCNA-positive cells per crypt in the functional and defunctioned intestine.

rather than increased apoptosis, which may be due to the lack of pro-proliferative microbial signals.

### Discussion

Our study has demonstrated a strong relationship between loop ileostomy-mediated fecal stream diversion and profound alterations in the intestinal microbiota, termed dysbiosis. This may be a causative factor in the observed mucosal atrophy and consequent post-surgical complications. These results provide novel insights into the effect of loop ileostomy-associated enteral nutrient deprivation on the intestinal microbiota, which may underpin the substantial morbidity rate observed following loop ileostomy closure.

The data presented demonstrates substantial distortion of intestinal mucosal architecture following fecal stream diversion, with significant atrophy of villi in the defunctioned limb. This is consistent with

findings reported in previous animal and human studies.<sup>10,11</sup> Furthermore, a comprehensive morphological study of the defunctioned ileum reported several additional physiologic changes, including loss of smooth muscle area and reduced isometric contractility.<sup>11</sup> Such physiologic consequences of loop ileostomy-mediated defunctioning, have previously been suggested to occur as a direct result of cellular nutrient deprivation.<sup>31,32</sup> As a result, present clinical studies aiming to reduce post-surgical complications following loop ileostomy reversal have administered a 'feed' to the defunctioned ileum before surgery. The feed is composed of a saline solution and thickening agent which is used to improve cellular functionality before reinstating luminal flow, but offers no nutritional value.<sup>14</sup> This study demonstrates for the first time that loop ileostomy leads to microbial dysbiosis at both the phylum and genus level. In contrast to mucosal cells, which receive blood-borne

nutrition, gut microbes in the defunctioned ileum are nutritionally deprived. Considering the microflora, the feed used in Abrisqueta *et al.* 2014 provides no nutritional sustenance and is therefore unlikely to restore or support the patient's microbiome before reversal surgery.<sup>14</sup>

Profound dysbiosis was observed in the defunctioned ileum at the time of reversal. We report a significant reduction in total bacterial load in the defunctioned intestine, as determined by a reduction in 16S rRNA gene copy number, as well as broad shifts in microbiota composition between functional and defunctioned intestine. Of particular note, we found a significant loss of the predominant phylum Firmicutes, reported to be decreased in IBD and associated with obesity.<sup>33,34</sup> A concomitant increase in  $\gamma$ -Proteobacteria is observed in the defunctioned limb. Increases in this phylum have also been described in IBD.<sup>35</sup> Similar dysbiotic changes were observed in a study investigating the effects of TPN on the microbiota of human small intestine.<sup>36</sup> Interestingly, the study reports a correlation between duration of TPN use and increased severity of dysbiosis; participants fed with TPN either partially, or for less than 6 weeks, somewhat maintained microbial diversity compared with one participant given TPN for >2 months. Given that the downstream intestine in participants of this study remained defunctioned for an average of one year, it is unsurprising that we observed such profound dysbiosis.

The influence of the gut microbiota upon intestinal function should not be underestimated as the importance of both bacterial derived nutrients and direct microbial stimulation for maintaining intestinal replenishment and consequently health is well documented. For example, bacterial derived butyrate is a primary energy source for IECs and recognition of commensal microbes by epithelial TLR is known to be crucial for maintaining intestinal homeostasis.<sup>18,37</sup> Intestinal dysbiosis has been linked to the pathogenesis of numerous chronic diseases due to the induction of a proinflammatory state within the intestine.<sup>38-40</sup> Interestingly, we identified that there was no significant inflammation observed in the defunctioned ileum at the time of loop ileostomy reversal. We consider this finding linked to the reduction observed in total bacterial load following nutrient deprivation. The intestinal microbiome is sensitive to local nutritional fluctuations and extreme prolonged starvation in the defunctioned ileum

appears to rapidly deplete bacterial load. It is likely that an initial period of inflammation following ileostomy formation occurs, as evidenced by the fibrotic nature of intestinal tissue. Subsequently a state of 'dysbiotic equilibrium' is reached and mucosal homeostasis, be it at a compromised capacity, is reinstated preventing chronic inflammation. However, reanastomosis to reinstate luminal flow through the defunctioned intestine could restore bacterial load while maintaining dysbiosis therefore putting patients at risk of complications.

Blood tests, measuring CRP, Albumin and WBC are routinely used as predictors of post-surgical complications and clinical outcomes.<sup>41,42</sup> We report a substantial elevation in post-surgical CRP levels with a concomitant reduction in serum albumin in our patient cohort. Serum albumin levels decrease during an inflammatory response to surgery or infection as the liver shifts its production toward acute phase proteins. Elevated CRP is a natural part of the inflammatory response to surgery, but may also be raised in infection, and can be an indicator of anastomotic leak. Elevated CRP is possibly due to incompetent barrier function of the defunctioned bowel during the period following reanastomosis. In addition to mucosal atrophy, depletion of the microbiome is associated with altered intestinal permeability and activation of local immune/stromal cells.<sup>43</sup> It is plausible that dysbiosis-driven changes in the defunctioned limb following reversal surgery, contribute to an increased risk of developing post-surgical complications, such as small bowel obstruction or ileus. This should be investigated further to evaluate future clinical applications, for example through provision of nutritional support to the defunctioned limb. Patients did not receive any 'bowel preparation' before ileostomy reversal; such preparations may influence, particularly luminal, microbiota.

We have also demonstrated that ileostomy-associated defunctioning results in a reduction in IEC proliferation. Mice fed exclusively on TPN also demonstrated a reduction in IEC proliferation in a MyD88 dependent manner.<sup>23</sup> MyD88 knockout ( $^{-/-}$ ) mice presented normal levels of IEC proliferation irrespective of enteral nutrient deprivation, but wild-type TPN mice demonstrated a characteristic significant shift in microbial dominance from Firmicutes to Proteobacteria, consistent with our present findings.<sup>23</sup> Furthermore, physiologic preservation of epithelial

barrier function in MyD88<sup>-/-</sup> TPN fed mice was also reported, indicating minimal disruption to intestinal morphology, suggesting that host immunity has an impact upon the microflora composition.<sup>23</sup> Collectively, it is reasonable to conclude that the reduction we observed in IEC proliferation and resultant intestinal atrophy is highly likely to be a consequence of dysbiosis, via altered host-microbial interactions at the intestinal surface, rather than due to nutrient deprivation exclusively.

Collectively, these findings could support future feasibility studies to provide the defunctioned bowel with nutritional sustenance before reanastomosis, supporting microbiome restoration. Nutritional support, in the form of elemental diet, could be supplemented with prebiotics or fecal effluent from the functioning limb.

### Conclusion

Loop ileostomy reversal surgery is associated with substantial morbidity and post-surgical complications. We have shown that loop ileostomy-associated fecal stream diversion results in intestinal dysbiosis and likely influences the development of impaired intestinal function. We propose that novel therapeutics should focus on restoring the microflora to health to promote intestinal functionality and potentially further reduce postoperative complications.

### Disclosure of potential conflicts of interest

No potential conflicts of interest were disclosed.

### Acknowledgment

We thank Dr. Sheena Cruickshank and Maria Glymenaki at The University of Manchester for DGGE assistance; Dr. Lora Hooper at UT Southwestern Medical Center for use of TopoTA plasmid; Charlotte Pattison and Meghan Acres for assistance with sample processing.

### Funding

This work was supported by Bowel Cancer Research Grant, University Hospitals of Morecambe Bay SIFT and Medical Research Council NIRG (Rigby) G1100211/1.

### ORCID

Elisabeth J. Shaw  <http://orcid.org/0000-0002-5653-0145>  
Rachael J. Rigby  <http://orcid.org/0000-0002-6605-9609>

### References

- [1] Winslet MC, Drolc Z, Allan A, Keighley MR. Assessment of the defunctioning efficiency of the loop ileostomy. *Dis Colon Rectum* 1991; 34(8):699-703; PMID:1855427; <https://doi.org/10.1007/BF02050354>
- [2] Pemberton JH, Kelly KA, Beart RW Jr, Dozois RR, Wolff BG, Ilstrup DM. Ileal pouch-anal anastomosis for chronic ulcerative colitis. Long-term results. *Ann Surg* 1987; 206(4):504-13; PMID:3662660; <https://doi.org/10.1097/00000658-198710000-00011>
- [3] Chow A, Tilney HS, Paraskeva P, Jeyarajah S, Zacharakis E, Purkayastha S. The morbidity surrounding reversal of defunctioning Ileostomies: A systematic review of 48 studies including 6,107 cases. *Int J Colorectal Dis* 2009; 24(6):711-23; PMID:19221766; <https://doi.org/10.1007/s00384-009-0660-z>
- [4] van Westreenen HL, Visser A, Tanis PJ, Bemelman WA. Morbidity related to defunctioning Ileostomy closure after Ileal Pouch-Anal anastomosis and low colonic anastomosis. *Int J Colorectal Dis* 2012; 27(1):49-54; PMID:21761119; <https://doi.org/10.1007/s00384-011-1276-7>
- [5] El-Hussuna A, Lauritsen M, Bulow S. Relatively High Incidence of complications after loop Ileostomy reversal. *Dan Med J* 2012; 59(10):A4517
- [6] Musters GD, Atema JJ, van Westreenen HL, Buskens CJ, Bemelman WA, Tanis PJ. Ileostomy closure by colorectal surgeons results in less major morbidity: Results from an institutional change in practice and awareness. *Int J Colorectal Dis* 2016; 31(3):661-7; PMID:26732261; <https://doi.org/10.1007/s00384-015-2478-1>
- [7] D'Haeninck A, Wolthuis AM, Penninckx F, D'Hondt M, D'Hoore A. Morbidity after closure of a defunctioning loop Ileostomy. *Acta Chir Belg* 2011; 111(3):136-41; PMID:21780519; <https://doi.org/10.1080/00015458.2011.11680724>
- [8] Hasegawa H, Radley S, Morton DG, Keighley MR. Stapled versus sutured closure of loop Ileostomy: A randomized controlled trial. *Ann Surg* 2000; 231(2):202-4; PMID:10674611; <https://doi.org/10.1097/00000658-200002000-00008>
- [9] Bailey CM, Wheeler JM, Birks M, Farouk R. The incidence and causes of permanent stoma after anterior resection. *Colorectal Dis* 2003; 5(4):331-4; PMID:12814411; <https://doi.org/10.1046/j.1463-1318.4.s1.1.78.x>
- [10] Ekelund KM, Ekblad E. Structural, neuronal, and functional adaptive changes in atrophic rat Ileum. *Gut* 1999; 45(2):236-45; PMID:10403736; <https://doi.org/10.1136/gut.45.2.236>
- [11] Williams L, Armstrong MJ, Finan P, Sagar P, Burke D. The effect of faecal diversion on human Ileum. *Gut* 2007; 56(6):796-801; PMID:17229794; <https://doi.org/10.1136/gut.2006.102046>



- [12] Miedema BW, Kohler L, Smith CD, Phillips SF, Kelly KA. Preoperative perfusion of bypassed ileum does not improve postoperative function. *Dig Dis Sci* 1998; 43(2):429-35; PMID:9512141; <https://doi.org/10.1023/A:1018887212921>
- [13] Abrisqueta J, Abellan I, Frutos MD, Lujan J, Parrilla P. [Afferent loop stimulation prior to ileostomy closure]. *Cir Esp* 2013; 91(1):50-2; PMID:23153779; <https://doi.org/10.1016/j.ciresp.2012.09.002>
- [14] Abrisqueta J, Abellan I, Lujan J, Hernandez Q, Parrilla P. Stimulation of the efferent limb before ileostomy closure: A randomized clinical trial. *Dis Colon Rectum* 2014; 57(12):1391-6; PMID:25380005; <https://doi.org/10.1097/DCR.0000000000000237>
- [15] Round JL, Mazmanian SK. The gut microbiota shapes intestinal immune responses during health and disease. *Nat Rev Immunol* 2009; 9(5):313-23; PMID:19343057; <https://doi.org/10.1038/nri2515>
- [16] Perey DY, Good RA. Experimental arrest and induction of lymphoid development in intestinal lymphoepithelial tissues of rabbits. *Lab Invest* 1968; 18(1):15-26; PMID:4966916
- [17] Savage DC, Siegel JE, Snellen JE, Whitt DD. Transit Time of epithelial cells in the small intestines of germfree mice and Ex-germfree mice associated with indigenous microorganisms. *Appl Environ Microbiol* 1981; 42(6):996-1001; PMID:7198427
- [18] Rakoff-Nahoum S, Paglino J, Eslami-Varzaneh F, Edberg S, Medzhitov R. Recognition of commensal microflora by toll-like receptors is required for intestinal homeostasis. *Cell* 2004; 118(2):229-41; PMID:15260992; <https://doi.org/10.1016/j.cell.2004.07.002>
- [19] De La Cochetiere MF, Durand T, Lepage P, Bourreille A, Galniche JP, Dore J. Resilience of the dominant human fecal microbiota upon short-course antibiotic challenge. *J Clin Microbiol* 2005; 43(11):5888-92
- [20] Gronlund MM, Lehtonen OP, Eerola E, Kero P. Fecal microflora in healthy infants born by different methods of delivery: permanent changes in intestinal flora after cesarean delivery. *J Pediatr Gastroenterol Nutr* 1999; 28(1):19-25; PMID:9890463; <https://doi.org/10.1097/00005176-199901000-00007>
- [21] De Filippo C, Cavalieri D, Di Paola M, Ramazzotti M, Poullet JB, Massart S, Collini S, Pieraccini G, Lionetti P. Impact of Diet in shaping gut microbiota revealed by a comparative study in children from Europe and rural Africa. *Proc Natl Acad Sci U S A* 2010; 107(33):14691-6; PMID:20679230; <https://doi.org/10.1073/pnas.1005963107>
- [22] Graf D, Di Cagno R, Fak F, Flint HJ, Nyman M, Saarela M, Watzl B. Contribution of diet to the composition of the human gut microbiota. *Microb Ecol Health Dis* 2015; 26:26164; PMID:25656825
- [23] Miyasaka EA, Feng Y, Poroyko V, Falkowski NR, Erb-Downward J, Gilliland MG 3rd, Mason KL, Huffnagle GB, Teitelbaum DH. Total parenteral nutrition-associated lamina propria inflammation in mice is mediated by a Myd88-dependent mechanism. *J Immunol* 2013; 190(12):6607-15; PMID:23667106; <https://doi.org/10.4049/jimmunol.1201746>
- [24] Feng Y, Teitelbaum DH. epidermal growth factor/Tnf-Alpha transactivation modulates epithelial cell proliferation and apoptosis in a mouse model of parenteral nutrition. *Am J Physiol Gastrointest Liver Physiol* 2012; 302(2):G236-49; PMID:22075779; <https://doi.org/10.1152/ajpgi.00142.2011>
- [25] Schneider CA, Rasband WS, Eliceiri KW. NIH image to ImageJ: 25 Years of image analysis. *Nat Methods* 2012; 9(7):671-5; PMID:22930834; <https://doi.org/10.1038/nmeth.2089>
- [26] Rath HC, Herfarth HH, Ikeda JS, Grenther WB, Hamm TE Jr, Balish E, Taugo JD, Hammer RE, Wilson KH, et al. Normal luminal bacteria, especially bacteroides species, mediate chronic colitis, gastritis, and arthritis in Hla-B27/Human Beta2 microglobulin transgenic rats. *J Clin Invest* 1996; 98(4):945-53; PMID:8770866; <https://doi.org/10.1172/JCI118878>
- [27] Muyzer G, de Waal EC, Uitterlinden AG. Profiling of complex microbial populations by denaturing gradient gel electrophoresis analysis of polymerase chain reaction-amplified genes coding for 16S rRNA. *Appl Environ Microbiol* 1993; 59(3):695-700; PMID:7683183
- [28] Livak KJ, Schmittgen TD. Analysis of relative gene expression data using real-time quantitative PCR and the 2<sup>-Delta Delta C(T)</sup> method. *Methods* 2001; 25(4):402-8; <https://doi.org/10.1006/meth.2001.1262>
- [29] Hartman AL, Lough DM, Barupal DK, Fiehn O, Fishbein T, Zasloff M, Eisen JA. Human gut microbiome adopts an alternative state following small bowel transplantation. *Proc Natl Acad Sci U S A* 2009; 106(40):17187-92; PMID:19805153; <https://doi.org/10.1073/pnas.0904847106>
- [30] Berg RD. The indigenous gastrointestinal microflora. *Trends Microbiol* 1996; 4(11):430-5; PMID:8950812; [https://doi.org/10.1016/0966-842X\(96\)10057-3](https://doi.org/10.1016/0966-842X(96)10057-3)
- [31] Altmann GG. Influence of bile and pancreatic secretions on the size of the intestinal villi in the Rat. *Am J Anat* 1971; 132(2):167-77; PMID:5112467; <https://doi.org/10.1002/aja.1001320204>
- [32] Keren DF, Elliott HL, Brown GD, Yardley JH. Atrophy of villi with hypertrophy and hyperplasia of paneth cells in isolated (Thiry-Vella) ileal loops in Rabbits. light-microscopic studies. *Gastroenterology* 1975; 68(1):83-93
- [33] Sokol H, Pigneur B, Watterlot L, Lakhdari O, Bermudez-Humaran LG, Gratadoux JJ, Blugeon S, Bridonneau C, Furet JP, et al. Faecalibacterium prausnitzii is an anti-inflammatory commensal bacterium identified by gut microbiota analysis of Crohn disease patients. *Proc Natl Acad Sci U S A* 2008; 105(43):16731-6; PMID:18936492; <https://doi.org/10.1073/pnas.0804812105>
- [34] Backhed F, Ding H, Wang T, Hooper LV, Koh GY, Nagy A, Semenkovich CF, Gordon JL. The gut microbiota as an environmental factor that regulates fat storage. *Proc Natl*

- Acad Sci U S A 2004; 101(44):15718-23; PMID:15505215; <https://doi.org/10.1073/pnas.0407076101>
- [35] Baumgart M, Dogan B, Rishniw M, Weitzman G, Bosworth B, Yantiss R, Orsi RH, Wiedmann M, McDonough P, et al. Culture independent analysis of Ileal mucosa reveals a selective increase in invasive escherichia coli of novel phylogeny relative to depletion of clostridiales in crohn's disease involving the Ileum. *Isme J* 2007; 1(5):403-18; PMID:18043660; <https://doi.org/10.1038/ismej.2007.52>
- [36] Ralls MW, Miyasaka E, Teitelbaum DH. Intestinal microbial diversity and perioperative complications. *JPEN J Parenter Enteral Nutr* 2014; 38(3):392-9; PMID:23636012; <https://doi.org/10.1177/0148607113486482>
- [37] Csordas A. Butyrate, aspirin and colorectal cancer. *Eur J Cancer Prev* 1996; 5(4):221-31; PMID:8894559; <https://doi.org/10.1097/00008469-199608000-00002>
- [38] Walker AW, Sanderson JD, Churcher C, Parkes GC, Hudspith BN, Rayment N, Brostoff J, Parkhill J, Dougan G, et al. High-throughput clone library analysis of the mucosa-associated microbiota reveals dysbiosis and differences between inflamed and non-inflamed regions of the intestine in inflammatory bowel disease. *BMC Microbiol* 2011; 11:7; PMID:21219646; <https://doi.org/10.1186/1471-2180-11-7>
- [39] Sobhani I, Tap J, Roudot-Thoraval F, Roperch JP, Letulle S, Langella P, Corthier G, Tran Van Nhieu J, Furet JP. Microbial dysbiosis in colorectal cancer (Crc) patients. *PLoS One* 2011; 6(1):e16393; PMID:21297998; <https://doi.org/10.1371/journal.pone.0016393>
- [40] Jiang W, Wu N, Wang X, Chi Y, Zhang Y, Qiu X, Hu Y, Li J, Liu Y. Dysbiosis gut microbiota associated with inflammation and impaired mucosal immune function in intestine of humans with non-alcoholic fatty liver disease. *Sci Rep* 2015; 5:8096; PMID:25644696; <https://doi.org/10.1038/srep08096>
- [41] Ortega-Deballon P, Radais F, Facy O, d'Athis P, Masson D, Charles PE, Cheynel N, Favre JP, Rat P. C-Reactive Protein Is an Early Predictor of Septic Complications after Elective Colorectal Surgery. *World J Surg* 2010; 34(4):808-14; PMID:20049435; <https://doi.org/10.1007/s00268-009-0367-x>
- [42] Hubner M, Mantziari S, Demartines N, Pralong F, Coti-Bertrand P, Schafer M. Postoperative albumin drop is a marker for surgical stress and a predictor for clinical outcome: A pilot study. *Gastroenterol Res Pract* 2016; 2016:8743187; PMID:26880899; <https://doi.org/10.1155/2016/8743187>
- [43] Cani PD, Possemiers S, Van de Wiele T, Guiot Y, Everard A, Rottier O, Geurts L, Naslain D, Neyrinck A, et al. Changes in gut microbiota control inflammation in obese mice through a mechanism involving Glp-2-driven improvement of gut permeability. *Gut* 2009; 58(8):1091-103; PMID:19240062; <https://doi.org/10.1136/gut.2008.165886>



# Appendices

## Appendix 1 - Surgical Study Clinical Documentation

### Participant Consent Form



Trust Headquarters  
Royal Preston Hospital,  
Sharoe Green Lane,  
Fulwood, Preston,  
Lancashire,  
PR2 9HT

Tel: 01772 716565

Web: <http://www.lancsteachinghospitals.nhs.uk/>

Centre Number:

Study Number:

Patient Identification Number for this study:

## Consent Form

Version 1 – 29/08/13

**Improving the outcome of stoma reversal surgery.**

**Name of Researchers: Mr Arnab Bhowmick, Mr Nigel Scott, Dr Andrew Stagg and Dr Rachael Rigby**

*Please initial the boxes [ ]*

• I confirm that I have read and understood the information sheet dated [29/08/13] for the above study. [ ]

• I have had the opportunity to consider the information and ask any questions I may have related to the study. [ ]

• I understand that I am under no obligation to participate in this study and that I am able to withdraw my data, without reason, for up to 2 weeks following participation. [ ]

• I understand that the researchers will hold all information and data collected securely and in confidence and that all efforts will be made to ensure that I cannot be identified as a participant in the study (except as might be required by law) and I give permission for the researchers to hold relevant personal data where relevant to my taking part in this research. [ ]

• I agree to take part in the above study. [ ]

**Name of Participant**                      **Signature**                      **Date**

**Name of person taking consent**    **Signature**                      **Date**

When completed: 1 copy for the subject; 1 copy for the researcher site file; original to be kept in medical notes

## Patient Information Sheet



Lancashire Teaching Hospitals **NHS**  
NHS Foundation Trust

**Trust Headquarters**  
Royal Preston Hospital,  
Sharoe Green Lane,  
Fulwood, Preston,  
Lancashire,  
PR2 9HT

Tel: 01772 716565  
Web: <http://www.lancsteachinghospitals.nhs.uk/>

## Patient Information Sheet Version 1 – 29/08/13

### Part 1

#### *Study title.*

Improving the outcome of stoma reversal surgery.

#### *Invitation to participate in the study.*

We would like to invite you to take part in our research study. Before you decide we would like you to understand why the research is being done and what it would involve. Please take time to read the following information carefully, and talk to others about the study, if you wish. Ask one of our team if there is anything that is not clear, or if you would like more information before deciding whether or not you wish to take part.

#### *What is the purpose of the study?*

Following surgical removal of diseased bowel, patients often require a temporary redirection of bowel contents to a stoma to allow healing prior to re-joining of the remaining bowel at a later date. The section of bowel that is 'non-functioning' undergoes muscle-wasting, due to lack of nutrition and stimulation and can become inflamed and scarred. Some patients may experience complications either during or after reversal surgery and it remains unclear how much of this may be due to these changes in the under-nourished and inactive bowel. This research aims to investigate ways to improve the health of the "non-functioning" bowel, reduce complications and thus possibly reduce the recovery time from bowel surgery.

#### *Why have I been invited?*

You have been invited to take part in the study because you are undergoing ileostomy reversal surgery at Royal Preston Hospital.

*Do I have to take part?*

Taking part is entirely voluntary and is up to you to decide whether or not you wish to join the study. If you agree to take part you will keep this information sheet and be invited to ask any questions, we will then ask you to sign a consent form. You are free to withdraw from the study up to 2 weeks following participation, without giving a reason. Any decision to not take part or withdraw from the study, will not affect the medical care you receive.

*What will happen to me if I take part?*

If you agree to take part, you will be asked to sign the consent form. Following this, any intestinal tissue that the surgeons will remove during your operation may be kept for research purposes. No extra tissue will be removed for this purpose as the surgeons always remove a margin of tissue from both sides of the bowel which were previously connected to your stoma. Neither you nor your doctors will receive a result from this tissue sample as it is purely for research purposes. The samples will not be used for any financial gain and will be treated as a gift from you to us, effectively belonging to Lancashire Teaching Hospitals NHS Foundation Trust. This procedure will not affect the standard diagnosis, treatment and management of your condition which will continue as normal. Patient information collected in connection with the study will be stored in a secure facility only accessible to the researchers involved.

*What will I have to do?*

If you agree to take part in the study, you will be asked to sign the consent form and any tissue that is removed, as part of your normal surgery, may be kept for research purposes.

*What are the possible risks and disadvantages of taking part?*

There are no additional risks associated with taking part in this research as the tissue being removed is always removed, but is usually discarded by the surgeons.

*What are the possible benefits of taking part?*

There is no immediate benefit to you taking part in this study. The information we get from this study will provide further insight into the changes that take place in the bowel when no food passes through it and may help improve treatment, ileostomy management and reversal in the future.

*What happens when the research study stops?*

The tissue samples may be stored and remain available for future authorised scientific studies.

*What if there is a problem?*

Any complaint about the way you have been dealt with during the study or any possible harm you might suffer will be addressed. The detailed information on this is given in Part 2.

*Will my taking part in the study be kept confidential?*

Yes, we will follow ethical and legal practice and all information about you will be handled in confidence. The details are included in Part 2.

If the information in Part 1 has interested you and you are considering participation, please read the additional information in Part 2 before making any decision.





*What will happen to the results of the research study?*

The results of the scientific study will be published in international medical journals and presented at scientific/ medical conferences. You will not be identified in any reports or publications.

*Who is organising and funding the research?*

This study is being organised by Dr Rachael Rigby, at Lancaster University, in collaboration with other researchers at Queen Mary's University London and consultants from Royal Preston Hospital. This study is supported by a Bowel Cancer Research Grant.

*Who has reviewed the study?*

All research in the NHS is looked at by an independent group of people, called a Research Ethics Committee (REC) to protect your interests. This study has been reviewed and approved by the North West Research Ethics Committee.

*Contact for further information.*

If you would like further information about this biological research study, or have any questions concerning it, please contact the study team:

Chief Investigator: Dr Rachael Rigby, Lecturer in Biomedicine, Faculty of Health & Medicine, Division of Biomedical & Life Sciences, University of Lancaster, Lancaster.  
Telephone: 01524 593420

Trial Co-ordinator (Research Nurse):

Medical Team at Royal Preston Hospital:

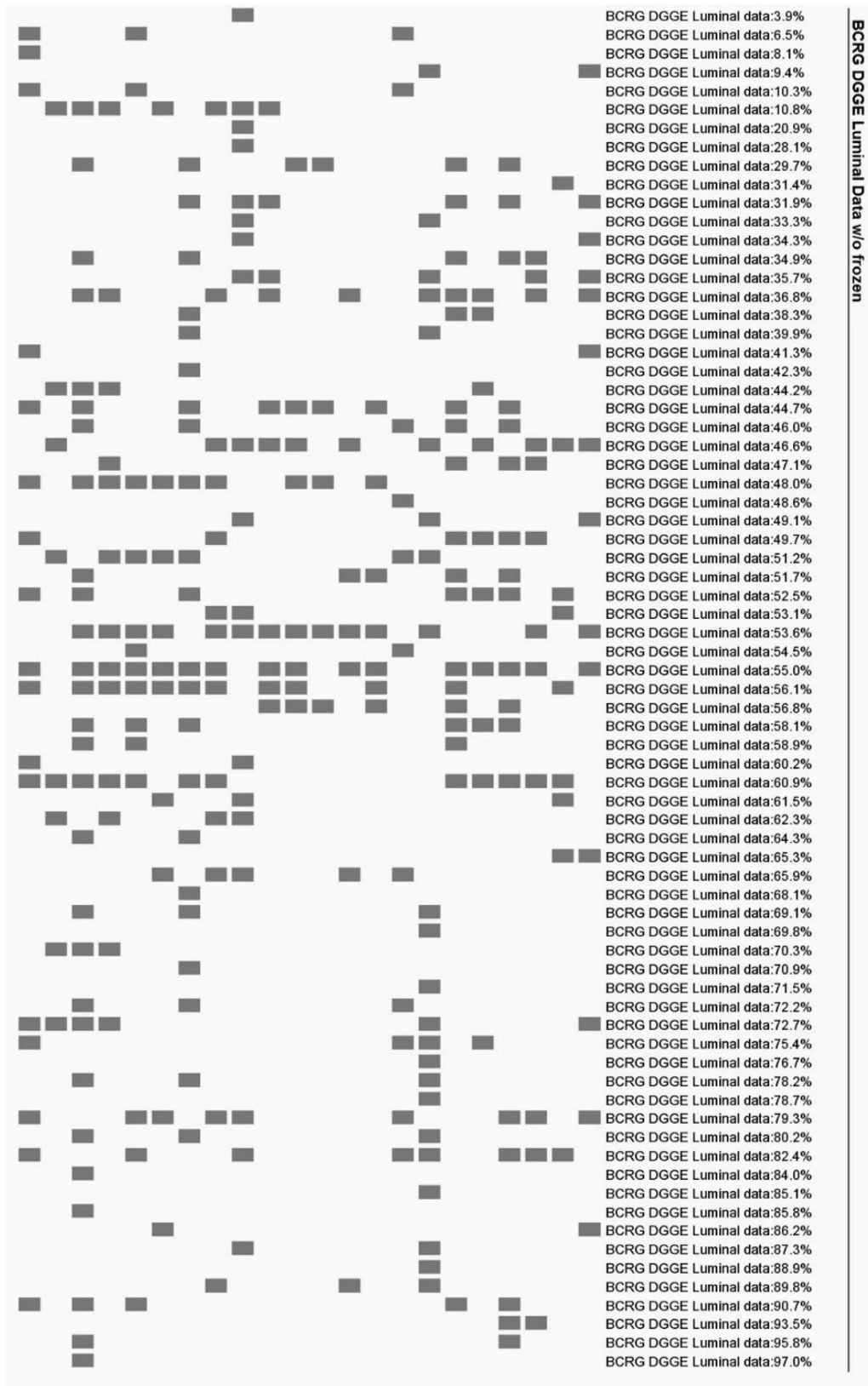
Mr Arnab Bhowmick, Consultant General/Colorectal Surgeon. Telephone: 01772 522372  
(ext2372)

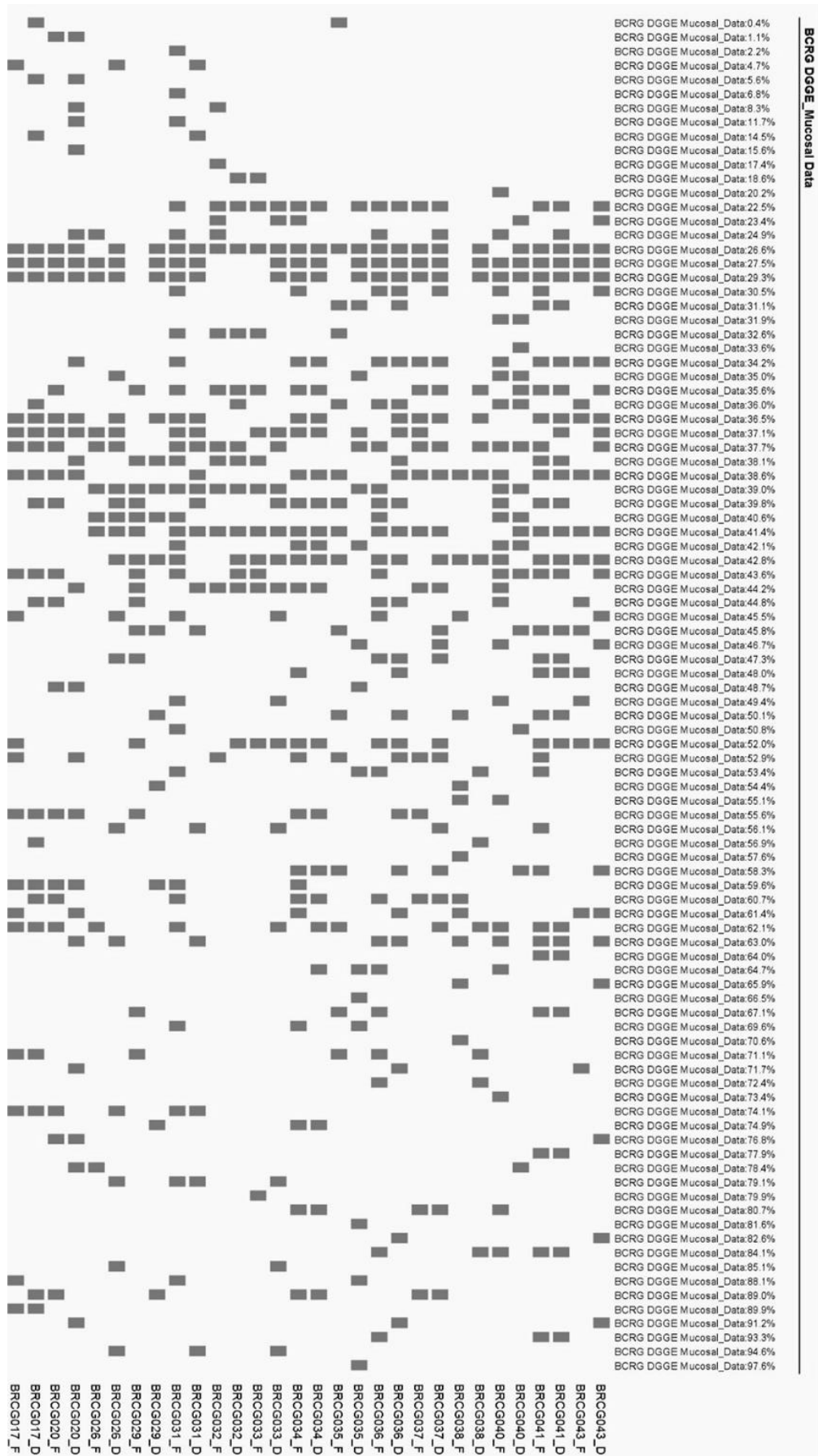
Mr Nigel Scott, Consultant General/Colorectal Surgeon.

**Thank you for reading this, and for your interest in this research study.**

If you wish to take part in the study, please sign the consent form. Whether or not you decide to take part, you may keep this information sheet for future reference.

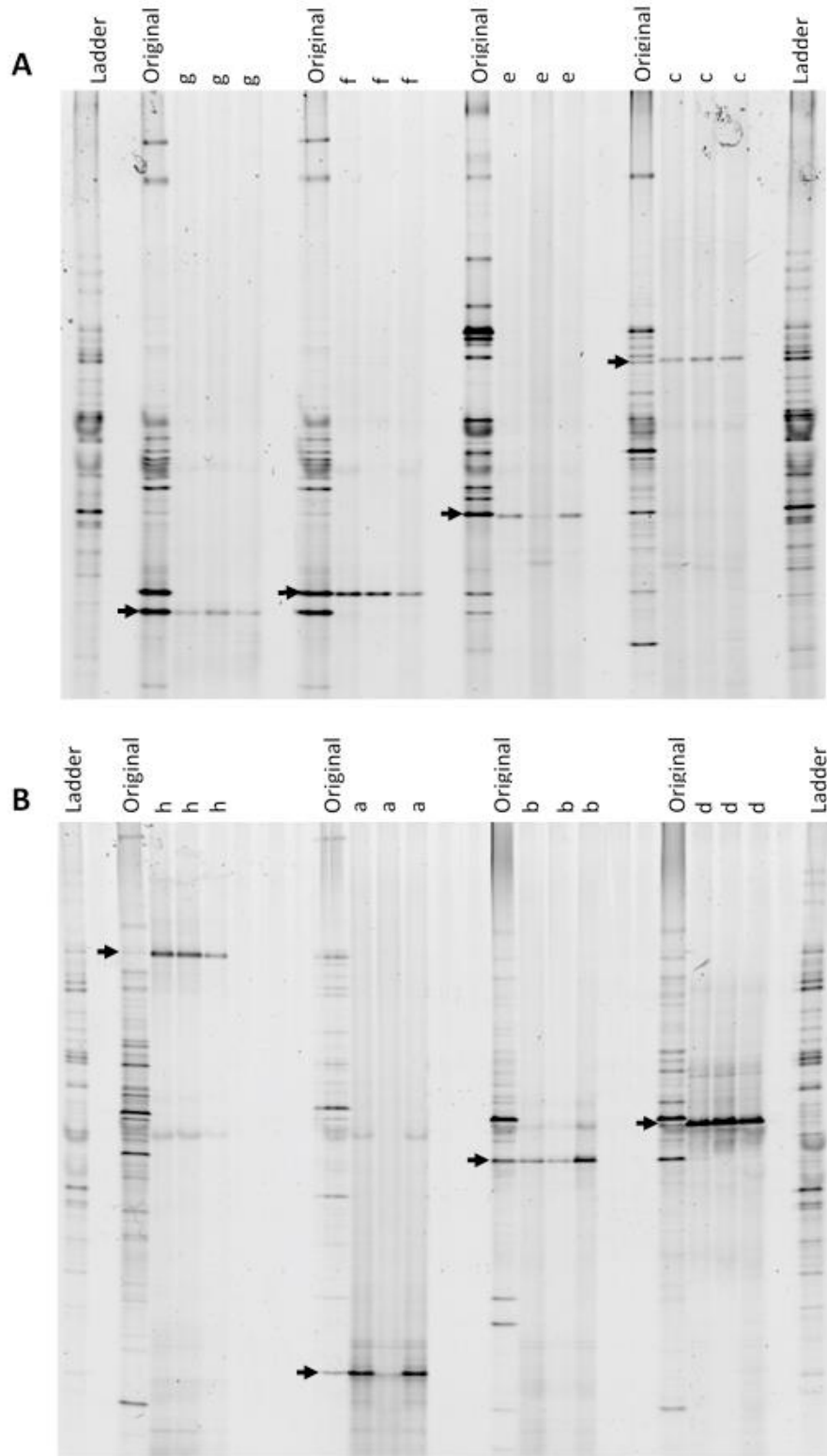
## Appendix 2 - Binary DGGE Banding Profiles of Luminal and Mucosal-associated Microbiota





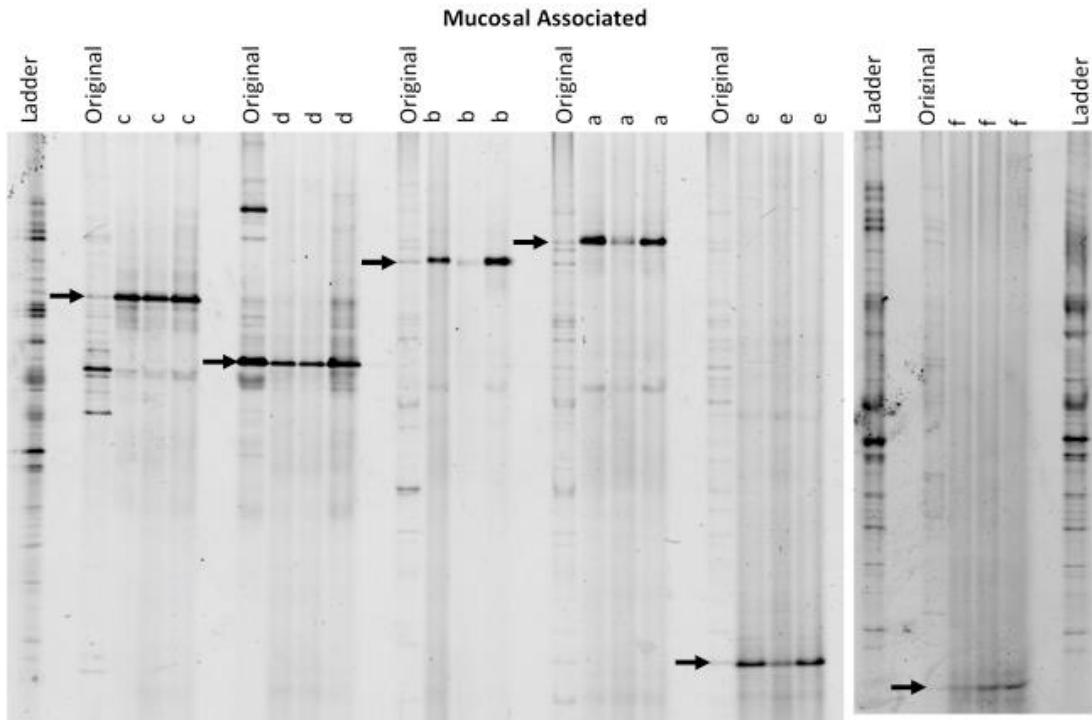


**Appendix 3 - Mucosal and Luminal DGGE band extraction and purification**



**Luminal band class extraction.** DGGE to confirm selection and purity of luminal-associated amplicons later sequenced. Band classes (A) f, g, e and c (B) h, a, b and d ran adjacent to corresponding original sample. Arrows indicate location of band class within original sample.

Data published Supplementary Information of (Beamish et al., 2017)



**Mucosal band class extraction.** DGGE to confirm selection and purity of mucosal-associated amplicons later sequenced. Band classes (A) c, d, b, a and e (B) f, ran adjacent to corresponding original sample. Arrows indicate location of band class within original sample.

#### **Appendix 4 - DGGE Band Class Consensus Sequences and Taxonomic Assignments for Optimisation Experiment, Mucosal and Luminal Microbiota Profiles.**

##### Consensus Sequences:

Selected bands are presented in Chapter 3, figure 3.3.

Band 1:

NNNNGGGAATCTTNNNGCAATGGACGAAAGNCTGACCNNAGCAACGCCGCGTGAGTGANGAAG  
GNTTTCGGATCGNAAAACCTCTGTTGTTANAGNNNAACANGGACGTTNNTAACTGANCGTCCCCTG  
ACGGTATCTAACCANAAAGCCACGG

Band 2:

GGGGAATATTGCACAATGGGCGCAAGCCTGATGCAGCGACGCCGCGTGCGGGATGGAGGCCTTCG  
GGTTGTAAACCGCTTTTGTTCAGGGCAAGGCACGTTTTCGGCCGTGTTGAGTGAT

Band 3:

GAGGAATATTGGTCAATGGGCGCTAGCCTGAACCAGCCAAGTAGCGTGAAGGATGAAGGCTCTAT  
GGGTCGTAAACTTCTTTATATAAGAATAAAGTGCAGTATGTATACTGTTTTGTATGTATTATATGAA  
TAAGGATCGGCTAACTCCGTGCCAGCAGCCGCGGTAATA

Band 4:

GGGAATCTTCGGCAATGGACGAAAGTCTGACCGAGCAACGCCGCGTGAGTGAAGAAGGTTTTTCGG  
ATCGTAAAACCTCTGTTGTTAGAGAAGAACAAGGACGTTAGTAACTGAACGTCCCCTGACGGTATCT  
AACCAGAA

Band 5:

CCTTCGGGTTGTAAAGTACTTTTCGACGGGGAGGAAGGGAGTCAAGTTAATACCTTTGCTCATTGAC  
GTTACCCGCACAAAAAGCACCGGCTAACTCCGTGCCAGCAGCCGCGGTAATA

Band 6:

GGGGAATATTGCACAATGGGCGCAAGCCTGATGCAGCCATGCCGCGTGTATGAAGAAGGCCTTCG  
GGTTGTAAAGTACTTTTCGACGGGGAGGAAGGGAGTCAAGTTAATACCTTTGCTCATTGACG

Band 7:

GGGGAATATTGCACAATGGGCGCAAGCCTGATGCAGCCATGCCGCGTGTATGAAGAAGGCCTTCG  
GGTTGTAAAGTACTTTTCAGCGGGGAGGAAGGGAGTAAAGTTA

Band 8:

GGGGAATATTGCACAATGGGCGCAAGCCTGATGCAGCCATGCCGCGTGTATGAAGAAGGCCTTCG  
GGTTGTAAAGTACTTTTCAGCGGGGAGGAAGGGAGTAAAGTTAATAC

Band 9:

GGGAATATTGCACAATGGGCGAAAGCCTGATGCAGCAACGCCGCGTGAGCGATGAAGGCCTTCGG  
GTCGTAAAGCTCTGTCCTCAAGGAAGATAATGACGGTACTTGAGGAG

Band 10:

GGGGAATATTGCACAATGGGGGAAACCCTGATGCAGCAACGCCGCGTGAGTGATGACGGCCTTCG  
GGTTGTAAAGCTCTGTCTTCAGGGACGATAATGACGGTACCTGAGGAGG

Consensus sequence Taxonomic Assignment:

Band Class	Assignment	Max Score	Query Cover	E Value	Accession
1	'No significant similarity found'	-	-	-	-
2	Uncultured <i>Bifidobacterium</i>	313	100%	1e-81	LT 858997.1
3	<i>Bacteroides fragilis</i>	318	100%	2e-83	LT692011.1
4	<i>Enterococcus faecalis</i>	257	100%	4e-65	CP022712.1
5	<i>Escherichia coli</i>	202	100%	2e-48	JX183942.1
6	Uncultured <i>Escherichia sp.</i>	222	100%	1e-54	GU132156.2
7	<i>Escherichia coli</i>	198	100%	2e-47	LT906474.1
8	<i>Escherichia coli</i>	206	100%	1e-49	LT906474.1
9	<i>Paraclostridium benzoelyticum</i>	207	100%	3e-50	NR 148815.1
10	Uncultured <i>Clostridium sp.</i>	281	100%	3e-72	LT625904.1

Luminal-associated Microbiota Consensus Sequences:

Band classes are presented in Chapter 3, figure 3.6.

Band Class a:

CTACGGGAGGCAGCAGTGAGGAATTTTGGTCAATGGGGGACCACTTGAACCAGCCAAGTAGCGTG  
AAGGATGACTGCCCTATGGGTTGTAAACTTCTTTTATAAAGGAATAAAGTCGGGTATGCATACCCGT  
TTGCATGTACTTTATGAATAAGGATC

Band Class b:

TACGCGTGCCATGGAAGCAGGCACCAGAGCCCCTGCCAGGTAATTAGAAAGATGACGGGATTAT  
GGGGGTATACTTCTTTTATAAAGGAATAAAGTCGGGTATGTATACCCGTTTGCATGTACTTTATGA  
ATAAGGATCGGCTAACTCCGTGCCAGCAGCCGCGGTAA

Band Class c:

GCAATGGGGGCAACCCTGACCGAGCAACGCCGCGTGAGTGAAGAAGGTTTTCGGATCGTAAAGCT  
CTGTTGTAAGTCAAGAACGAGTGTGAGAGTGAAAGTTCACACTGTGACGGTAGCTTACCAGA

Band Class d:

AGCAGTAGGGAATCTTTGGCAATGGACGGAAGTCTGACCGAGCAACGCCGCGTGAGTGAAGAAG  
GTTTTCGGATCGTAAAGCTCTGTTGTAAAGAGAAGAACGAGTGTGAGAGTGAAAGTTCACACTGT  
GACGGTAACTTACCAGAAAGGG

Band Class e:

CGGGAGGCAGCAGTGGGGAATCTTGACAATGGGGAAAAGCCTGATGCAGCGATGCCGCGTGAG  
TGATGAAGGCCTTCGGGTTGTAAAGCTCTTTCAGCGGGGAAGAAAAGAGTAAAGTTAATACCTTG  
CTCATTGACGGTACTTGACTAGGAA

Band Class f:

ATATTGACAATGGGGGAAACCCTGATGCAGCAACGCCGCGTGAGTGATGACGGCCTTCGGGTTG  
TAAAGCTCTGTCTTCAGGGACGATAATGACGGTACCTGAGGAGGAAGCCACGGCT

Band Class g:

GTGGGGAATATTGACAATGGGCGAAAGCCTGATGCAGCAACGCCGCGTGAGCGATGAAGGCCTT  
CGGGTCGTAAAGCTCTGTCTCAAGGAAGATAATGACGGTACTTGAGGAG

Band Class h:

GGAATACTCGAAAGACAGGCTGTGTGGAAACCCAGCAGAGAGGAGGTGCTGTGTGAAGTCTGTGC  
CAGTAGCCGCGTAATAAAATTATATCGGTGAAGAACTCTGGTCTGCGGGGTCAGTTGACGGTAG  
CCGAGGAATAAGCACCGGCTAACTCCGTGCCAGCAGCCGCGGTAATA

Luminal-associated Microbiota Taxonomic Assignment:

Band Class	Assignment	Max Score	Query Cover	E Value	Accession	Assigned Genus ID
a	<i>Bacteroides dorei</i>	259	100%	3e-69	NR 041351.1	Bacteroides
b	<i>Bacteroides vulgatus</i>	178	72%	8e-45	NR 074515.1	Bacteroides
c	<i>Streptococcus vestibularis</i>	237	100%	9e-63	NR 042777.1	Streptococci
d	<i>Streptococcus oligofermentans</i>	268	100%	4e-72	NR 103943.1	Streptococci
e	<i>Shigella sonnei</i>	189	92%	3e-48	NR 104826.1	Shigella
f	<i>Clostridium aurantibutyricum</i>	222	100%	2e-58	NR 044841.2	Clostridia
g	<i>Clostridium ghonii</i>	213	100%	1e-55	NR 119036.1	Clostridia
h	<i>Spirosoma endophyticum</i>	134	92%	2e-31	NR 135723.1	Spirosoma

Mucosal-associated Microbiota Consensus Sequences:

Band classes are presented in Chapter 3, figure 3.11.

Band Class a:

CATAAATTAATATCCTACTGAATGCCCTATGGGATGTAACTTCTTTTATAAGGGAATAAAGTGGAG  
TATGCATACTCCTTTCATGTACCGTATGAATAAGGATCGGCTAACTCCGTGCCAGCAGCCGCGGTA  
ATAA

Band Class b: Sequence quality not suitable.

Band Class c:

TACGGGAGGCAGCAGTAGGGAATCTCCGCAATGGGCGAAAGCCTGACGGAGCAACGCCGCGTG  
AGTGAAGAAGGATTTTCGGTTCGTAAAGCTCTGTTGTTAGGGAAGAATGATTGTGTAGTAACTATAC  
ACAGTAGAGACGGTACCTAACCAGAAAGCC

Band Class d:

GGAGGCAGCAGTAGGGAATCTTCGGCAATGGACGAAAGTCTGACCGAGCAACGCCGCGTGAGTG  
AAGAAGGTTTTTCGGATCGTAAACTCTGTTGTTAGAGAAGAACAAGGACGTTAGTAACTGAACGTC  
CCCTGACGGTATCTAACCAGAAAGCCACGGCTAACTACGTGCCAGCAGCC

Band Class e: Sequence quality not suitable.

Band Class f: Sequence quality not suitable.

Mucosal-associated Microbiota Taxonomic Assignment:

Band Class	Assignment	Max Score	Query Cover	E Value	Accession	Assigned Genus ID
a	<i>Bacteroides eggerthi</i>	198	86%	5e-51	NR 112935.1	Bacteroides
c	<i>Gemella taiwanensis</i>	296	100%	2e-80	NR 133753.1	Gemella
d	<i>Enterococcus faecalis</i>	333	100%	2e-91	NR 113901.1	Enterococcus

## Appendix 5 - pCR®2.1-TOPO® Plasmid Standard Curve Calculations

**Step 1** – Mass of single recombinant plasmid calculation

$$m = (n) \left( \frac{1 \text{ mole}}{6.023e23 \text{ molecules (bp)}} \right) \left( \frac{660g}{\text{mole}} \right)$$

$$m = (n) \left( \frac{1.096e^{-21}g}{bp} \right)$$

$$m = (4057bp) \left( \frac{1.096e^{-21}g}{bp} \right)$$

$$m = 4.447e^{-18}g$$

**Where:** *n* = Plasmid + insert size (bp), *m* = mass, **Avogadros number** = 6.023e23 molecules / 1 mole, **Average MW of a double-stranded DNA molecule** = 660 g/mole.

**Step 2** – Mass of plasmid copy number of interest calculation

Typical bacterial abundances within the small intestine are  $3 \times 10^9$ .

Copy # of interest x mass of single plasmid = mass of plasmid DNA required

$$(3 \times 10^9) \times (4.447 \times 10^{-18}) = 1.33 \times 10^8$$

**Step 3** – Plasmid Standard Curve Dilutions:

$$C_1V_1 = C_2V_2$$

See table for  $C_1$ ,  $V_1$ ,  $C_2$ ,  $V_2$  values.

Initial Concentration of plasmid DNA ( $C_1$ ) was determined using a NanoDrop™ 2000c Spectrophotometer (Thermo-Fisher).

$$(1.19 \times 10^7)(V_1) = (3 \times 10^9)(100\mu\text{L})$$

$$V_1 = 11.3 \mu\text{L}$$

Dilution #	Plasmid DNA Source	Initial Conc. (g/ $\mu$ L) <b>C<sub>1</sub></b>	Vol of plasmid DNA ( $\mu$ L) <b>V<sub>1</sub></b>	Volume of PCR H <sub>2</sub> O ( $\mu$ L)	Final Volume ( $\mu$ L) <b>V<sub>2</sub></b>	Final conc. in (g/ $\mu$ l) <b>C<sub>2</sub></b>	Resulting copy #
1	Stock	1.19E-07	11.3	88.7	100	1.34E-08	3.00E+09
2	D1	1.34118E-08	10	90	100	1.34E-09	3.00E+08
3	D2	1.34118E-09	10	90	100	1.34E-10	3.00E+07
4	D3	1.34118E-10	10	90	100	1.34E-11	3.00E+06
5	D4	1.33394E-11	10	90	100	1.33E-12	3.00E+05
6	D5	1.34118E-12	10	90	100	1.34E-13	3.00E+04
7	D6	1.34118E-13	10	90	100	1.34E-14	3.00E+03
8	D7	1.34118E-14	10	90	100	1.34E-15	3.00E+02

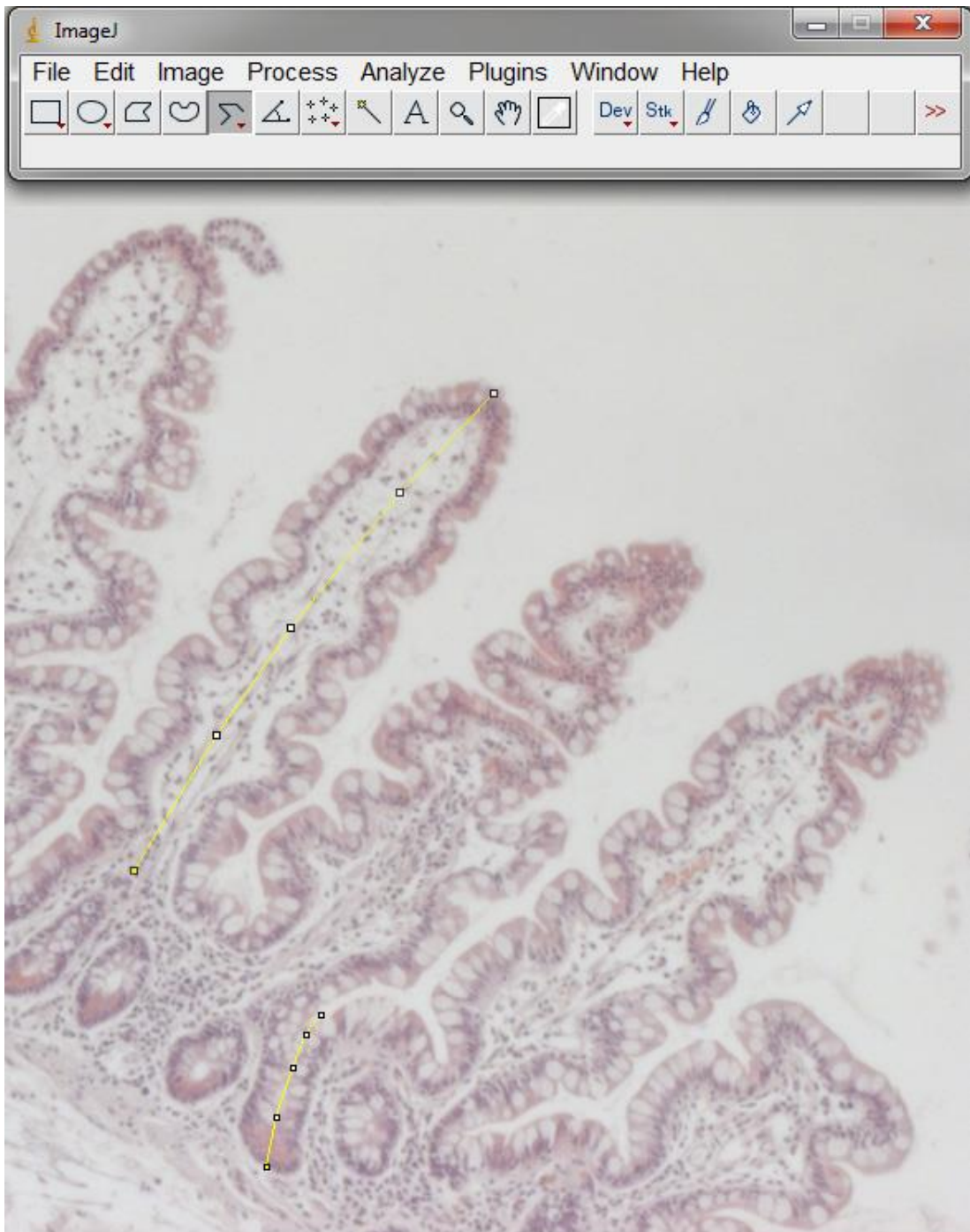
Dilutions 1 – 5 were selected for standard curve construction in 16S rDNA qRT-PCR detailed in section 2.2.10.7.



## Appendix 6 - Measurement of Villous Height and Crypt Depth using ImageJ Software.

Tool: Segmented Line

Analyze: Measure (Pixels)



**Appendix 7 - Endoscopy Study Clinical Documentation**

Participant Consent Form - Furness General Hospital



Westmorland General Hospital  
Burton Road  
Kendal  
LA9 7RG

Tel: 01539 716621

Centre Number:

Study Number:

Patient Identification Number for this study:

**Consent Form**

**Version 4 - 24/02/16**

**Identification of bacterial 'signatures' characteristic of intestinal disease**

**Name of Researchers: Dr Albert Davies, Emma Beamish and Dr Rachael Rigby**

*Please initial the boxes [ ]*

- I confirm that I have read and understood the information sheet dated 24/02/16 for the above study. [ ]
- I have had the opportunity to consider the information and ask any questions I may have related to the study. [ ]
- I understand that I am under no obligation to participate in this study and that I am able to withdraw my data, without reason, for up to 2 weeks following participation. [ ]
- I agree to gift my tissue sample for research [ ]
- I understand that my midstream urine sample will be screened for a urinary tract infection and, if identified, I will be excluded from the study and referred to my GP for further diagnosis and treatment. [ ]
- I understand that relevant sections of my medical notes and data collected from the study may be looked at by regulatory authorities or by persons from the Trust where it is relevant to my taking part in this study. I give permission for these individuals to have access to this information [ ]
- I understand that the researchers will hold all information and data collected securely and in confidence and that all efforts will be made to ensure that I cannot be identified as a participant in the study (except as might be required by law) and I give permission for the researchers to hold relevant personal data where relevant to my taking part in this research. [ ]
- I agree to take part in the above study. [ ]

**Name of Participant**

**Signature**

**Date**

**Name of person taking consent**

**Signature**

**Date**



Royal Preston Hospital  
Sharoe Green Lane  
Fulwood, Preston  
PR2 9HT

Tel: 01772 716565

Centre Number:

Study Number:

Patient Identification Number for this study:

## Consent Form

Version 4 – 08/11/16

### Identification of bacterial 'signatures' characteristic of intestinal disease

**Name of Researchers: Dr Abhishek Sharma, Ailsa Watt, Janet Mills, Emma Beamish and Dr Rachael Rigby**

*Please initial the boxes [ ]*

- I confirm that I have read and understood the information sheet dated 08/11/16 for the above study. [ ]
- I have had the opportunity to consider the information and ask any questions I may have related to the study. [ ]
- I understand that I am under no obligation to participate in this study and that I am able to withdraw my data, without reason, for up to 2 weeks following participation. [ ]
- I agree to gift my tissue sample for research [ ]
- I understand that my midstream urine sample will be screened for a urinary tract infection and, if identified, I will be excluded from the study and referred to my GP for further diagnosis and treatment. [ ]
- I understand that relevant sections of my medical notes and data collected from the study may be looked at by regulatory authorities or by persons from the Trust where it is relevant to my taking part in this study. I give permission for these individuals to have access to this information [ ]
- I understand that the researchers will hold all information and data collected securely and in confidence and that all efforts will be made to ensure that I cannot be identified as a participant in the study (except as might be required by law) and I give permission for the researchers to hold relevant personal data where relevant to my taking part in this research. [ ]
- I agree to take part in the above study. [ ]

**Name of Participant**

**Signature**

**Date**

**Name of person taking consent**

**Signature**

**Date**

When completed: 1 copy for the subject; 1 copy for the researcher site file; original to be kept in medical notes





**Trust Headquarters**  
Westmorland General Hospital  
Burton Road  
Kendal  
LA9 7RG

Tel: 01539 716621  
Web: <http://www.uhmb.nhs.uk/>

**Patient Information Sheet**  
**Version 4 – 24/02/16**

**Part 1**

*Study title.*

Identification of bacterial 'signatures' characteristic of intestinal disease

*Invitation to participate in the study.*

We would like to invite you to take part in our research study. Before you decide we would like you to understand why the research is being done and what it would involve. Please take time to read the following information carefully, and talk to others about the study, if you wish. Ask one of our team if there is anything that is not clear, or if you would like more information before deciding whether or not you wish to take part.

*What is the purpose of the study?*

It is estimated that around 1000 different types of bacteria live within the gut and usually exist in harmony with the host. Evidence suggests that changes in the amount and type of gut bacteria may promote the development of gut inflammation. New methods can detect changes in the bacteria through analysis of the bacterial waste products present in the urine. Our research aims to identify bacterial-product profiles present in the urine, which can then be used to provide new, non-invasive techniques for diagnosis of intestinal disease.

*Why have I been invited?*

You have been invited to take part in the study because you are undergoing a flexible sigmoidoscopy or colonoscopy examination at Furness General Hospital.

*Do I have to take part?*

Taking part is entirely voluntary and is up to you to decide whether or not you wish to join the study. If you agree to take part you will keep this information sheet and be invited to ask any questions, we will then ask you to sign a consent form. You are free to withdraw from the study up to 2 weeks following participation, without giving a reason. Any decision to not take part or withdraw from the study, will not affect the medical care you receive.

*What will happen to me if I take part?*

If you agree to take part, you will be asked to sign the consent form. Following this, during your examination the doctor will take two extra colonic tissue biopsies which may be kept for research purposes. Before the procedure starts, you will also be required to provide a midstream urine sample which, although is not part of the normal examination, will not affect the procedure in any way.

Because we will be looking at the bacterial waste products present in your urine, we need to make sure that you do not have a bacterial infection, as this would compromise your sample. To do this, we will screen you for a urinary tract infection (UTI) using a dipstick test on the urine sample you provide. The test result is instant and if we identify that you may have a UTI you will be excluded from the study and referred to your GP for a confirmed diagnosis and treatment. If you are excluded for this reason, your endoscopic examination will continue as normal, but the two additional biopsies for the study will not be taken. If there is no evidence of a UTI, your participation in the study can continue and the two additional biopsies will be taken during your examination.

The samples will not be used for any financial gain and will be treated as a gift from you to us, effectively belonging to University Hospitals of Morecambe Bay NHS Foundation Trust. This procedure will not affect the standard diagnosis, treatment and management of your condition which will continue as normal. Neither you nor your doctors will receive a result from the tissue or urine sample as it is purely for research purposes. Patient information collected in connection with the study will be stored in a secure facility only accessible to the researchers involved.

*What will I have to do?*

If you agree to take part in the study, you will be asked to sign the consent form then provide a mid-stream urine sample. Your examination will take place as normal and the extra tissue biopsy samples which will be taken may be kept for research purposes.

*What are the possible risks and disadvantages of taking part?*

As two additional biopsies will be taken, there is a slightly elevated risk associated with taking part. However, as biopsies are likely to be taken during your normal procedure, regardless of participation in this study, the additional risk is minimal. There are also no risks associated with providing a midstream urine sample.

We will also be screening you for a urinary tract infection by testing your midstream urine sample. Although we expect that this will affect a very small number of participants, if a positive result is obtained, we will need to refer you to your GP for a confirmed diagnosis and treatment. This will involve you making a separate appointment with your GP and, if required, receiving treatment for the infection.

*What are the possible benefits of taking part?*

There is no immediate benefit to you taking part in this study. The information we get from this study will provide further insight into the alterations in the intestinal bacteria. This research may also help to improve the techniques used to diagnose and treat intestinal disease in the future.

*What happens when the research study stops?*

The tissue and urine samples may be stored and remain available for future authorised scientific studies.

*What if there is a problem?*

Any complaint about the way you have been dealt with during the study or any possible harm you might suffer will be addressed. The detailed information on this is given in Part 2.

*Will my taking part in the study be kept confidential?*

Yes, all samples will be anonymised and no patient identifiable information will be used for this study. All information which is collected about you during the course of the research will be kept strictly confidential. We will follow ethical and legal practice and all information about you will be handled in confidence. The details are included in Part 2.

If the information in Part 1 has interested you and you are considering participation, please read the additional information in Part 2 before making any decision.

## Part 2

### *What if relevant new information becomes available?*

If any important new information becomes available that might affect the management or treatment of your condition during the period of the study, the investigators will contact you to tell you about it.

### *What will happen if I don't want to carry on with the study?*

If you withdraw from the study within 2 weeks of participation, we will destroy all your samples. Beyond 2 weeks, your identifiable data will no longer be traceable and therefore your data will be included in the study.

### *What if there is a problem?*

If you have a concern or complaints about any aspect of this study, you should speak to the researchers who will do their best to answer your questions or contact the Chief Investigator:

Dr Rachael Rigby

Tel: 01524 593420

Email: rachael.rigby@lancaster.ac.uk

Or you can speak to someone outside of the research team at Lancaster University:

Prof. Roger Pickup

Dean of Research, Division of Biomedical & Life Sciences,  
Faculty of Health & Medicine, Lancaster University,  
Lancaster. LA1 4YQ

Tel: 01524 593746

Email: r.pickup@lancaster.ac.uk

If you remain unhappy and wish to complain formally, you can do this through the NHS Complaints Procedure by contacting:

Customer Care Department

Tel: 01539 716621

*Or in writing to:*

Patient Advice and Liaison Services (PALS)  
Royal Lancaster Infirmary  
Ashton Road  
Lancaster  
LA1 4RP

Tel: 01539 795497

In the event that something does go wrong and you are harmed during the research and this is due to someone's negligence then you may have grounds for a legal action for compensation against the University Hospitals of Morecambe Bay NHS Foundation Trust but you may have to pay your legal costs. The normal National Health Service complaints mechanisms will still be available to you.

*What will happen to any samples I give?*



The samples will be anonymised and then processed in the research labs at Lancaster University. Any left-over material (e.g. urine) may be stored and remain available for future authorised scientific studies. If not used, remaining material will be discarded at the end of the study period. No patient identifiable information will be used and samples will only be accessible to researchers associated with the study.

*What will happen to the results of the research study?*

The results of the scientific study will be published in international medical journals and presented at scientific/ medical conferences. You will not be identified in any reports or publications.

*Who is organising and funding the research?*

This study is being organised by Dr Rachael Rigby, at Lancaster University, in collaboration with consultants from Royal Lancaster Infirmary, Royal Preston Hospital and Blackpool Victoria Hospital. This study is supported by University Hospitals of Morecambe Bay NHS Foundation Trust.

*Who has reviewed the study?*

All research in the NHS is looked at by an independent group of people, called a Research Ethics Committee (REC) to protect your interests. This study has been reviewed and approved by the North West Research Ethics Committee.

*Contact for further information.*

If you would like further information about this biological research study, or have any questions concerning it, please contact the study team:

Chief Investigator: Dr Rachael Rigby, Lecturer in Biomedicine, Faculty of Health & Medicine, Division of Biomedical & Life Sciences, University of Lancaster, Lancaster.  
Telephone: 01524 593420

Trial Co-ordinator: Emma Beamish, Post Graduate PhD Student. Lancaster University.  
Email: e.beamish@lancaster.ac.uk

Medical Team at Furness General Hospital:

Dr Albert Davies, Consultant Gastroenterologist. Telephone: 01229 403722

**Thank you for reading this, and for your interest in this research study.**

If you wish to take part in the study, please sign the consent form. Whether or not you decide to take part, you may keep this information sheet for future reference.

Study Cover Letter - Furness General Hospital



**Trust Headquarters**  
Westmorland General Hospital  
Burton Road  
Kendal  
LA9 7RG

Date:

Dear

I am writing to inform you of a clinical research study we are currently conducting in collaboration with researchers at Lancaster University. The primary aim of this study is to improve the diagnosis and management of various intestinal diseases. As you are scheduled to attend Furness General Hospital on \_\_\_\_\_ for either a Flexible Sigmoidoscopy or Colonoscopy examination, we would like to inform you that you are a suitable candidate for the study. We would therefore like to offer you the opportunity to participate in this research and invite you to review the information provided on the enclosed Patient Information Sheet. I would also like to stress that taking part is entirely voluntary and you are under no obligation to do so. Should you decide you are interested in participating, or have any questions regarding the study, please do not hesitate to contact me, prior to your appointment, using the details below.

Kind regards,

**Dr Albert Davies**  
Consultant Gastroenterologist  
Tel: 01229 491118





**Trust Headquarters**  
Royal Preston Hospital  
Sharoe Green Lane  
Fulwood, Preston  
Lancashire  
PR2 9HT

Date:

Dear

I am writing to inform you of a clinical research study we are currently conducting in collaboration with researchers at Lancaster University. The primary aim of this study is to improve the diagnosis and management of various intestinal diseases. As you are scheduled to attend Royal Preston Hospital on \_\_\_\_\_ for either a Flexible Sigmoidoscopy or Colonoscopy examination, we would like to inform you that you are a suitable candidate for the study. We would therefore like to offer you the opportunity to participate in this research and invite you to review the information provided on the enclosed Patient Information Sheet. Our research nurse, Emma Durant, is coordinating the study at the hospital and will contact you before your appointment to provide further details and discuss your decision on participation. I would also like to stress that taking part is entirely voluntary and you are under no obligation to do so. In the meantime, if you have any questions, or would like any further information, please do not hesitate to contact Emma using the details below.

Emma Durant  
Upper GI Research Sister  
Royal Preston Hospital  
Tel: 01772 528272

Kind regards,

**Dr Abhishek Sharma**  
Consultant Gastroenterologist

Letter to GP Following UTI-based Exclusion

University Hospitals   
of Morecambe Bay  
NHS Foundation Trust

**Trust Headquarters**  
Westmorland General Hospital  
Burton Road  
Kendal  
LA9 7RG

Tel: 01229 403722

GP Address

Dear Dr

Re: Patient name:

DOB:

Your patient, with a diagnosis of \_\_\_\_\_, was invited and consented to participate in a research study entitled 'identification of bacterial signatures characteristic of intestinal disease'.

The study participant consented to providing two additional intestinal biopsies and a midstream urine sample during their endoscopic examination, which took place on \_\_\_\_\_.

As part of our study exclusion criteria we are required to screen for urinary tract infections via urinary dipstick analysis. Our test results for your patient were suggestive of a UTI and we therefore advise that they are given a confirmed diagnosis and appropriate treatment. The participant was excluded from the study and although their examination went ahead as normal, the additional two biopsies were not obtained.

Please find enclosed a copy of the patient information sheet for your information. If you require any further information, or have any comments about this, please feel free to contact me on the details listed above.

Yours sincerely,

**Dr Albert Davies**  
Consultant Gastroenterologist

## Appendix 8 - Pattern File for Computational Bucket Processing of <sup>1</sup>H NMR Spectral Peaks

10/04/17

PATTERN = 1

DESCRIPTION = /raid/usr/EBeamish/Urine\_NMR/EBeamish\_urine3mm\_080217\_6/291

AUTHOR = ebeamish

DIM = 2

ORIGIN = 1

ITEMS = 237

9.312 9.273 1-Methylnicotinamide 1  
9.152 9.097 Trigoneline 1  
9.069 9.034 Unknown  
9.002 8.959 1-Methylnicotinamide 2  
8.939 8.892 1-Methylnicotinamide 3  
8.886 8.823 Trigoneline 2  
8.818 8.788 Unknown  
8.774 8.727 Unknown  
8.700 8.659 Unknown  
8.654 8.631 Unknown\_Nicotinate  
8.602 8.502 IMP\_Hippurate 1\_ADP  
8.487 8.414 Unknown  
8.410 8.360 Unknown  
8.359 8.310 Inosine\_Unknown  
8.308 8.121 Oxypurinol\_Adenine\_Hypoxanthine  
8.120 8.049 Unknown  
8.045 8.000 Theophylline\_Riboflavin 1\_Quinolate  
7.997 7.954 Riboflavin 2\_Unknown  
7.953 7.912 N,N-Dimethylformamide\_Na-Aceyllysine\_Xanthine  
7.910 7.853 4-Pyridoxate\_Kynurenate  
7.852 7.785 Hippurate 2\_Salicyurate 1  
7.778 7.749 Indole-3-lactate  
7.748 7.739 N-Phenylacetylphenylalanine  
7.738 7.714 Tryptophan 1  
7.713 7.701 Unknown  
7.700 7.682 T-Methylhistidine  
7.667 7.626 Hippurate 3  
7.582 7.537 Hippurate 4\_Tryptophan 2  
7.534 7.507 Indole-3-Lactate  
7.507 7.491 Salicyurate 2  
7.474 7.444 Unknown  
7.384 7.346 3,5-Dibromotyrosine\_N-Phenylacetylglycine  
7.345 7.334 Tryptophan 2\_Acetylsalicylate  
7.333 7.302 Unknown  
7.300 7.266 Tryptophan 3\_Unknown  
7.264 7.230 Unknown  
7.192 7.161 Tryptophan 4\_Tyrosine 2\_Unknown  
7.159 7.121 Unknown  
7.088 7.055 T-Methylhistidine  
7.055 7.030 Epicatechin 1  
7.017 6.985 Unknown  
6.984 6.934 Epicatechin 2  
6.933 6.902 Tyrosine 2  
6.892 6.863 3,4-Dihydroxybenzeneacetate 1  
6.844 6.812 Unknown  
6.798 6.759 3 Hydroxyphenylacetate  
6.719 6.696 3,4-Dihydroxybenzeneacetate 2

6.691 6.663 Unknown  
6.662 6.634 2-Furoylglycine\_Unknown  
6.625 6.608 Unknown  
6.608 6.595 Trans-Aconitate  
6.591 6.550 Unknown  
6.539 6.524 Fumarate  
6.520 6.486 Unknown\_2,3,4,-Trihydroxybenzoate  
6.460 6.448 2,6-Dihydroxybenzoate  
6.434 6.359 Urocanate  
6.313 6.289 Unknown  
6.208 6.192 Unknown  
6.156 6.121 IMP\_Unknown  
6.120 6.071 Inosine  
6.062 6.027 Unknown  
6.001 5.878 Unknown  
5.873 5.850 Xanthosine  
5.829 5.805 Uracil  
5.730 5.676 cis-Aconitate  
5.634 5.572 UDP-glucose  
5.570 5.511 Unknown  
5.485 5.468 Unknown  
5.424 5.404 Sucrose\_Maltose  
5.402 5.377 Allantoin\_Ribose 1  
5.376 5.353 Unknown  
5.352 5.285 Unknown  
5.284 5.249 Galactose\_Cellobiose\_Lactose  
5.235 5.216 Glucose  
5.209 5.174 Trehalose  
5.169 5.135 Riboflavin  
5.130 5.095 Unknown  
5.058 4.953 Mandelate  
4.950 4.926 Ribose 2  
4.925 4.760 Water  
4.759 4.719 Unknown  
4.713 4.683 Unknown  
4.681 4.651 Glucose\_Glucuronate  
4.646 4.634 Unknown  
4.619 4.598 Unknown  
4.594 4.559 Unknown  
4.551 4.518 Ascorbate  
4.512 4.475 1-Methylnicotinamide 4\_Unknown  
4.468 4.456 Lactose 1  
4.455 4.444 Trigonelline  
4.443 4.403 1,3-Dihydroxyacetone\_Hydroxyacetone  
4.392 4.323 Tartrate\_sn-Glycero-3-phosphocholine 1  
4.319 4.257 Glycylproline 1\_Galactonate 1  
4.250 4.212 Sucrose  
4.211 4.143 Gluconate  
4.142 4.114 Ribose 1\_Lactulose  
4.109 4.083 5-Aminolevulinate\_N-Methylhydantoin  
4.075 4.057 Creatinine 1  
4.056 4.025 Ascorbate  
4.024 4.002 Fructose  
4.001 3.968 Galactonate 2\_Hippurate 5  
3.967 3.961 Glycylproline 2  
3.958 3.936 1,7-Dimethylxanthine 1

3.930 3.894 Syringate\_Unknown  
3.894 3.878 Unknown  
3.877 3.857 Homovanillate\_Arabinitol 1  
3.856 3.828 Ribose 2\_Arabinitol 2  
3.827 3.812 Xylitol  
3.811 3.788 Erythritol 1  
3.787 3.722 Ascorbate  
3.715 3.704 Unknown  
3.701 3.650 Lactose 2\_Arabinitol 3\_Erythritol 2  
3.649 3.593 Unknown  
3.587 3.575 Glycine  
3.572 3.543 myo-Inositol  
3.542 3.473 Ribose 3\_Cellobiose  
3.469 3.457 Acetoacetate  
3.457 3.407 Fucose\_Unknown  
3.400 3.384 Unknown  
3.383 3.364 Methanol  
3.361 3.338 Caffeine  
3.331 3.313 Cellobiose  
3.305 3.300 1,7-Dimethylxanthine 2  
3.296 3.285 Unknown  
3.285 3.276 Unknown  
3.274 3.267 Betane\_Trimethylamine N-oxide  
3.261 3.254 Carnosine 1  
3.252 3.245 sn-Glycero-3-phosphocholine 2  
3.243 3.237 Unknown  
3.237 3.224 Carnitine  
3.212 3.190 O-Acetylcarnitine\_choline  
3.189 3.179 Unknown  
3.179 3.141 N-Nitrosodimethylamine\_Ethanolamine  
3.139 3.128 Malonate  
1.127 3.105 cis-Aconitate\_Unknown  
3.103 3.075 Carnosine 2  
3.067 3.045 Creatinine 2  
3.043 3.038 Creatine Phosphate  
3.035 2.942 Na-Acetyllysine\_Unknown  
2.940 2.926 N-Methylhydantoin\_Unknown  
2.926 2.904 Unknown  
2.904 2.898 Unknown  
2.896 2.875 Unknown  
2.875 2.862 Unknown  
2.861 2.846 Unknown  
2.845 2.824 Unknown  
2.819 2.809 Methylguanidine  
2.808 2.794 Unknown  
2.792 2.784 Unknown  
2.874 2.752 Unknown  
2.752 2.724 Unknown  
2.723 2.704 Dimethylamine  
2.703 2.680 Unknown  
2.679 2.657 Unknown  
2.657 2.634 Unknown  
2.634 2.622 Unknown  
2.621 2.610 Methylamine  
2.610 2.577 Unknown  
2.568 2.538 Unknown

2.537 2.524 Unknown  
2.524 2.512 Unknown  
2.512 2.483 Unknown  
2.483 2.438 Glutamine  
2.435 2.415 Unknown  
2.415 2.401 Unknown  
2.399 2.390 Unknown  
2.390 2.384 Pyruvate  
2.384 2.364 N-Carbamoyl-B-alanine  
2.357 2.343 Unknown  
2.340 2.297 3-Hydroxybutyrate 1  
2.296 2.283 Acetoacetate  
2.282 2.248 Unknown  
2.245 2.238 Acetone  
2.235 2.222 Unknown  
2.221 2.193 Unknown  
2.193 2.183 Adipate 1  
2.182 2.177 Unknown  
2.177 2.164 Unknown  
2.164 2.156 Unknown\_Acetaminophen  
2.156 2.151 Unknown  
2.149 2.135 Methylsuccinate  
2.135 2.126 Unknown  
2.114 2.089 Unknown  
2.087 2.060 Unknown  
2.058 2.027 Unknown  
2.026 2.006 Unknown  
2.004 1.983 2-Aminobutyrate  
1.983 1.959 Unknown  
1.954 1.936 Unknown  
1.936 1.927 Acetate  
1.927 1.917 Unknown  
1.917 1.912 Melatonin  
1.912 1.894 Unknown  
1.894 1.872 Unknown  
1.870 1.855 Unknown  
1.855 1.835 Unknown  
1.834 1.817 Unknown  
1.816 1.797 Unknown  
1.797 1.771 Unknown  
1.771 1.747 Unknown  
1.747 1.699 Cadaverine\_N-Acetylornithine  
1.697 1.654 Unknown  
1.654 1.628 Arginine  
1.627 1.580 Biotin\_2-Hydroxyvalerate  
1.579 1.533 Adipate 2  
1.534 1.509 Unknown  
1.503 1.479 Alanine  
1.475 1.457 Unknown  
1.454 1.434 Unknown  
1.415 1.373 Acetonin  
1.372 1.359 2-Hydroxyisobutyrate  
1.353 1.330 Threonine\_Lactate  
1.330 1.322 3-Hydroxy-3-methylglutarate\_Unknown  
1.322 1.297 Unknown  
1.297 1.281 Unknown

1.281 1.271 3-Hydroxyisovalerate  
1.270 1.248 Unknown  
1.246 1.227 Fucose  
1.223 1.196 3-Hydroxybutyrate 2  
1.196 1.187 3-Aminoisobutyrate  
1.185 1.176 Unknown  
1.176 1.162 Unknown  
1.161 1.131 Unknown  
1.125 1.101 Unknown  
1.100 1.084 Unknown  
1.084 1.063 Methylsuccinate  
1.063 1.057 Unknown  
1.057 0.961 Valine\_Butanone\_2-Aminobutyrate\_Unknown  
0.961 0.928 Unknown  
0.921 0.853 2-Hydroxybutyrate 3\_Unknown  
0.850 0.818 Unknown  
0.796 0.734 Unknown  
0.734 0.695 Unknown  
0.681 0.630 Unknown  
0.579 0.527 Unknown  
0.176 0.164 Unknown  
0.102 0.092 Unknown  
0.011 0.000 TSP

**Appendix 9 - PQN Normalised and Pareto Scaled Relative Concentrations of Annotated Urine Metabolites.**

Table A

	Sample	LANC001	LANC011	LANC002	LANC023	LANC036	LANC003	LANC024	LANC004	LANC015	LANC025	LANC005	LANC026	LANC006	LANC017	LANC027	LTHTr002	LANC007	LANC008	LANC019	LTHTr005
	Group	Control	Control	Control	Control	Control	Control	Control	Control	Control	Control	Control	Control	Control	Control	Control	Control	Control	Control	Control	Control
X1.3.Dihydroxyacetone		-0.014	-0.014	-0.014	-0.014	0.11	-0.014	-0.014	-0.014	-0.014	-0.014	-0.014	-0.014	-0.014	-0.014	-0.014	-0.014	-0.014	-0.014	-0.014	-0.014
X1.3.Dimethylurate		-0.112	0.176	0.151	-0.155	0.497	-0.019	0.204	0.073	0.195	-0.091	-0.078	-0.036	-0.076	0.174	-0.058	-0.11	-0.105	-0.118	-0.111	-0.093
X1.6.Anhydro...D.glucose		-0.077	-0.077	0.003	-0.077	-0.077	-0.077	0.029	0.776	-0.077	0.045	-0.077	-0.077	-0.077	-0.002	-0.077	-0.077	-0.077	-0.077	0.029	0.047
X1.7.Dimethylxanthine		-0.011	0.005	0.118	0.244	0.254	0.079	0.04	-0.04	-0.041	0.226	-0.148	-0.036	-0.175	-0.293	-0.22	-0.163	-0.053	-0.109	-0.178	-0.162
X1.Methylnicotinamide		-0.024	0.056	0.572	0.164	-0.25	-0.25	-0.102	-0.105	-0.003	0.175	-0.148	0.082	-0.124	0.382	-0.131	-0.25	-0.141	-0.137	0.018	0.074
X2..Deoxyadenosine		-0.043	-0.043	0.283	-0.043	-0.043	-0.043	0.133	-0.043	-0.043	-0.043	-0.043	-0.043	-0.043	-0.043	-0.043	-0.043	-0.043	-0.043	-0.043	-0.043
X2..Deoxyguanosine		-0.027	-0.027	-0.027	-0.027	-0.027	-0.027	-0.027	0.022	-0.027	-0.027	-0.027	0.123	-0.027	-0.027	0.096	-0.027	0.15	-0.027	-0.027	-0.027
X2..Deoxyinosine		0.092	-0.011	-0.011	-0.011	-0.011	-0.011	-0.011	-0.011	-0.011	-0.011	-0.011	-0.011	-0.011	0.122	-0.011	-0.011	-0.011	0.083	-0.011	-0.011
X2.Aminoacidipate		-0.113	-0.113	-0.113	-0.113	-0.113	-0.113	-0.113	0.861	-0.113	-0.113	-0.113	-0.113	-0.113	-0.113	-0.113	-0.113	-0.113	-0.113	-0.113	-0.113
X2.Aminobutyrate		0.147	0.223	-0.149	0.075	-0.212	0.077	0.255	-0.212	-0.086	0.421	-0.086	0.074	-0.147	-0.212	0.84	0.229	0.116	-0.147	-0.11	-0.212
X2.Ethylacrylate		0.161	-0.034	-0.034	-0.034	-0.034	0.266	-0.034	-0.034	-0.034	0.231	0.165	-0.034	-0.034	-0.034	-0.034	-0.034	-0.034	-0.034	-0.034	-0.034
X2.Furoylglycine		0.038	-0.063	-0.063	-0.063	0.176	-0.063	-0.063	-0.063	-0.063	-0.063	0.15	0.134	0.013	0.027	-0.063	-0.063	0.057	0.038	0.033	0.048
X2.Hydroxy.3.methylvalerate		-0.035	-0.035	-0.035	-0.035	-0.035	-0.035	-0.035	-0.035	0.197	0.176	-0.035	-0.035	-0.035	-0.035	-0.035	-0.035	-0.035	-0.035	-0.035	-0.035
X2.Hydroxybutyrate		-0.009	-0.009	-0.009	-0.009	-0.009	-0.009	-0.009	-0.009	0.346	-0.009	-0.009	-0.009	-0.009	-0.009	-0.009	-0.009	-0.009	-0.009	-0.009	-0.009
X2.Hydroxyisobutyrate		-0.049	-0.1	0.388	0.197	-0.241	-0.058	-0.14	-0.089	0.057	-0.113	-0.114	-0.104	-0.042	0.336	-0.102	-0.183	-0.002	-0.051	0.208	0.061
X2.Hydroxyisocaproate		-0.015	0.105	-0.015	0.181	-0.015	-0.015	-0.015	0.197	-0.015	-0.015	-0.015	-0.015	-0.015	-0.015	-0.015	-0.015	-0.015	-0.015	-0.015	-0.015
X2.Hydroxyisovalerate		-0.011	-0.011	-0.011	-0.011	-0.011	-0.011	-0.011	-0.011	-0.011	-0.011	-0.011	-0.011	-0.011	-0.011	-0.011	-0.011	-0.011	-0.011	-0.011	-0.011
X2.Hydroxyphenylacetate		0.176	0.104	0.004	0.063	0.023	-0.119	-0.119	-0.119	0.076	-0.025	-0.013	-0.119	0.005	0.028	0.054	0.065	0.053	0.109	0.039	-0.119
X2.Hydroxyvalerate		-0.044	-0.044	-0.044	-0.044	-0.044	-0.044	-0.044	-0.044	-0.044	-0.044	-0.044	-0.044	-0.044	-0.044	-0.044	-0.044	1.2	-0.044	-0.044	-0.044
X2.Methylglutarate		-0.022	-0.022	-0.022	-0.022	-0.022	-0.022	-0.022	-0.022	-0.022	-0.022	-0.022	-0.022	-0.022	-0.022	-0.022	-0.022	-0.022	-0.022	-0.022	-0.022
X2.Oxocaproate		-0.012	-0.012	-0.012	-0.012	-0.012	-0.012	-0.012	-0.012	-0.012	-0.012	-0.012	-0.012	-0.012	-0.012	-0.012	-0.012	-0.012	-0.012	-0.012	-0.012
X2.Oxoglutarate		0.166	-0.111	-0.111	-0.111	-0.111	0.613	-0.111	-0.111	0.591	-0.111	-0.111	-0.111	-0.111	-0.111	-0.111	-0.111	-0.111	-0.111	-0.111	-0.111
X2.Oxoisocaproate		-0.004	-0.004	-0.004	-0.004	-0.004	-0.004	-0.004	-0.004	-0.004	-0.004	-0.004	-0.004	-0.004	-0.004	-0.004	-0.004	-0.004	-0.004	-0.004	-0.004
X2.Phenylpropionate		-0.006	-0.006	-0.006	-0.006	-0.006	-0.006	-0.006	-0.006	-0.006	-0.006	-0.006	-0.006	-0.006	0.1	-0.006	-0.006	-0.006	-0.006	-0.006	-0.006
X3.4.Dihydroxybenzeneacetate		0.084	0.04	-0.085	-0.085	-0.085	-0.085	-0.085	-0.085	-0.085	0.007	0.09	0.072	0.098	-0.085	-0.085	-0.085	0.088	0.126	0.031	-0.085
X3.4.Dihydroxymandelate		-0.076	-0.076	0.019	0.096	-0.076	-0.076	0.113	0.041	0.085	0.048	-0.076	-0.076	-0.076	-0.076	-0.076	-0.076	0.077	-0.076	0.079	0.092
X3.5.Dibromotyrosine		-0.123	-0.123	-0.123	-0.123	0.134	-0.041	0.586	-0.123	-0.123	-0.123	-0.123	-0.123	0.293	-0.103	-0.093	-0.123	-0.057	0.298	-0.123	-0.123
X3.Aminoisobutyrate		-0.331	1.421	0.322	0.168	-0.331	0.055	0.554	-0.24	-0.107	0.845	-0.04	0.058	-0.12	0.097	0.043	0.019	-0.331	-0.122	-0.079	0.045
X3.Chlorotyrosine		-0.055	-0.055	-0.055	-0.055	0.404	-0.055	-0.055	0.27	-0.055	-0.055	-0.055	0.113	-0.001	-0.055	-0.055	-0.055	-0.055	0.186	-0.055	-0.055
X3.Hydroxy.3.methylglutarate		0.089	0.087	0.013	-0.054	-0.101	-0.026	0.056	-0.108	-0.058	-0.005	-0.11	-0.04	-0.069	0.011	0.052	-0.04	0.094	0.001	0.004	0.011
X3.Hydroxybutyrate		-0.62	-0.053	-0.542	-0.445	-0.62	-0.513	-0.014	-0.62	-0.62	-0.34	-0.595	-0.543	-0.579	-0.584	-0.468	-0.524	14.413	-0.579	-0.379	-0.606
X3.Hydroxyisobutyrate		-0.062	-0.062	-0.062	-0.062	-0.062	-0.062	-0.062	-0.062	-0.062	-0.062	-0.062	-0.062	-0.062	-0.062	-0.062	-0.062	1.2	-0.062	-0.062	-0.062
X3.Hydroxyisovalerate		-0.173	0.009	0.325	0.262	-0.206	-0.011	-0.207	-0.05	-0.075	-0.112	-0.163	0.059	-0.069	0.126	-0.079	-0.009	0.239	-0.078	0.105	0.021
X3.Hydroxykynurenine		-0.038	-0.038	-0.038	-0.038	-0.038	-0.038	-0.038	-0.038	0.151	-0.038	-0.038	-0.038	-0.038	-0.038	0.18	-0.038	-0.038	-0.038	-0.038	-0.038
X3.Hydroxymandelate		0.027	-0.105	-0.105	-0.022	0.232	-0.105	-0.105	0.005	-0.105	0.046	-0.105	-0.007	-0.013	0.029	0.038	-0.105	0.02	-0.105	-0.105	-0.105
X3.Hydroxyphenylacetate		-0.019	-0.164	-0.164	-0.011	0.157	-0.002	-0.045	0.036	-0.018	-0.018	-0.053	-0.036	-0.029	-0.023	-0.019	0.553	-0.072	-0.035	-0.041	-0.03
X3.Indoxylsulfate		-0.205	-0.205	0.02	0.058	-0.205	-0.205	0.137	0.035	0.087	-0.205	0.052	0.122	-0.205	0.129	0.025	-0.205	0.051	-0.205	0.099	-0.205
X3.Methyl.2.oxovalerate		-0.014	0.342	-0.014	-0.014	-0.014	-0.014	-0.014	-0.014	-0.014	-0.014	-0.014	-0.014	-0.014	-0.014	-0.014	-0.014	-0.014	-0.014	-0.014	-0.014
X3.Methyladipate		-0.012	-0.012	-0.012	-0.012	-0.012	-0.012	-0.012	-0.012	-0.012	-0.012	-0.012	-0.012	-0.012	-0.012	-0.012	-0.012	-0.012	-0.012	-0.012	0.291
X3.Methylglutarate		-0.108	0.229	-0.108	0.12	0.06	-0.108	-0.108	-0.108	-0.108	-0.108	-0.108	0.187	-0.108	-0.108	0.304	0.232	0.338	-0.108	-0.108	-0.108
X3.Methylxanthine		0.156	-0.092	-0.093	0.12	-0.14	-0.087	-0.098	0.031	-0.101	0.016	-0.004	-0.053	-0.14	-0.042	-0.047	0.136	-0.048	-0.099	0.071	-0.14



Sample	LANC001	LANC011	LANC002	LANC023	LANC036	LANC003	LANC024	LANC004	LANC015	LANC025	LANC005	LANC026	LANC006	LANC017	LANC027	LTHTr002	LANC007	LANC008	LANC019	LTHTr005
Group	Control	Control	Control	Control	Control	Control	Control	Control	Control	Control	Control	Control	Control	Control	Control	Control	Control	Control	Control	Control
X3.Methylxanthine	0.156	-0.092	-0.093	0.12	-0.14	-0.087	-0.098	0.031	-0.101	0.016	-0.004	-0.053	-0.14	-0.042	-0.047	0.136	-0.048	-0.099	0.071	-0.14
X3.Phenylpropionate	-0.034	-0.034	-0.034	-0.034	0.534	-0.034	-0.034	-0.034	-0.034	-0.034	0.323	-0.034	-0.034	-0.034	-0.034	-0.034	-0.034	-0.034	-0.034	-0.034
X4.Aminohippurate	-0.011	-0.011	-0.011	-0.011	-0.011	-0.011	-0.011	-0.011	-0.011	-0.011	-0.011	-0.011	0.23	-0.011	-0.011	-0.011	-0.011	-0.011	-0.011	-0.011
X4.Guanidinobutanoate	-0.018	-0.018	-0.018	-0.018	-0.018	-0.018	-0.018	-0.018	-0.018	-0.018	-0.018	-0.018	-0.018	-0.018	-0.018	0.708	-0.018	-0.018	-0.018	-0.018
X4.Hydroxy.3.methoxymandelate	0.152	-0.198	-0.036	-0.058	-0.049	0.217	-0.001	-0.028	0.049	0.041	-0.02	-0.042	-0.039	-0.091	0.06	0.019	-0.135	0.04	-0.067	0.011
X4.Hydroxybenzoate	-0.069	-0.069	-0.069	-0.069	-0.069	0.276	-0.069	0.304	0.247	-0.069	-0.069	-0.069	-0.069	0.212	-0.069	-0.069	-0.069	-0.069	-0.069	-0.069
X4.Hydroxyphenylacetate	0.017	-0.217	-0.104	-0.217	-0.027	-0.217	0.03	0.058	0.013	-0.015	-0.021	0.054	-0.217	-0.023	0.206	0.449	-0.034	-0.217	0.021	-0.06
X4.Pyridoxate	-0.002	0.03	0.057	0.225	-0.125	-0.058	0.402	-0.112	0.206	0.092	0.007	-0.089	0.112	-0.045	-0.059	-0.046	-0.067	0.107	0.157	-0.053
X5.6.Dihydrothymine	0.162	0.194	-0.078	-0.078	-0.078	-0.078	-0.078	-0.078	-0.078	-0.078	-0.078	-0.078	-0.078	-0.078	-0.078	-0.078	-0.078	0.12	-0.078	-0.078
X5.6.Dihydrouracil	-0.021	0.828	-0.021	-0.021	-0.021	-0.021	-0.021	-0.021	-0.021	-0.021	-0.021	-0.021	-0.021	-0.021	-0.021	-0.021	-0.021	-0.021	-0.021	-0.021
X5.Aminolevulinate	-0.052	0.53	-0.177	-0.288	0.311	-0.117	-0.01	0.4	0.025	0.31	0.088	0.033	0.065	-0.062	0.158	-0.103	-0.231	0.05	-0.135	0.095
X5.Hydroxyindole.3.acetate	0.084	-0.158	-0.04	-0.029	0.041	0.017	-0.158	0.041	0.012	-0.101	-0.082	-0.055	-0.04	-0.074	0.06	0.189	-0.158	0.019	-0.036	-0.158
X5.Hydroxyllysine	-0.031	-0.031	-0.031	-0.031	-0.031	-0.031	-0.031	-0.031	-0.031	-0.031	-0.031	-0.031	-0.031	-0.031	-0.031	-0.031	-0.031	-0.031	-0.031	-0.031
X5.Hydroxytryptophan	0.098	-0.175	-0.034	0.065	0.156	-0.175	0.084	-0.175	-0.175	0.035	0.006	0.089	0.029	-0.01	-0.068	-0.175	0.052	0.034	-0.108	0.017
X5.Methoxysalicylate	-0.06	-0.06	-0.06	-0.06	0.259	0.107	-0.06	0.181	-0.06	0.135	-0.06	-0.06	-0.06	-0.06	-0.06	-0.06	-0.06	-0.06	-0.06	-0.06
Acetaminophen	-0.085	-0.085	-0.085	-0.085	-0.085	-0.048	0.559	-0.032	-0.085	-0.085	-0.085	0.054	-0.085	-0.085	-0.085	1.123	-0.085	-0.085	-0.085	-0.085
Acetate	-0.052	0.204	-0.12	-0.107	-0.318	0.169	-0.048	-0.11	-0.07	-0.123	-0.196	-0.037	-0.091	-0.076	-0.067	1.175	-0.088	-0.089	-0.113	-0.091
Acetoacetate	-0.487	1.302	-0.422	-0.434	-0.484	-0.36	0.164	-0.525	-0.474	0.326	-0.424	-0.059	-0.398	-0.438	-0.126	-0.167	7.821	-0.491	0.286	-0.505
Acetoin	0.149	0.906	-0.093	-0.093	0.069	-0.093	-0.093	-0.093	0.032	-0.093	-0.093	-0.093	0.063	-0.093	-0.093	-0.093	-0.093	0.076	-0.093	0.047
Acetone	-0.206	-0.117	-0.015	0.039	-0.17	0.359	0.247	-0.221	-0.19	0.013	0.159	-0.037	-0.167	-0.192	-0.1	-0.157	1.882	-0.188	0.132	-0.207
Acetylsalicylate	-0.038	0.124	-0.125	-0.051	0.224	-0.125	0.056	0.007	0.039	-0.033	0.041	0.046	-0.125	-0.019	0.009	0.026	-0.125	-0.125	-0.049	0.093
Adenine	-0.021	-0.021	-0.021	-0.021	-0.021	-0.021	-0.021	-0.021	-0.021	-0.021	-0.021	-0.021	-0.021	-0.021	-0.021	-0.021	-0.021	-0.021	0.664	-0.021
Adenosine	-0.012	-0.012	-0.012	-0.012	-0.012	-0.012	-0.012	-0.012	-0.012	-0.012	-0.012	-0.012	-0.012	-0.012	-0.012	0.078	-0.012	-0.012	-0.012	-0.012
Adipate	-0.023	-0.023	-0.023	-0.023	-0.023	-0.023	-0.023	-0.023	-0.023	-0.023	-0.023	-0.023	-0.023	-0.023	-0.023	-0.023	-0.023	-0.023	-0.023	-0.023
ADP	-0.013	-0.013	-0.013	-0.013	-0.013	-0.013	-0.013	-0.013	-0.013	-0.013	-0.013	-0.013	-0.013	0.205	-0.013	-0.013	-0.013	-0.013	0.094	-0.013
Alanine	-0.36	-0.36	-0.184	-0.079	-0.121	0.074	0.075	0.471	0.287	-0.125	-0.165	-0.117	0.121	-0.107	-0.122	-0.08	-0.142	0.116	0.051	0.288
Allantoin	0.048	-0.167	0.032	-0.167	0.042	-0.167	-0.017	0.007	0.028	-0.167	-0.167	-0.167	0.047	0.023	0.163	-0.167	0.094	0.039	0.063	0.085
Alloisoleucine	0.099	-0.076	0.215	-0.076	-0.076	-0.076	-0.076	-0.076	0.252	-0.076	-0.008	0.066	0.006	-0.076	-0.076	0.095	-0.076	0.095	-0.076	-0.076
Anserine	0.05	0.102	-0.024	0.042	-0.125	0.146	-0.07	-0.032	-0.093	-0.06	0.143	0.008	-0.144	-0.127	0.106	-0.027	-0.013	0.054	-0.096	0.097
Anthranilate	-0.03	-0.03	-0.03	-0.03	0.515	-0.03	-0.03	-0.03	-0.03	-0.03	-0.03	-0.03	-0.03	-0.03	-0.03	-0.03	-0.03	-0.03	-0.03	-0.03
Arabinitol	0.953	-0.121	-0.121	-0.121	-0.121	-0.121	-0.121	-0.121	-0.121	-0.121	0.462	-0.121	-0.121	-0.121	0.526	-0.121	-0.121	-0.121	-0.121	-0.121
Arabinose	-0.328	-0.328	-0.328	-0.328	-0.328	-0.328	-0.137	-0.328	-0.328	-0.328	0.952	-0.328	0.488	-0.148	0.687	-0.266	0.636	-0.328	0.574	-0.328
Arginine	-0.073	-0.073	-0.073	-0.073	-0.073	-0.073	-0.073	-0.073	-0.073	1.128	-0.073	-0.073	-0.073	-0.073	-0.073	-0.073	-0.073	-0.073	-0.073	-0.073
Ascorbate	0.839	-1.445	0.874	-0.039	-1.5	0.852	-0.994	-1.214	0.579	0.74	-0.374	-0.742	-1.078	0.458	-0.925	-1.376	-0.227	-1.09	-0.329	2.559
ATP	0.143	-0.012	-0.012	0.147	-0.012	-0.012	-0.012	-0.012	-0.012	-0.012	-0.012	-0.012	-0.012	0.09	-0.012	-0.012	-0.012	-0.012	-0.012	-0.012
Azelate	-0.023	-0.023	-0.023	-0.023	-0.023	-0.023	-0.023	-0.023	-0.023	-0.023	-0.023	-0.023	-0.023	-0.023	-0.023	-0.023	-0.023	-0.023	-0.023	-0.023
Betaine	0.05	-0.073	-0.068	-0.078	-0.142	0.082	-0.127	-0.035	0.084	-0.04	-0.108	-0.12	-0.154	0.156	0.021	0.504	-0.027	-0.154	0.002	0.125
Biotin	-0.261	-0.261	0.07	0.047	0.269	-0.261	0.283	-0.261	0.06	-0.261	0.399	0.007	0.073	0.127	0.26	0.005	-0.009	0.176	0.159	
Butanone	-0.097	-0.097	-0.097	-0.097	0.129	0.217	0.482	-0.097	0.045	0.105	-0.097	0.171	0.098	-0.097	-0.097	0.048	0.183	-0.097	-0.097	-0.097
Cadaverine	-0.022	-0.022	-0.022	-0.022	-0.022	-0.022	-0.022	-0.022	-0.022	-0.022	-0.022	-0.022	-0.022	-0.022	-0.022	-0.022	-0.022	-0.022	-0.022	-0.022
Caffeine	-0.167	0.074	0.191	-0.025	0.221	0.355	-0.094	-0.043	-0.102	0.067	-0.019	-0.007	-0.087	0.098	-0.063	-0.047	-0.084	-0.167	0.037	-0.064
Caprate	-0.045	-0.045	-0.045	-0.045	-0.045	-0.045	-0.045	-0.045	0.441	-0.045	-0.045	-0.045	-0.045	-0.045	-0.045	-0.045	-0.045	-0.045	-0.045	-0.045
Carnitine	-0.069	-0.17	-0.029	-0.051	0.006	0.246	-0.038	0.259	-0.125	0.085	-0.012	-0.141	-0.042	-0.17	-0.071	-0.071	-0.006	-0.038	0.006	-0.064

	Sample	LANC001	LANC011	LANC002	LANC023	LANC036	LANC003	LANC024	LANC004	LANC015	LANC025	LANC005	LANC026	LANC006	LANC017	LANC027	LTHTr002	LANC007	LANC008	LANC019	LTHTr005
	Group	Control	Control	Control	Control	Control	Control	Control	Control	Control	Control	Control	Control	Control	Control	Control	Control	Control	Control	Control	Control
Carnosine		0.231	0.378	-0.24	-0.124	-0.24	-0.001	0.02	0.477	-0.178	-0.24	-0.08	-0.13	0.581	-0.159	-0.13	-0.15	-0.137	-0.194	-0.064	0.717
Cellobiose		0.456	-0.445	-0.399	0.496	-0.316	-0.445	0.561	-0.445	0.354	0.317	-0.023	0.162	-0.445	-0.445	-0.445	-0.326	0.496	0.078	0.28	0.277
Chlorogenate		-0.01	-0.01	-0.01	-0.01	-0.01	-0.01	-0.01	-0.01	-0.01	-0.01	-0.01	-0.01	-0.01	0.262	-0.01	-0.01	-0.01	-0.01	-0.01	-0.01
Cholate		-0.024	-0.024	-0.024	0.03	-0.024	-0.024	-0.024	-0.024	-0.024	-0.024	-0.024	-0.024	0.003	-0.024	-0.024	-0.024	-0.024	0.127	-0.024	0.028
Choline		-0.173	0.206	-0.066	-0.029	0.217	-0.101	0.097	-0.083	0.006	-0.066	-0.086	0.032	-0.173	-0.062	-0.018	-0.064	0.023	-0.173	0.104	-0.173
cis.Aconitate		0.013	0.423	0.015	0.016	-0.573	0.003	0.225	0.081	0.116	-0.46	-0.126	0.029	0.306	-0.132	-0.368	-0.236	0.622	0.289	0.117	-0.469
Citraconate		-0.037	-0.037	-0.037	-0.037	-0.037	-0.037	0.246	-0.037	0.074	0.308	-0.037	-0.037	-0.037	-0.037	-0.037	-0.037	-0.037	-0.037	-0.037	-0.037
Citrate		-0.092	-0.092	-0.092	0.125	-0.011	-0.092	-0.092	-0.092	0.34	0.092	-0.092	0.126	0.094	0.178	-0.092	0.136	0.132	-0.092	-0.092	-0.092
Citrulline		0.571	-0.047	-0.047	-0.047	-0.047	-0.047	-0.047	-0.047	-0.047	-0.047	-0.047	-0.047	-0.047	-0.047	-0.047	-0.047	-0.047	-0.047	0.548	-0.047
Creatine		-0.013	-0.245	1.374	-0.222	-0.111	-0.14	-0.225	-0.05	1.8	-0.161	-0.039	-0.196	-0.07	0.665	-0.078	0.601	-0.263	-0.105	0.078	-0.21
Creatine.phosphate		0.078	0.997	0.055	0.037	-0.22	-0.116	-0.124	-0.174	-0.017	-0.132	-0.181	-0.171	-0.081	-0.181	0.085	-0.112	0.751	-0.069	-0.217	-0.174
Creatinine		2.258	-0.473	1.516	-3.446	-0.874	-0.168	-1.276	0.622	0.741	0.598	-0.2	-3.499	-0.176	-3.285	0.269	-0.933	1.736	-0.2	2.171	-2.91
Cytidine		0.1	-0.035	0.096	-0.035	-0.035	-0.035	-0.035	-0.035	-0.035	-0.035	-0.035	-0.035	-0.035	0.152	-0.035	-0.035	0.227	-0.035	-0.035	0.138
dCTP		-0.006	-0.006	-0.006	-0.006	-0.006	-0.006	-0.006	-0.006	-0.006	-0.006	-0.006	-0.006	-0.006	-0.006	-0.006	-0.006	-0.006	-0.006	-0.006	-0.006
Desaminotyrosine		-0.024	-0.024	-0.024	-0.024	-0.024	-0.024	-0.024	-0.024	-0.024	-0.024	-0.024	-0.024	-0.024	-0.024	-0.024	-0.024	-0.024	-0.024	-0.024	-0.024
Dimethylamine		0.692	-0.023	0.008	0.267	0.017	-0.214	-0.299	-0.24	0.116	0.016	-0.12	-0.22	-0.112	0.183	0.069	-0.599	0.055	-0.124	0.124	0.369
Dimethyl.sulfone		-0.032	0.056	-0.104	0.036	-0.115	-0.07	0.024	-0.145	0.004	-0.089	-0.105	-0.115	0.029	0.004	-0.092	0.621	-0.038	0.038	0.031	0.065
dTTP		0.102	-0.027	-0.027	-0.027	-0.027	-0.027	-0.027	-0.027	-0.027	-0.027	-0.027	-0.027	0.096	-0.027	-0.027	-0.027	-0.027	0.077	0.205	0.163
Epicatechin		0.102	-0.046	-0.046	-0.046	0.141	-0.046	-0.046	-0.046	0.109	-0.046	-0.046	0.059	-0.046	-0.046	-0.046	0.071	-0.046	0.075	-0.046	-0.046
Erythritol		0.773	0.117	-0.144	0.004	-0.808	0.129	-0.808	0.122	-0.808	0.061	-0.234	-0.034	0.111	-0.429	0.153	-0.182	-0.045	0.182	0.338	-0.808
Ethanol		-0.156	-0.156	-0.156	-0.156	0.012	0.038	-0.156	-0.156	-0.156	-0.156	-0.156	-0.008	-0.156	-0.156	-0.156	-0.156	-0.156	-0.156	-0.156	-0.156
Ethanolamine		-0.057	-0.057	-0.057	-0.057	-0.057	-0.057	-0.057	0.978	-0.057	-0.057	-0.057	-0.057	-0.057	-0.057	-0.057	-0.057	-0.057	-0.057	-0.057	-0.057
Ethylene.glycol		-0.042	-0.042	-0.042	-0.042	-0.042	-0.042	0.244	-0.042	-0.042	-0.042	-0.042	-0.042	-0.042	-0.042	-0.042	-0.042	0.091	-0.042	-0.042	-0.042
Ethylmalonate		-0.031	-0.031	-0.031	-0.031	-0.031	-0.031	-0.031	-0.031	-0.031	0.528	-0.031	-0.031	-0.031	-0.031	-0.031	-0.031	-0.031	-0.031	-0.031	-0.031
Ferulate		-0.067	-0.067	-0.02	-0.067	0.055	0.085	-0.067	-0.067	-0.009	0.003	-0.067	0.1	0.068	-0.009	-0.067	-0.067	-0.018	0.042	0.12	0.239
Formate		-0.283	0.6	-0.284	-0.203	-0.17	0.87	0.254	-0.025	-0.145	-0.083	0.056	0.011	-0.287	-0.208	-0.023	0.022	-0.299	-0.232	-0.168	-0.081
Fructose		0.183	-0.25	-0.179	-0.069	0.439	-0.511	-0.511	1.016	0.345	0.287	0.094	-0.511	-0.511	0.254	-0.511	0.826	0.504	-0.243	-0.511	0.133
Fucose		-0.277	-0.016	0.26	0.296	-0.401	0.03	-0.023	-0.273	-0.31	-0.015	-0.117	-0.195	0	-0.01	-0.127	-0.12	1.042	-0.005	0.637	0.118
Fumarate		-0.013	0.152	-0.033	-0.013	-0.091	0.06	-0.071	-0.034	0.045	-0.001	-0.091	-0.03	0.024	-0.024	0.018	-0.091	-0.006	0.026	-0.009	-0.091
Galactarate		0.055	-0.326	-0.032	0.192	-0.083	-0.212	0.181	-0.157	-0.013	-0.033	-0.326	-0.078	0.263	-0.03	0.019	0.054	-0.146	0.253	-0.004	0.386
Galactitol		-0.225	0.032	-0.225	-0.225	0.176	-0.105	0.508	0.521	-0.225	-0.083	1.132	-0.123	-0.225	-0.225	0.109	0.035	-0.225	-0.225	-0.225	-0.056
Galactonate		0.412	-0.373	-0.086	-0.144	-0.129	0.129	0.399	-0.373	0.208	-0.055	-0.148	-0.064	0.098	0.313	-0.083	0.791	0.21	0.084	-0.013	-0.373
Galactose		-0.177	0.39	-0.177	-0.177	0.744	-0.177	1.014	-0.177	-0.177	0.74	0.561	-0.177	-0.177	0.869	-0.177	0.185	-0.177	0.274	-0.177	-0.177
Gallate		-0.024	0.08	-0.008	-0.045	0.022	-0.045	0.408	0.003	0.007	-0.045	-0.045	-0.007	-0.045	-0.045	0.38	-0.045	-0.045	-0.045	-0.045	-0.045
Gentisate		-0.062	-0.062	0.086	-0.062	-0.062	-0.062	0.195	0.119	-0.062	-0.062	-0.062	-0.062	-0.062	-0.062	0.114	-0.062	-0.062	-0.062	-0.062	0.057
Glucarate		0.166	-0.137	-0.137	-0.137	-0.137	-0.137	-0.137	-0.137	-0.137	-0.137	-0.137	0.081	-0.137	-0.137	0.936	0.199	-0.137	0.345	-0.137	-0.137
Glucitol		-0.259	-0.259	-0.259	-0.259	-0.259	-0.259	-0.259	-0.259	-0.259	-0.259	-0.259	0.523	0.622	0.767	-0.259	-0.259	-0.259	-0.259	0.767	-0.259
Gluconate		0.317	0.321	-0.743	0.497	0.005	0.216	-0.383	-0.515	0.49	0.392	-0.078	-0.622	0.261	0.395	-0.743	-0.743	-0.743	0.241	-0.743	0.433
Glucose		1.333	-0.121	-0.121	-0.121	0.302	-0.121	-0.121	-0.121	-0.121	0.215	0.486	-0.121	-0.121	-0.121	0.538	-0.121	-0.121	-0.121	-0.121	-0.121
Glucose.6.phosphate		-0.239	-0.239	-0.163	-0.239	0.107	0.027	-0.239	-0.239	-0.239	0.493	-0.239	-0.239	-0.239	-0.239	-0.239	-0.239	-0.239	-0.239	0.37	-0.239
Glucuronate		0.299	0.109	-0.383	-0.383	0.193	0.36	0.349	-0.383	0.183	0.088	-0.383	-0.383	0.351	-0.383	0.812	-0.383	-0.383	0.021	0.114	-0.383
Glutamine		1.003	-0.084	-0.084	-0.084	-0.084	-0.084	-0.084	-0.084	-0.084	1.131	-0.084	-0.084	-0.084	-0.084	-0.084	-0.084	-0.084	-0.084	-0.084	-0.084
Glutaric.acid.monomethyl.ester		-0.023	-0.023	-0.023	-0.023	0.17	-0.023	-0.023	-0.023	-0.023	-0.023	-0.023	-0.023	-0.023	-0.023	-0.023	0.208	-0.023	-0.023	-0.023	-0.023

	Sample	LANC001	LANC011	LANC002	LANC023	LANC036	LANC003	LANC024	LANC004	LANC015	LANC025	LANC005	LANC026	LANC006	LANC017	LANC027	LTHTr002	LANC007	LANC008	LANC019	LTHTr005	
	Group	Control	Control	Control	Control	Control	Control	Control	Control	Control	Control	Control	Control	Control	Control	Control	Control	Control	Control	Control	Control	
Glutathione		-0.031	-0.031	-0.031	-0.031	-0.031	-0.031	-0.031	-0.031	-0.031	-0.031	-0.031	-0.031	-0.031	-0.031	-0.031	-0.031	-0.031	-0.031	-0.031	-0.031	-0.031
Glycerate		-0.036	-0.036	-0.036	-0.036	-0.036	-0.036	-0.036	-0.036	-0.036	-0.036	-0.036	-0.036	-0.036	-0.036	-0.036	-0.036	-0.036	-0.036	-0.036	-0.036	-0.036
Glycine		-0.443	0.503	-0.541	0.55	-0.739	1.071	0.364	-0.134	1.074	-0.493	-0.521	0.169	-0.123	0.298	-0.451	0.774	-0.719	-0.126	-0.775	0.274	
Glycocholate		-0.042	-0.042	-0.042	0.09	-0.042	-0.042	0.05	-0.042	0.123	0.06	-0.042	-0.042	0.099	-0.042	-0.042	-0.042	-0.042	-0.042	-0.042	0.082	
Glycolate		-0.572	-0.225	-0.091	-0.488	-0.572	0.168	-0.535	0.229	0.361	-0.466	-0.506	0.252	0.205	0.47	-0.531	0.143	-0.102	0.222	0.369	0.272	
Glycylproline		-0.09	-0.351	0.643	-0.363	-0.267	-0.18	-0.369	0.734	-0.149	-0.357	-0.151	-0.264	-0.355	-0.233	-0.168	-0.133	-0.484	-0.254	-0.14	0.613	
GTP		-0.012	-0.012	-0.012	-0.012	-0.012	-0.012	-0.012	-0.012	-0.012	-0.012	-0.012	-0.012	-0.012	-0.012	0.237	-0.012	-0.012	-0.012	-0.012	-0.012	
Guanidinosuccinate		0.364	-0.127	-0.127	-0.127	0.57	-0.127	-0.127	-0.127	-0.127	-0.127	0.332	0.201	-0.127	0.335	-0.127	-0.127	-0.127	-0.127	-0.127	-0.127	
Guanidoacetate		-0.296	-0.139	0.315	0.203	-0.223	-0.196	-0.296	0.407	0.458	-0.182	0.008	-0.22	-0.296	0.355	-0.296	0.661	-0.296	-0.296	-0.214	0.133	
Guanosine		0.099	-0.013	0.045	0.261	-0.07	-0.176	-0.093	0.05	0.117	0.125	0.066	0.071	-0.045	-0.058	-0.176	-0.176	0.03	-0.142	0.108	0.098	
Hippurate		-0.372	0.926	-0.255	-0.256	1.42	0.09	-0.034	0.472	-0.104	-0.256	-0.575	-0.272	-0.08	-0.197	-0.242	0.532	-0.288	-0.071	-0.193	0.11	
Histamine		0.621	-0.019	-0.08	-0.063	-0.106	0.072	-0.005	-0.087	-0.057	-0.07	0.152	-0.071	-0.085	-0.087	-0.056	0.426	-0.062	-0.091	-0.072	-0.151	
Histidine		0.223	-0.099	-0.099	-0.099	-0.099	-0.099	-0.048	-0.056	-0.099	-0.099	-0.099	-0.099	-0.099	0.493	-0.004	-0.099	0.046	-0.058	-0.022	-0.04	
Homocitrulline		-0.151	-0.151	0.623	-0.151	-0.151	-0.151	-0.151	0.563	0.477	-0.151	0.252	-0.151	0.426	0.183	-0.151	-0.151	-0.151	-0.151	-0.151	-0.151	
Homogentisate		-0.02	-0.02	-0.02	-0.02	-0.02	-0.02	0.061	-0.02	0.112	0.147	-0.02	-0.02	-0.02	-0.02	-0.02	-0.02	-0.02	-0.02	-0.02	-0.02	
Homovanillate		-0.132	-0.014	-0.05	-0.008	0.134	-0.195	-0.019	-0.071	0.005	-0.128	-0.052	-0.085	-0.046	0.027	-0.027	0.22	-0.03	-0.024	-0.106	0.084	
Hydroxyacetone		0.214	-0.182	-0.182	0.125	0.109	0.234	-0.182	-0.043	0.146	0.187	0.124	0.099	0.126	-0.182	0.109	0.086	-0.182	0.13	0.086	-0.182	
Hypoxanthine		-0.05	-0.05	-0.05	-0.05	-0.05	-0.05	0.309	-0.013	-0.05	-0.05	-0.05	-0.05	-0.05	-0.05	-0.05	-0.05	-0.05	0.369	-0.05	-0.05	
Ibuprofen		-0.093	0.385	0.023	-0.036	-0.019	-0.093	0.01	0.018	0.155	-0.093	0.202	-0.015	0.198	-0.028	-0.093	-0.01	-0.093	0.19	-0.093	-0.093	
Imidazole		0.087	0.426	0.119	0.201	0.02	0.079	0.178	-0.096	-0.093	-0.167	-0.012	-0.091	0.018	0.037	-0.158	-0.049	0.273	0.011	-0.006	0.268	
IMP		0.096	-0.102	0.096	0.095	-0.102	0.106	-0.058	-0.043	-0.102	-0.027	-0.102	0.049	-0.007	0.093	0.099	-0.102	0.141	0.095	-0.102	0.137	
Indole.3.acetate		-0.12	-0.12	-0.05	0.02	0.033	-0.12	-0.12	0.008	-0.023	0.028	0.103	-0.029	0.088	-0.015	-0.12	-0.12	-0.042	0.068	-0.034	0.024	
Indole.3.lactate		0.042	0.053	-0.035	-0.061	-0.069	0.201	-0.193	0.127	-0.063	0	0.04	-0.065	-0.193	-0.042	0.227	-0.193	-0.06	0.052	-0.042	0.088	
Inosine		0.093	-0.031	0.033	-0.031	-0.031	-0.031	-0.031	-0.031	-0.031	-0.031	-0.031	-0.031	0.105	0.221	-0.031	-0.031	0.049	0.072	0.147	0.035	
Isocitrate		-0.555	-0.555	0.232	0.447	-0.555	0.279	-0.555	-0.555	-0.555	0.42	-0.555	0.288	0.325	0.278	0.605	0.517	-0.555	0.355	-0.555	0.294	
Isoeugenol		0.023	-0.071	0.093	0.035	-0.071	-0.071	0.028	0.082	0.077	-0.071	0.08	0.096	-0.071	-0.071	-0.071	-0.071	0.03	0.123	-0.071	0.069	
Isoleucine		-0.042	-0.042	-0.042	-0.042	-0.042	0.211	-0.042	-0.042	-0.042	-0.042	-0.042	-0.042	-0.042	-0.042	-0.042	-0.042	0.44	-0.042	0.066	-0.042	
Isopropanol		-0.009	-0.009	-0.009	-0.009	-0.009	-0.009	-0.009	-0.009	-0.009	-0.009	-0.009	-0.009	-0.009	-0.009	0.133	-0.009	-0.009	-0.009	-0.009	-0.009	
Kynurenate		0.029	0.072	-0.003	0.042	0.146	-0.063	0.081	-0.063	-0.063	-0.063	-0.063	-0.063	0.085	-0.063	-0.063	0.036	-0.021	0.002	0.048	0.016	
Kynurenine		-0.079	-0.079	-0.079	0.184	0.136	-0.079	0.13	-0.079	-0.079	0.259	-0.079	-0.079	-0.079	-0.079	-0.079	0.393	-0.079	0.151	-0.079	-0.079	
Lactate		-0.064	-0.262	0.128	-0.1	-0.166	-0.002	0.231	0.129	0.069	-0.262	-0.143	-0.102	-0.014	-0.071	-0.022	0.14	0.415	-0.012	0.018	0.086	
Lactose		-0.183	0.092	-0.04	0.695	-0.524	-0.524	-0.524	-0.029	0.188	0.266	0.4	0.135	-0.294	0.892	0.695	-0.164	-0.524	0.077	-0.013	-0.267	
Lactulose		0.458	0.208	0.126	0.029	0.156	-0.067	-0.273	-0.235	-0.447	0.638	0.526	-0.286	0.062	-0.811	0.531	-0.35	-0.103	0.043	0.062	0.06	
Leucine		-0.041	0.212	0.216	-0.041	0.131	-0.041	-0.041	-0.041	0.257	-0.041	-0.041	-0.041	-0.041	-0.041	-0.041	-0.041	-0.041	-0.041	-0.041	-0.041	
Levulinat		-0.102	-0.102	0.17	0.234	-0.102	-0.102	-0.102	-0.102	-0.102	-0.102	0.226	0.144	-0.102	0.11	-0.102	0.368	0.002	0.082	0.232	-0.102	
Maleate		0.02	-0.029	-0.029	0.029	-0.029	-0.029	0.152	-0.029	-0.029	-0.029	-0.029	-0.029	-0.001	0.013	-0.029	-0.029	0.151	-0.029	-0.029	-0.029	
Malonate		0.113	-0.024	-0.107	0.236	-0.134	-0.186	0.098	-0.075	-0.158	-0.036	-0.031	-0.162	0.111	-0.14	-0.204	-0.143	-0.166	0.115	1.996	-0.198	
Maltose		-0.082	-0.082	-0.082	0.125	0.096	-0.082	-0.082	0.447	0.297	0.07	-0.082	-0.082	0.178	-0.082	-0.082	-0.082	-0.082	-0.014	0.249	-0.082	
Mandelate		-0.055	-0.192	-0.067	-0.061	-0.015	0.004	0.182	-0.164	-0.023	-0.192	-0.192	-0.049	-0.047	-0.04	-0.007	0.177	-0.053	-0.04	-0.056	-0.033	
Mannitol		-0.186	0.464	0.302	-0.186	1.269	0.336	0.464	-0.186	-0.186	-0.186	-0.186	0.312	-0.186	-0.186	-0.186	-0.186	-0.186	-0.186	-0.186	-0.186	
Mannose		-0.047	-0.047	0.146	0.22	-0.047	-0.047	0.459	-0.047	-0.047	-0.047	-0.047	-0.047	-0.047	-0.047	-0.047	0.23	-0.047	-0.047	-0.047	-0.047	
Melatonin		-0.083	-0.156	-0.086	0	0.141	0.018	-0.156	-0.068	-0.084	-0.107	0.053	-0.015	-0.016	-0.104	-0.051	0.682	-0.074	-0.02	-0.059	-0.065	
Methanol		0.062	-0.109	-0.213	-0.006	-0.065	-0.029	-0.213	0.419	-0.154	-0.159	-0.144	-0.148	-0.213	0.512	-0.213	-0.079	0.056	-0.213	0.916	0.226	

Sample	LANC001	LANC011	LANC002	LANC023	LANC036	LANC003	LANC024	LANC004	LANC015	LANC025	LANC005	LANC026	LANC006	LANC017	LANC027	LTHTr002	LANC007	LANC008	LANC019	LTHTr005
Group	Control	Control	Control	Control	Control	Control	Control	Control	Control	Control	Control	Control	Control	Control	Control	Control	Control	Control	Control	Control
Methionine	0.191	0.008	-0.061	0.087	-0.191	-0.094	0.254	-0.191	-0.191	0.252	0.243	-0.191	0.282	-0.136	-0.191	0.331	-0.191	0.311	-0.191	0.431
Methylamine	0.061	-0.158	-0.128	0.011	-0.158	-0.105	0.27	0.005	-0.071	0.418	0.08	0.077	0.014	0.036	-0.158	-0.158	-0.027	-0.089	0.078	-0.037
Methylguanidine	-0.049	0.241	-0.172	-0.1	0.056	0.332	-0.123	0.198	-0.172	0.059	-0.172	-0.074	-0.081	-0.082	0.076	0.292	-0.172	-0.084	-0.11	0.022
Methylsuccinate	0.006	0.12	-0.027	0.358	-0.309	-0.049	0.009	0.127	0.033	0.108	-0.159	-0.051	-0.126	0.11	-0.11	0.218	-0.137	-0.131	0.333	0.275
myo.Inositol	0.907	-0.15	-0.15	-0.15	0.387	-0.15	0.186	-0.15	-0.15	0.242	-0.15	-0.15	0.512	-0.15	-0.15	-0.15	-0.15	-0.15	1.854	-0.15
N.N.Dimethylformamide	-0.031	0.086	0.074	0.023	-0.295	-0.147	-0.165	-0.068	0.047	0.076	-0.112	-0.035	0.015	0.29	-0.092	-0.106	-0.033	0.035	0.217	0.071
N.N.Dimethylglycine	-0.077	-0.064	-0.077	-0.056	-0.095	-0.095	-0.007	-0.02	0.059	0.051	-0.074	0.113	-0.061	0.02	0.143	0.001	-0.081	0.108	-0.022	0.065
N6.Acetyllysine	0.324	-0.114	-0.114	-0.114	0.313	0.186	-0.114	-0.114	-0.114	0.033	-0.114	-0.114	-0.114	0.03	0.34	-0.114	0.007	-0.114	-0.008	0.237
N.Acetylaspartate	0.142	-0.14	0.287	-0.14	0.215	-0.14	-0.14	-0.14	0.171	0.349	-0.14	-0.14	-0.14	0.262	-0.14	-0.14	-0.017	-0.14	0.054	0.153
N.Acetylcysteine	-0.02	-0.02	-0.02	-0.02	-0.02	-0.02	0.798	-0.02	-0.02	-0.02	-0.02	-0.02	-0.02	-0.02	-0.02	-0.02	-0.02	-0.02	-0.02	-0.02
N.Acetylglucosamine	0.791	-0.087	-0.087	-0.087	-0.087	-0.087	-0.087	-0.087	0.248	-0.087	-0.087	-0.087	-0.087	0.006	-0.087	-0.087	0.241	-0.087	-0.087	-0.087
N.Acetylglutamate	-0.199	0.14	-0.199	0.082	0.33	0.017	-0.033	0.025	0.067	0.048	-0.006	0.112	-0.199	-0.006	-0.199	-0.076	0.011	-0.199	-0.001	0.231
N.Acetylglutamine	-0.033	-0.033	-0.033	-0.033	-0.033	-0.033	-0.033	-0.033	-0.033	-0.033	-0.033	-0.033	-0.033	-0.033	0.64	-0.033	-0.033	-0.033	-0.033	-0.033
N.Acetyllysine	-0.016	-0.016	-0.016	-0.016	-0.016	-0.016	-0.016	-0.016	-0.016	-0.016	-0.016	-0.016	-0.016	-0.016	-0.016	-0.016	-0.016	-0.016	-0.016	-0.016
N.Acetylmethionine	-0.074	-0.074	-0.074	-0.074	-0.074	0.096	-0.074	-0.074	-0.074	-0.074	-0.074	-0.074	-0.074	-0.074	-0.074	-0.074	-0.074	-0.074	-0.074	-0.074
N.Acetylserotonin	-0.013	0.217	-0.051	-0.128	-0.018	0.119	0.085	-0.049	0.025	0	0.003	-0.001	0.042	0.068	0.031	0.119	-0.128	-0.128	-0.128	-0.128
N.Acetyltyrosine	0.048	-0.096	-0.011	-0.096	0.135	-0.096	0.033	0.011	0.027	-0.096	-0.096	0.019	0.027	-0.096	0.065	-0.096	0	0.034	-0.096	0.015
NADH	-0.015	-0.015	-0.015	-0.015	-0.015	-0.015	0.078	-0.015	-0.015	-0.015	-0.015	-0.015	-0.015	0.142	-0.015	-0.015	-0.015	-0.015	-0.015	-0.015
NADPH	-0.01	-0.01	-0.01	-0.01	-0.01	-0.01	-0.01	-0.01	-0.01	-0.01	-0.01	-0.01	0.162	-0.01	-0.01	-0.01	-0.01	-0.01	-0.01	-0.01
N.Carbamoylaspartate	-0.232	-0.232	-0.232	0.648	-0.232	-0.232	-0.232	-0.232	-0.232	0.548	0.624	-0.232	-0.232	-0.232	-0.232	-0.232	-0.232	0.164	-0.232	-0.232
N.Carbamoyl...alanine	1.009	-0.026	-0.026	-0.026	-0.026	-0.026	-0.026	-0.026	-0.026	-0.026	-0.026	-0.026	-0.026	-0.026	-0.026	-0.026	-0.026	-0.026	-0.026	-0.026
Nicotinurate	-0.005	-0.005	-0.005	-0.005	-0.005	-0.005	-0.005	-0.005	-0.005	-0.005	-0.005	-0.005	-0.005	-0.005	-0.005	-0.005	-0.005	0.198	-0.005	-0.005
N.Methylhydantoin	0.088	0.074	-0.157	-0.072	-0.157	0.008	-0.074	0.112	-0.061	-0.045	-0.174	-0.029	-0.053	-0.017	-0.089	0.496	-0.103	-0.032	0.265	0.081
N.Nitrosodimethylamine	-0.076	0.285	0.237	-0.08	-0.317	0.093	0.128	-0.092	-0.082	-0.233	-0.077	0.117	-0.054	-0.112	0.053	-0.185	-0.058	-0.053	0.331	0.598
N.Phenylacetyllysine	-0.046	0.107	0.027	-0.033	0.224	0.024	0.288	-0.142	-0.265	-0.155	-0.183	-0.21	-0.164	-0.029	-0.184	0.526	-0.076	-0.168	-0.18	-0.19
N.Phenylacetylphenylalanine	-0.011	-0.011	-0.011	-0.011	-0.011	-0.011	-0.011	-0.011	-0.011	-0.011	-0.011	-0.011	-0.011	-0.011	-0.011	-0.011	-0.011	-0.011	-0.011	-0.011
N..Acetyllysine	0.364	0.372	-0.168	-0.168	-0.168	0.211	-0.168	-0.168	0.169	-0.005	-0.168	-0.009	0.308	0.014	-0.039	-0.168	-0.168	0.324	-0.168	-0.113
O.Acetylcarnitine	-0.213	-0.088	0.598	0.79	-0.315	-0.009	0.663	-0.255	0.191	0.373	0.094	0.333	-0.253	-0.001	-0.152	-0.288	0.168	-0.253	-0.3	-0.152
O.Acetylcholine	-0.133	-0.133	-0.092	-0.083	0.01	0.218	-0.088	-0.046	0.123	0.211	-0.006	0.06	-0.133	0.047	0.112	0.034	0.055	-0.133	0.057	-0.011
o.Cresol	-0.105	-0.105	0.21	-0.105	0.29	-0.105	0.167	-0.105	-0.105	0.181	-0.105	-0.105	-0.105	-0.105	-0.105	0.196	0.123	-0.105	-0.105	0.127
O.Phosphocholine	-0.106	0.024	0.071	0.04	-0.027	0	-0.008	-0.035	-0.058	-0.081	0.09	-0.03	-0.027	0.255	-0.066	-0.052	-0.106	-0.027	0.14	0.941
Ornithine	-0.06	-0.06	-0.06	-0.06	-0.06	-0.06	-0.06	-0.06	-0.06	-0.06	-0.06	-0.06	-0.06	-0.06	-0.06	-0.06	-0.06	-0.06	-0.06	1.274
Oxypurinol	0.081	-0.303	0.147	-0.494	-1.091	0.002	-0.985	3.381	-0.25	0.779	-0.502	0.009	0.006	0.578	-0.711	-0.905	-0.748	-0.016	2.806	1.397
Pantothenate	-0.043	-0.07	-0.032	-0.033	0.138	0.102	-0.037	-0.06	0.001	0.102	-0.069	-0.041	0.05	0.002	-0.123	-0.172	0.111	-0.172	0.129	-0.035
p.Cresol	0.048	-0.118	-0.006	0.01	-0.118	0.038	0.033	0.066	0.011	-0.118	-0.118	0.018	0.027	0.04	0.007	-0.118	0.007	-0.118	-0.118	-0.003
Phenylacetate	-0.005	0.02	-0.02	-0.039	0.005	0.105	0.134	0.144	0.043	-0.062	-0.012	-0.103	0.163	-0.002	-0.13	-0.068	0.014	0.156	0.014	0.011
Propylene.glycol	-0.093	0.619	-0.014	-0.093	-0.093	-0.012	0.213	-0.093	-0.093	-0.02	0.08	0.044	-0.093	-0.093	-0.022	0.1	0.194	-0.093	-0.011	-0.093
Protocatechuate	-0.01	-0.01	-0.01	-0.01	-0.01	-0.01	-0.01	-0.01	-0.01	-0.01	-0.01	-0.01	0.119	-0.01	-0.01	-0.01	-0.01	-0.01	-0.01	0.277
Pyridoxine	-0.043	0.052	-0.021	0.018	0.086	0.076	0.007	0.031	0.024	-0.012	-0.007	-0.026	-0.01	-0.011	0.005	0.004	-0.068	-0.003	-0.014	0.024
Pyrimidine	0.073	-0.034	-0.034	-0.034	-0.034	-0.034	-0.034	0.084	-0.034	-0.034	-0.034	-0.034	-0.034	-0.034	-0.034	0.535	-0.034	-0.034	-0.034	-0.034
Pyroglutamate	-0.028	-0.028	-0.028	-0.028	-0.028	-0.028	-0.028	-0.028	-0.028	-0.028	-0.028	-0.028	-0.028	-0.028	-0.028	-0.028	-0.028	-0.028	-0.028	-0.028
Pyruvate	0.116	-0.104	-0.104	-0.104	-0.104	0.241	0.169	0.018	0.131	0.627	0.041	-0.104	-0.104	-0.104	0.068	-0.104	0.049	-0.104	0.086	0.147
Quinolate	0.102	-0.14	-0.14	0.08	-0.14	-0.14	-0.14	-0.14	-0.14	0.131	-0.14	-0.14	-0.14	0.2	-0.14	-0.14	0.135	-0.14	0.079	0.099

Sample	LANC001	LANC011	LANC002	LANC023	LANC036	LANC003	LANC024	LANC004	LANC015	LANC025	LANC005	LANC026	LANC006	LANC017	LANC027	LTHTr002	LANC007	LANC008	LANC019	LTHTr005
Group	Control	Control	Control	Control	Control	Control	Control	Control	Control	Control	Control	Control	Control	Control	Control	Control	Control	Control	Control	Control
Riboflavin	-0.018	0.239	0.063	-0.04	-0.129	0.16	-0.077	0.058	0.138	-0.064	-0.033	-0.073	-0.058	-0.129	0.01	0.221	0.057	-0.054	-0.02	
Ribose	0.543	-0.793	0.009	0.432	0.661	0.652	-0.793	-0.793	0.458	0.335	0.707	-0.173	0.159	-0.793	-0.088	0.168	-0.793	0.642	0.416	-0.793
Saccharopine	-0.12	-0.12	0.623	-0.12	-0.12	-0.12	-0.12	-0.12	-0.12	0.738	-0.12	-0.12	-0.12	-0.12	-0.12	0.582	-0.12	-0.12	-0.12	-0.12
S.Adenosylhomocysteine	-0.014	-0.014	-0.014	-0.014	-0.014	-0.014	-0.014	-0.014	-0.014	-0.014	-0.014	-0.014	-0.014	-0.014	-0.014	-0.014	-0.014	-0.014	-0.014	-0.014
Salicylate	0.052	-0.031	-0.031	-0.031	-0.031	-0.031	-0.031	-0.031	-0.031	-0.031	0.35	-0.031	0.062	-0.031	-0.031	-0.031	-0.031	-0.031	-0.031	-0.031
Salicylurate	0.028	-0.089	-0.089	-0.089	-0.089	-0.089	-0.089	-0.089	0.142	0.039	-0.089	-0.089	0.101	-0.089	0.28	-0.089	-0.007	0.099	-0.089	-0.089
Sarcosine	-0.053	-0.053	-0.053	-0.053	0.164	0.014	0.28	0.031	-0.053	-0.053	-0.053	-0.053	-0.053	-0.053	-0.053	0.087	-0.053	-0.053	-0.053	0.04
Serotonin	-0.081	0.195	-0.081	-0.081	-0.081	-0.081	0.46	-0.019	0.006	-0.002	0.043	-0.081	-0.081	0.206	-0.081	-0.081	-0.081	-0.081	-0.081	-0.081
sn.Glycero.3.phosphocholine	-0.207	-0.096	-0.183	0.453	-0.158	-0.171	0.068	-0.108	0.856	-0.169	0.067	0.455	-0.207	-0.034	-0.091	-0.169	-0.207	-0.207	0.118	-0.09
Succinate	-0.043	0.363	-0.118	0.067	-0.307	-0.067	-0.194	-0.099	0.065	-0.084	-0.163	0.014	0.123	0.147	-0.128	0.137	-0.307	0.13	-0.084	0.069
Succinylacetone	-0.076	0.4	0.54	0.027	0.161	-0.167	-0.003	-0.053	-0.114	0.05	-0.29	-0.015	0.118	0.134	-0.049	0.347	0.401	0.115	0.006	-0.21
Sucrose	-0.068	-0.068	0.009	-0.068	-0.068	-0.068	-0.068	-0.068	-0.068	-0.068	0.068	0.084	0.483	-0.009	-0.068	0.006	0.14	0.478	-0.068	-0.068
Syringate	-0.024	0.36	-0.044	-0.023	-0.079	-0.044	0.569	-0.045	0.142	-0.071	-0.048	-0.079	-0.028	-0.018	0.006	0.599	-0.057	-0.034	-0.079	-0.054
Tartrate	-0.02	0.058	-0.014	-0.133	-0.063	-0.005	-0.052	-0.076	-0.031	-0.133	-0.009	-0.025	-0.133	-0.01	-0.133	0.283	-0.018	-0.133	-0.133	-0.022
Taurine	0.378	-0.207	0.317	-0.207	-0.207	0.151	0.158	1.154	-0.207	-0.207	1.362	0.047	-0.207	-0.207	-0.207	-0.207	-0.207	-0.207	-0.207	0.031
Theophylline	-0.056	0.027	0.087	-0.062	0.042	-0.071	0.071	-0.013	0.186	-0.092	-0.003	-0.128	0.155	-0.026	-0.036	0.35	-0.04	0.166	-0.093	-0.046
Threonate	-0.819	-0.159	0.196	0.605	0.494	-0.15	0.357	0.885	-0.142	0.017	0.663	0.092	-0.218	0.225	-0.466	1.199	0.325	-0.218	0.421	-0.819
Threonine	0.072	-0.226	-0.226	0.146	0.058	0.151	0.053	0.113	0.082	-0.226	-0.226	0.194	0.036	0.056	0.024	0.175	-0.226	0.032	0.218	0.239
Thymidine	-0.013	-0.013	-0.013	-0.013	-0.013	-0.013	-0.013	-0.013	0.139	-0.013	-0.013	-0.013	-0.013	-0.013	-0.013	-0.013	-0.013	-0.013	-0.013	-0.013
Thymol	-0.17	0.07	0.08	0.112	0.073	-0.05	0.014	0.047	0.056	0.047	0.085	0.051	0.045	0.109	0.048	-0.17	-0.17	0.016	-0.17	0.148
trans.4.Hydroxy.L.proline	-0.071	-0.071	-0.071	-0.071	-0.071	-0.071	-0.071	0.341	-0.071	-0.071	-0.071	-0.071	-0.071	-0.071	-0.071	-0.071	-0.071	-0.071	-0.071	-0.071
trans.Aconitate	0.12	-0.065	0.018	0.072	0.066	-0.101	-0.055	0.128	0.106	0.024	-0.186	-0.074	-0.01	0.012	0.014	-0.08	0.1	-0.02	0.116	0.112
Trehalose	-0.042	-0.042	-0.042	-0.042	-0.042	-0.042	-0.042	-0.042	-0.042	-0.042	-0.042	0.034	-0.007	-0.042	-0.042	0.015	-0.042	-0.042	-0.042	-0.042
Trigonelline	-0.01	0.265	-0.107	-0.095	-0.02	0.613	-0.06	-0.035	-0.105	-0.055	0.307	0.032	-0.08	0.402	-0.044	0.318	-0.187	-0.084	-0.106	-0.121
Trimethylamine.N.oxide	-0.15	0.101	-0.163	0.039	-0.148	-0.166	-0.162	0.282	-0.153	-0.16	-0.152	-0.003	-0.058	-0.154	-0.169	-0.165	-0.167	-0.048	-0.171	-0.162
Tropate	-0.023	-0.023	-0.023	-0.023	-0.023	-0.023	-0.023	-0.023	-0.023	-0.023	-0.023	-0.023	-0.023	-0.023	-0.023	-0.023	-0.023	-0.023	-0.023	-0.023
Tryptophan	0.103	-0.223	-0.144	-0.014	0.005	-0.223	-0.104	-0.045	-0.057	-0.072	-0.043	0.034	0.037	-0.074	-0.223	-0.05	-0.065	0.044	-0.12	-0.017
Tyramine	-0.049	-0.049	-0.049	-0.049	-0.049	-0.049	-0.049	-0.049	0.132	-0.049	-0.049	-0.049	-0.049	-0.049	-0.049	0.358	0.22	-0.049	-0.049	-0.049
Tyrosine	-0.143	-0.143	-0.143	-0.143	-0.143	-0.143	-0.143	-0.143	0.323	-0.143	0.053	-0.143	0.183	0.235	-0.143	-0.143	0.11	0.191	0.457	0.213
UDP.galactose	-0.017	-0.017	-0.017	0.259	-0.017	-0.017	-0.017	-0.017	-0.017	-0.017	-0.017	-0.017	-0.017	-0.017	-0.017	-0.017	-0.017	-0.017	0.257	-0.017
UDP.glucose	-0.032	-0.032	-0.032	-0.032	-0.032	-0.032	-0.032	-0.032	-0.032	-0.032	0.312	-0.032	0.051	-0.032	-0.032	-0.032	-0.032	0.068	0.1	-0.032
UDP.glucuronate	-0.053	-0.053	-0.053	-0.053	0.133	-0.053	0.076	-0.053	-0.053	-0.053	-0.053	0.182	-0.053	-0.053	-0.053	-0.053	0.107	-0.053	-0.053	0.054
UDP.N.Acetylglucosamine	-0.08	-0.08	-0.08	0.125	-0.08	0.102	-0.08	-0.08	0.041	-0.08	-0.08	0.005	0.01	0.094	0.084	0.019	-0.08	-0.08	0.102	0.008
UMP	0.217	-0.038	-0.038	-0.038	-0.038	-0.038	0.07	-0.038	-0.038	-0.038	-0.038	-0.038	0.109	0.074	-0.038	-0.038	0.083	-0.038	-0.038	-0.038
Uracil	-0.088	-0.088	0.106	-0.088	-0.088	-0.088	-0.088	-0.088	-0.088	-0.088	-0.088	-0.088	0.23	0.11	-0.088	-0.088	-0.088	0.096	0.227	-0.088
Uridine	-0.027	-0.027	-0.027	-0.027	-0.027	-0.027	-0.027	-0.027	-0.027	-0.027	0.345	-0.027	-0.027	-0.027	-0.027	-0.027	-0.027	-0.027	-0.027	-0.027
Urocanate	-0.055	-0.055	0.079	-0.055	-0.055	-0.055	0.047	-0.055	-0.055	0.129	-0.055	-0.055	-0.055	0.148	-0.055	-0.055	-0.055	-0.055	0.128	-0.055
Valerate	-0.046	-0.046	-0.046	-0.046	-0.046	-0.046	0.714	-0.046	-0.046	-0.046	-0.046	-0.046	-0.046	-0.046	-0.046	-0.046	-0.046	-0.046	0.146	-0.046
Valine	-0.05	0.052	-0.036	0.172	-0.153	-0.114	-0.005	-0.042	0.097	0.051	-0.079	0.133	0.024	-0.021	-0.046	-0.09	-0.257	0.028	0.173	-0.047
Vanillate	0.014	0.156	-0.035	-0.035	-0.035	0.179	-0.035	-0.035	-0.035	-0.035	-0.035	-0.035	-0.035	0.006	0.081	-0.035	-0.035	-0.035	-0.035	0.081
Xanthine	0.117	0.14	-0.028	0.022	-0.048	0.07	0.353	-0.164	-0.039	-0.164	0.076	-0.044	-0.099	-0.039	-0.164	0.017	-0.084	-0.108	0.024	-0.164
Xanthosine	0.105	-0.034	-0.001	0.009	-0.034	-0.034	-0.034	-0.034	-0.034	-0.034	-0.034	-0.034	-0.034	-0.034	-0.034	0.2	0.001	-0.034	-0.034	-0.034
Xanthurenate	-0.009	-0.102	0.052	0.096	-0.102	0.157	0.102	0.038	-0.022	-0.102	-0.102	-0.032	-0.032	-0.032	-0.032	0.001	-0.068	-0.06	-0.05	-0.048

Sample	LANC001	LANC011	LANC002	LANC023	LANC036	LANC003	LANC024	LANC004	LANC015	LANC025	LANC005	LANC026	LANC006	LANC017	LANC027	LTHTr002	LANC007	LANC008	LANC019	LTHTr005
Group	Control	Control	Control	Control	Control	Control	Control	Control	Control	Control	Control	Control	Control	Control	Control	Control	Control	Control	Control	Control
Xylitol	-0.177	-0.177	-0.177	-0.177	0.299	-0.177	-0.177	0.292	-0.177	-0.177	0.763	-0.177	-0.177	-0.177	-0.177	-0.177	-0.177	0.361	-0.177	-0.177
Xylose	-0.066	-0.066	0.021	-0.066	0.332	-0.066	-0.066	-0.066	-0.066	-0.066	-0.066	-0.066	-0.066	-0.066	-0.066	-0.066	-0.066	-0.066	-0.066	-0.066
X..Alanine	-0.031	-0.031	-0.031	-0.031	-0.031	-0.031	-0.031	-0.031	-0.031	-0.031	-0.031	-0.031	-0.031	-0.031	-0.031	-0.031	-0.031	-0.031	-0.031	-0.031
X..Glutamylphenylalanine	0.11	-0.064	-0.064	-0.064	-0.064	-0.064	-0.064	-0.064	-0.064	-0.064	-0.064	-0.064	-0.064	-0.064	-0.064	-0.064	-0.064	-0.064	0.145	-0.064
X..Methylhistidine	-0.205	0.405	0.104	0.583	-0.286	-0.29	-0.329	-0.441	0.15	0.064	0.48	0.26	-0.034	-0.379	-0.085	-0.313	0.225	-0.165	0.32	-0.185
X..Methylhistidine.1	-0.031	0.022	-0.071	-0.04	0.514	-0.065	-0.13	-0.155	-0.144	-0.052	0.101	-0.009	0.016	-0.029	0.18	0.134	-0.145	0.032	-0.059	-0.109

Table B

Sample Group	LANC009	LANC020	LTHTr006	LANC010	LANC032	LTHTr010		LANC034	LANC012	LANC013	LANC037	LANC038	LANC016	LANC040	LANC018	LANC028	LTHTr003	LANC029	LANC030	LANC021	LTHTr013	
	Control	Control	Control	Control	Control	Control		IBD	IBD	IBD	IBD	IBD	IBD	IBD	IBD	IBD	IBD	IBD	IBD	IBD	IBD	
X1.3.Dihydroxyacetone	-0.014	-0.014	-0.014	-0.014	-0.014	-0.014		-0.014	-0.014	0.435	-0.014	-0.014	-0.014	-0.014	-0.014	-0.014	-0.014	-0.014	-0.014	-0.014	-0.014	-0.014
X1.3.Dimethylurate	-0.155	0.136	-0.04	-0.095	0.316	-0.006		0.034	0.091	-0.07	-0.037	-0.07	-0.082	-0.01	0.011	-0.105	-0.072	0.026	-0.106	0.08	-0.155	
X1.6.Anhydro...D.glucose	-0.077	-0.077	0.473	-0.077	-0.009	-0.035		0.07	-0.077	-0.077	0.103	-0.077	0.053	-0.077	-0.077	0.061	-0.077	0.017	-0.077	0.084	0.023	
X1.7.Dimethylxanthine	-0.093	-0.198	-0.045	-0.09	0.193	0.158		0.315	-0.02	0.32	0.003	0.09	-0.171	-0.041	0.244	-0.174	-0.054	0.052	-0.029	0.202	0.003	
X1.Methylnicotinamide	0.084	0.415	-0.006	0.016	-0.021	-0.09		-0.033	-0.25	-0.051	-0.083	0.072	0.199	0.156	-0.12	0.035	0.103	-0.05	-0.25	-0.179	0.197	
X2..Deoxyadenosine	-0.043	-0.043	0.119	-0.043	-0.043	0.231		-0.043	-0.043	-0.043	-0.043	-0.043	-0.043	-0.043	0.236	0.179	-0.043	-0.043	-0.043	-0.043	0.255	
X2..Deoxyguanosine	-0.027	-0.027	0.04	-0.027	-0.027	-0.027		-0.027	-0.027	0.109	-0.027	-0.027	-0.027	-0.027	-0.027	-0.027	0.113	-0.027	0.106	0.076	-0.027	
X2..Deoxyinosine	-0.011	-0.011	-0.011	-0.011	-0.011	-0.011		0.092	-0.011	-0.011	-0.011	-0.011	-0.011	-0.011	-0.011	-0.011	-0.011	-0.011	-0.011	-0.011	-0.011	
X2.Aminoadipate	0.497	-0.113	-0.113	-0.113	-0.113	-0.113		-0.113	0.792	-0.113	-0.113	1.469	-0.113	-0.113	-0.113	-0.113	-0.113	-0.113	-0.113	-0.113	0.324	
X2.Aminobutyrate	-0.212	-0.212	-0.212	0.477	-0.02	-0.212		0.225	-0.212	-0.044	-0.137	-0.11	-0.212	-0.008	-0.212	0.249	-0.136	0.669	-0.212	-0.136	-0.212	
X2.Ethylacrylate	-0.034	-0.034	-0.034	-0.034	-0.034	-0.034		-0.034	-0.034	-0.034	-0.034	-0.034	-0.034	0.104	-0.034	0.231	-0.034	-0.034	-0.034	-0.034	-0.034	
X2.Furoylglycine	0.022	-0.063	-0.063	-0.063	0.21	-0.063		0.03	0.254	0.222	-0.063	-0.063	-0.063	-0.063	-0.063	0.062	-0.063	-0.063	-0.063	-0.063	-0.063	
X2.Hydroxy.3.methylvalerate	-0.035	0.147	-0.035	-0.035	0.178	-0.035		-0.035	-0.035	-0.035	-0.035	-0.035	0.068	-0.035	0.164	0.21	-0.035	-0.035	-0.035	-0.035	-0.035	
X2.Hydroxybutyrate	-0.009	-0.009	-0.009	-0.009	-0.009	-0.009		-0.009	-0.009	-0.009	-0.009	-0.009	-0.009	-0.009	-0.009	-0.009	-0.009	-0.009	-0.009	-0.009	-0.009	
X2.Hydroxyisobutyrate	0.063	0.137	-0.234	0.094	-0.002	-0.251		-0.106	-0.228	-0.035	-0.014	0.019	0.102	0.167	0.06	0	0.124	-0.033	0.078	0.216	-0.018	
X2.Hydroxyisocaproate	-0.015	-0.015	-0.015	-0.015	-0.015	-0.015		-0.015	-0.015	-0.015	-0.015	-0.015	-0.015	-0.015	-0.015	-0.015	0.023	-0.015	-0.015	-0.015	0.036	
X2.Hydroxyisovalerate	-0.011	-0.011	-0.011	-0.011	-0.011	0.415		-0.011	-0.011	-0.011	-0.011	-0.011	-0.011	-0.011	-0.011	-0.011	-0.011	-0.011	-0.011	-0.011	-0.011	
X2.Hydroxyphenylacetate	-0.119	0.04	0.005	0.133	-0.119	-0.119		0.107	-0.119	-0.119	-0.01	0.051	-0.119	-0.119	-0.119	-0.008	-0.119	0.256	0.061	-0.119	0.395	
X2.Hydroxyvalerate	-0.044	-0.044	-0.044	-0.044	-0.044	-0.044		-0.044	-0.044	-0.044	-0.044	-0.044	-0.044	-0.044	-0.044	0.486	-0.044	-0.044	-0.044	-0.044	-0.044	
X2.Methylglutarate	-0.022	-0.022	0.269	-0.022	-0.022	-0.022		-0.022	-0.022	-0.022	-0.022	-0.022	-0.022	-0.022	-0.022	-0.022	-0.022	-0.022	-0.022	-0.022	-0.022	
X2.Oxocaproate	-0.012	-0.012	-0.012	-0.012	-0.012	-0.012		-0.012	-0.012	-0.012	-0.012	-0.012	-0.012	-0.012	0.485	-0.012	-0.012	-0.012	-0.012	-0.012	-0.012	
X2.Oxoglutarate	-0.111	-0.111	0.615	-0.111	-0.111	0.205		0.555	0.293	-0.111	-0.111	-0.111	-0.111	0.528	-0.111	-0.111	-0.111	-0.111	-0.111	-0.111	-0.111	
X2.Oxoisocaproate	-0.004	-0.004	-0.004	-0.004	-0.004	-0.004		-0.004	0.175	-0.004	-0.004	-0.004	-0.004	-0.004	-0.004	-0.004	-0.004	-0.004	-0.004	-0.004	-0.004	
X2.Phenylpropionate	-0.006	-0.006	-0.006	-0.006	-0.006	-0.006		-0.006	-0.006	0.124	-0.006	-0.006	-0.006	-0.006	-0.006	-0.006	-0.006	-0.006	-0.006	-0.006	-0.006	
X3.4.Dihydroxybenzeneacetate	-0.085	0.064	0.042	-0.085	0.089	-0.085		0.026	0.151	0.134	0.061	0.136	0.003	-0.085	0.127	-0.085	-0.001	0.06	-0.085	-0.085	0.011	
X3.4.Dihydroxymandelate	-0.076	-0.076	0.167	0.027	-0.076	0.141		0.023	-0.076	0.104	-0.076	0.169	0.022	-0.076	-0.076	0.001	-0.076	0.113	-0.076	0.053	0.049	
X3.5.Dibromotyrosine	0.242	-0.123	-0.123	-0.112	-0.113	-0.123		-0.123	-0.123	-0.123	-0.123	0.535	0.013	-0.123	-0.123	-0.113	0.605	-0.123	-0.073	0.026	0.681	
X3.Aminoisobutyrate	-0.224	-0.194	-0.331	0.518	0.032	-0.15		-0.095	-0.144	0.584	-0.18	-0.084	0.173	-0.171	-0.232	-0.331	-0.331	-0.331	0.085	-0.331	-0.188	
X3.Chlorotyrosine	0.195	-0.055	-0.055	-0.055	-0.055	-0.055		-0.055	-0.055	-0.055	-0.055	0.207	0.086	-0.055	-0.055	-0.055	-0.055	0.231	-0.055	-0.055	-0.055	
X3.Hydroxy.3.methylglutarate	-0.099	-0.042	-0.028	-0.018	-0.097	-0.02		0.016	0.632	0.007	-0.111	-0.016	-0.04	-0.055	-0.057	0.182	-0.114	0.027	-0.112	0.306	-0.167	
X3.Hydroxybutyrate	-0.62	-0.62	-0.62	-0.461	-0.398	-0.62		-0.489	-0.62	-0.62	-0.558	-0.598	-0.575	-0.614	-0.62	5.107	-0.525	0.132	-0.62	-0.62	-0.615	
X3.Hydroxyisobutyrate	-0.062	-0.062	0.013	-0.062	-0.062	-0.062		-0.062	-0.062	-0.062	-0.062	-0.062	-0.062	-0.062	-0.062	1.086	-0.062	-0.062	-0.062	-0.062	-0.062	
X3.Hydroxyisovalerate	-0.067	0.353	-0.171	0.047	-0.165	0.009		-0.082	-0.171	-0.071	-0.062	0.053	0.177	-0.059	0.042	0.273	0	-0.128	0.23	0.011	-0.131	
X3.Hydroxykynurenine	-0.038	-0.038	-0.038	-0.038	0.084	-0.038		-0.038	-0.038	-0.038	0.194	-0.038	-0.038	0.147	0.107	-0.038	0.228	-0.038	-0.038	0.14	-0.038	
X3.Hydroxymandelate	0.022	-0.006	-0.04	0.008	0.013	-0.105		0.06	-0.105	-0.105	-0.105	-0.105	0.046	-0.105	-0.035	0.049	0.127	0.044	-0.105	-0.007	1.15	
X3.Hydroxyphenylacetate	0.086	-0.164	-0.049	-0.041	-0.036	-0.07		-0.062	0.125	-0.008	0.126	-0.01	-0.03	0.046	-0.066	-0.035	-0.025	-0.004	0.18	-0.046	0.116	
X3.Indoxylsulfate	0.226	0.251	0.082	-0.205	0.013	0.283		0.039	-0.205	0.04	-0.205	0.403	0.334	-0.205	0.277	0.041	-0.005	-0.205	0.084	0.188	-0.205	
X3.Methyl.2.oxovalerate	-0.014	-0.014	-0.014	-0.014	-0.014	-0.014		-0.014	-0.014	-0.014	-0.014	-0.014	-0.014	-0.014	-0.014	-0.014	-0.014	0.192	-0.014	-0.014	-0.014	
X3.Methyladipate	-0.012	-0.012	-0.012	-0.012	-0.012	-0.012		-0.012	-0.012	-0.012	-0.012	-0.012	-0.012	-0.012	-0.012	-0.012	0.163	-0.012	-0.012	-0.012	-0.012	
X3.Methylglutarate	-0.108	0.057	0.08	0.291	-0.108	-0.108		0.127	-0.108	-0.108	0.03	0.094	0.106	-0.108	-0.108	-0.108	-0.108	0.248	0.083	-0.108	-0.108	
X3.Methylxanthine	-0.14	0.221	0.052	-0.036	0.219	-0.14		-0.083	-0.14	0.231	0.253	0.038	-0.026	0.25	-0.026	-0.094	0.142	-0.1	-0.044	0.069	0.004	

Sample	LANC009	LANC020	LHTR006	LANC010	LANC032	LHTR010		LANC034	LANC012	LANC013	LANC037	LANC038	LANC016	LANC040	LANC018	LANC028	LHTR003	LANC029	LANC030	LANC021	LHTR013
Group	Control	Control	Control	Control	Control	Control		IBD	IBD	IBD	IBD	IBD	IBD	IBD	IBD	IBD	IBD	IBD	IBD	IBD	IBD
X3.Methylxanthine	-0.14	0.221	0.052	-0.036	0.219	-0.14		-0.083	-0.14	0.231	0.253	0.038	-0.026	0.25	-0.026	-0.094	0.142	-0.1	-0.044	0.069	0.004
X3.Phenylpropionate	0.41	-0.034	-0.034	-0.034	-0.034	-0.034		-0.034	-0.034	-0.034	-0.034	-0.034	-0.034	-0.034	-0.034	-0.034	-0.034	-0.034	-0.034	-0.034	-0.034
X4.Aminohippurate	-0.011	-0.011	-0.011	-0.011	-0.011	-0.011		-0.011	-0.011	-0.011	0.207	-0.011	-0.011	-0.011	-0.011	-0.011	-0.011	-0.011	-0.011	-0.011	-0.011
X4.Guanidinobutanoate	-0.018	-0.018	-0.018	-0.018	-0.018	-0.018		-0.018	-0.018	-0.018	-0.018	-0.018	-0.018	-0.018	-0.018	-0.018	-0.018	-0.018	-0.018	-0.018	-0.018
X4.Hydroxy.3.methoxymandelate	0.102	0.024	-0.078	-0.015	-0.01	-0.021		-0.047	0.146	-0.107	0.095	-0.015	-0.062	-0.094	-0.12	-0.131	0.081	0.093	0.435	-0.061	-0.038
X4.Hydroxybenzoate	-0.069	-0.069	-0.069	-0.069	-0.069	-0.069		0.293	-0.069	0.215	-0.069	-0.069	-0.069	0.256	0.402	-0.069	-0.069	-0.069	-0.069	-0.069	-0.069
X4.Hydroxyphenylacetate	-0.217	-0.012	0.051	-0.05	0.061	-0.011		-0.069	0.087	-0.016	-0.217	0.068	-0.093	-0.029	0.467	-0.031	-0.082	0.389	0.133	-0.217	0.304
X4.Pyridoxate	-0.139	-0.121	0.068	0.03	0.089	0.136		0.231	-0.098	0.064	-0.012	-0.092	-0.118	-0.068	-0.129	-0.108	-0.144	-0.135	-0.099	-0.091	-0.005
X5.6.Dihydrothymine	0.131	-0.078	-0.078	-0.078	-0.078	-0.078		-0.078	0.228	0.344	-0.078	-0.078	-0.078	0.317	0.155	-0.078	0.762	-0.078	-0.078	-0.078	-0.078
X5.6.Dihydrouracil	-0.021	-0.021	-0.021	-0.021	-0.021	-0.021		-0.021	-0.021	-0.021	-0.021	-0.021	-0.021	-0.021	-0.021	-0.021	-0.021	-0.021	-0.021	-0.021	-0.021
X5.Aminolevulinate	0.075	0.028	0.001	-0.171	-0.173	-0.118		-0.248	-0.277	0.286	-0.099	-0.054	-0.186	-0.082	-0.131	0.357	0.055	-0.051	-0.019	0.025	-0.107
X5.Hydroxyindole.3.acetate	0.066	-0.014	-0.066	0.057	-0.066	-0.022		-0.077	0.206	0.051	0.014	0.075	-0.108	-0.158	-0.122	-0.078	-0.088	-0.045	0.275	0.04	0.681
X5.Hydroxylysine	-0.031	-0.031	-0.031	-0.031	-0.031	-0.031		-0.031	-0.031	-0.031	-0.031	-0.031	1.21	-0.031	-0.031	-0.031	-0.031	-0.031	-0.031	-0.031	-0.031
X5.Hydroxytryptophan	0.145	-0.175	-0.066	-0.104	0.074	-0.115		-0.011	-0.175	-0.175	0.053	-0.175	-0.042	0.032	0.001	-0.105	0.021	0.063	0.126	-0.004	1.059
X5.Methoxysalicylate	-0.06	-0.06	-0.06	0.064	-0.06	-0.06		-0.06	-0.06	0.086	0.212	-0.06	-0.06	0.468	-0.06	-0.06	0.127	-0.06	0.161	-0.06	-0.06
Acetaminophen	-0.085	-0.085	-0.085	-0.085	-0.002	-0.085		-0.085	-0.085	-0.085	0.169	-0.046	-0.085	0.277	-0.085	-0.085	-0.085	0.006	-0.085	-0.085	0.411
Acetate	-0.205	-0.01	-0.205	-0.051	0.009	-0.064		-0.052	0.029	0.244	1.31	0.016	-0.104	-0.178	-0.108	-0.041	-0.007	-0.065	0.003	0.047	-0.318
Acetoacetate	-0.504	-0.525	-0.516	0.128	-0.076	-0.505		-0.202	-0.451	-0.47	-0.446	-0.366	-0.269	-0.492	-0.525	2.153	-0.383	0.324	-0.048	-0.511	-0.42
Acetoin	-0.093	-0.093	0.057	-0.093	-0.093	-0.093		-0.093	0.218	0.041	0.056	-0.093	-0.093	0.013	0.357	-0.093	-0.093	-0.093	-0.093	0.094	0.138
Acetone	-0.133	-0.049	-0.201	0.076	-0.086	-0.221		-0.067	-0.174	-0.181	-0.182	-0.122	0.078	-0.191	-0.053	0.888	-0.072	0.002	0.182	-0.209	-0.152
Acetylsalicylate	0.074	-0.013	0.046	-0.021	-0.125	0.082		0.178	0.37	-0.125	-0.125	-0.125	0.094	-0.083	0.004	-0.037	0.088	-0.076	-0.009	0.074	-0.125
Adenine	-0.021	-0.021	-0.021	-0.021	-0.021	0.024		-0.021	-0.021	-0.021	-0.021	-0.021	0.096	-0.021	-0.021	-0.021	-0.021	-0.021	-0.021	-0.021	-0.021
Adenosine	0.233	-0.012	0.15	-0.012	-0.012	-0.012		-0.012	-0.012	-0.012	-0.012	-0.012	-0.012	-0.012	-0.012	-0.012	-0.012	-0.012	-0.012	-0.012	-0.012
Adipate	-0.023	-0.023	-0.023	-0.023	-0.023	-0.023		0.899	-0.023	-0.023	-0.023	-0.023	-0.023	-0.023	-0.023	-0.023	-0.023	-0.023	-0.023	-0.023	-0.023
ADP	-0.013	-0.013	-0.013	-0.013	-0.013	0.183		-0.013	-0.013	-0.013	-0.013	-0.013	-0.013	-0.013	-0.013	-0.013	-0.013	-0.013	-0.013	-0.013	-0.013
Alanine	-0.104	0.411	-0.118	0.029	0.156	-0.034		0.036	0.525	-0.032	0.681	-0.017	0.02	-0.097	-0.36	-0.182	0.056	-0.064	-0.081	-0.36	0.014
Allantoin	-0.002	-0.031	-0.024	0	0.021	-0.092		0.383	0.594	0.027	-0.167	-0.167	0.011	-0.167	0.051	0.037	-0.019	-0.167	0.053	0.181	-0.013
Alloisoleucine	0.096	-0.076	-0.076	-0.076	-0.076	-0.076		-0.076	-0.013	-0.076	0.203	0.241	-0.076	0.002	-0.076	-0.076	-0.076	-0.076	0.049	0.24	-0.076
Anserine	-0.037	0.043	-0.035	-0.036	-0.053	-0.144		-0.019	-0.04	0.085	0.063	-0.087	0.059	0.158	0.143	-0.195	-0.026	-0.025	0.026	0.087	0.098
Anthranilate	-0.03	-0.03	-0.03	-0.03	-0.03	-0.03		-0.03	-0.03	0.244	-0.03	-0.03	-0.03	-0.03	-0.03	-0.03	-0.03	-0.03	-0.03	-0.03	-0.03
Arabinitol	-0.121	-0.121	1.704	-0.121	-0.121	-0.121		-0.121	-0.121	0.605	-0.121	-0.121	-0.121	-0.121	-0.121	-0.121	-0.121	-0.121	-0.121	-0.121	-0.121
Arabinose	0.059	-0.328	0.285	-0.328	0.241	-0.328		-0.328	-0.328	0.348	-0.328	-0.137	0.924	0.93	-0.328	-0.328	-0.328	0.736	1.141	-0.328	-0.108
Arginine	-0.073	-0.073	-0.073	-0.073	-0.073	-0.073		-0.073	-0.073	-0.073	-0.073	-0.073	0.55	-0.073	-0.073	1.025	-0.073	-0.073	-0.073	-0.073	-0.073
Ascorbate	-0.816	1.452	4.786	0.523	0.398	-0.848		-0.287	-1.512	0.37	4.066	-1.055	1.843	0.187	-0.899	-0.185	-0.075	-0.902	-1.098	0.005	-1.523
ATP	-0.012	-0.012	-0.012	-0.012	-0.012	0.06		-0.012	-0.012	-0.012	-0.012	-0.012	-0.012	-0.012	-0.012	-0.012	-0.012	-0.012	-0.012	-0.012	-0.012
Azelate	-0.023	-0.023	-0.023	-0.023	-0.023	-0.023		-0.023	-0.023	-0.023	-0.023	-0.023	-0.023	-0.023	-0.023	-0.023	-0.023	0.897	-0.023	-0.023	-0.023
Betaine	-0.145	-0.124	-0.199	-0.029	-0.065	-0.073		-0.105	-0.077	-0.117	1.578	-0.099	0.026	-0.13	-0.002	-0.14	-0.191	0.088	-0.028	0.023	-0.092
Biotin	0.018	-0.261	0.308	0.09	-0.261	-0.1		0.154	-0.261	0.409	0.081	-0.261	0.133	-0.261	0.065	0.12	0.102	0.08	-0.261	0.003	-0.261
Butanone	-0.097	-0.097	0.106	-0.097	-0.097	-0.097		0.111	-0.097	-0.097	-0.097	-0.097	-0.097	-0.097	0.078	0.231	-0.097	0.396	-0.097	-0.097	0.035
Cadaverine	-0.022	-0.022	-0.022	-0.022	-0.022	-0.022		-0.022	-0.022	-0.022	0.862	-0.022	-0.022	-0.022	-0.022	-0.022	-0.022	-0.022	-0.022	-0.022	-0.022
Caffeine	0.085	0.207	-0.048	0.021	0.073	-0.101		-0.105	0.039	0.062	-0.092	0.121	-0.051	-0.042	0.009	-0.089	0.03	-0.044	0.004	-0.101	-0.054
Caprate	-0.045	-0.045	-0.045	-0.045	-0.045	-0.045		-0.045	0.445	-0.045	-0.045	-0.045	-0.045	-0.045	-0.045	0.782	-0.045	-0.045	-0.045	-0.045	-0.045
Carnitine	0.046	-0.047	-0.097	-0.17	0.553	-0.029		-0.127	0.218	-0.113	0.086	0.384	-0.123	-0.031	-0.116	-0.107	-0.084	-0.116	0.143	-0.122	0.349



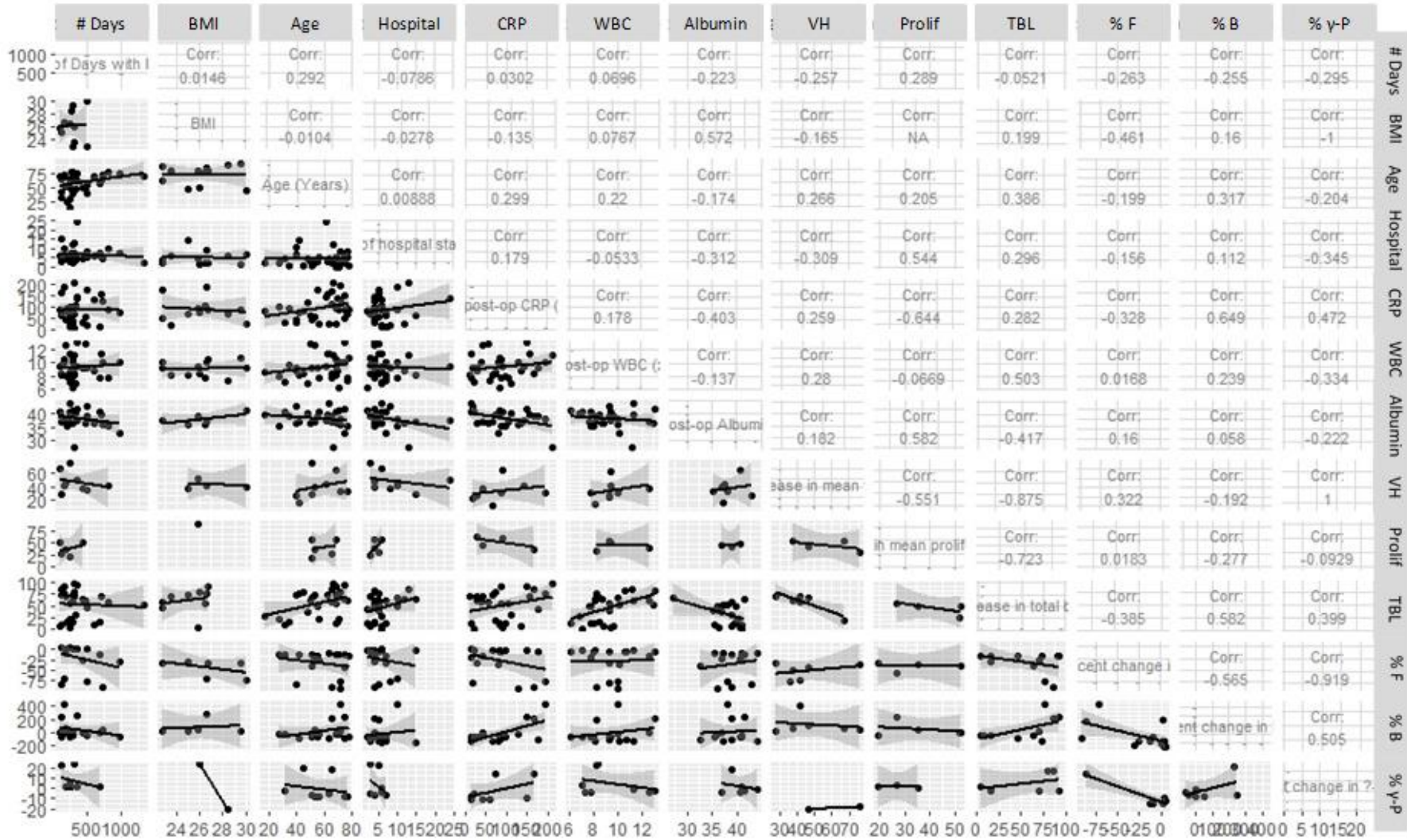
Sample Group	LANC009 Control	LANC020 Control	LHTR006 Control	LANC010 Control	LANC032 Control	LHTR010 Control		LANC034 IBD	LANC012 IBD	LANC013 IBD	LANC037 IBD	LANC038 IBD	LANC016 IBD	LANC040 IBD	LANC018 IBD	LANC028 IBD	LHTR003 IBD	LANC029 IBD	LANC030 IBD	LANC021 IBD	LHTR013 IBD
Carnosine	-0.116	0.156	0.472	0.21	-0.064	-0.24		-0.17	0.151	-0.116	0.044	-0.11	-0.156	0.17	0.074	0.088	-0.095	-0.24	-0.134	-0.117	-0.141
Cellobiose	-0.159	-0.445	1.251	-0.445	0.44	-0.445		0.14	-0.255	-0.445	-0.445	-0.445	0.084	0.233	0.151	0.304	0.466	0.271	0.303	0.148	-0.445
Chlorogenate	-0.01	-0.01	-0.01	-0.01	-0.01	0.11		-0.01	-0.01	-0.01	-0.01	-0.01	-0.01	-0.01	-0.01	-0.01	-0.01	-0.01	-0.01	-0.01	-0.01
Cholate	0.019	-0.024	-0.024	-0.024	0.014	0.063		-0.024	0.331	-0.024	-0.024	-0.024	-0.024	-0.024	-0.024	-0.024	-0.024	-0.024	-0.024	-0.024	-0.024
Choline	0.189	-0.14	-0.173	0.209	-0.063	-0.016		-0.05	-0.117	0.195	-0.173	-0.014	0.132	-0.003	0.153	0.225	0.233	0.056	-0.03	0.064	-0.09
cis.Aconitate	-0.179	-0.455	0.949	-0.033	0.349	-0.027		0.473	-0.287	-0.089	0.014	0.095	0.046	-0.091	-0.037	0.349	0.085	-0.41	-0.558	0.01	-0.097
Citraconate	-0.037	-0.037	-0.037	-0.037	-0.037	0.183		-0.037	-0.037	-0.037	0.07	-0.037	-0.037	-0.037	-0.037	-0.037	-0.037	0.391	-0.037	-0.037	-0.037
Citrate	0.074	-0.092	-0.092	-0.092	-0.092	-0.092		-0.092	-0.092	-0.092	-0.092	0.118	0.138	0.276	-0.092	-0.092	-0.092	0.574	-0.092	-0.092	-0.092
Citrulline	0.617	-0.047	-0.047	-0.047	-0.047	-0.047		-0.047	-0.047	-0.047	-0.047	-0.047	-0.047	-0.047	-0.047	-0.047	-0.047	-0.047	-0.047	-0.047	-0.047
Creatine	-0.102	0.038	-0.25	-0.226	-0.183	-0.216		-0.13	0.23	-0.236	-0.078	-0.184	0.074	-0.154	-0.267	0.164	-0.061	-0.239	-0.086	-0.284	-0.201
Creatine.phosphate	0.097	-0.138	0.154	-0.097	0.069	-0.075		0.031	-0.157	0.067	-0.107	-0.23	-0.045	-0.172	0.616	-0.209	-0.029	0.133	-0.25	0.149	0.158
Creatinine	1.005	2.169	-0.272	-3.461	-0.336	0.11		1.242	-0.662	-0.663	0.34	0.965	1.947	-0.068	1.082	0.866	2.047	-0.2	0.951	0.047	0.421
Cytidine	-0.035	0.153	-0.035	0.087	-0.035	-0.035		-0.035	-0.035	-0.035	-0.035	-0.035	-0.035	-0.035	-0.035	-0.035	-0.035	-0.035	-0.035	-0.035	-0.035
dCTP	-0.006	-0.006	-0.006	-0.006	-0.006	0.25		-0.006	-0.006	-0.006	-0.006	-0.006	-0.006	-0.006	-0.006	-0.006	-0.006	-0.006	-0.006	-0.006	-0.006
Desaminotyrosine	-0.024	-0.024	-0.024	-0.024	-0.024	-0.024		-0.024	-0.024	-0.024	0.109	-0.024	-0.024	-0.024	-0.024	-0.024	0.084	-0.024	-0.024	-0.024	0.69
Dimethylamine	0.036	0.047	0.036	0.107	-0.083	0.01		0.417	-1.099	-0.064	0.011	0.004	0.125	0.362	-0.145	0.118	0.108	0.277	-0.133	-0.067	-0.031
Dimethyl.sulfone	0.126	-0.078	-0.062	0.036	0.049	-0.13		-0.12	-0.123	-0.072	0.121	0.112	-0.002	-0.015	0.054	-0.118	0.115	0.065	0.01	-0.014	0.043
dTTP	-0.027	-0.027	-0.027	-0.027	-0.027	-0.027		0.163	-0.027	-0.027	-0.027	-0.027	-0.027	-0.027	-0.027	-0.027	0.096	-0.027	-0.027	-0.027	-0.027
Epicatechin	-0.046	0.098	-0.046	0.102	0.088	0.018		0.081	-0.046	0.07	-0.046	-0.046	-0.046	-0.046	0.081	0.089	-0.046	-0.046	-0.046	-0.046	-0.046
Erythritol	0.155	0.713	-0.808	-0.131	0.27	0.314		0.494	0.079	-0.034	-0.613	0.489	0.347	0.016	0.508	-0.086	0.315	0.557	0.124	0.414	-0.808
Ethanol	-0.156	-0.156	5.29	-0.156	-0.156	-0.156		-0.156	-0.156	0.022	-0.156	-0.156	-0.156	-0.156	-0.156	-0.156	-0.156	-0.156	-0.156	-0.156	-0.058
Ethanolamine	-0.057	-0.057	-0.057	-0.057	-0.057	-0.057		-0.057	1.182	-0.057	-0.057	-0.057	-0.057	-0.057	-0.057	-0.057	-0.057	-0.057	-0.057	-0.057	-0.057
Ethylene.glycol	-0.042	-0.042	0.706	-0.042	-0.042	-0.042		-0.042	-0.042	-0.042	-0.042	-0.042	-0.042	-0.042	-0.042	0.059	-0.042	-0.042	0.214	-0.042	0.102
Ethylmalonate	-0.031	-0.031	0.329	-0.031	-0.031	-0.031		-0.031	-0.031	0.279	-0.031	-0.031	-0.031	-0.031	-0.031	-0.031	-0.031	-0.031	-0.031	-0.031	-0.031
Ferulate	-0.067	-0.004	0.09	0.002	-0.009	-0.067		-0.067	0.084	0.026	0.085	-0.067	-0.004	-0.067	0.035	-0.021	-0.033	0.031	-0.067	-0.015	0.015
Formate	-0.078	-0.008	-0.199	-0.06	-0.145	0.059		-0.218	0.852	-0.246	0.764	0.205	-0.182	0.051	-0.125	-0.063	0.119	-0.315	0.384	0.114	-0.228
Fructose	0.285	0.134	1.031	0.141	-0.511	-0.511		-0.511	-0.511	0.083	0.116	-0.511	-0.511	0.695	-0.354	0.076	-0.21	-0.011	0.238	0.392	0.173
Fucose	-0.145	-0.344	-0.586	0.07	0.038	0.605		-0.139	-0.248	-0.465	-0.236	0.235	0.176	-0.392	-0.055	1.177	0.241	-0.027	0.294	-0.369	-0.324
Fumarate	-0.091	-0.053	0.227	-0.032	0.141	0.001		0.172	-0.034	-0.025	0.094	-0.027	-0.034	-0.011	-0.029	-0.041	-0.021	0.062	-0.019	0.043	-0.049
Galactarate	0.138	0.026	0.347	-0.201	-0.09	0.061		0.032	-0.154	-0.156	0.029	-0.007	0.028	0.286	-0.082	0.038	-0.022	-0.01	0.17	-0.07	-0.326
Galactitol	-0.225	-0.225	0.262	-0.225	-0.024	-0.225		-0.225	0.329	-0.225	-0.225	-0.068	-0.225	0.015	-0.225	0.021	-0.004	-0.008	-0.028	0.972	0.438
Galactonate	-0.373	-0.055	-0.373	0.205	-0.02	0.085		0.016	0.01	0.44	-0.373	-0.026	-0.185	-0.373	0.011	0.104	0.205	0.084	0.113	-0.101	-0.196
Galactose	0.359	-0.177	-0.177	-0.177	-0.177	-0.177		0.106	-0.095	-0.177	-0.177	-0.177	-0.177	-0.177	-0.177	-0.177	-0.177	-0.177	-0.177	-0.177	-0.177
Gallate	0.046	-0.045	-0.045	-0.045	-0.011	-0.045		-0.045	-0.045	-0.002	0.179	-0.045	-0.005	-0.045	-0.008	-0.045	-0.045	-0.045	-0.045	-0.045	0.024
Gentisate	-0.062	0.119	0.021	-0.062	-0.062	-0.062		-0.062	-0.062	-0.062	0.059	-0.062	0.058	-0.062	0.085	0.048	0.124	-0.062	-0.062	0.064	0.462
Glucarate	0.221	0.127	-0.137	-0.137	-0.137	-0.137		0.379	0.781	0.179	-0.137	-0.137	-0.137	-0.137	0.564	-0.137	-0.137	-0.137	-0.137	-0.137	-0.137
Glucitol	0.633	1.048	-0.259	0.907	0.86	0.803		-0.259	-0.259	-0.259	0.854	-0.259	-0.259	-0.259	-0.259	-0.259	-0.259	-0.259	-0.259	-0.259	-0.259
Glucuronate	0.185	0.057	0.155	0.491	-0.181	0.624		0.476	-0.743	-0.019	0.242	0.209	-0.017	-0.105	-0.18	-0.743	0.298	0.637	0.056	-0.061	0.366
Glucose	-0.121	-0.121	0.191	-0.121	-0.121	-0.121		-0.121	-0.121	-0.121	-0.121	-0.121	-0.121	-0.121	-0.024	0.196	-0.121	-0.121	0.517	-0.121	-0.121
Glucose.6.phosphate	-0.239	-0.239	0.432	-0.239	-0.239	-0.08		0.414	0.417	-0.239	-0.239	-0.239	-0.239	0.34	0.673	0.247	0.639	1.615	0.433	-0.239	-0.239
Glucuronate	-0.383	-0.383	0.765	-0.383	-0.383	0.303		0.045	0.044	-0.383	0.435	0.002	0.283	0.205	0.432	0.084	-0.229	0.299	-0.383	0.064	0.138
Glutamine	-0.084	-0.084	-0.084	-0.084	0.972	-0.084		-0.084	-0.084	-0.084	-0.084	-0.084	-0.084	-0.084	-0.084	-0.084	-0.084	-0.084	-0.084	-0.084	-0.084
Glutaric.acid.monomethyl.ester	-0.023	-0.023	0.487	-0.023	-0.023	-0.023		-0.023	-0.023	-0.023	-0.023	-0.023	-0.023	-0.023	-0.023	-0.023	-0.023	-0.023	-0.023	-0.023	-0.023

Sample Group	LANC009 Control	LANC020 Control	LHTR006 Control	LANC010 Control	LANC032 Control	LHTR010 Control		LANC034 IBD	LANC012 IBD	LANC013 IBD	LANC037 IBD	LANC038 IBD	LANC016 IBD	LANC040 IBD	LANC018 IBD	LANC028 IBD	LHTR003 IBD	LANC029 IBD	LANC030 IBD	LANC021 IBD	LHTR013 IBD
Methionine	-0.191	0.077	-0.191	-0.191	0.013	-0.191		-0.014	-0.191	0.079	0.309	-0.015	0.07	-0.095	-0.191	0.254	-0.191	0.115	-0.191	0.156	-0.191
Methylamine	0.047	-0.061	-0.158	0.13	0.127	-0.158		0.153	-0.079	-0.158	-0.023	-0.05	0.084	-0.083	-0.112	0.422	0.042	0.16	-0.063	-0.074	-0.109
Methylguanidine	-0.172	-0.172	-0.099	-0.113	-0.172	0.009		0.751	0.006	-0.096	-0.088	0.137	-0.172	0.435	0.06	-0.066	-0.042	-0.077	0.06	-0.084	0.007
Methylsuccinate	-0.176	-0.041	-0.381	0.066	0.206	-0.079		0.044	-0.141	-0.206	0.321	0.133	-0.04	-0.055	0.047	-0.381	0.314	0.104	-0.258	0.066	-0.141
myo-Inositol	-0.15	-0.15	-0.15	-0.15	-0.15	-0.15		-0.15	-0.15	-0.15	0.854	-0.15	-0.15	-0.15	-0.15	-0.15	-0.15	-0.15	-0.15	-0.15	-0.15
N.N.Dimethylformamide	-0.027	0.2	0.037	0.079	0.087	-0.04		-0.028	-0.062	0.158	0.021	0.01	-0.006	-0.197	0.067	-0.105	0.162	0.009	0.031	0.027	-0.275
N.N.Dimethylglycine	-0.095	0.075	-0.069	-0.056	-0.054	-0.062		0.166	-0.001	-0.055	-0.055	0.168	0.008	-0.001	0.171	-0.035	-0.095	-0.026	0.054	0.006	0.127
N6.Acetylysine	-0.114	0.025	-0.114	0.217	-0.114	-0.114		0.218	0.213	-0.114	-0.114	0.247	0.01	-0.114	-0.114	0.011	-0.114	-0.114	-0.114	0.224	-0.114
N.Acetylaspartate	-0.14	-0.14	0.067	0.032	0.084	0.002		0.163	-0.14	0.071	-0.14	-0.14	0.267	-0.14	0.027	0.179	-0.14	0.225	-0.14	0.078	-0.14
N.Acetylcysteine	-0.02	-0.02	-0.02	-0.02	-0.02	-0.02		-0.02	-0.02	-0.02	-0.02	-0.02	-0.02	-0.02	-0.02	-0.02	-0.02	-0.02	-0.02	-0.02	-0.02
N.Acetylglucosamine	-0.087	-0.087	-0.087	-0.087	-0.087	-0.087		0.679	0.316	-0.087	-0.087	-0.025	-0.087	-0.087	0.54	-0.087	-0.087	-0.087	-0.087	-0.087	-0.087
N.Acetylglutamate	-0.199	0.128	0.026	0.386	0.027	0.083		-0.022	0.067	0.13	0.032	0.083	0.059	-0.029	-0.199	-0.199	-0.199	-0.199	0.007	0.052	0.02
N.Acetylglutamine	-0.033	-0.033	-0.033	0.231	-0.033	-0.033		-0.033	0.359	-0.033	-0.033	-0.033	-0.033	-0.033	-0.033	-0.033	-0.033	-0.033	-0.033	-0.033	-0.033
N.Acetylglycine	-0.016	-0.016	-0.016	-0.016	-0.016	-0.016		-0.016	-0.016	-0.016	-0.016	-0.016	-0.016	-0.016	-0.016	-0.016	-0.016	-0.016	0.606	-0.016	-0.016
N.Acetylornithine	-0.074	-0.074	0.421	0.509	-0.074	-0.074		-0.074	-0.074	-0.074	0.501	-0.074	-0.074	-0.074	-0.074	0.425	-0.074	0.56	-0.074	-0.074	-0.074
N.Acetylserotonin	-0.019	0.041	-0.128	-0.128	-0.128	-0.057		-0.043	0.146	0.114	-0.128	0.072	-0.128	-0.128	0.11	0.006	0.064	0.057	0.19	0.059	0.086
N.Acetyltyrosine	-0.096	0.002	-0.096	0.042	0.02	0.094		0.021	0.032	0.041	-0.096	0.004	-0.096	-0.096	0.034	0.018	-0.008	-0.096	0.159	-0.096	0.578
NADH	-0.015	-0.015	0.107	-0.015	-0.015	0.214		-0.015	-0.015	-0.015	-0.015	-0.015	-0.015	-0.015	-0.015	-0.015	-0.015	-0.015	-0.015	-0.015	-0.015
NADPH	-0.01	-0.01	-0.01	-0.01	-0.01	0.056		-0.01	-0.01	-0.01	-0.01	-0.01	-0.01	-0.01	-0.01	-0.01	-0.01	-0.01	-0.01	-0.01	0.157
N.Carbamoylaspartate	-0.232	0.768	-0.232	0.78	-0.232	-0.232		-0.232	-0.232	0.4	0.413	-0.232	0.661	-0.232	-0.232	0.679	-0.232	0.349	-0.232	-0.232	0.468
N.Carbamoyl...alanine	-0.026	-0.026	-0.026	-0.026	-0.026	-0.026		-0.026	-0.026	-0.026	-0.026	-0.026	-0.026	-0.026	-0.026	-0.026	-0.026	-0.026	-0.026	-0.026	-0.026
Nicotinurate	-0.005	-0.005	-0.005	-0.005	-0.005	-0.005		-0.005	-0.005	-0.005	-0.005	-0.005	-0.005	-0.005	-0.005	-0.005	-0.005	-0.005	-0.005	-0.005	-0.005
N.Methylhydantoin	-0.238	-0.049	-0.048	0.155	-0.088	0.023		-0.071	-0.051	0.02	0.695	0.077	0.005	-0.03	-0.11	-0.008	-0.137	-0.099	-0.115	0.001	-0.14
N.Nitrosodimethylamine	0.017	0.237	-0.317	-0.036	-0.017	-0.131		0.12	0.427	-0.317	-0.091	0.082	-0.317	-0.027	-0.011	-0.045	0.289	0.04	-0.003	-0.317	-0.01
N.Phenylacetyl glycine	0.39	-0.136	0.002	-0.142	-0.269	-0.111		-0.154	-0.037	-0.193	0.239	0.326	-0.087	0.44	-0.17	-0.133	-0.118	0.238	-0.213	0.041	0.916
N.Phenylacetylphenylalanine	-0.011	-0.011	-0.011	-0.011	-0.011	-0.011		-0.011	-0.011	0.422	-0.011	-0.011	-0.011	-0.011	-0.011	-0.011	-0.011	-0.011	-0.011	-0.011	-0.011
N...Acetylysine	-0.168	0.055	-0.168	-0.168	-0.168	-0.168		-0.168	-0.101	0.218	-0.168	-0.01	-0.025	0.243	-0.168	-0.168	0.317	0.19	-0.038	0.286	0.289
O.Acetylcarnitine	-0.227	-0.232	-0.266	-0.173	0.04	-0.31		0.209	-0.173	-0.215	-0.305	-0.021	0.107	-0.323	-0.3	0.814	0.298	0.743	-0.133	-0.175	-0.291
O.Acetylcholine	0.343	0.128	-0.133	0.018	-0.085	-0.056		-0.051	-0.133	0.231	-0.133	0.03	-0.045	-0.078	-0.133	0.086	0.167	-0.037	-0.081	-0.045	-0.063
o.Cresol	0.246	-0.105	-0.105	-0.105	0.162	-0.105		0.078	0.204	-0.105	-0.105	0.314	-0.105	-0.105	0.199	0.237	-0.105	-0.105	-0.105	-0.105	-0.105
O.Phosphocholine	-0.106	-0.066	-0.106	-0.106	-0.076	-0.022		-0.04	-0.068	-0.106	-0.006	-0.075	-0.025	-0.01	-0.063	0.043	-0.038	-0.074	0.003	-0.036	0.04
Ornithine	-0.06	-0.06	-0.06	1.018	-0.06	-0.06		-0.06	-0.06	-0.06	-0.06	-0.06	-0.06	-0.06	-0.06	-0.06	-0.06	-0.06	-0.06	-0.06	-0.06
Oxypurinol	0.04	0.702	-0.105	-0.082	0.716	0.087		-0.678	-0.664	-0.491	-0.899	-0.128	0.197	-0.385	-0.241	-0.169	0.334	-0.706	-0.407	-0.734	0.431
Pantothenate	0.056	0.004	0.082	-0.055	-0.048	0.165		-0.071	0.02	-0.032	-0.071	0.216	-0.075	-0.08	0.107	0.1	0.004	-0.1	-0.035	0.061	0.008
p.Cresol	-0.118	-0.01	-0.011	0.054	-0.118	-0.118		0.004	0.282	0.039	0.025	0.054	-0.009	-0.027	-0.118	-0.118	0.072	-0.118	0.328	0.003	0.435
Phenylacetate	-0.024	0.098	-0.347	-0.059	0.044	-0.347		0.011	-0.121	-0.019	0.265	0.174	-0.057	0.189	0.041	-0.347	-0.045	-0.108	0.087	-0.053	0.254
Propylene.glycol	-0.093	-0.093	0.522	-0.01	-0.093	-0.093		-0.093	-0.093	-0.054	-0.04	-0.018	-0.093	-0.029	-0.093	0.223	-0.093	-0.093	-0.093	0.184	-0.093
Protocatechuate	-0.01	-0.01	-0.01	-0.01	-0.01	-0.01		-0.01	-0.01	-0.01	-0.01	-0.01	-0.01	-0.01	-0.01	-0.01	-0.01	-0.01	-0.01	-0.01	-0.01
Pyridoxine	-0.043	-0.032	-0.026	0.01	-0.041	-0.107		-0.021	0.12	-0.006	-0.048	-0.04	-0.006	-0.012	-0.01	-0.018	-0.024	0.013	0.021	0.013	0.141
Pyrimidine	-0.034	-0.034	0.058	-0.034	-0.034	-0.034		-0.034	-0.034	0.214	-0.034	-0.034	-0.034	-0.034	-0.034	-0.034	-0.034	-0.034	0.19	-0.034	-0.034
Pyroglutamate	-0.028	-0.028	-0.028	-0.028	-0.028	-0.028		-0.028	-0.028	-0.028	-0.028	-0.028	-0.028	-0.028	-0.028	-0.028	-0.028	-0.028	-0.028	-0.028	1.081
Pyruvate	-0.104	-0.104	-0.104	0.072	-0.104	-0.104		-0.104	-0.014	-0.104	0.238	-0.104	0.082	-0.104	-0.104	0.024	-0.104	0.125	-0.104	-0.104	0.07
Quinolate	0.007	0.297	-0.14	0.022	0.182	0.444		0.317	-0.14	0.212	0.142	-0.14	-0.14	0.211	0.18	0.066	-0.14	0.034	-0.14	-0.14	-0.14

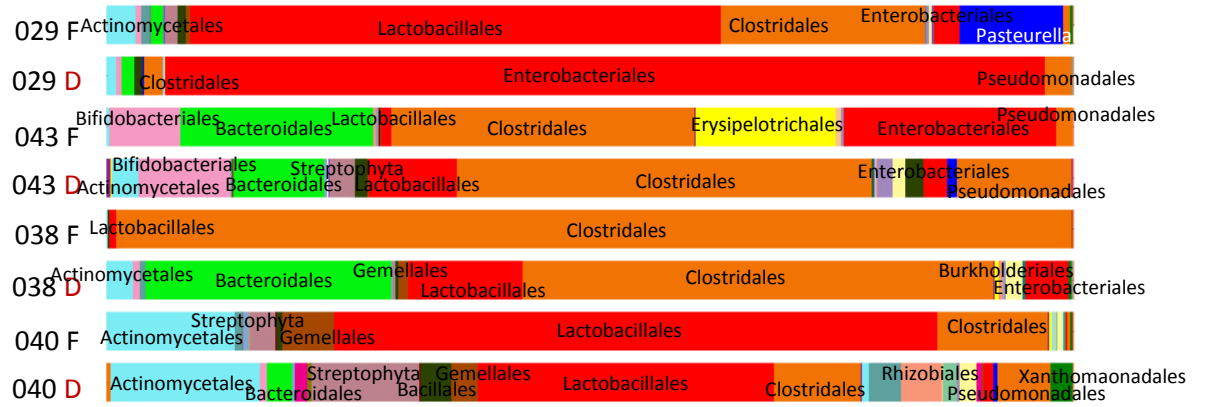
Sample	LANC009	LANC020	LHTR006	LANC010	LANC032	LHTR010		LANC034	LANC012	LANC013	LANC037	LANC038	LANC016	LANC040	LANC018	LANC028	LHTR003	LANC029	LANC030	LANC021	LHTR013
Group	Control	Control	Control	Control	Control	Control		IBD	IBD	IBD	IBD	IBD	IBD	IBD	IBD	IBD	IBD	IBD	IBD	IBD	IBD
Riboflavin	-0.016	0.103	-0.067	-0.059	-0.045	-0.03		-0.044	-0.129	0.052	-0.071	0.049	-0.078	-0.033	0.071	0.125	-0.037	-0.067	-0.048	-0.068	0.108
Ribose	0.167	0.242	-0.793	0.394	0.435	-0.503		0.247	0.051	0.747	0.113	0.456	-0.793	-0.793	0.666	-0.564	-0.793	0.131	0.105	0.581	-0.252
Saccharopine	-0.12	-0.12	0.632	0.727	0.355	-0.12		-0.12	-0.12	-0.12	-0.12	-0.12	-0.12	0.312	-0.12	-0.12	-0.12	-0.12	-0.12	-0.12	-0.12
S.Adenosylhomocysteine	0.075	-0.014	-0.014	-0.014	0.071	0.141		-0.014	-0.014	-0.014	-0.014	-0.014	-0.014	-0.014	0.208	-0.014	-0.014	-0.014	-0.014	-0.014	-0.014
Salicylate	-0.031	-0.031	-0.031	-0.031	-0.031	-0.031		-0.031	0.196	-0.031	-0.031	-0.031	0.183	-0.031	0.223	-0.031	-0.031	-0.031	-0.031	-0.031	-0.031
Salicylurate	0.186	-0.089	0.055	-0.012	0.131	0.102		0.144	0.198	-0.089	-0.089	-0.089	0.064	0.168	0.034	-0.089	0.206	-0.089	-0.089	-0.089	-0.089
Sarcosine	-0.053	-0.053	-0.053	-0.053	-0.053	-0.053		-0.053	0.093	-0.053	0.085	0.171	-0.053	-0.053	-0.053	-0.053	-0.053	0.148	0.052	-0.053	0.309
Serotonin	-0.021	0.157	-0.081	-0.081	-0.081	-0.081		-0.081	-0.081	-0.081	-0.081	-0.081	0.07	0.275	0.226	-0.081	0.123	-0.081	-0.081	0.186	0.122
sn.Glycero.3.phosphocholine	0.322	-0.031	-0.207	0.063	-0.05	-0.207		0.138	-0.114	0.297	-0.167	-0.104	0.146	-0.179	-0.108	-0.096	0.278	0.236	-0.077	0.098	-0.159
Succinate	-0.104	0.24	0.111	-0.194	0.194	0.084		0.449	0.144	0.072	0.039	-0.029	-0.132	-0.015	-0.057	-0.162	0.003	-0.21	-0.019	0.353	-0.287
Succinylacetone	-0.133	-0.09	-0.223	0.043	-0.038	-0.173		-0.046	0.001	-0.122	-0.117	-0.043	0.001	-0.117	-0.09	-0.1	-0.027	0.279	-0.018	-0.218	-0.089
Sucrose	-0.068	-0.068	-0.068	-0.068	-0.068	-0.068		-0.068	0.098	-0.068	-0.068	0.083	-0.068	0.113	-0.068	0.082	-0.068	-0.068	0.138	-0.068	-0.003
Syringate	-0.008	-0.05	-0.053	-0.069	-0.079	-0.054		-0.079	-0.016	-0.079	-0.079	0.03	-0.06	-0.059	-0.061	-0.071	0.116	-0.079	-0.079	-0.053	-0.066
Tartrate	-0.133	0.015	-0.025	-0.133	0.001	-0.133		-0.039	-0.032	0.028	0.015	-0.053	-0.001	-0.011	-0.066	0.007	-0.001	0.056	-0.133	0.015	1.432
Taurine	-0.207	-0.207	0.107	1.408	-0.207	0.466		-0.207	-0.207	-0.207	-0.207	-0.207	-0.207	0.212	-0.207	-0.207	-0.207	-0.207	-0.207	-0.207	-0.207
Theophylline	0.018	-0.048	-0.128	-0.013	-0.104	0.046		-0.059	0.081	-0.091	0.046	0.019	-0.038	-0.096	-0.064	-0.1	-0.083	-0.003	0.054	-0.075	0.222
Threonate	-0.819	0.802	-0.819	0.599	-0.17	-0.196		-0.197	-0.008	-0.819	0.641	-0.005	0.5	-0.069	-0.311	-0.205	0.088	-0.819	-0.152	-0.819	0.294
Threonine	0.016	0.263	-0.226	0.347	-0.226	-0.226		0.099	0.469	0.044	0.221	0.161	-0.226	-0.226	-0.226	0.205	-0.226	-0.226	-0.226	-0.226	-0.078
Thymidine	-0.013	-0.013	-0.013	0.197	-0.013	-0.013		-0.013	-0.013	-0.013	-0.013	-0.013	-0.013	-0.013	-0.013	-0.013	0.154	-0.013	-0.013	-0.013	-0.013
Thymol	-0.17	-0.051	0.007	0.038	-0.056	0.018		0.033	0.02	0.067	-0.17	-0.005	0.083	-0.17	0.118	0.016	-0.17	-0.17	0.066	0.06	0.163
trans.4.Hydroxy.L.proline	-0.071	-0.071	-0.071	-0.071	-0.071	-0.071		0.94	-0.071	-0.071	-0.071	-0.071	-0.071	-0.071	-0.071	0.819	-0.071	0.441	-0.071	-0.071	-0.071
trans.Aconitate	0.022	-0.014	-0.047	-0.218	0.101	0		0.068	0.006	0.245	0.102	-0.005	0.039	-0.063	0.006	-0.215	0.07	-0.259	0.049	0.007	-0.194
Trehalose	-0.042	-0.042	0.422	-0.042	-0.042	-0.042		-0.042	-0.042	-0.042	0.955	-0.042	0.01	-0.042	-0.042	-0.042	-0.042	-0.042	-0.042	-0.042	-0.042
Trigonelline	0.168	-0.187	0.105	-0.101	0.054	-0.187		-0.148	-0.139	0.116	-0.187	-0.028	-0.1	-0.129	-0.088	-0.074	0.097	-0.07	0.221	-0.013	-0.135
Trimethylamine.N.oxide	1.926	0.073	-0.158	-0.16	-0.148	-0.171		-0.158	-0.147	-0.162	-0.168	0.158	-0.168	0.424	-0.154	-0.17	-0.168	-0.147	-0.17	-0.143	1.738
Tropate	-0.023	-0.023	-0.023	-0.023	-0.023	-0.023		-0.023	-0.023	-0.023	-0.023	-0.023	-0.023	-0.023	-0.023	-0.023	-0.023	0.888	-0.023	-0.023	-0.023
Tryptophan	-0.223	-0.223	0.014	0.071	-0.223	0.652		0.013	0.201	-0.126	0.079	-0.223	0.035	0.508	0.022	-0.075	0.17	-0.223	0.106	0.053	0.641
Tyramine	-0.049	0.178	-0.049	0.187	-0.049	-0.049		0.229	-0.049	-0.049	-0.049	-0.049	-0.049	-0.049	0.127	-0.049	0.134	-0.049	-0.049	-0.049	-0.049
Tyrosine	0.251	0.438	0.219	0.2	-0.143	-0.143		-0.143	-0.143	-0.143	-0.143	-0.143	0.242	-0.143	-0.143	-0.143	0.256	-0.143	-0.143	0.214	-0.143
UDP.galactose	-0.017	-0.017	-0.017	-0.017	-0.017	-0.017		-0.017	-0.017	0.132	-0.017	-0.017	-0.017	-0.017	-0.017	-0.017	-0.017	-0.017	-0.017	-0.017	-0.017
UDP.glucose	-0.032	-0.032	-0.032	-0.032	-0.032	-0.032		-0.032	0.256	-0.032	-0.032	-0.032	-0.032	-0.032	0.151	-0.032	0.126	-0.032	-0.032	-0.032	-0.032
UDP.glucuronate	0.026	-0.053	-0.053	-0.053	0.06	-0.053		-0.053	0.15	-0.053	0.154	-0.053	-0.053	0.25	-0.053	-0.053	0.096	-0.053	0.194	-0.053	-0.053
UDP.N.Acetylglucosamine	-0.08	-0.08	-0.023	0.096	0.079	-0.015		0.013	0.084	-0.024	-0.08	0.179	0.017	-0.08	0.119	-0.08	-0.032	-0.08	0.091	0.104	-0.002
UMP	-0.038	0.116	0.035	-0.038	0.053	0.031		-0.038	-0.038	-0.038	-0.038	-0.038	0.074	-0.038	-0.038	0.228	-0.038	-0.038	-0.038	-0.038	-0.038
Uracil	0.457	-0.088	0.102	0.096	-0.088	0.092		-0.088	0.453	0.084	-0.088	-0.088	-0.088	-0.088	-0.088	0.323	0.012	-0.088	-0.088	-0.088	-0.088
Uridine	-0.027	0.136	-0.027	-0.027	-0.027	-0.027		-0.027	0.183	-0.027	-0.027	-0.027	0.313	-0.027	-0.027	-0.027	-0.027	-0.027	-0.027	-0.027	-0.027
Urocanate	0.21	0.155	0.11	0.142	-0.055	0.054		0.08	-0.055	-0.055	-0.055	-0.055	0.092	-0.055	-0.055	0.115	-0.055	-0.055	-0.055	-0.055	-0.055
Valerate	-0.046	-0.046	-0.046	-0.046	-0.046	-0.046		-0.046	-0.046	-0.046	0.292	-0.046	-0.046	0.098	-0.046	-0.046	0.347	-0.046	-0.046	-0.046	-0.046
Valine	-0.068	0.076	-0.137	-0.002	0.107	-0.004		0.023	-0.034	-0.119	0.031	0.133	0.033	-0.01	0.062	0.072	0.038	-0.009	0.131	-0.032	-0.082
Vanillate	-0.035	0.029	-0.035	0.287	-0.035	-0.035		-0.035	-0.035	-0.035	-0.035	0.104	-0.035	0.105	-0.035	-0.035	-0.035	-0.035	-0.035	-0.035	-0.035
Xanthine	0.048	-0.085	0.28	-0.039	-0.076	-0.031		-0.102	-0.038	-0.164	0.326	-0.164	-0.164	0.038	-0.085	0.081	-0.075	-0.164	-0.164	-0.076	0.985
Xanthosine	-0.034	-0.034	-0.034	-0.034	-0.034	0.005		-0.034	-0.034	-0.034	-0.034	-0.034	-0.034	0.026	-0.034	-0.034	0.004	-0.034	-0.034	-0.034	0.694
Xanthurenate	-0.061	-0.024	-0.102	-0.038	-0.102	-0.082		-0.102	0.094	0.08	0.253	-0.102	-0.04	0.213	-0.059	-0.076	-0.039	-0.049	-0.102	-0.04	0.827

Sample	LANC009	LANC020	LTHTr006	LANC010	LANC032	LTHTr010		LANC034	LANC012	LANC013	LANC037	LANC038	LANC016	LANC040	LANC018	LANC028	LTHTr003	LANC029	LANC030	LANC021	LTHTr013
Group	Control	Control	Control	Control	Control	Control		IBD	IBD	IBD	IBD	IBD	IBD	IBD	IBD	IBD	IBD	IBD	IBD	IBD	IBD
Xylitol	-0.177	-0.177	1.621	-0.177	-0.177	-0.177		-0.177	0.17	-0.177	1.345	0.799	-0.177	-0.177	-0.177	-0.177	-0.177	-0.177	-0.177	-0.177	-0.177
Xylose	-0.066	-0.066	-0.066	0.374	-0.066	-0.066		-0.066	-0.066	-0.066	1.141	-0.066	-0.066	-0.066	0.425	-0.066	-0.066	-0.066	-0.066	-0.066	-0.066
X..Alanine	-0.031	-0.031	-0.031	-0.031	-0.031	0.416		-0.031	0.397	-0.031	-0.031	-0.031	-0.031	-0.031	0.324	-0.031	-0.031	-0.031	-0.031	-0.031	-0.031
X..Glutamylphenylalanine	0.624	-0.064	-0.064	-0.064	-0.064	0.24		-0.064	0.824	0.228	-0.064	-0.064	-0.064	-0.064	-0.064	-0.064	-0.064	-0.064	-0.064	-0.064	-0.064
X..Methylhistidine	0.64	0.012	-0.01	-0.255	0.072	-0.034		0.064	-0.348	0.025	0.158	0.227	0.306	-0.188	0.011	-0.117	0.265	-0.024	-0.193	-0.187	-0.306
X..Methylhistidine.1	0.72	0.013	-0.025	-0.191	-0.005	-0.137		-0.121	-0.07	-0.191	-0.03	-0.104	-0.135	0.039	0.078	-0.191	-0.061	-0.006	0.007	0.23	0.221

Appendix 10 - Scatterplot Matrix



Appendix 11 - Complete and Annotated Proportionate Microbiota Data at Order Level.



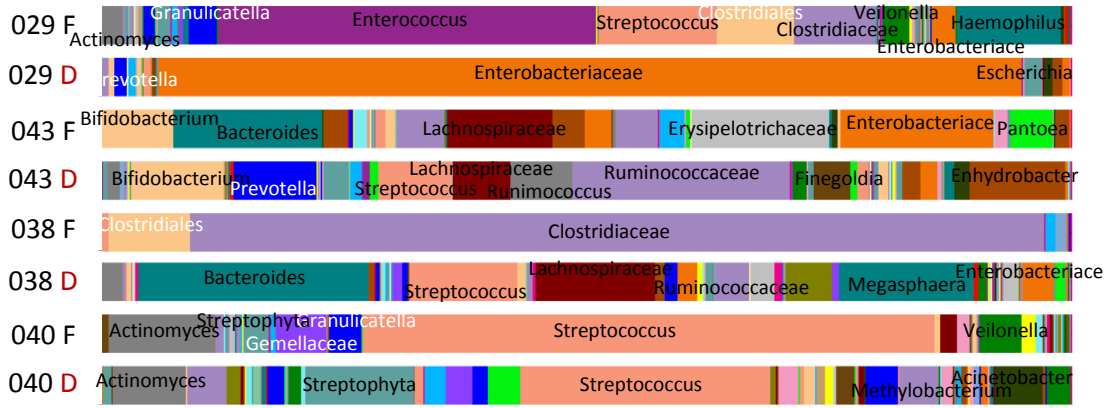
- k\_Archaea;p\_Euryarchaeota;c\_Methanobacteria;o\_Methanobacteriales
- k\_Archaea;p\_Euryarchaeota;c\_Thermoplasmata;o\_E2
- k\_Bacteria;p\_Acidobacteria;c\_Acidobacteria-6;o\_iii1-15
- k\_Bacteria;p\_Acidobacteria;c\_Holophagae;o\_Holophagales
- k\_Bacteria;p\_Acidobacteria;c\_[Chloracidobacteria];o\_RB41
- k\_Bacteria;p\_Actinobacteria;c\_Acidimicrobia;o\_Acidimicrobiales
- k\_Bacteria;p\_Actinobacteria;c\_Actinobacteria;o\_Actinomycetales
- k\_Bacteria;p\_Actinobacteria;c\_Actinobacteria;o\_Bifidobacteriales
- k\_Bacteria;p\_Actinobacteria;c\_Coriobacteriia;o\_Coriobacteriales
- k\_Bacteria;p\_Actinobacteria;c\_Thermoleophilla;o\_Gaellales
- k\_Bacteria;p\_Actinobacteria;c\_Thermoleophilla;o\_Solirubrobacterales
- k\_Bacteria;p\_Bacteroidetes;c\_Bacteroidia;o\_Bacteroidales
- k\_Bacteria;p\_Bacteroidetes;c\_Cytophagia;o\_Cytophagales
- k\_Bacteria;p\_Bacteroidetes;c\_Flavobacteriia;o\_Flavobacteriales
- k\_Bacteria;p\_Bacteroidetes;c\_Sphingobacteriia;o\_Sphingobacteriales
- k\_Bacteria;p\_Bacteroidetes;c\_VC2\_1\_Bac22;o\_
- k\_Bacteria;p\_Bacteroidetes;c\_[Saprosirae];o\_[Saprosirales]
- k\_Bacteria;p\_Chlorobi;c\_OPB56;o\_
- k\_Bacteria;p\_Chloroflexi;c\_Anaerolineae;o\_Anaerolineales
- k\_Bacteria;p\_Chloroflexi;c\_Gitt-GS-136;o\_
- k\_Bacteria;p\_Chloroflexi;c\_Thermomicrobia;o\_JG30-KF-CM45
- k\_Bacteria;p\_Cyanobacteria;c\_4C0d-2;o\_YS2
- k\_Bacteria;p\_Cyanobacteria;c\_Chloroplast;o\_Chlorophyta
- k\_Bacteria;p\_Cyanobacteria;c\_Chloroplast;o\_Stramenopiles
- k\_Bacteria;p\_Cyanobacteria;c\_Chloroplast;o\_Streptophyta
- k\_Bacteria;p\_Cyanobacteria;c\_ML635J-21;o\_
- k\_Bacteria;p\_Elusimicrobia;c\_Elusimicrobia;o\_Ilb
- k\_Bacteria;p\_Firmicutes;c\_Bacilli;o\_Bacillales
- k\_Bacteria;p\_Firmicutes;c\_Bacilli;o\_Gemellales
- k\_Bacteria;p\_Firmicutes;c\_Bacilli;o\_Lactobacillales
- k\_Bacteria;p\_Firmicutes;c\_Bacilli;o\_Turicibacterales
- k\_Bacteria;p\_Firmicutes;c\_Clostridia;o\_Clostridiales
- k\_Bacteria;p\_Firmicutes;c\_Clostridia;o\_Natranaerobiales
- k\_Bacteria;p\_Firmicutes;c\_Clostridia;o\_Thermoanaerobacteriales
- k\_Bacteria;p\_Firmicutes;c\_Erysipelotrichi;o\_Erysipelotrichales
- k\_Bacteria;p\_Fusobacteriia;c\_Fusobacteriia;o\_Fusobacteriales
- k\_Bacteria;p\_Gemmatimonadetes;c\_Gemmatimonadetes;o\_Gemmatimonadales
- k\_Bacteria;p\_OD1;c\_ZB2;o\_
- k\_Bacteria;p\_Planctomycetes;c\_Planctomycetia;o\_Planctomycetales
- k\_Bacteria;p\_Proteobacteria;c\_Alphaproteobacteria;o\_Caulobacteriales
- k\_Bacteria;p\_Proteobacteria;c\_Alphaproteobacteria;o\_RF32
- k\_Bacteria;p\_Proteobacteria;c\_Alphaproteobacteria;o\_Rhizobiales
- k\_Bacteria;p\_Proteobacteria;c\_Alphaproteobacteria;o\_Rhodobacteriales
- k\_Bacteria;p\_Proteobacteria;c\_Alphaproteobacteria;o\_Rhodospirillales
- k\_Bacteria;p\_Proteobacteria;c\_Alphaproteobacteria;o\_Rickettsiales
- k\_Bacteria;p\_Proteobacteria;c\_Alphaproteobacteria;o\_Sphingomonadales
- k\_Bacteria;p\_Proteobacteria;c\_Betaproteobacteria;o\_Burkholderiales
- k\_Bacteria;p\_Proteobacteria;c\_Betaproteobacteria;o\_Ellin6067
- k\_Bacteria;p\_Proteobacteria;c\_Betaproteobacteria;o\_Neisseriales

■ k\_Bacteria;p\_Proteobacteria;c\_Betaproteobacteria;o\_Rhodocyclales  
■ k\_Bacteria;p\_Proteobacteria;c\_Betaproteobacteria;o\_SBl14  
■ k\_Bacteria;p\_Proteobacteria;c\_Deltaproteobacteria;o\_  
■ k\_Bacteria;p\_Proteobacteria;c\_Deltaproteobacteria;o\_Bdellovibrionales  
■ k\_Bacteria;p\_Proteobacteria;c\_Deltaproteobacteria;o\_Desulfobacterales  
■ k\_Bacteria;p\_Proteobacteria;c\_Deltaproteobacteria;o\_Desulfovibrionales  
■ k\_Bacteria;p\_Proteobacteria;c\_Epsilonproteobacteria;o\_Campylobacterales  
■ k\_Bacteria;p\_Proteobacteria;c\_Gammaproteobacteria;o\_Aeromonadales  
■ k\_Bacteria;p\_Proteobacteria;c\_Gammaproteobacteria;o\_Alteromonadales  
■ k\_Bacteria;p\_Proteobacteria;c\_Gammaproteobacteria;o\_Enterobacterales  
■ k\_Bacteria;p\_Proteobacteria;c\_Gammaproteobacteria;o\_Pasteurellales  
■ k\_Bacteria;p\_Proteobacteria;c\_Gammaproteobacteria;o\_Pseudomonadales  
■ k\_Bacteria;p\_Proteobacteria;c\_Gammaproteobacteria;o\_Xanthomonadales  
■ k\_Bacteria;p\_SR1;c\_;o\_  
■ k\_Bacteria;p\_Spirochaetes;c\_Spirochaetes;o\_Spirochaetales  
■ k\_Bacteria;p\_TM6;c\_SJA-4;o\_  
■ k\_Bacteria;p\_TM7;c\_TM7-3;o\_CW040  
■ k\_Bacteria;p\_Tenericutes;c\_Mollicutes;o\_RF39  
■ k\_Bacteria;p\_Verrucomicrobia;c\_Verrucomicrobiae;o\_Verrucomicrobiales  
■ k\_Bacteria;p\_Verrucomicrobia;c\_[Spartobacteria];o\_[Chthoniobacterales]  
■ k\_Bacteria;p\_[Thermi];c\_Deinococci;o\_Deinococcales  
■ k\_Bacteria;p\_[Thermi];c\_Deinococci;o\_Thermales

Relative taxonomic composition of 16S rRNA amplicon sequences in mucosal-associated microbiota, at order level. K, kingdom; p, phylum; c, class; o, order; F, functional; D, defunctioned. n=4.



**Appendix 12 - Complete and Annotated Proportionate Microbiota Data at Genus Level.**



- k\_Archaea;p\_Euryarchaeota;c\_Methanobacteria;o\_Methanobacteriales;f\_Methanobacteriaceae;g\_Methanobrevibacter
- k\_Archaea;p\_Euryarchaeota;c\_Thermoplasmata;o\_E2;f\_Marine group II;g\_
- k\_Bacteria;p\_Acidobacteria;c\_Acidobacteria-6;o\_III1-15;f\_g\_
- k\_Bacteria;p\_Acidobacteria;c\_Holophagae;o\_Holophagales;f\_Holophagaceae;g\_
- k\_Bacteria;p\_Acidobacteria;c\_[Chloracidobacteria];o\_RB41;f\_Ellin6075;g\_
- k\_Bacteria;p\_Actinobacteria;c\_Acidimicrobia;o\_Acidimicrobiales;f\_g\_
- k\_Bacteria;p\_Actinobacteria;c\_Acidimicrobia;o\_Acidimicrobiales;f\_Microthrixaceae;g\_
- k\_Bacteria;p\_Actinobacteria;c\_Actinobacteria;o\_Actinomycetales;f\_g\_
- k\_Bacteria;p\_Actinobacteria;c\_Actinobacteria;o\_Actinomycetales;f\_ACK-M1;g\_
- k\_Bacteria;p\_Actinobacteria;c\_Actinobacteria;o\_Actinomycetales;f\_Actinomycetaceae;g\_
- k\_Bacteria;p\_Actinobacteria;c\_Actinobacteria;o\_Actinomycetales;f\_Actinomycetaceae;g\_Actinomycetes
- k\_Bacteria;p\_Actinobacteria;c\_Actinobacteria;o\_Actinomycetales;f\_Actinomycetaceae;g\_Mobiluncus
- k\_Bacteria;p\_Actinobacteria;c\_Actinobacteria;o\_Actinomycetales;f\_Actinomycetaceae;g\_Trueperella
- k\_Bacteria;p\_Actinobacteria;c\_Actinobacteria;o\_Actinomycetales;f\_Actinomycetaceae;g\_Varibaculum
- k\_Bacteria;p\_Actinobacteria;c\_Actinobacteria;o\_Actinomycetales;f\_Brevibacteriaceae;g\_Brevibacterium
- k\_Bacteria;p\_Actinobacteria;c\_Actinobacteria;o\_Actinomycetales;f\_Cellulomonadaceae;g\_Cellulomonas
- k\_Bacteria;p\_Actinobacteria;c\_Actinobacteria;o\_Actinomycetales;f\_Corynebacteriaceae;g\_Corynebacterium
- k\_Bacteria;p\_Actinobacteria;c\_Actinobacteria;o\_Actinomycetales;f\_Dermacoccaceae;g\_Dermacoccus
- k\_Bacteria;p\_Actinobacteria;c\_Actinobacteria;o\_Actinomycetales;f\_Dietziaceae;g\_Dietzia
- k\_Bacteria;p\_Actinobacteria;c\_Actinobacteria;o\_Actinomycetales;f\_Gordoniaceae;g\_Gordonia
- k\_Bacteria;p\_Actinobacteria;c\_Actinobacteria;o\_Actinomycetales;f\_Intrasporangiaceae;g\_
- k\_Bacteria;p\_Actinobacteria;c\_Actinobacteria;o\_Actinomycetales;f\_Intrasporangiaceae;g\_Janibacter
- k\_Bacteria;p\_Actinobacteria;c\_Actinobacteria;o\_Actinomycetales;f\_Intrasporangiaceae;g\_Knoellia
- k\_Bacteria;p\_Actinobacteria;c\_Actinobacteria;o\_Actinomycetales;f\_Intrasporangiaceae;g\_Kytococcus
- k\_Bacteria;p\_Actinobacteria;c\_Actinobacteria;o\_Actinomycetales;f\_Intrasporangiaceae;g\_Phycoccus
- k\_Bacteria;p\_Actinobacteria;c\_Actinobacteria;o\_Actinomycetales;f\_Kineosporiaceae;g\_
- k\_Bacteria;p\_Actinobacteria;c\_Actinobacteria;o\_Actinomycetales;f\_Microbacteriaceae;g\_
- k\_Bacteria;p\_Actinobacteria;c\_Actinobacteria;o\_Actinomycetales;f\_Microbacteriaceae;g\_Candidatus Aquiluna
- k\_Bacteria;p\_Actinobacteria;c\_Actinobacteria;o\_Actinomycetales;f\_Microbacteriaceae;g\_Candidatus Rhodoluna
- k\_Bacteria;p\_Actinobacteria;c\_Actinobacteria;o\_Actinomycetales;f\_Microbacteriaceae;g\_Curtobacterium
- k\_Bacteria;p\_Actinobacteria;c\_Actinobacteria;o\_Actinomycetales;f\_Microbacteriaceae;g\_Glaciibacter
- k\_Bacteria;p\_Actinobacteria;c\_Actinobacteria;o\_Actinomycetales;f\_Microbacteriaceae;g\_Microbacterium
- k\_Bacteria;p\_Actinobacteria;c\_Actinobacteria;o\_Actinomycetales;f\_Micrococcaceae;g\_
- k\_Bacteria;p\_Actinobacteria;c\_Actinobacteria;o\_Actinomycetales;f\_Micrococcaceae;g\_Arthrobacter
- k\_Bacteria;p\_Actinobacteria;c\_Actinobacteria;o\_Actinomycetales;f\_Micrococcaceae;g\_Kocuria
- k\_Bacteria;p\_Actinobacteria;c\_Actinobacteria;o\_Actinomycetales;f\_Micrococcaceae;g\_Micrococcus
- k\_Bacteria;p\_Actinobacteria;c\_Actinobacteria;o\_Actinomycetales;f\_Micrococcaceae;g\_Nesterenkonia
- k\_Bacteria;p\_Actinobacteria;c\_Actinobacteria;o\_Actinomycetales;f\_Micrococcaceae;g\_Rothia
- k\_Bacteria;p\_Actinobacteria;c\_Actinobacteria;o\_Actinomycetales;f\_Nocardiaceae;g\_Rhodococcus
- k\_Bacteria;p\_Actinobacteria;c\_Actinobacteria;o\_Actinomycetales;f\_Nocardiopsaceae;g\_Nocardiopsis
- k\_Bacteria;p\_Actinobacteria;c\_Actinobacteria;o\_Actinomycetales;f\_Williamsiaceae;g\_Williamsia
- k\_Bacteria;p\_Actinobacteria;c\_Actinobacteria;o\_Bifidobacteriales;f\_Bifidobacteriaceae;g\_
- k\_Bacteria;p\_Actinobacteria;c\_Actinobacteria;o\_Bifidobacteriales;f\_Bifidobacteriaceae;g\_Alloscardovia
- k\_Bacteria;p\_Actinobacteria;c\_Actinobacteria;o\_Bifidobacteriales;f\_Bifidobacteriaceae;g\_Bifidobacterium
- k\_Bacteria;p\_Actinobacteria;c\_Actinobacteria;o\_Bifidobacteriales;f\_Bifidobacteriaceae;g\_Gardnerella
- k\_Bacteria;p\_Actinobacteria;c\_Actinobacteria;o\_Bifidobacteriales;f\_Bifidobacteriaceae;g\_Scardovia
- k\_Bacteria;p\_Actinobacteria;c\_Coriobacteriia;o\_Coriobacteriales;f\_Coriobacteriaceae;g\_
- k\_Bacteria;p\_Actinobacteria;c\_Coriobacteriia;o\_Coriobacteriales;f\_Coriobacteriaceae;g\_Atopobium
- k\_Bacteria;p\_Actinobacteria;c\_Coriobacteriia;o\_Coriobacteriales;f\_Coriobacteriaceae;g\_Collinsella
- k\_Bacteria;p\_Actinobacteria;c\_Coriobacteriia;o\_Coriobacteriales;f\_Coriobacteriaceae;g\_Eggerthella
- k\_Bacteria;p\_Actinobacteria;c\_Coriobacteriia;o\_Coriobacteriales;f\_Coriobacteriaceae;g\_Slackia
- k\_Bacteria;p\_Actinobacteria;c\_Thermoleophila;o\_Gaiellales;f\_Gaiellaceae;g\_
- k\_Bacteria;p\_Actinobacteria;c\_Thermoleophila;o\_Solirubrobacterales;f\_Patulibacteraceae;g\_Patulibacter
- k\_Bacteria;p\_Bacteroidetes;c\_Bacteroidia;o\_Bacteroidales;f\_g\_



■ k\_Bacteria;p\_Bacteroidetes;c\_Bacteroidia;o\_Bacteroidales;f\_Bacteroidaceae;g\_Bacteroides  
 ■ k\_Bacteria;p\_Bacteroidetes;c\_Bacteroidia;o\_Bacteroidales;f\_Porphyrimonadaceae;g\_  
 ■ k\_Bacteria;p\_Bacteroidetes;c\_Bacteroidia;o\_Bacteroidales;f\_Porphyrimonadaceae;g\_Paludibacter  
 ■ k\_Bacteria;p\_Bacteroidetes;c\_Bacteroidia;o\_Bacteroidales;f\_Porphyrimonadaceae;g\_Parabacteroides  
 ■ k\_Bacteria;p\_Bacteroidetes;c\_Bacteroidia;o\_Bacteroidales;f\_Porphyrimonadaceae;g\_Porphyrimonas  
 ■ k\_Bacteria;p\_Bacteroidetes;c\_Bacteroidia;o\_Bacteroidales;f\_Prevotellaceae;g\_Prevotella  
 ■ k\_Bacteria;p\_Bacteroidetes;c\_Bacteroidia;o\_Bacteroidales;f\_Rikenellaceae;g\_  
 ■ k\_Bacteria;p\_Bacteroidetes;c\_Bacteroidia;o\_Bacteroidales;f\_Rikenellaceae;g\_Alistipes  
 ■ k\_Bacteria;p\_Bacteroidetes;c\_Bacteroidia;o\_Bacteroidales;f\_Rikenellaceae;g\_Bivii28  
 ■ k\_Bacteria;p\_Bacteroidetes;c\_Bacteroidia;o\_Bacteroidales;f\_S24-7;g\_  
 ■ k\_Bacteria;p\_Bacteroidetes;c\_Bacteroidia;o\_Bacteroidales;f\_[Barnesiellaceae];g\_  
 ■ k\_Bacteria;p\_Bacteroidetes;c\_Bacteroidia;o\_Bacteroidales;f\_[Odoribacteraceae];g\_Butyricimonas  
 ■ k\_Bacteria;p\_Bacteroidetes;c\_Bacteroidia;o\_Bacteroidales;f\_[Odoribacteraceae];g\_Odoribacter  
 ■ k\_Bacteria;p\_Bacteroidetes;c\_Bacteroidia;o\_Bacteroidales;f\_[Paraprevotellaceae];g\_  
 ■ k\_Bacteria;p\_Bacteroidetes;c\_Bacteroidia;o\_Bacteroidales;f\_[Paraprevotellaceae];g\_Paraprevotella  
 ■ k\_Bacteria;p\_Bacteroidetes;c\_Bacteroidia;o\_Bacteroidales;f\_[Paraprevotellaceae];g\_[Prevotella]  
 ■ k\_Bacteria;p\_Bacteroidetes;c\_Cytophagia;o\_Cytophagales;f\_Cytophagaceae;g\_  
 ■ k\_Bacteria;p\_Bacteroidetes;c\_Cytophagia;o\_Cytophagales;f\_Cytophagaceae;g\_Hymenobacter  
 ■ k\_Bacteria;p\_Bacteroidetes;c\_Flavobacteriia;o\_Flavobacteriales;f\_Cryomorphaceae;g\_Fluviicola  
 ■ k\_Bacteria;p\_Bacteroidetes;c\_Flavobacteriia;o\_Flavobacteriales;f\_Flavobacteriaceae;g\_  
 ■ k\_Bacteria;p\_Bacteroidetes;c\_Flavobacteriia;o\_Flavobacteriales;f\_Flavobacteriaceae;g\_Flavobacterium  
 ■ k\_Bacteria;p\_Bacteroidetes;c\_Flavobacteriia;o\_Flavobacteriales;f\_[Weeksellaceae];g\_  
 ■ k\_Bacteria;p\_Bacteroidetes;c\_Flavobacteriia;o\_Flavobacteriales;f\_[Weeksellaceae];g\_Chryseobacterium  
 ■ k\_Bacteria;p\_Bacteroidetes;c\_Flavobacteriia;o\_Flavobacteriales;f\_[Weeksellaceae];g\_Cloacibacterium  
 ■ k\_Bacteria;p\_Bacteroidetes;c\_Flavobacteriia;o\_Flavobacteriales;f\_[Weeksellaceae];g\_Elizabethkingia  
 ■ k\_Bacteria;p\_Bacteroidetes;c\_Sphingobacteriia;o\_Sphingobacteriales;f\_  
 ■ k\_Bacteria;p\_Bacteroidetes;c\_Sphingobacteriia;o\_Sphingobacteriales;f\_Sphingobacteriaceae;g\_  
 ■ k\_Bacteria;p\_Bacteroidetes;c\_Sphingobacteriia;o\_Sphingobacteriales;f\_Sphingobacteriaceae;g\_Pedobacter  
 ■ k\_Bacteria;p\_Bacteroidetes;c\_VC2\_1\_Bac22;o\_;f;g\_  
 ■ k\_Bacteria;p\_Bacteroidetes;c\_[Saprosirae];o\_[Saprosirales];f\_Chitinophagaceae;g\_  
 ■ k\_Bacteria;p\_Bacteroidetes;c\_[Saprosirae];o\_[Saprosirales];f\_Chitinophagaceae;g\_Chitinophaga  
 ■ k\_Bacteria;p\_Bacteroidetes;c\_[Saprosirae];o\_[Saprosirales];f\_Chitinophagaceae;g\_Sediminibacterium  
 ■ k\_Bacteria;p\_Bacteroidetes;c\_[Saprosirae];o\_[Saprosirales];f\_Saprosiraceae;g\_  
 ■ k\_Bacteria;p\_Chlorobi;c\_OPB56;o\_;f;g\_  
 ■ k\_Bacteria;p\_Chloroflexi;c\_Anaerolineae;o\_Anaerolineales;f\_Anaerolinaceae;g\_Anaerolinea  
 ■ k\_Bacteria;p\_Chloroflexi;c\_Anaerolineae;o\_Anaerolineales;f\_Anaerolinaceae;g\_T78  
 ■ k\_Bacteria;p\_Chloroflexi;c\_Gitt-GS-136;o\_;f;g\_  
 ■ k\_Bacteria;p\_Chloroflexi;c\_Thermomicrobia;o\_JG30-KF-CM45;f;g\_  
 ■ k\_Bacteria;p\_Cyanobacteria;c\_4C0d-2;o\_YS2;f;g\_  
 ■ k\_Bacteria;p\_Cyanobacteria;c\_Chloroplast;o\_Chlorophyta;f;g\_  
 ■ k\_Bacteria;p\_Cyanobacteria;c\_Chloroplast;o\_Stramenopiles;f;g\_  
 ■ k\_Bacteria;p\_Cyanobacteria;c\_Chloroplast;o\_Streptophyta;f;g\_  
 ■ k\_Bacteria;p\_Cyanobacteria;c\_ML635J-21;o\_;f;g\_  
 ■ k\_Bacteria;p\_Elusimicrobia;c\_Elusimicrobia;o\_llb;f;g\_  
 ■ k\_Bacteria;p\_Firmicutes;c\_Bacilli;o\_Bacillales;f;g\_  
 ■ k\_Bacteria;p\_Firmicutes;c\_Bacilli;o\_Bacillales;f\_Bacillaceae;g\_  
 ■ k\_Bacteria;p\_Firmicutes;c\_Bacilli;o\_Bacillales;f\_Bacillaceae;g\_Anaerobacillus  
 ■ k\_Bacteria;p\_Firmicutes;c\_Bacilli;o\_Bacillales;f\_Bacillaceae;g\_Bacillus  
 ■ k\_Bacteria;p\_Firmicutes;c\_Bacilli;o\_Bacillales;f\_Listeriaceae;g\_Listeria  
 ■ k\_Bacteria;p\_Firmicutes;c\_Bacilli;o\_Bacillales;f\_Paenibacillaceae;g\_Paenibacillus  
 ■ k\_Bacteria;p\_Firmicutes;c\_Bacilli;o\_Bacillales;f\_Planococcaceae;g\_  
 ■ k\_Bacteria;p\_Firmicutes;c\_Bacilli;o\_Bacillales;f\_Planococcaceae;g\_Planomicrobium  
 ■ k\_Bacteria;p\_Firmicutes;c\_Bacilli;o\_Bacillales;f\_Staphylococcaceae;g\_Jeotgalicoccus  
 ■ k\_Bacteria;p\_Firmicutes;c\_Bacilli;o\_Bacillales;f\_Staphylococcaceae;g\_Staphylococcus  
 ■ k\_Bacteria;p\_Firmicutes;c\_Bacilli;o\_Bacillales;f\_[Thermicanaceae];g\_Thermicanus  
 ■ k\_Bacteria;p\_Firmicutes;c\_Bacilli;o\_Gemellales;f;g\_  
 ■ k\_Bacteria;p\_Firmicutes;c\_Bacilli;o\_Gemellales;f\_Gemellaceae;g\_  
 ■ k\_Bacteria;p\_Firmicutes;c\_Bacilli;o\_Gemellales;f\_Gemellaceae;g\_Gemella  
 ■ k\_Bacteria;p\_Firmicutes;c\_Bacilli;o\_Lactobacillales;f;g\_  
 ■ k\_Bacteria;p\_Firmicutes;c\_Bacilli;o\_Lactobacillales;f\_Aerococcaceae;g\_  
 ■ k\_Bacteria;p\_Firmicutes;c\_Bacilli;o\_Lactobacillales;f\_Aerococcaceae;g\_Aerococcus  
 ■ k\_Bacteria;p\_Firmicutes;c\_Bacilli;o\_Lactobacillales;f\_Aerococcaceae;g\_Alloiococcus  
 ■ k\_Bacteria;p\_Firmicutes;c\_Bacilli;o\_Lactobacillales;f\_Carnobacteriaceae;g\_  
 ■ k\_Bacteria;p\_Firmicutes;c\_Bacilli;o\_Lactobacillales;f\_Carnobacteriaceae;g\_Granulicatella  
 ■ k\_Bacteria;p\_Firmicutes;c\_Bacilli;o\_Lactobacillales;f\_Carnobacteriaceae;g\_Isobaculum  
 ■ k\_Bacteria;p\_Firmicutes;c\_Bacilli;o\_Lactobacillales;f\_Enterococcaceae;g\_  
 ■ k\_Bacteria;p\_Firmicutes;c\_Bacilli;o\_Lactobacillales;f\_Enterococcaceae;g\_Enterococcus  
 ■ k\_Bacteria;p\_Firmicutes;c\_Bacilli;o\_Lactobacillales;f\_Enterococcaceae;g\_Melissococcus  
 ■ k\_Bacteria;p\_Firmicutes;c\_Bacilli;o\_Lactobacillales;f\_Enterococcaceae;g\_Vagococcus  
 ■ k\_Bacteria;p\_Firmicutes;c\_Bacilli;o\_Lactobacillales;f\_Lactobacillaceae;g\_Lactobacillus  
 ■ k\_Bacteria;p\_Firmicutes;c\_Bacilli;o\_Lactobacillales;f\_Leuconostocaceae;g\_Leuconostoc  
 ■ k\_Bacteria;p\_Firmicutes;c\_Bacilli;o\_Lactobacillales;f\_Leuconostocaceae;g\_Weissella  
 ■ k\_Bacteria;p\_Firmicutes;c\_Bacilli;o\_Lactobacillales;f\_Streptococcaceae;g\_  
 ■ k\_Bacteria;p\_Firmicutes;c\_Bacilli;o\_Lactobacillales;f\_Streptococcaceae;g\_Lactococcus  
 ■ k\_Bacteria;p\_Firmicutes;c\_Bacilli;o\_Lactobacillales;f\_Streptococcaceae;g\_Streptococcus

■ k\_Bacteria;p\_Firmicutes;c\_Bacilli;o\_Turicibacterales;f\_Turicibacteraceae;g\_Turicibacter  
 ■ k\_Bacteria;p\_Firmicutes;c\_Clostridia;o\_Clostridiales;f\_;g\_  
 ■ k\_Bacteria;p\_Firmicutes;c\_Clostridia;o\_Clostridiales;f\_Christensenellaceae;g\_  
 ■ k\_Bacteria;p\_Firmicutes;c\_Clostridia;o\_Clostridiales;f\_Clostridiaceae;g\_  
 ■ k\_Bacteria;p\_Firmicutes;c\_Clostridia;o\_Clostridiales;f\_Clostridiaceae;g\_02d06  
 ■ k\_Bacteria;p\_Firmicutes;c\_Clostridia;o\_Clostridiales;f\_Clostridiaceae;g\_Caloramator  
 ■ k\_Bacteria;p\_Firmicutes;c\_Clostridia;o\_Clostridiales;f\_Clostridiaceae;g\_Clostridium  
 ■ k\_Bacteria;p\_Firmicutes;c\_Clostridia;o\_Clostridiales;f\_Clostridiaceae;g\_SMB53  
 ■ k\_Bacteria;p\_Firmicutes;c\_Clostridia;o\_Clostridiales;f\_Clostridiaceae;g\_Sarcina  
 ■ k\_Bacteria;p\_Firmicutes;c\_Clostridia;o\_Clostridiales;f\_Clostridiaceae;g\_Thermoanaerobacterium  
 ■ k\_Bacteria;p\_Firmicutes;c\_Clostridia;o\_Clostridiales;f\_Dehalobacteriaceae;g\_  
 ■ k\_Bacteria;p\_Firmicutes;c\_Clostridia;o\_Clostridiales;f\_Eubacteriaceae;g\_Anaerofustis  
 ■ k\_Bacteria;p\_Firmicutes;c\_Clostridia;o\_Clostridiales;f\_Eubacteriaceae;g\_Pseudoramibacter\_Eubacterium  
 ■ k\_Bacteria;p\_Firmicutes;c\_Clostridia;o\_Clostridiales;f\_Lachnospiraceae;g\_  
 ■ k\_Bacteria;p\_Firmicutes;c\_Clostridia;o\_Clostridiales;f\_Lachnospiraceae;g\_Anaerostipes  
 ■ k\_Bacteria;p\_Firmicutes;c\_Clostridia;o\_Clostridiales;f\_Lachnospiraceae;g\_Blautia  
 ■ k\_Bacteria;p\_Firmicutes;c\_Clostridia;o\_Clostridiales;f\_Lachnospiraceae;g\_Clostridium  
 ■ k\_Bacteria;p\_Firmicutes;c\_Clostridia;o\_Clostridiales;f\_Lachnospiraceae;g\_Coprococcus  
 ■ k\_Bacteria;p\_Firmicutes;c\_Clostridia;o\_Clostridiales;f\_Lachnospiraceae;g\_Dorea  
 ■ k\_Bacteria;p\_Firmicutes;c\_Clostridia;o\_Clostridiales;f\_Lachnospiraceae;g\_Epuloiscium  
 ■ k\_Bacteria;p\_Firmicutes;c\_Clostridia;o\_Clostridiales;f\_Lachnospiraceae;g\_Lachnobacterium  
 ■ k\_Bacteria;p\_Firmicutes;c\_Clostridia;o\_Clostridiales;f\_Lachnospiraceae;g\_Lachnospira  
 ■ k\_Bacteria;p\_Firmicutes;c\_Clostridia;o\_Clostridiales;f\_Lachnospiraceae;g\_Moryella  
 ■ k\_Bacteria;p\_Firmicutes;c\_Clostridia;o\_Clostridiales;f\_Lachnospiraceae;g\_Oribacterium  
 ■ k\_Bacteria;p\_Firmicutes;c\_Clostridia;o\_Clostridiales;f\_Lachnospiraceae;g\_Roseburia  
 ■ k\_Bacteria;p\_Firmicutes;c\_Clostridia;o\_Clostridiales;f\_Lachnospiraceae;g\_Shuttleworthia  
 ■ k\_Bacteria;p\_Firmicutes;c\_Clostridia;o\_Clostridiales;f\_Lachnospiraceae;g\_[Ruminococcus]  
 ■ k\_Bacteria;p\_Firmicutes;c\_Clostridia;o\_Clostridiales;f\_Peptococcaceae;g\_Peptococcus  
 ■ k\_Bacteria;p\_Firmicutes;c\_Clostridia;o\_Clostridiales;f\_Peptococcaceae;g\_WCHB1-84  
 ■ k\_Bacteria;p\_Firmicutes;c\_Clostridia;o\_Clostridiales;f\_Peptostreptococcaceae;g\_  
 ■ k\_Bacteria;p\_Firmicutes;c\_Clostridia;o\_Clostridiales;f\_Peptostreptococcaceae;g\_Peptostreptococcus  
 ■ k\_Bacteria;p\_Firmicutes;c\_Clostridia;o\_Clostridiales;f\_Peptostreptococcaceae;g\_[Clostridium]  
 ■ k\_Bacteria;p\_Firmicutes;c\_Clostridia;o\_Clostridiales;f\_Ruminococcaceae;g\_  
 ■ k\_Bacteria;p\_Firmicutes;c\_Clostridia;o\_Clostridiales;f\_Ruminococcaceae;g\_Anaerotruncus  
 ■ k\_Bacteria;p\_Firmicutes;c\_Clostridia;o\_Clostridiales;f\_Ruminococcaceae;g\_Faecalibacterium  
 ■ k\_Bacteria;p\_Firmicutes;c\_Clostridia;o\_Clostridiales;f\_Ruminococcaceae;g\_Oscillospira  
 ■ k\_Bacteria;p\_Firmicutes;c\_Clostridia;o\_Clostridiales;f\_Ruminococcaceae;g\_Ruminococcus  
 ■ k\_Bacteria;p\_Firmicutes;c\_Clostridia;o\_Clostridiales;f\_Veillonellaceae;g\_  
 ■ k\_Bacteria;p\_Firmicutes;c\_Clostridia;o\_Clostridiales;f\_Veillonellaceae;g\_Acidaminococcus  
 ■ k\_Bacteria;p\_Firmicutes;c\_Clostridia;o\_Clostridiales;f\_Veillonellaceae;g\_Dialister  
 ■ k\_Bacteria;p\_Firmicutes;c\_Clostridia;o\_Clostridiales;f\_Veillonellaceae;g\_Megamonas  
 ■ k\_Bacteria;p\_Firmicutes;c\_Clostridia;o\_Clostridiales;f\_Veillonellaceae;g\_Megasphaera  
 ■ k\_Bacteria;p\_Firmicutes;c\_Clostridia;o\_Clostridiales;f\_Veillonellaceae;g\_Mitsuokella  
 ■ k\_Bacteria;p\_Firmicutes;c\_Clostridia;o\_Clostridiales;f\_Veillonellaceae;g\_Pectinatus  
 ■ k\_Bacteria;p\_Firmicutes;c\_Clostridia;o\_Clostridiales;f\_Veillonellaceae;g\_Pelosinus  
 ■ k\_Bacteria;p\_Firmicutes;c\_Clostridia;o\_Clostridiales;f\_Veillonellaceae;g\_Phascolarctobacterium  
 ■ k\_Bacteria;p\_Firmicutes;c\_Clostridia;o\_Clostridiales;f\_Veillonellaceae;g\_Selenomonas  
 ■ k\_Bacteria;p\_Firmicutes;c\_Clostridia;o\_Clostridiales;f\_Veillonellaceae;g\_Succiniclasticum  
 ■ k\_Bacteria;p\_Firmicutes;c\_Clostridia;o\_Clostridiales;f\_Veillonellaceae;g\_Veillonella  
 ■ k\_Bacteria;p\_Firmicutes;c\_Clostridia;o\_Clostridiales;f\_[Acidaminobacteraceae];g\_  
 ■ k\_Bacteria;p\_Firmicutes;c\_Clostridia;o\_Clostridiales;f\_[Mogibacteriaceae];g\_  
 ■ k\_Bacteria;p\_Firmicutes;c\_Clostridia;o\_Clostridiales;f\_[Mogibacteriaceae];g\_Mogibacterium  
 ■ k\_Bacteria;p\_Firmicutes;c\_Clostridia;o\_Clostridiales;f\_[Tissierellaceae];g\_1-68  
 ■ k\_Bacteria;p\_Firmicutes;c\_Clostridia;o\_Clostridiales;f\_[Tissierellaceae];g\_Anaerococcus  
 ■ k\_Bacteria;p\_Firmicutes;c\_Clostridia;o\_Clostridiales;f\_[Tissierellaceae];g\_Finegoldia  
 ■ k\_Bacteria;p\_Firmicutes;c\_Clostridia;o\_Clostridiales;f\_[Tissierellaceae];g\_Parvimonas  
 ■ k\_Bacteria;p\_Firmicutes;c\_Clostridia;o\_Clostridiales;f\_[Tissierellaceae];g\_Peptoniphilus  
 ■ k\_Bacteria;p\_Firmicutes;c\_Clostridia;o\_Clostridiales;f\_[Tissierellaceae];g\_WAL\_1855D  
 ■ k\_Bacteria;p\_Firmicutes;c\_Clostridia;o\_Clostridiales;f\_[Tissierellaceae];g\_ph2  
 ■ k\_Bacteria;p\_Firmicutes;c\_Clostridia;o\_Natranaerobiales;f\_Anaerobranchaceae;g\_Dethiobacter  
 ■ k\_Bacteria;p\_Firmicutes;c\_Clostridia;o\_Thermoanaerobacteriales;f\_Caldicellulosiruptoraceae;g\_Caldicellulosiruptor  
 ■ k\_Bacteria;p\_Firmicutes;c\_Clostridia;o\_Thermoanaerobacteriales;f\_Thermoanaerobacteraceae;g\_Moorella  
 ■ k\_Bacteria;p\_Firmicutes;c\_Clostridia;o\_Thermoanaerobacteriales;f\_Thermoanaerobacteraceae;g\_Thermoanaerobacter  
 ■ k\_Bacteria;p\_Firmicutes;c\_Erysipelotrichi;o\_Erysipelotrichales;f\_Erysipelotrichaceae;g\_  
 ■ k\_Bacteria;p\_Firmicutes;c\_Erysipelotrichi;o\_Erysipelotrichales;f\_Erysipelotrichaceae;g\_Bulleidia  
 ■ k\_Bacteria;p\_Firmicutes;c\_Erysipelotrichi;o\_Erysipelotrichales;f\_Erysipelotrichaceae;g\_Catenibacterium  
 ■ k\_Bacteria;p\_Firmicutes;c\_Erysipelotrichi;o\_Erysipelotrichales;f\_Erysipelotrichaceae;g\_Clostridium  
 ■ k\_Bacteria;p\_Firmicutes;c\_Erysipelotrichi;o\_Erysipelotrichales;f\_Erysipelotrichaceae;g\_Coprobacillus  
 ■ k\_Bacteria;p\_Firmicutes;c\_Erysipelotrichi;o\_Erysipelotrichales;f\_Erysipelotrichaceae;g\_Holdmania  
 ■ k\_Bacteria;p\_Firmicutes;c\_Erysipelotrichi;o\_Erysipelotrichales;f\_Erysipelotrichaceae;g\_Sharpea  
 ■ k\_Bacteria;p\_Firmicutes;c\_Erysipelotrichi;o\_Erysipelotrichales;f\_Erysipelotrichaceae;g\_[Eubacterium]  
 ■ k\_Bacteria;p\_Fusobacteria;c\_Fusobacteriia;o\_Fusobacteriales;f\_Fusobacteriaceae;g\_Fusobacterium



■ k\_Bacteria;p\_Fusobacteria;c\_Fusobacteriia;o\_Fusobacteriales;f\_Leptotrichiaceae;g\_Leptotrichia  
 ■ k\_Bacteria;p\_Fusobacteria;c\_Fusobacteriia;o\_Fusobacteriales;f\_Leptotrichiaceae;g\_Sneathia  
 ■ k\_Bacteria;p\_Gemmatimonadetes;c\_Gemmatimonadetes;o\_Gemmatimonadales;f\_A1-B1;g\_  
 ■ k\_Bacteria;p\_OD1;c\_ZB2;o\_f;g\_  
 ■ k\_Bacteria;p\_Planctomycetes;c\_Planctomycetia;o\_Planctomycetales;f\_Planctomycetaceae;g\_Planctomyces  
 ■ k\_Bacteria;p\_Proteobacteria;c\_Alphaproteobacteria;o\_Caulobacterales;f\_Caulobacteraceae;g\_  
 ■ k\_Bacteria;p\_Proteobacteria;c\_Alphaproteobacteria;o\_Caulobacterales;f\_Caulobacteraceae;g\_Asticcacaulis  
 ■ k\_Bacteria;p\_Proteobacteria;c\_Alphaproteobacteria;o\_Caulobacterales;f\_Caulobacteraceae;g\_Brevundimonas  
 ■ k\_Bacteria;p\_Proteobacteria;c\_Alphaproteobacteria;o\_Caulobacterales;f\_Caulobacteraceae;g\_Caulobacter  
 ■ k\_Bacteria;p\_Proteobacteria;c\_Alphaproteobacteria;o\_Caulobacterales;f\_Caulobacteraceae;g\_Phenylobacterium  
 ■ k\_Bacteria;p\_Proteobacteria;c\_Alphaproteobacteria;o\_RF32;f;g\_  
 ■ k\_Bacteria;p\_Proteobacteria;c\_Alphaproteobacteria;o\_Rhizobiales;f;g\_  
 ■ k\_Bacteria;p\_Proteobacteria;c\_Alphaproteobacteria;o\_Rhizobiales;f\_Beijerinckiaceae;g\_  
 ■ k\_Bacteria;p\_Proteobacteria;c\_Alphaproteobacteria;o\_Rhizobiales;f\_Bradyrhizobiaceae;g\_  
 ■ k\_Bacteria;p\_Proteobacteria;c\_Alphaproteobacteria;o\_Rhizobiales;f\_Bradyrhizobiaceae;g\_Bradyrhizobium  
 ■ k\_Bacteria;p\_Proteobacteria;c\_Alphaproteobacteria;o\_Rhizobiales;f\_Brucellaceae;g\_Ochrobactrum  
 ■ k\_Bacteria;p\_Proteobacteria;c\_Alphaproteobacteria;o\_Rhizobiales;f\_Brucellaceae;g\_Pseudochrobactrum  
 ■ k\_Bacteria;p\_Proteobacteria;c\_Alphaproteobacteria;o\_Rhizobiales;f\_Methylobacteriaceae;g\_  
 ■ k\_Bacteria;p\_Proteobacteria;c\_Alphaproteobacteria;o\_Rhizobiales;f\_Methylobacteriaceae;g\_Methylobacterium  
 ■ k\_Bacteria;p\_Proteobacteria;c\_Alphaproteobacteria;o\_Rhizobiales;f\_Phyllobacteriaceae;g\_Mesorhizobium  
 ■ k\_Bacteria;p\_Proteobacteria;c\_Alphaproteobacteria;o\_Rhizobiales;f\_Phyllobacteriaceae;g\_Phyllobacterium  
 ■ k\_Bacteria;p\_Proteobacteria;c\_Alphaproteobacteria;o\_Rhizobiales;f\_Rhizobiaceae;g\_  
 ■ k\_Bacteria;p\_Proteobacteria;c\_Alphaproteobacteria;o\_Rhizobiales;f\_Rhizobiaceae;g\_Agrobacterium  
 ■ k\_Bacteria;p\_Proteobacteria;c\_Alphaproteobacteria;o\_Rhizobiales;f\_Xanthobacteraceae;g\_  
 ■ k\_Bacteria;p\_Proteobacteria;c\_Alphaproteobacteria;o\_Rhizobiales;f\_Xanthobacteraceae;g\_Labrys  
 ■ k\_Bacteria;p\_Proteobacteria;c\_Alphaproteobacteria;o\_Rhodobacterales;f\_Rhodobacteraceae;g\_  
 ■ k\_Bacteria;p\_Proteobacteria;c\_Alphaproteobacteria;o\_Rhodobacterales;f\_Rhodobacteraceae;g\_Paracoccus  
 ■ k\_Bacteria;p\_Proteobacteria;c\_Alphaproteobacteria;o\_Rhodospirillales;f\_Acetobacteraceae;g\_  
 ■ k\_Bacteria;p\_Proteobacteria;c\_Alphaproteobacteria;o\_Rhodospirillales;f\_Acetobacteraceae;g\_Acidocella  
 ■ k\_Bacteria;p\_Proteobacteria;c\_Alphaproteobacteria;o\_Rhodospirillales;f\_Acetobacteraceae;g\_Roseomonas  
 ■ k\_Bacteria;p\_Proteobacteria;c\_Alphaproteobacteria;o\_Rhodospirillales;f\_Rhodospirillaceae;g\_  
 ■ k\_Bacteria;p\_Proteobacteria;c\_Alphaproteobacteria;o\_Rhodospirillales;f\_Rhodospirillaceae;g\_Azospirillum  
 ■ k\_Bacteria;p\_Proteobacteria;c\_Alphaproteobacteria;o\_Rhodospirillales;f\_Rhodospirillaceae;g\_Phaeospirillum  
 ■ k\_Bacteria;p\_Proteobacteria;c\_Alphaproteobacteria;o\_Rickettsiales;f\_Rickettsiaceae;g\_  
 ■ k\_Bacteria;p\_Proteobacteria;c\_Alphaproteobacteria;o\_Rickettsiales;f\_mitochondria;g\_Acanthamoeba  
 ■ k\_Bacteria;p\_Proteobacteria;c\_Alphaproteobacteria;o\_Rickettsiales;f\_mitochondria;g\_Carludovica  
 ■ k\_Bacteria;p\_Proteobacteria;c\_Alphaproteobacteria;o\_Rickettsiales;f\_mitochondria;g\_Diplazium  
 ■ k\_Bacteria;p\_Proteobacteria;c\_Alphaproteobacteria;o\_Rickettsiales;f\_mitochondria;g\_Sarcandra  
 ■ k\_Bacteria;p\_Proteobacteria;c\_Alphaproteobacteria;o\_Rickettsiales;f\_mitochondria;g\_Zea  
 ■ k\_Bacteria;p\_Proteobacteria;c\_Alphaproteobacteria;o\_Sphingomonadales;f;g\_  
 ■ k\_Bacteria;p\_Proteobacteria;c\_Alphaproteobacteria;o\_Sphingomonadales;f\_Erythrobacteraceae;g\_  
 ■ k\_Bacteria;p\_Proteobacteria;c\_Alphaproteobacteria;o\_Sphingomonadales;f\_Sphingomonadaceae;g\_  
 ■ k\_Bacteria;p\_Proteobacteria;c\_Alphaproteobacteria;o\_Sphingomonadales;f\_Sphingomonadaceae;g\_Kaistobacter  
 ■ k\_Bacteria;p\_Proteobacteria;c\_Alphaproteobacteria;o\_Sphingomonadales;f\_Sphingomonadaceae;g\_Novosphingobium  
 ■ k\_Bacteria;p\_Proteobacteria;c\_Alphaproteobacteria;o\_Sphingomonadales;f\_Sphingomonadaceae;g\_Sphingobium  
 ■ k\_Bacteria;p\_Proteobacteria;c\_Alphaproteobacteria;o\_Sphingomonadales;f\_Sphingomonadaceae;g\_Sphingomonas  
 ■ k\_Bacteria;p\_Proteobacteria;c\_Betaproteobacteria;o\_Burkholderiales;f;g\_  
 ■ k\_Bacteria;p\_Proteobacteria;c\_Betaproteobacteria;o\_Burkholderiales;f\_Alcaligenaceae;g\_Achromobacter  
 ■ k\_Bacteria;p\_Proteobacteria;c\_Betaproteobacteria;o\_Burkholderiales;f\_Alcaligenaceae;g\_Rhodospirillum  
 ■ k\_Bacteria;p\_Proteobacteria;c\_Betaproteobacteria;o\_Burkholderiales;f\_Alcaligenaceae;g\_Sutterella  
 ■ k\_Bacteria;p\_Proteobacteria;c\_Betaproteobacteria;o\_Burkholderiales;f\_Burkholderiaceae;g\_Lautropia  
 ■ k\_Bacteria;p\_Proteobacteria;c\_Betaproteobacteria;o\_Burkholderiales;f\_Comamonadaceae;g\_  
 ■ k\_Bacteria;p\_Proteobacteria;c\_Betaproteobacteria;o\_Burkholderiales;f\_Comamonadaceae;g\_Alicyclophilus  
 ■ k\_Bacteria;p\_Proteobacteria;c\_Betaproteobacteria;o\_Burkholderiales;f\_Comamonadaceae;g\_Comamonas  
 ■ k\_Bacteria;p\_Proteobacteria;c\_Betaproteobacteria;o\_Burkholderiales;f\_Comamonadaceae;g\_Delftia  
 ■ k\_Bacteria;p\_Proteobacteria;c\_Betaproteobacteria;o\_Burkholderiales;f\_Comamonadaceae;g\_Giesbergia  
 ■ k\_Bacteria;p\_Proteobacteria;c\_Betaproteobacteria;o\_Burkholderiales;f\_Comamonadaceae;g\_Hylemonella  
 ■ k\_Bacteria;p\_Proteobacteria;c\_Betaproteobacteria;o\_Burkholderiales;f\_Comamonadaceae;g\_Leptothrix  
 ■ k\_Bacteria;p\_Proteobacteria;c\_Betaproteobacteria;o\_Burkholderiales;f\_Comamonadaceae;g\_Limnochabans  
 ■ k\_Bacteria;p\_Proteobacteria;c\_Betaproteobacteria;o\_Burkholderiales;f\_Comamonadaceae;g\_Methylobium  
 ■ k\_Bacteria;p\_Proteobacteria;c\_Betaproteobacteria;o\_Burkholderiales;f\_Comamonadaceae;g\_Polaromonas  
 ■ k\_Bacteria;p\_Proteobacteria;c\_Betaproteobacteria;o\_Burkholderiales;f\_Comamonadaceae;g\_Rubrivivax  
 ■ k\_Bacteria;p\_Proteobacteria;c\_Betaproteobacteria;o\_Burkholderiales;f\_Comamonadaceae;g\_Schlegelella  
 ■ k\_Bacteria;p\_Proteobacteria;c\_Betaproteobacteria;o\_Burkholderiales;f\_Comamonadaceae;g\_Simplicispira  
 ■ k\_Bacteria;p\_Proteobacteria;c\_Betaproteobacteria;o\_Burkholderiales;f\_Comamonadaceae;g\_Variovorax  
 ■ k\_Bacteria;p\_Proteobacteria;c\_Betaproteobacteria;o\_Burkholderiales;f\_Oxalobacteraceae;g\_  
 ■ k\_Bacteria;p\_Proteobacteria;c\_Betaproteobacteria;o\_Burkholderiales;f\_Oxalobacteraceae;g\_Collimonas  
 ■ k\_Bacteria;p\_Proteobacteria;c\_Betaproteobacteria;o\_Burkholderiales;f\_Oxalobacteraceae;g\_Polynucleobacter  
 ■ k\_Bacteria;p\_Proteobacteria;c\_Betaproteobacteria;o\_Burkholderiales;f\_Oxalobacteraceae;g\_Ralstonia  
 ■ k\_Bacteria;p\_Proteobacteria;c\_Betaproteobacteria;o\_Ellin6067;f;g\_  
 ■ k\_Bacteria;p\_Proteobacteria;c\_Betaproteobacteria;o\_Neisseriales;f\_Neisseriaceae;g\_  
 ■ k\_Bacteria;p\_Proteobacteria;c\_Betaproteobacteria;o\_Neisseriales;f\_Neisseriaceae;g\_Aquaspirillum  
 ■ k\_Bacteria;p\_Proteobacteria;c\_Betaproteobacteria;o\_Neisseriales;f\_Neisseriaceae;g\_Eikenella  
 ■ k\_Bacteria;p\_Proteobacteria;c\_Betaproteobacteria;o\_Neisseriales;f\_Neisseriaceae;g\_Kingella



k\_Bacteria;p\_Proteobacteria;c\_Betaproteobacteria;o\_Neisseriales;f\_Neisseriaceae;g\_Neisseria  
 k\_Bacteria;p\_Proteobacteria;c\_Betaproteobacteria;o\_Rhodocyclales;f\_Rhodocyclaceae;g\_  
 k\_Bacteria;p\_Proteobacteria;c\_Betaproteobacteria;o\_Rhodocyclales;f\_Rhodocyclaceae;g\_KD1-23  
 k\_Bacteria;p\_Proteobacteria;c\_Betaproteobacteria;o\_Rhodocyclales;f\_Rhodocyclaceae;g\_Methyloversatilis  
 k\_Bacteria;p\_Proteobacteria;c\_Betaproteobacteria;o\_Rhodocyclales;f\_Rhodocyclaceae;g\_Rhodocyclus  
 k\_Bacteria;p\_Proteobacteria;c\_Betaproteobacteria;o\_SBl14;f\_;g\_  
 k\_Bacteria;p\_Proteobacteria;c\_Deltaproteobacteria;o\_;f\_;g\_  
 k\_Bacteria;p\_Proteobacteria;c\_Deltaproteobacteria;o\_Bdellovibrionales;f\_Bdellovibrionaceae;g\_Bdellovibrio  
 k\_Bacteria;p\_Proteobacteria;c\_Deltaproteobacteria;o\_Desulfobacterales;f\_Nitrospinaceae;g\_Nitrospina  
 k\_Bacteria;p\_Proteobacteria;c\_Deltaproteobacteria;o\_Desulfovibrionales;f\_Desulfovibrionaceae;g\_  
 k\_Bacteria;p\_Proteobacteria;c\_Deltaproteobacteria;o\_Desulfovibrionales;f\_Desulfovibrionaceae;g\_Bilophila  
 k\_Bacteria;p\_Proteobacteria;c\_Deltaproteobacteria;o\_Desulfovibrionales;f\_Desulfovibrionaceae;g\_Desulfovibrio  
 k\_Bacteria;p\_Proteobacteria;c\_Epsilonproteobacteria;o\_Campylobacteriales;f\_Campylobacteriaceae;g\_Campylobacter  
 k\_Bacteria;p\_Proteobacteria;c\_Epsilonproteobacteria;o\_Campylobacteriales;f\_Campylobacteriaceae;g\_Sulfurospirillum  
 k\_Bacteria;p\_Proteobacteria;c\_Gammaproteobacteria;o\_Aeromonadales;f\_Aeromonadaceae;g\_  
 k\_Bacteria;p\_Proteobacteria;c\_Gammaproteobacteria;o\_Aeromonadales;f\_Aeromonadaceae;g\_Aeromonas  
 k\_Bacteria;p\_Proteobacteria;c\_Gammaproteobacteria;o\_Alteromonadales;f\_Alteromonadaceae;g\_Cellvibrio  
 k\_Bacteria;p\_Proteobacteria;c\_Gammaproteobacteria;o\_Enterobacteriales;f\_Enterobacteriaceae;g\_  
 k\_Bacteria;p\_Proteobacteria;c\_Gammaproteobacteria;o\_Enterobacteriales;f\_Enterobacteriaceae;g\_Brenneria  
 k\_Bacteria;p\_Proteobacteria;c\_Gammaproteobacteria;o\_Enterobacteriales;f\_Enterobacteriaceae;g\_Citrobacter  
 k\_Bacteria;p\_Proteobacteria;c\_Gammaproteobacteria;o\_Enterobacteriales;f\_Enterobacteriaceae;g\_Dickeya  
 k\_Bacteria;p\_Proteobacteria;c\_Gammaproteobacteria;o\_Enterobacteriales;f\_Enterobacteriaceae;g\_Enterobacter  
 k\_Bacteria;p\_Proteobacteria;c\_Gammaproteobacteria;o\_Enterobacteriales;f\_Enterobacteriaceae;g\_Erwinia  
 k\_Bacteria;p\_Proteobacteria;c\_Gammaproteobacteria;o\_Enterobacteriales;f\_Enterobacteriaceae;g\_Escherichia  
 k\_Bacteria;p\_Proteobacteria;c\_Gammaproteobacteria;o\_Enterobacteriales;f\_Enterobacteriaceae;g\_Klebsiella  
 k\_Bacteria;p\_Proteobacteria;c\_Gammaproteobacteria;o\_Enterobacteriales;f\_Enterobacteriaceae;g\_Morganella  
 k\_Bacteria;p\_Proteobacteria;c\_Gammaproteobacteria;o\_Enterobacteriales;f\_Enterobacteriaceae;g\_Pantoea  
 k\_Bacteria;p\_Proteobacteria;c\_Gammaproteobacteria;o\_Enterobacteriales;f\_Enterobacteriaceae;g\_Plesiomonas  
 k\_Bacteria;p\_Proteobacteria;c\_Gammaproteobacteria;o\_Enterobacteriales;f\_Enterobacteriaceae;g\_Proteus  
 k\_Bacteria;p\_Proteobacteria;c\_Gammaproteobacteria;o\_Enterobacteriales;f\_Enterobacteriaceae;g\_Rahnella  
 k\_Bacteria;p\_Proteobacteria;c\_Gammaproteobacteria;o\_Enterobacteriales;f\_Enterobacteriaceae;g\_Salmonella  
 k\_Bacteria;p\_Proteobacteria;c\_Gammaproteobacteria;o\_Enterobacteriales;f\_Enterobacteriaceae;g\_Serratia  
 k\_Bacteria;p\_Proteobacteria;c\_Gammaproteobacteria;o\_Enterobacteriales;f\_Enterobacteriaceae;g\_Shigella  
 k\_Bacteria;p\_Proteobacteria;c\_Gammaproteobacteria;o\_Enterobacteriales;f\_Enterobacteriaceae;g\_Stenotrophomonas  
 k\_Bacteria;p\_Proteobacteria;c\_Gammaproteobacteria;o\_Enterobacteriales;f\_Enterobacteriaceae;g\_Trabulsiella  
 k\_Bacteria;p\_Proteobacteria;c\_Gammaproteobacteria;o\_Enterobacteriales;f\_Enterobacteriaceae;g\_Xenorhabdus  
 k\_Bacteria;p\_Proteobacteria;c\_Gammaproteobacteria;o\_Enterobacteriales;f\_Enterobacteriaceae;g\_Yersinia  
 k\_Bacteria;p\_Proteobacteria;c\_Gammaproteobacteria;o\_Pasteurellales;f\_Pasteurellaceae;g\_  
 k\_Bacteria;p\_Proteobacteria;c\_Gammaproteobacteria;o\_Pasteurellales;f\_Pasteurellaceae;g\_Actinobacillus  
 k\_Bacteria;p\_Proteobacteria;c\_Gammaproteobacteria;o\_Pasteurellales;f\_Pasteurellaceae;g\_Aggregatibacter  
 k\_Bacteria;p\_Proteobacteria;c\_Gammaproteobacteria;o\_Pasteurellales;f\_Pasteurellaceae;g\_Haemophilus  
 k\_Bacteria;p\_Proteobacteria;c\_Gammaproteobacteria;o\_Pseudomonadales;f\_Moraxellaceae;g\_  
 k\_Bacteria;p\_Proteobacteria;c\_Gammaproteobacteria;o\_Pseudomonadales;f\_Moraxellaceae;g\_Acinetobacter  
 k\_Bacteria;p\_Proteobacteria;c\_Gammaproteobacteria;o\_Pseudomonadales;f\_Moraxellaceae;g\_Enhydrobacter  
 k\_Bacteria;p\_Proteobacteria;c\_Gammaproteobacteria;o\_Pseudomonadales;f\_Moraxellaceae;g\_Moraxella  
 k\_Bacteria;p\_Proteobacteria;c\_Gammaproteobacteria;o\_Pseudomonadales;f\_Moraxellaceae;g\_Psychrobacter  
 k\_Bacteria;p\_Proteobacteria;c\_Gammaproteobacteria;o\_Pseudomonadales;f\_Pseudomonadaceae;g\_Pseudomonas  
 k\_Bacteria;p\_Proteobacteria;c\_Gammaproteobacteria;o\_Xanthomonadales;f\_Xanthomonadaceae;g\_  
 k\_Bacteria;p\_Proteobacteria;c\_Gammaproteobacteria;o\_Xanthomonadales;f\_Xanthomonadaceae;g\_Dokdonella  
 k\_Bacteria;p\_Proteobacteria;c\_Gammaproteobacteria;o\_Xanthomonadales;f\_Xanthomonadaceae;g\_Luteimonas  
 k\_Bacteria;p\_Proteobacteria;c\_Gammaproteobacteria;o\_Xanthomonadales;f\_Xanthomonadaceae;g\_Lysobacter  
 k\_Bacteria;p\_Proteobacteria;c\_Gammaproteobacteria;o\_Xanthomonadales;f\_Xanthomonadaceae;g\_Stenotrophomonas  
 k\_Bacteria;p\_SR1;c\_;o\_;f\_;g\_  
 k\_Bacteria;p\_Spirochaetes;c\_Spirochaetes;o\_Spirochaetales;f\_Spirochaetaceae;g\_Spirochaeta  
 k\_Bacteria;p\_TM6;c\_SJA-4;o\_;f\_;g\_  
 k\_Bacteria;p\_TM7;c\_TM7-3;o\_CW040;f\_;g\_  
 k\_Bacteria;p\_Tenericutes;c\_Mollicutes;o\_RF39;f\_;g\_  
 k\_Bacteria;p\_Verrucomicrobia;c\_Verrucomicrobiae;o\_Verrucomicrobiales;f\_Verrucomicrobiaceae;g\_  
 k\_Bacteria;p\_Verrucomicrobia;c\_Verrucomicrobiae;o\_Verrucomicrobiales;f\_Verrucomicrobiaceae;g\_Akkermansia  
 k\_Bacteria;p\_Verrucomicrobia;c\_Verrucomicrobiae;o\_Verrucomicrobiales;f\_Verrucomicrobiaceae;g\_Luteolibacter  
 k\_Bacteria;p\_Verrucomicrobia;c\_Verrucomicrobiae;o\_Verrucomicrobiales;f\_Verrucomicrobiaceae;g\_Prostheobacter  
 k\_Bacteria;p\_Verrucomicrobia;c\_[Spartobacteria];o\_[Chthoniobacteriales];f\_[Chthoniobacteriaceae];g\_DA101  
 k\_Bacteria;p\_[Thermi];c\_Deinococci;o\_Deinococcales;f\_Trueperaceae;g\_Truepera  
 k\_Bacteria;p\_[Thermi];c\_Deinococci;o\_Thermales;f\_Thermaceae;g\_Thermus

Relative taxonomic composition of 16S rRNA amplicon sequences in mucosal-associated microbiota, at genus level. K, kingdom; p, phylum; c, class; o, order; f, family; g, genus; F, functional; D, defunctioned. n=4.